HYDROGEOLOGICAL ASSESSMENT AND GROUNDWATER VULNERABILITY MAP OF BASARA BASIN, SULAIMANI GOVERNORATE, IRAQI KURDISTAN REGION

A THESIS
SUBMITTED TO THE COUNCIL OF THE COLLEGE OF SCIENCE, UNIVERSITY OF SULAIMANI, IN PARTIAL FULFILLMENT OF THE REQUIREMENTS FOR THE DEGREE OF DOCTOR OF PHILOSOPHY IN GEOLOGY

By

DARA FAEQ HAMAMIN

M.Sc. IN HYDROGEOLOGY - 2004

Supervised by

Asst. Professor SALAHLADDIN S. ALI

May, 2011 A.D *JOZARDAN, 2711 KU*

Supervisor's Certification

I certify that this thesis was prepared under my supervision at the *University of Sulaimani, College of Science, Department of Geology* as a partial requirement for the degree of Doctor of Philosophy in ***Geology (Hydrogeology)***

Signature:

Supervisor: Dr. Salahalddin S. Ali

Scientific title: Assistant Professor

Address: Dean of the College of Science / University of Sulaimani

Date:

Certification of the Department

In view of the available recommendation, I forward this thesis for debate by the examining committee.

Signature:

Name: Dr. Kamal Haji Kareem

Scientific title: Professor

Address: Head of Geology Department, College of Science / University of Sulaimani

Date:

Linguistic Evaluation Certification

I hereby certify that this thesis has been checked by me and after indicating all the grammatical and spelling mistakes, the thesis was given again to the candidate to make the adequate corrections. After the second reading I found that the candidate corrected the indicated mistakes. Therefore, I certify that this thesis is free from mistakes.

Signature: Saz

Name: Saza Ahmed Fakhry

Date: 1/ 3 / 2011

Sulaimani University/ College of Languages/ English Department

Certification of the Examination Committee

We certify that we have read this thesis and as examining committee examined the student in its contents and whatever relevant to it and that in our opinion it is adequate thesis for the degree of Doctor of philosophy in **Geology (Hydrogeology).**

Signature
Name: Dr. Mukdad H. Al Jabbary
Scientific title: Professor
Address: University of Baghdad
Date:
(Chairman)

Signature
Name: Dr. Ayser M. Al-Shamae
Scientific title: Professor
Address: University of Baghdad
Date:
(Member)

Signature
Name: Dr. Qusai Y. Al-Qubaisi
Scientific title: Professor
Address: University of Baghdad
Date:
(Member)

Signature
Name: Dr. Sabbar A. Salih
Scientific title: Professor
Address: University of Tikrit
Date:
(Member)

Signature
Name: Dr. Bakhtiar Q. Aziz
Scientific title: Assistant Professor
Address: University of Sulaimani
Date:
(Member)

Signature
Name: Dr. Salahalddin S. Ali
Scientific title: Assistant Professor
Address: University of Sulaimani
Date:
(Supervisor)

Approved by the College Committee of Graduate Studies:

Signature
Name: **Dr. Salahalddin Saeed Ali**
Scientific title: **Assistant Professor**
Dean of the College of Science/ University of Sulaimani
Date:

بِسْمِ اللّهِ الرَّحْمَنِ الرَّحِيم

قُلْ أَرَأَيْتُمْ إِنْ أَصْبَحَ مَاؤُكُمْ غَوْرًا فَمَن يَأْتِيكُم بِمَاءٍ مَّعِينٍ

Say: Have you thought: If (all) your water were to disappear into the earth, who then could bring you gushing water?

سورة المُلك، آية (٣٠)

Dedication

- To my adorable wife, Naska for all her love, support, patience and encouragement
- To my children, for being my joy and inspiration.
- To all my family and my friends, which they have made their time in my life a truly wonderful experience.

Dara

ACKNOWLEDGEMENTS

First of all; my debt is to the creator "Allah" for giving me power and patience to make this dream comes true.

I am deeply indebted to my supervisor, Ass. Professor Salahaddin S. Ali for supervising this thesis and whose guidance and advice contributed tremendously in enhancing this thesis. My appreciation is due to the Deanery of the College of Science, the Presidency of the University of Sulaimani and the Ministry of Higher Education of the Kurdistan Region for funding part of this study. Special thanks are due to the head of the Department of Geology - University of Sulaimani, especially Dr.Kamal Haji and Dr. Dyari for their assistance and the valuable references they provided me throughout this work.

I am grateful to the Governorate of Sulaimaniyah for funding isotope analyses and drilling two piezometer wells inside the studied area. Without this it would have been impossible for this study to be completed.

I am also grateful to the Ministry of Higher Education and Scientific Research of Iraq and all related directorates for funding fellowship for my training course at the University of Belgrade–Serbia during preparing this research.

My sincere thanks to all the colleagues of the teaching staff, of the "Department of Hydrogeology - Belgrade University", especially prof. Zoran Stevanovic, Dr. Branislav Trivic and Dr. Sasha Milanovic.

I cannot fully express my sincere appreciation and gratitude to the members of the "Joanneum Research Institute – Austria" staff for their tireless efforts and the best hospitality during my training course there, with particular thanks to Prof. Zojer, "Head of the Institute", Dr. Albrechet Lies, Dr. Beyene for their helps, providing Lab, field work, and the valuable references they provided during my stay in Austria.

I owe great thanks to the Groundwater Directorate and Directorate of Irrigation of Sulaimani, especially Mr. Baba Rassol, Mr. Hoshyar Shali and all the other geologists who helped me by providing data related to my study.

Appreciation is also extended to Mr. Farhad from Map Com Company, for his technical help in providing some shape files at the early stage of this study.

My special thanks are extended to the American University of Sulaimani in Iraq- Twin River Institute especially Laboratory staff for chemical analyses of the wet season samples. I am indebted to the Kurdistan Institute for Strategic Studies and Scientific Research (KISSR) in Sulaimani, Department of Chemistry, College of Science from University of Sulaimani, especially Dr. Polla Khanaqa, Mr. Dler and D.Bakhtiar and all other staffs for chemical analyses of dry season.

To my wife and my parents, I have much to thank for their continuous spiritual support and for their patience during the period of my study.

Last but not least, much sincere gratitude to all those who gave me their helps and whom I have forgot to mention.

Abstract

The Basara basin is located in north east of Iraq, 25 km west of Sulaimani city, between the 496652 - 537752 East and 3911038 - 3951906 North in Universal Transverse Mercator (UTM) and lie in Zone 38N. The basin has a rectangular shape and covering an area of 571 km². Tectonically, the basin is complex and located in the unstable platform of the Arabian plate within the Zagros fold thrust belt, exactly along the south western boundary of the High folded with foot hill zones of this belt with intense folding and faulting which resulted from several phases of deformations during Alpine Orogeny.

The entire surface and groundwater of the basin is discharged towards the Basara gorge through three main and several smaller streams.

All the lithological units that are encountered and cropping out in the area are sedimentary and belonging to the Cenozoic in which Kolosh is the oldest formation, while Quaternary deposit, which belongs to Holocene, is the youngest.

Crop Water Balance method using (CROPWAT 8.0) software program was used on the monthly basis for the period of (1980-2009) to estimate reference evapotranspiration on the basis of FAO-Penman Monteith equation, effective precipitation and actual irrigation required water for different cultivated crops in the studied area.

According to the soil water balance and SCS methods, the total expected runoff of the entire area is 149 mm (21.5 %) and the net recharge is 168 mm (24%) from the average annual precipitation of 691mm.

The present hydrogeological investigations have revealed three inhomogeneous and anisotropic water bearing formations: Eocene Karstic Fissured Aquifer (EKFA), Intergranular Aquifer represented by Alluvium and Pliocene (AIA) & (PIA), as well as Miocene Complex Aquifer (MCA).

For the current study, two piezometer wells were drilled and three pumping tests on the basis of observation wells were carried out to obtain aquifer characteristics of the EKFA and AIA which are considered as the most important aquifers of the whole studied area.

The total annual effective recharge to the groundwater from precipitation in the study basin, has estimated by 96 million m^3, among this volume about 10 million m^3 annually is consumed by domestic, irrigation and industrial activities. Approximately 71.5%, 68% and 16% of annual production from annual recharge in Bazian, Hanjeera and Tile sub basins is expected respectively.

Based on the analysis of 65 water points from springs, shallow and deep wells, almost all the tested samples are of very good quality and under maximal permitted limits of the WHO and Iraqi standards, with exception groundwater from shallow or deep wells that tap the water of evaporate formation in the southern part of the basin. The calcium-bicarbonates are the most dominant groundwater type in the study area.

For the first time, not only in Kurdistan but also in all Iraq, Groundwater Vulnerability Map was constructed in this study, using DRASTIC method with the assistance of Geographic Information System (GIS) to show zonation area of high and low groundwater susceptible to pollution. Accordingly, vulnerability classes of the study area were classified into four classes. Most of the basin shows the highest extension of the zones with very low and low vulnerability zones, in contrast the zones with high vulnerability are distributed mainly in the mountain areas, solely in the eastern Uloblagh and Kuwaik mountains, in addition to that small zones in the farthest northern corner and south western corner of the area have less or no human activity.

List of Contents

Subject **Page**

Chapter Three - Hydroclimatic and Water Balance Analysis

Chapter Four – Hydrogeology

Chapter Five - Hydrochemistry

Chapter Six – Groundwater Vulnerability Mapping

Chapter Seven – Conclusions and Recommendations

LIST OF APPENDICES

LIST OF FIGURES

LIST OF TABLES

CHAPTER ONE

INTRODUCTION

1.1 Preface

The hydrogeological knowledge of Kurdistan Region is still unproportionate with the importance of groundwater in present and perspective uses. The abstraction of groundwater from the Basara basin, supplies water for more than 90% of populations inside the area, moreover it provides potable water for other inhabitants outside the studied basin (such as Takiya and Chamchamal towns). Within the last few years, rapid urbanization, growth in industries and agricultural activities are the main phenomena that everyone can felt. Establishing Bazian and Mass Cement factories, as well as Bazian Oil Refinery and several water bottling factories such as Ala Cola and Ice Water are examples of this growth in the area.

In contrast, providing water with high quality and sufficient quantity for those sectors have been increased dramatically, while the over-exploitation of the aquifers and the occasional depletion of annual precipitation have also been increased the decline of the groundwater supply. Its wealth to mention also, although this region has 700mm of annual rainfall in average which precipitated during winter and spring seasons, but a problem of water shortage rises during dry season represented by Summer and Autumn where no or very limited rainfall occur. Moreover, lack of knowledge of groundwater management and little or no regulated protection of aquifer will be affected negatively in the future.

Accordingly, this study is an attempt to fill the gap in the knowledge of hydrogeology, and encourages all those who support active use and protection of groundwater, as one of the most important available resources in one hand. On the other hand, it tries to build up a systematic base of the methodology of the study for the protection of groundwater in geologically complex and sensitive area. In other basins where absence of preventative actions, Industrial and Agricultural practices might result in deterioration of groundwater quality, the number of potential and pollution sources may influence the quality of groundwater.

1.2 Location

As a whole, the studied area is located 25 km west of Sulaimani city. It is situated between 496652 - 537752 East and 3911038 - 3951906 North in Universal Transverse Mercator (UTM) and lie in Zone 38N, covering 571 km^2 and has a rectangular shape with the same trend of the strike of the main structure of the area (Fig 1.1). The entire surface and groundwater of the basin is discharged towards the Basara gorge through three main and several smaller streams.

Each of those streams is dissected into smaller one forming a dendritic drainage patterns. The first two largest streams which are called Tainal stream and Khaldan stream within the Bazian and Hanjeera subbasins are confluence near the Balulan village, where they form a single main stream flowing south west until it reaches to Chami Mastar valley, where they change their directions southwards towards the Basara gorge. The other quite dominant stream which is located in the southern area within the Tile sub basin is the Tile stream that stretches from the Basara gorge toward the south-east for more than 12km and splits near Maryam beg into three smaller valleys. The first one called Chami Hurgena valley, directed toward the north, the second valley directed towards the east and called Chami Zayir valley, while the last one stretches towards the south and ends near the Dolan village, where the divide line of this catchment in the southern part is separated from Darbandikhan basin (Fig 1.2).

Approximately, 45% of the total area is considered as mountainous region which cropping out mostly by outcrops of Sinjar and Pilaspi formations and the remainder area is covered by agriculture plain area. Several inhabitant communities, small towns with tenth of villages are spread out overall the area. Many large factories in addition to several industrial and agricultural projects provide hundredth of job chances for people inside and outside the area for employment.

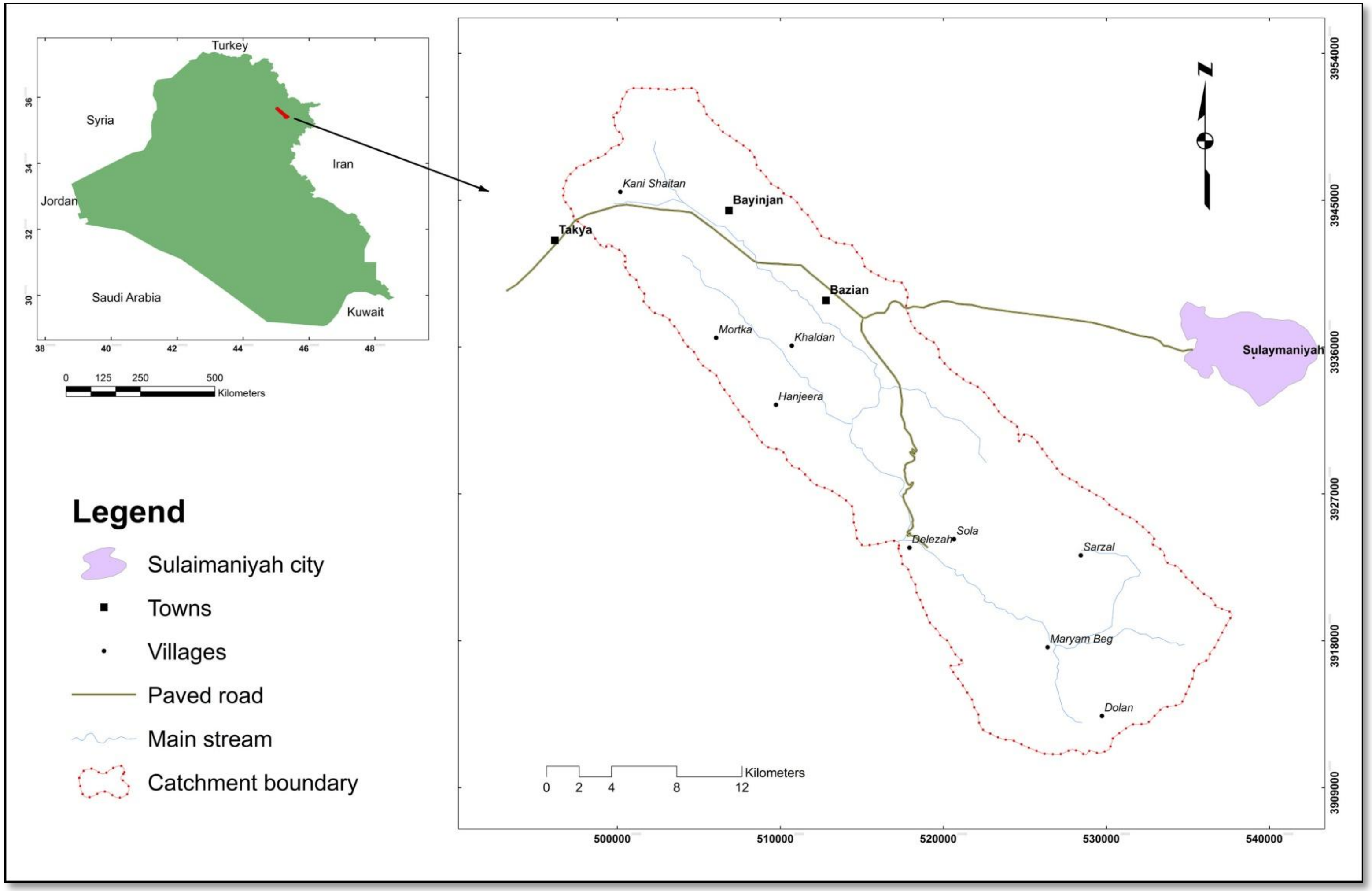

Fig (1.1) Location map of the Basara basin

1.3 Division of the basin

Basara catchment is divided into three sub-basins based on the following criteria:

- Topography. The northern area is divided into two main sub-basins where the two streams namely (Tainal and Khaldan streams) are confluence before reaching the inlet of the Basara gorge, while the drainage basin of the southern part collected water from all small valleys surrounding this sub basin to accumulate in one main stream named as Tile stream.
- Most of the Neogene formations are cropping out only within the Tile sub basin, while most of the Paleogene formations are cropping out within the Bazian and Hanjeera sub basins.
- Structural setting also has its influence for making this sub division.

Generally the Basara basin has a rectangular shape, resemble the dominant structural feature of the area. The previous three sub-basins as suggested in this study are named according to the main towns, mountains and in the basin, (Fig 1.2).

Each sub basin is briefly explained below:

1.3.1 Bazian sub basin

Aziz (2005), named this sub basin as recent sub basin, but in the present study the name has been changed to Bazian sub basin, related to the Bazian community which is considered as the largest town inside the area. This sub-basin is the largest one; it occupies an area of 242 km^2 and this located at the northern and north-eastern part of the studied basin. The collected surface runoff is drained westwards to confluence with Hanjeera sub basin near Balulan village, where they drained exclusively towards the Basara gorge by Mastar stream which collects water from tens of tributaries. Most of the valleys surface consists of gently sloping plain towards the center of the sub basin where most of the large inhabitant communities are settled such as (Bazian, Baiynjan, Allai and Gopala). The basin boundary at the north, northeast, east, south, west and southwest consists of flow divide on the summit of Tasluja, Chaqz, Daragha, Bakhsi, Kuwaik, Uloblagh and Bazian mountains respectively, (Fig 1.2).

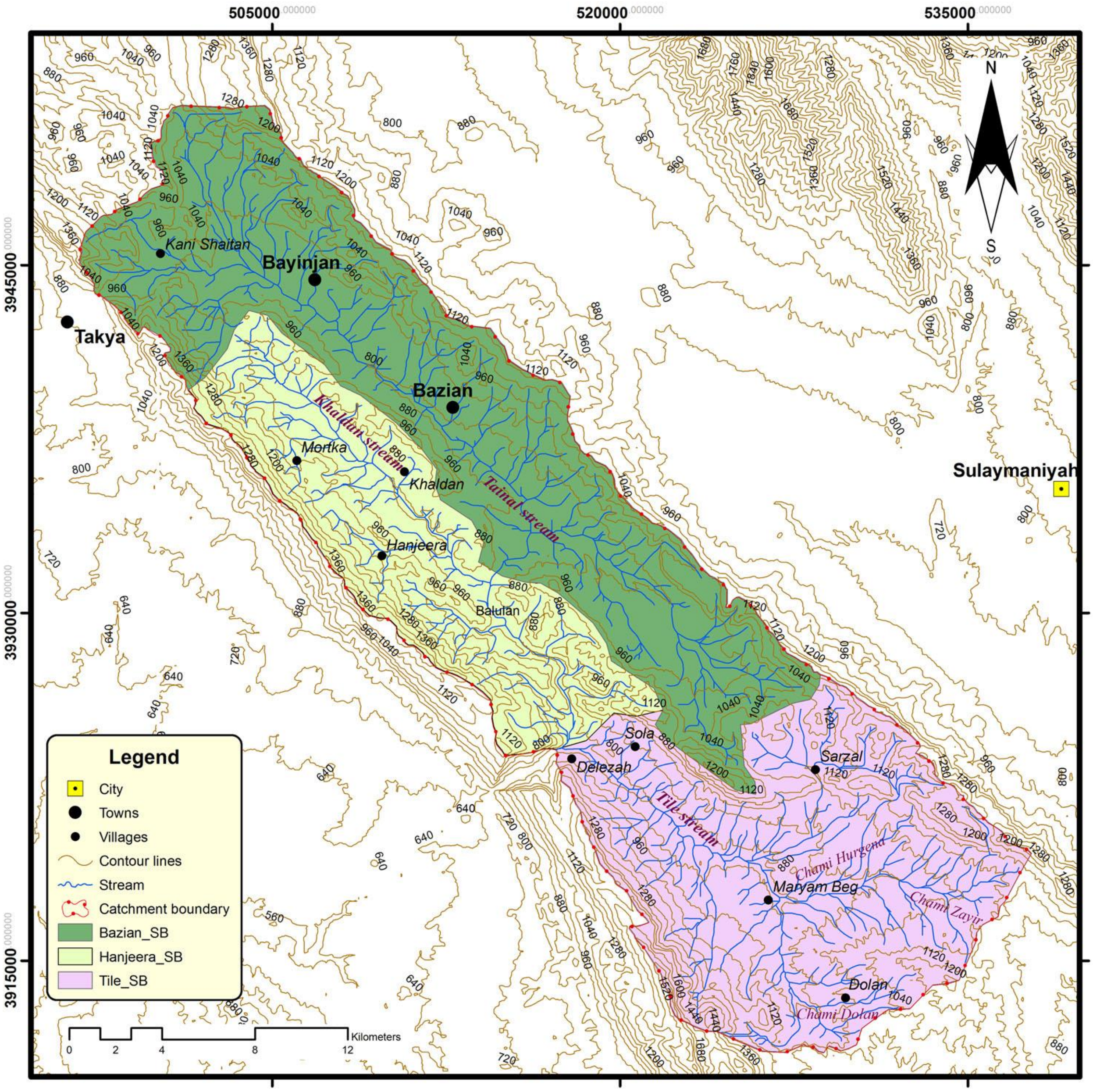

Fig (1.2) Sub-division of the Basara basin into three smaller sub-basins

1.3.2 Hanjeera sub basin

Pilaspi sub basin was the name that suggested by Aziz (2005) in his work, but due to the fact that Pilaspi Formation is not exposed and considered as the major aquifer solely within this sub basin, but also within the Tile sub basin, as a result, its name is suggested to be Hanjeera sub basin, because Hanjeera mountain is completely bordering western part and has influenced the direction of most tributaries flowing eastwards.

This sub-basin is occupying nearly half of the western part of the catchment and covering a total area of 126.6 km^2. The sub-basin has an elongated shape, all the surface runoff are drained exclusively to the Basara gorge by Khaldan stream, which collected water from several springs flowing throughout the year among them, (Cholmak, Mortka, Hanjeera, and Ali-goran) that flowing directly from Hanjeera mountain and the other springs that added their water to this sub basin and flowing from eastern part of the basin are (Khaldan, Ali-bizaw and Gomatta kach). In addition to other several smaller springs that flowing in winter and spring. Relatively the surface of this subbasin consists of higher sloping area as it compared to the previous one, (Fig 6.9).

1.3.3 Tile sub basin

Most of the southern catchment area is represented by this sub basin which contains tenth of villages, like (Delezah, Qazanqaya, Maryam Beg, Timar, Hurgena and Sarzal). It has a surface area of 202.5 km^2 and is semi-circular in shape. All the surface runoff and the groundwater discharge of this sub-basin are drained towards the Basara gorge by the Tile, Chami Zaiyr and Chami Hurgena streams from eastern part and by Chami Dolan, Chami Balakjar and Chami Qirkha streams from South. The divide line of the previous two sub basins have bounded at the north, while the eastern, southern and western part of this sub basin is indicated by the runoff divide line at the summit of Kani Gamka, Kani Bi, Qala Mayman, Sagirma, Darbandi Basara mountains respectively.

1.4 Previous Works

Since this study deals with hydrogeological assessment and groundwater vulnerability mapping, thus the light will shed basically on two main different subjects; the first attempt is going to assess hydrogeological setting and then to make vulnerability mapping.

Concerning making of vulnerability mapping, this study is considered as the first attempt not only in Kurdistan, but also overall the Iraq, which tries to construct such a kind of zonation map especially with the aid of using most recently tool in such field of study, that is called geographic information system (GIS).

Some regional studies are indirectly related to hydrogeological and hydrological conditions were done on and around this area. These studies can be summarized as follows:

The first investigation of groundwater resources was made by Parsons Company in (1957), who collected and evaluated the basic data about geological and hydrogeological information around the studied area.

Lawa, et al (2002) conducted a hydrogeological study of Sulaimaniyah and part of Kirkuk areas, under the FAO projects, part of these studies was carried out in Bazian-Sangaw Basin.

Markovic and Iurkiewicz (2002) have conducted geological and geomorphological studies of Basara Gorge under the FAO projects; the main purpose was to find promising sites for building dam sites and managing of water resources in Kurdistan region.

Lawa et al (2003) performed a geological and hydrogeological study of Qaradagh- Kalar basin, which is bordered in the southern part of the studied catchment.

Basara watershed studied by Barzinji (2003). The study demonstrated the climatic condition and clarified land use and vegetation covers, classified the main soil types in the texture point of view, achieved morphometrical characteristics and a few hydrological analyses for the entire area.

Stevanovic and Iurkiewicz (2004) in the second volume of their studies under a comprehensive program of FAO projects studied the climate, hydrology, geomorphology and regional geology of the three northern governorates "Sulaimani, Erbil and Dohuk", which might be considered the first regional and systematic hydrogeological study conducted up to the present time. Their attempts were followed by a study of general hydrogeology and aquifer system for the same governorates and were published in the second volume in 2004.

Several 1D and 2D geo-electrical surveys were carried out (from 2001 to 2005) by Aziz to demonstrate lithological profiles, subsurface structure and select optimum promising sites for production wells. Most of these surveys were done within Bazian and Hanjeera sub basins. The study also prepared a geological map of a scale of 1:100000 of the northern part of the study area.

A study of physical geography for the catchment area of Basara River was conducted by Jabbar (2007). The study deals with the climatical, geographical, and geomorphological process that occurs inside the Basara basin.

Environmental impact assessment about constructing the Basara dam site were done by Agrocomplet Consultant Engineers Company – Bulgarian in (1979) "unavailable data", Sogreah (France, 1983) and ITSC Hydroengineering - British company in (2006).

Recently, Hamasur (2009) has accomplished a study on rock mass engineering of the proposed Basara dam site, near Delaizha village. The study also prepared a geological map of the central part of the study area of a scale of 1:20000.

In conclusion, there is no detailed and systematic study of the hydrogeology of the basin. This dissertation attempts to contribute to framing a relevant hydrogeological base for more detailed analysis in hydrogeology, hydrochemistry and groundwater vulnerability mapping points of view, considering the importance of groundwater use for water supply, industrial and irrigation.

1.5 Aims of the study

The present work aimed to:

1- Analyzing the climatic characters using the most recently methods with the assistance of modern softwares in such sectors to estimate water balance components using well-known and the widely used methods in such field of study.
2- Demonstrating hydrogeological and geological investigations of the basin including constructing and geo-referencing the geological and hydrogeological maps as well as making some cross sections to show the impacts of topography, stratigraphy and structural geology on the directions of flow and accumulating of groundwater.
3- Hydrogeological assessment of groundwater resources, including the evaluation of the aquifers' characteristics, such as geometry of the aquifers, the recharge and discharge areas within the basin, and estimating hydraulic parameters such as transmissivity, storage coefficients and specific capacity.
4- The analysis of groundwater regime (groundwater table, spring yield versus time, estimation of minimum yield in recession period and storage capacity of the aquifer).
5- The evaluation of hydrochemical properties of the aquifers and validity for drinking, irrigation and industrial uses.
6- Preparing groundwater vulnerability mapping using DRASTIC method with the assistance of GIS tool, to explain the zonation of area of high and low groundwater susceptible to pollution.

1.6 The Used Data

Once, basic information, available report and documents about geology, geophysics, hydrology and hydrogeology were collected, the used data in the course of this survey has been classified into three types:

1.6.1 Field Data

Field data includes the hydrogeological, infiltration, hydrochemical and isotope data were collected, during a long term field work (started in April 2009 and continued along 15 months), covering the following activities:

- Mapping all geological formations and structures for the southern part of the basin, because the prepared previous map was in a regional scale that some important features were missed.
- Inventory of the most remarkable water points, such as deep and shallow drilling wells, springs as well as streams.
- Performing infiltration test for 19 sites throughout the basin during June (2009), using double ring infiltrometers to assess and classify the soil infiltration capacity.
- Monthly monitoring of three piezometer wells in addition to several other drilling wells, were possible with the aid of electrical sounder for measuring static water level.
- Drilling two piezometer wells, one penetrating Sinjar Fn. and the other was percolated Pilaspi Fn. in order to study the lithology, achieve pumping test and monitoring water level fluctuation.
- Three pumping tests which penetrating the main three aquifers inside the area were done from 3 observation wells located between several meters to some tenth of meters with duration between 240 – 400 minutes. These tests were performed during summer and autumn, 2009 after completing drilling the piezometer wells.
- Sampling of groundwater for two seasons (wet and dry) were done to determine hydrochemical characteristics and assessing seasonal variation. 40 samples and 25 samples were collected for the wet and dry periods respectively from deep wells, shallow wells and springs for chemical analyses including major and minor ions in addition to some trace and heavy metal for the selected samples. As well as *in situ* measuring of temperature, pH, electrical conductivity and total dissolved solids (TDS). Multi-parameter portable device model

(TPS/90FL-T Field Lab Analyzer) was used for this purpose. This was carried out during April and September (2009), (Fig 1.3 A and 1.3 B).

1.6.2 Laboratory Data

Laboratory work focused on the chemical and isotopic analysis of collected groundwater samples during field work. 65 samples for the two seasons were analyzed, in which 40 samples for wet season were sent to the Laboratories division in the Twin River Institute, the American University of Iraq _ Sulaimani, for analyzing major ions as well as heavy metals. The techniques used for analysis was the standard methods of water analysis as specified by the APHA (2005) and other approved procedures. A summary of the laboratory work is shown in table (1.1), while the other 25 samples of dry season were analyzed in the laboratory of Chemistry department of college of Science, Sulaimani and laboratory of Kurdistan Institute for Strategic studies and Scientific Research (KISSR) in Sulaimani, results of chemical analyses methods are shown in table (1.2).

Table (1.1) Summary of chemical analyses methods used by Twin River Institute for the collected samples in wet season

Parameter	*Methodology*	*Method No. in APHA 2005*
Phosphate (PO_4^{3-})	Ascorbic Acid	4500-P E
Alkalinity	Titration	Modified Lind, 1979
Calcium (Ca^{2+})	Ion Chromatography	4110B
Chloride (*Cl*)	Ion Chromatography	4110B
Magnesium (Mg^{2+})	Ion Chromatography	4110B
Potassium (K^+)	Ion Chromatography	4110B
Sodium (Na^+)	Ion Chromatography	4110B
Sulfate (SO_4^{2-})	Ion Chromatography	4110B
Nitrate (NO_3^-)	Ion Chromatography	4110B
Heavy metals	FAAS	3111B

Table (1.2) Summary of chemical analyses methods used by both Chemical department and (KISSR) for the collected samples in dry season

Parameters	*Methodology*	*Instruments*
Ca^{2+}, Mg^{2+} Na^{+}, K^{+}	ICP (Inductive Coupled Plasma)	Inductive Coupled plasma_ Optima 2100 Perkin Elmer
HCO_3^{-}, CO_3^{2-}	Titration	Normal Instruments for wet analysis
F, Cl^{-}, Br, PO_4^{3-}, SO_4^{2-}	Ion Chromatography	Ion Chromatography System (Dionex)
Alkalinity	**Photometer**	Flame Photometer

1.6.3 Office Work

The office work included representation of the field work and analyzing laboratory data. Among those softwares and programs which were used in this study for analysis and mapping are:

- CROPWAT version 8.0 (FAO-2009): For making crop water requirements and estimating evapotranspiration using FAO Penman-Monteith method as well as effective rainfall.
- SPSS statistics program for estimating infiltration capacity using Horton's equation.
- ArcGIS 9.3 (2008), for constructing all basic maps and required maps for preparing vulnerability mapping.
- AQTESOLV version 4.0 (2006) for pumping test analysis.
- Adobe Photoshop CS3, for creating and editing some sketches and cross-sections.
- Aq.QA version 1.1 (2005) software for hydrochemical data presentation, such as Piper and Pie charts diagrams.

Fig (1.3) Collecting groundwater samples for chemical analyses

CHAPTER TWO

TECTONIC SETTING AND GEOLOGICAL FRAMEWORK

2.1 Tectonics

From the tectonic points of view, the area of the study is complex and located in the unstable platform of the Arabian plate, Jassim & Goff (2006).

According to Beydoun (1993), this platform comprises the outer mobile part of the Arabian plate which extends mainly over eastern Saudi Arabia, most of the Arabian Gulf, central – northern Iraq, northern Jordan, and western Syria, Lebanon, Palestine and northern part of Senia. The main characteristics of this platform are:

- ❖ Thickness of the sedimentary cover with successive marginal sedimentary basins of broad subsidence and variety deposits separated by intra shelf swells.
- ❖ Basement is relatively deep.
- ❖ Affected to various degrees by the Alpine orogeny with folding and deformation intensity increased north – northeast wards and developed by direct compression forces, tangential shearing, vertical block movement and diapiric growth movements.
- ❖ This platform could be subdivided into (Mesopotamia, Arabian Gulf fore deep and Zagros – Taurus fold Thrust belt.

Generally, the studied basin is located within the Zagros fold thrust belt, exactly along the south western boundary of the High folded with foot hill zones of this belt (Fig 2.1). It is characterized by high mountains elevation (up to 1600m a.s.l. in the south-western part of the area) and intense folding and faulting are resulted from several phases of deformations during Alpine orogeny.

The basin lies between two mountain series, from the North and East by Tasluja, Daragha, and Baranan mountains, while from North West and western part by Bazian, Hanjeera, Darbandi-Basara, Sagrma, and Qala Mayman mountains. The later series represents the boundary between the low and high folded zones in the area. In addition to the series of Kawaik and Uloblagh mountains which divided the catchment in the northern and central parts into two hydrologic sub-basins (Fig 2.2 and 2.10).

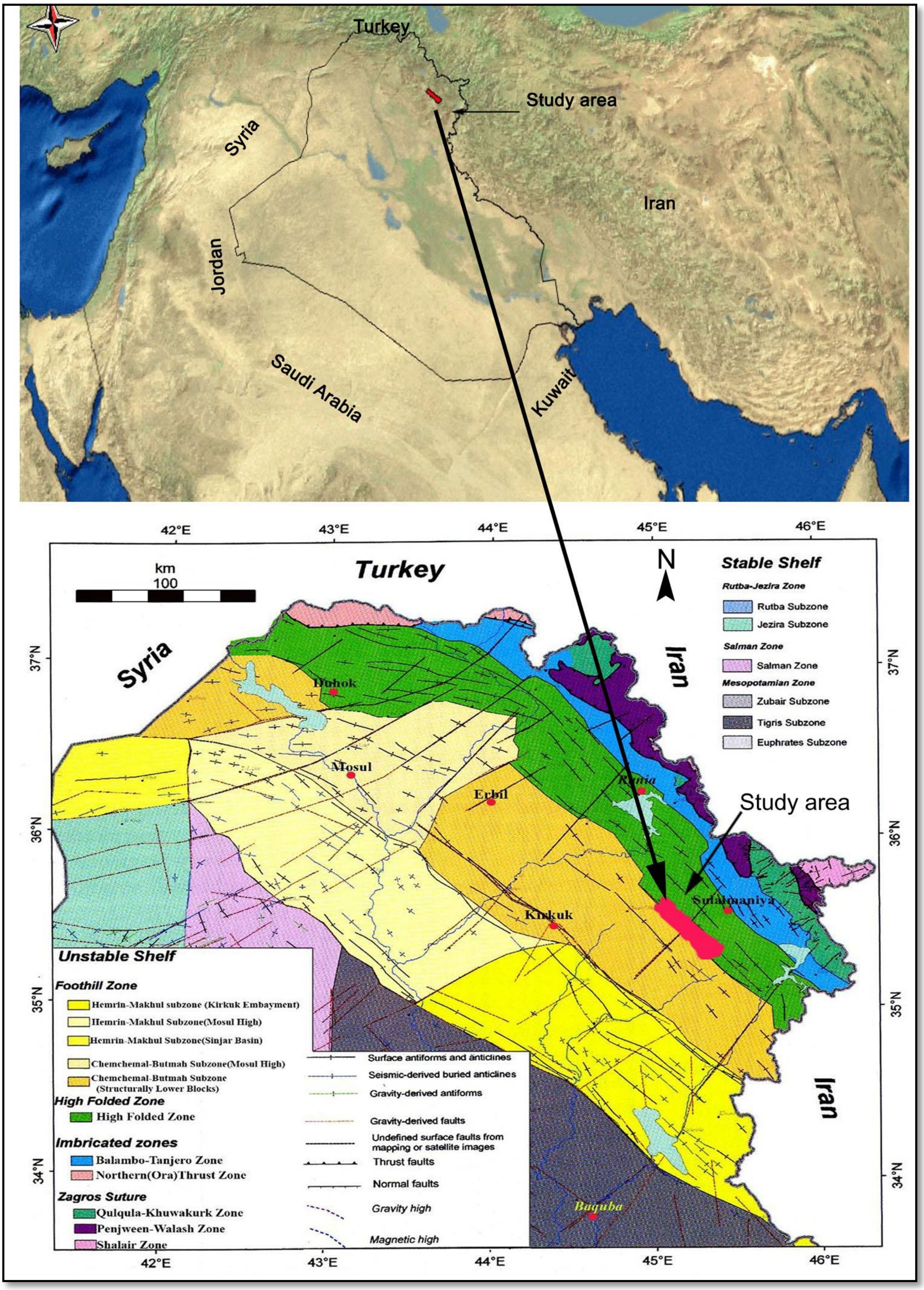

Fig (2.1) Tectonic maps and structural elements for the entire and surrounding the studied area, "after ESRI Arc Globe documents and Jassim & Goff, (2006)"

Based on the results of the tectonic map of Iraq that prepared by Jassim and Goff (2006) which is shown in Fig (2.1), the basin is controlled by NW-SE trending major folds and faults, similar to the lineaments trend of structural features associated with some minor NE-SW directions of the region.

Stevanovic and Markovic (2003) have described regional tectonic framework of Kurdistan (northern of Iraq) in terms of geo-flexures, they have mentioned that these structures are considered to be large folds of geotectonic scale, reconstructed by compilation of field and remote sensing data. On a geotectonic scale, geo-flexures could be parts of high uplifted lands or parts of subsided areas (basins).

Referring to Numan and Ameen (1983), most of the geo-flexures detected in Iraq are generally monoclinal, mostly double plunging with an echelon arrangement. The axial lengths range from 50 to 107 km and usually coincide with the hinges of major anticline structures.

Darbandi Bazian double plunging geo-flexures with monoclinal style and an echelon arrangement exist in the Zagros part of the folded zone of Iraq with NW-SE trend. It is considered as the largest detected one in Iraq. It extends about 107 km from Diyala River north-westwards. The hinge line of the geoflexure is coincident with that of the Darbandi Bazian Anticline. It is parallel and very close to the mountain front. The amplitude of this geoflexure is about 3200 m and the width is about 155 km as compared with other geoflexures in Iraq, this one is very peculiar. It has a long and relatively straight hinge line with a swing corresponding to that in the axis of Darbandi Bazian Anticline, near its eastern plunge. The southwestern limb shows local overturning due to major rotational faults. The dips of the southwestern and northeastern limbs along Sulaimaniyah traverse are 65^0 and 20^0 respectively (Stevanovic and Markovic, 2003). They also mentioned Bazian south anticline as a double plunging fold which extends about 50 km in a NW-SE direction. Its both plunges are gentle. The anticline is normal and asymmetrical with a northeastward vergence. The dips of the northeastern and south-western limbs are 45^0 and 15^0 respectively (Fig 2.3).

The Bazian South Anticline is parallel with the Darbandi Bazian Anticline to the southwest, and an arranged echelon overlapping with the Bazian North Anticline to the northeast. The latter is separated from the Bazian South Anticline by a syncline approximately wide 8 km. The landslides and gravity faults intensively affected the northeastern limb of the Bazian South Anticline. A longitudinal gravity fault has a displacement of about 600 m near Tasluja (Stevanovic & Markovic, 2003).

2.2 Regional lineaments

Generally, lineaments and other structures of the entire and around the studied area were presented based on the digital elevation model (DEM) from NASA srtm satellite image with resolution of 80m benefited from previous work carried out by FAO projects in 2003, the result is shown in Fig (2.2).

As can be seen, most of the lineaments presented as linear feature with blackish color, and oriented in NE-SW direction, perpendicular to the major strike of folded structures. In contrast, some other lineaments with NW-SE directions parallel to the main structure within the catchment area, and E-W oriented lineaments are well pronounced out of the area toward the south eastern part.

Stevanovic & Markovic (2003) assumed that, the oldest lineaments are those belonging to the N-S orientation. They could inherit Precambrian N-S trends. The E-W and NW-SE lineaments are younger, and are related to the opening of the Neo-Tethys Ocean which involved separation of the Iranian and Turkish plates in the Triassic. The NE-SW lineaments are the youngest and have developed during the closure of the Neo-Tethys Ocean and the following continental plate collision. They also found a considerable discrepancy between lineaments determined on aerial photos and the joints measured in the field; they mentioned that the first order tension joint is the transversal joint set. Such set is usually called extension joints set, formed parallel to the prime tectonic force and perpendicular to the strike of folds. While the second order tension joints make the longitudinal joint set formed perpendicular to the compressive tectonic force, as a result of elastic pressure release. They are parallel to the folds strike.

Accordingly, the majority of the joints within the studied area could be classified as the transversal joint sets, because most of the lineaments are perpendicular to the strike of the folds, in addition to that some sets of longitudinal joints are expected due to the presence of two main lineaments which are oriented NW-SE parallel to the main fold of the study area.

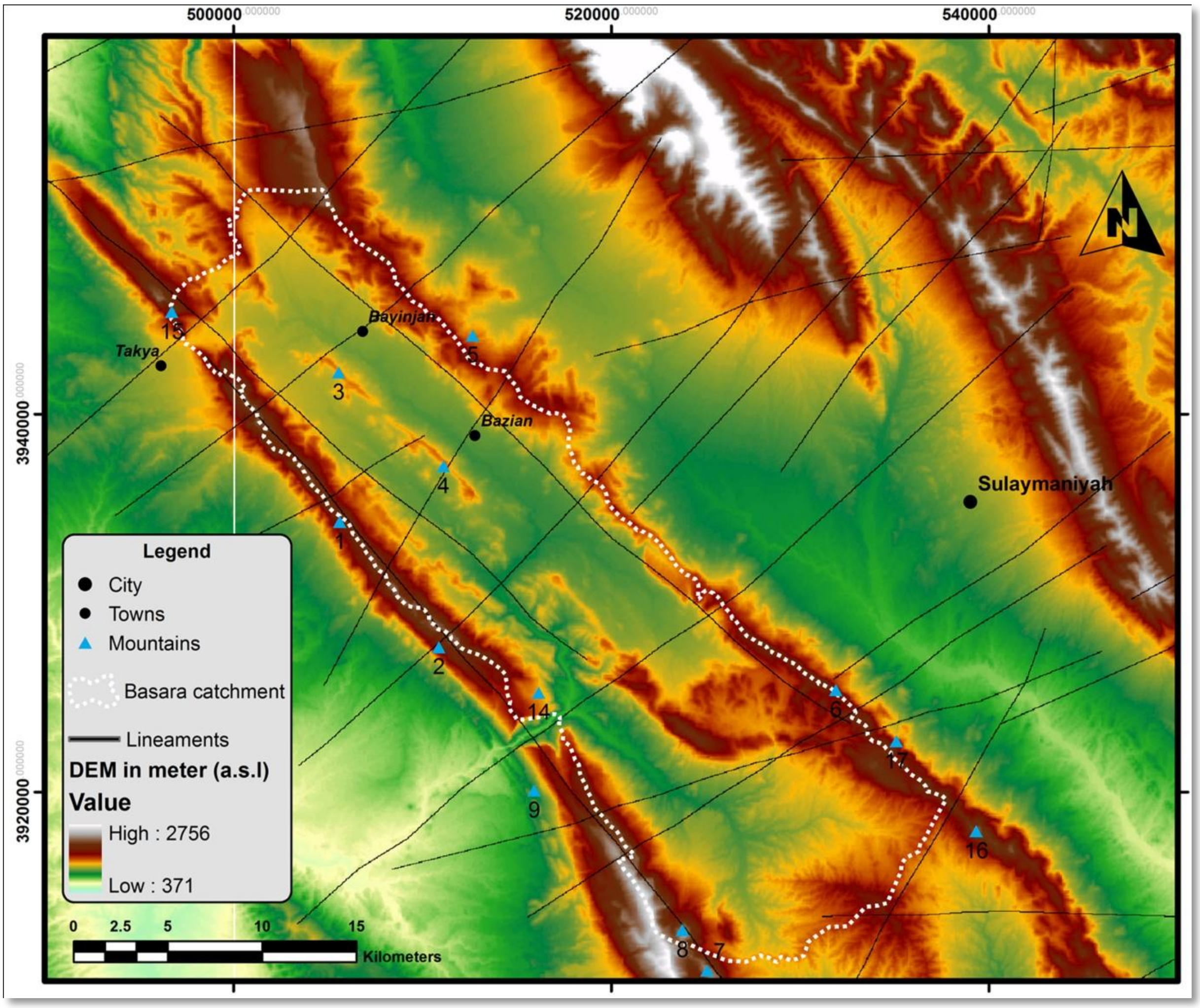

Fig (2.2) Digital Elevation Model "DEM" with Lineament pattern and the main mountains surrounding the Basara catchment (modified from Stevanovic and Markovic, 2003)

1. Bazian Mount. 2. Hanjeera Mount. 3. Uloblagh Mount. 4. Kuwaik Mount. 5. Tasluja Mount. 6. Daragha Mount. 7. Kani Bi Mount. 8. Qala Mayman Mount. 9. Sagirma Mount. 14. Darbandi Basara Mount. 15. Darbandi Bazian Mount. 16. Kani Gamka Mount. 17. Baranan Dagh Mount.

2.3 Stratigraphy

The different lithological units that are exposed to the surface in the area are belonging to the Cenozoic.

Description of the geological formations in this study is mainly based on Dubertret (1959), previous studies which carried out in this area by (Aziz, 2005), (Hamasur, 2009). In addition to the field work during the study, and finally geological map of the area was rearranged and presented in Fig (2.3). As can be noted from this map, Kolosh is the oldest formation, while recent deposits which belongs to Holocene, is the youngest. The existing formations for each period within Cenozoic are briefly descried from oldest to youngest as follows:

2.3.1 Paleogene formations

Based on Stevanovic and Markovic (2003), during Paleogene, a different deposition environments (Neritic and Bathyal) and lateral variation has dictated the creation of alternately carbonate and flysch sediments (Sinjar, Gercus and Pilaspi formations).

2.3.1.1 Kolosh Formation

Kolosh clastic Formation has been formed in a very deep and mobile sedimentary basin during Paleocene-Lower Eocene (Bellen et al., 1959).

Lithologically, it is composed of grey calcareous shale; siltstone, sandstone and sandy limestone, in some cases thin bed of limestone occupies the top of the formation. Well profile by Bazian Oil Company for oil exploring, close to the Kupala village near Bayinjan community, its thickness reached 600m.

According to Surdashy (1988), Surdashy & Lawa (1993), the upper contact is regarded as gradational conformable contact with Sinjar Formation, while Lawa (2004) believed that it is of unconformable contact with Sinjar at least in the sections (Sagrma and Kani Gopala) adjacent to the study area. Inter-fingering is the main characteristics of this formation with overlain Sinjar limestone, this was clearly obvious from well profiles drilled in the central and most northern part of the area.

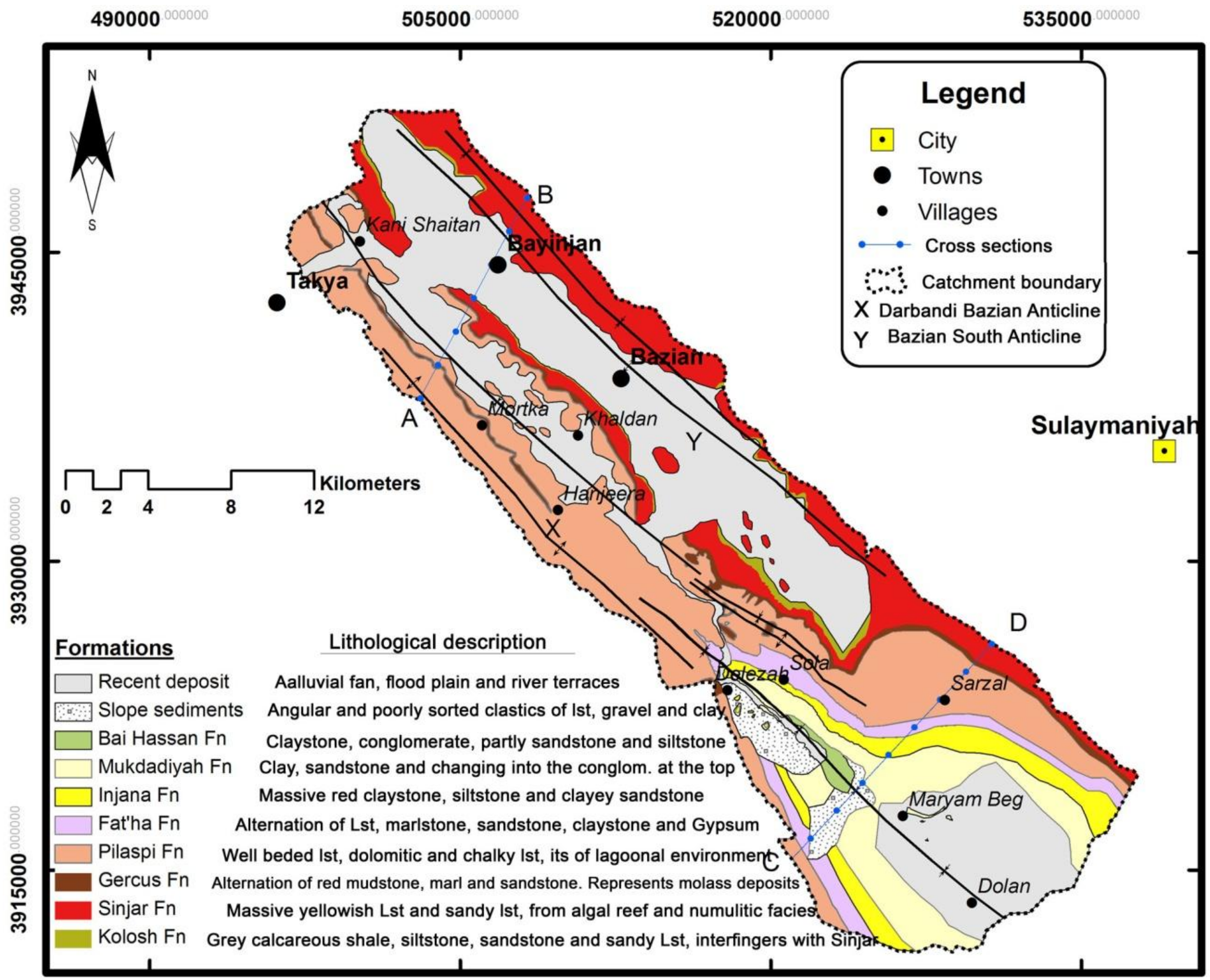

Fig (2.3) Geological map of the Basara catchment area

Generally, Kolosh Formation cropped out on an area of about 7 km^2 (Table 2.1), in the south-eastern and north-western boundary of the Bazian sub basin (Fig 2.3).

Table (2.1) Total exposed area and percent of each formation overall the Basara catchment

Formations	Area in (Km^2)	Percent of total area (%)
Recent deposit	219.81	38.5
Recent_Slope deposit	14.36	2.5
Bai Hassan Fn	2.88	0.5
Mukdadiyah Fn	43.52	7.6
Injana Fn	23.56	4.1
Fat'ha Fn	20.52	3.6
Pilaspi Fn	144.63	25.3
Gercus Fn	13.19	2.3
Sinjar Fn	81.97	14.3
Kolosh Fn	6.83	1.2

2.3.1.2 Sinjar Formation

This formation is of Early Eocene (Lawa, 2004). It is mainly composed of massive yellowish gray limestone, sandy limestone and conglomeratic limestone from algal reef and shoal nummulitic facies

Based on Hamasur (2009), the upper contact is unconformable with Gercus Formation which is indicated by red color and lithological variation into red clastic with weak conglomerate bed at this boundary. It occupies an area of about 82 km^2 or (14% of the total area), and crops out at most of the north and north-eastern boundary of the catchment area, as well as north eastern limb of Uloblagh Mountain (Fig 2.3). Surdashi (1988) has believed that the thickness of this formation is around 98m in the Bazian area, but according to the profiles and well sketches from 12 drilling wells penetrating this formation entire the area of the study, the mean average thickness varies between 50m and 70m (Fig 2.8), except some wells close to Kani-shaitan apparent thickness reaches 85m.

2.3.1.3 Gercus Formation

The overlain Gercus Formation is a Middle Eocene (Bellen et al., 1959). It is composed of consolidated red mudstones, green marl, and gray sandstone with lenses of basal conglomerate bed at the top, showing unconformity with Pilaspi Formation (Fig 2.4).

Fig (2.4) (A) Lithology and (B) unconformity contact of Gercus with overlain Pilaspi Formation, (photo was taken in March-2010, near Qala sura village)

The reddish colour that often characterizes the sediments of this formation probably indicates the oxidizing chemical condition that was prevailing in the area. This formation occupying an area of about 13 km^2 and crops out along most of the south-western exposed of Sinjar Formation, and along north-eastern limb of Hanjeera Mountain (Fig 2.3). Aziz (2005) believed that the thickness of this formation is around 80m based on two geo-electrical sections carried out and passing the Pilaspi sub basin (Hanjeera sub basin).

2.3.1.4 Pilaspi Formation

Pilaspi Formation is composed of well bedded limestone, dolomitic and chalky limestone (Fig 2.5). Some authors have assigned Middle – Upper Eocene age for this formation (Bellen et al., 1959). It is unconformable with the overlain Fat'ha Formation. According to Stevanovic and Markovic (2003) the sedimentary environment of Pilaspi Formation is mainly lagoon and the thickness varies between 100-200 m, while Aziz (2005) constructed an isopach map for this formation, he gave ranges of thickness from 20m to 130m. But the dominant thickness of this formation is around 80m based on the well profiles and cross sections prepared by previous work done by FAO project which was located close to the southern part of the area passing Tile sub basin, (Fig 2.6 & 2.8).

Fig (2.5) (A) Well bedded limestone and (B) tectonic effect on the Pilaspi Formation (photo was taken in March-2010, near Khamza village)

As a whole, this formation is the second most exposing formation overall the studied basin, it occupies an area of about 145 km^2 or more than 25% of the whole catchment area, cropping out as ridges at western and south-eastern parts of the area.

2.3.2 Neogene Formations

During Oligocene and Lower Miocene, the regression phase has partly caused the absence of sediments of these ages in the area. The sedimentation cycle continued during Middle and Upper Miocene when thick Fat'ha and Injana formations have been formed. These are lithologically very heterogeneous facies (marls, sandstones, anhydrite, gypsum, conglomerates, and clays) outcropped dominantly at Foothill (Low Folded) Zone (Stevanovic and Markovic, 2003).

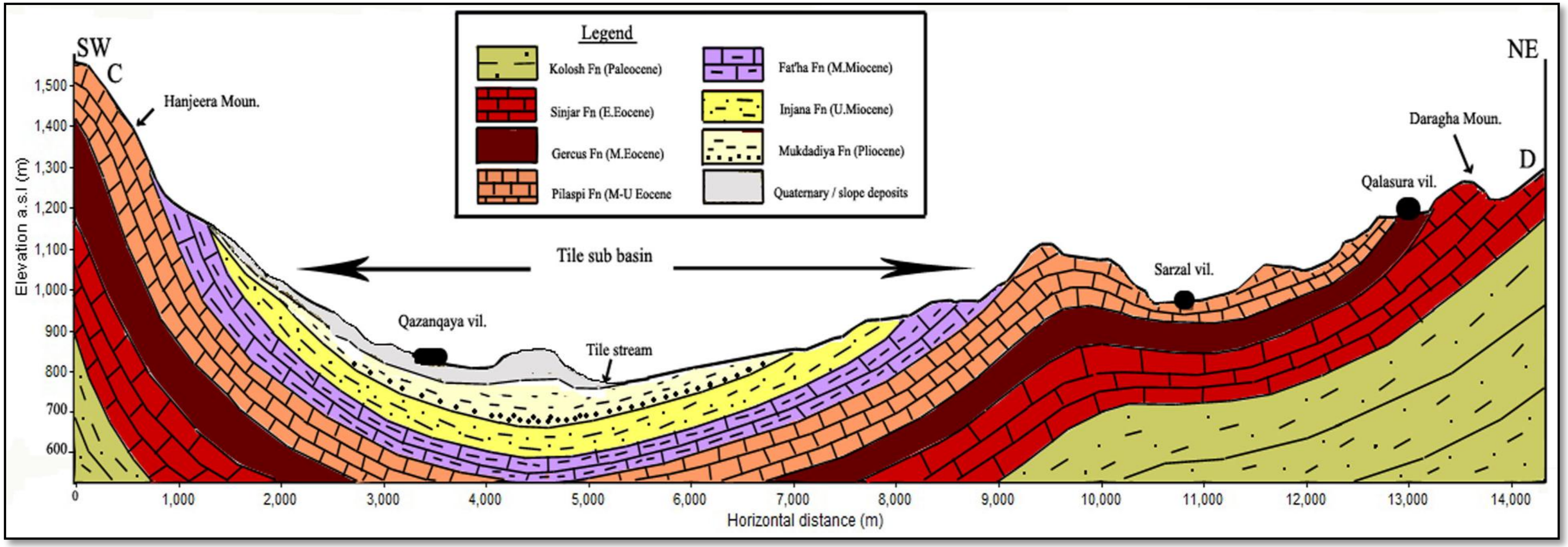

Fig (2.6) Geologic cross section (C-D) of the southern side of the area passing through the Tile sub basin

2.3.2.1 Fat'ha Formation (Lower Fars Fn)

This formation is composed of variable lithology from gypsum, yellowish limestone, green marlstone, sandstone, siltstone and claystone. Based on Bellen et al. (1959), the age is Middle Miocene. The contact is gradational and conformable with overlain Injana Formation. It occupies an area of around 20 km^2, and crops out within Tile sub basin in the southern area (Fig 2.3). As can be seen from Fig (2.6), the mean average thickness of 60m is expected, particularly in the southern part of the area.

2.3.2.2 Injana Formation (Upper Fars Fn)

Injana Formation consists of massive red claystone, siltstone and clayey sandstone. Based on Bellen et al. (1959) the age refers to Upper Miocene. Buday (1980) has believed that the deposition environment had been marine (lagoonal) but was progressively changed into fluvio-lacustrine toward overlying Mukdadiya Formation (the first conglomeratic layer marks the contact).

2.3.2.3 Mukdadiya Formation (Lower Bakhtiari Fn)

This formation is composed of clay, sandstone and changing into the conglomerate at the top with the overlain Bai Hassan Formation, having conformable contact. The age is Pliocene (Bellen et al., 1959). Based on Buday (1980), a general trend of grain size decreasing can be partly observed along the axis of the main deposition areas. This formation occupies an area of about 43.5 km^2, and crops out in the southern part of studied area, within Tile sub-basin (Fig 2.3). As can be noted from Fig (2.6), the thickness varies from few meters in the foot hill zones of the mountain and attains more than 100m in the depression area, especially around the trough axis of the main syncline in the southern area, adjacent to Tile stream.

2.3.2.4 Bai Hassan Formation (Upper Bakhtiari Fn)

It is composed mainly of claystone, conglomerates, partly sandstones and siltstones, with great lateral and vertical variations from one place to another (Fig 2.7). Bellen et al. (1959) have believed that this formation was deposited during the Pliocene.

Fig (2.7) profile of Bai Hassan Formation, near Sollai Darband village

2.3.3 Quaternary deposits

These deposits cover a wide range of the catchment and occupy 41% of the total area. It crops out at most central and southern parts of the area, due to erosion with the aid of mass wasting in the surrounded carbonate rocks. It consists of deposits of river terraces, alluvial fans, slope deposits and flood plains (Fig 2.3).

Nature of the unconsolidated with coarse material of these deposits, made it as the optimum resource for providing potable water for irrigation and domestic uses for most inhabitants settling on the places where Quaternary deposits are cropping out. According to the geo-electrical survey carried out in the area by Aziz (2005), the thickness of these deposits may reach 150m, especially at Bayinjan town, and it decreased to less than 30m within the Hanjeera sub basin, that confirmed from the drilling well profiles and from geo-electrical survey carried out in the area (Fig 2.8).

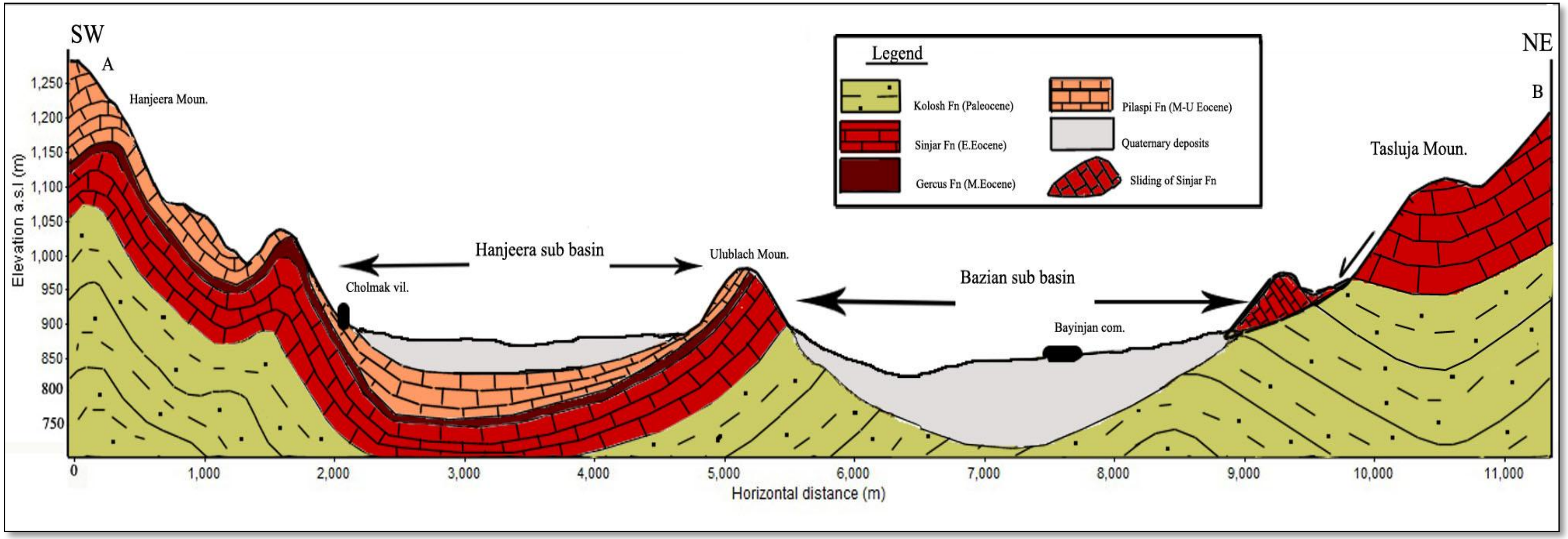

Fig (2.8) Geologic cross section (A-B) of the northern side of the area passing through both Hanjeera and Bazian sub basins

- **River terraces**

It spreads along major rivers represented by Tainal and Tile streams; it is composed of various sizes of gravel cemented by carbonate, clay and silty material (Fig 2.3).

Based on Stevanovic & Markovic (2003), the differentiation between these deposits and underlying Bai Hassan Formation is extremely difficult, due to lithological similarity and absence of fossils in both units.

Fig (2.9) Quaternary with thick recent deposits in Bazian town, (photo was taken in April-2010)

- **Alluvial fans**

During the field survey and with the aid of Google earth map, several large and small alluvial fans were observed; most of them follow flow direction of perennial and intermittent streams, as well as extending from the outlets of valleys of the high land area into the lowland of the plains (Fig 2.9 & 2.10).

Most of the large fans are predominant in the central part of the catchment area, especially within the Bazian sub basin. Most of the small fans are hardly distinguished by their shapes, because they have been dissected and separated by several small intermittent streams which have modified their shapes. Relatively low vegetal cover and minimum infiltration rate may cause the generation of these small fans to be derived from surrounded carbonate rocks represented mainly by Sinjar and Pilaspi formations.

- **Slope deposits**

These deposits accumulated along the mountain slopes (as colluviums); in the south western part (close to Basara gorge). It consists of succession of angular and poorly sorted clastics with various sizes of gravel with clay as separate deposits. Mostly, they are composed of limestone which derived from pilaspi Formation (Fig 2.3).

- **Flood plains:**

Generally, these deposits composed of gravel, sand, clay and silt on the river banks of the main streams in the catchment.

As can be seen from topographic map in Fig (6.9), most of the central part within the Bazian sub basin have slope less than 2 %, thus a heavy load with coarse sediments as channel deposit, as well as fine clastics on the flood plain which are expected during wet seasons.

Finally, all previous Quaternary deposits are described and grouped as recent deposits for the next chapter and entitled as recent deposits in the legend of the geological map in Fig (2.3), except slope deposit which is classified and described as separate zone within the geological map, because it is characterized by higher infiltration rate as compared to the other Quaternary deposits.

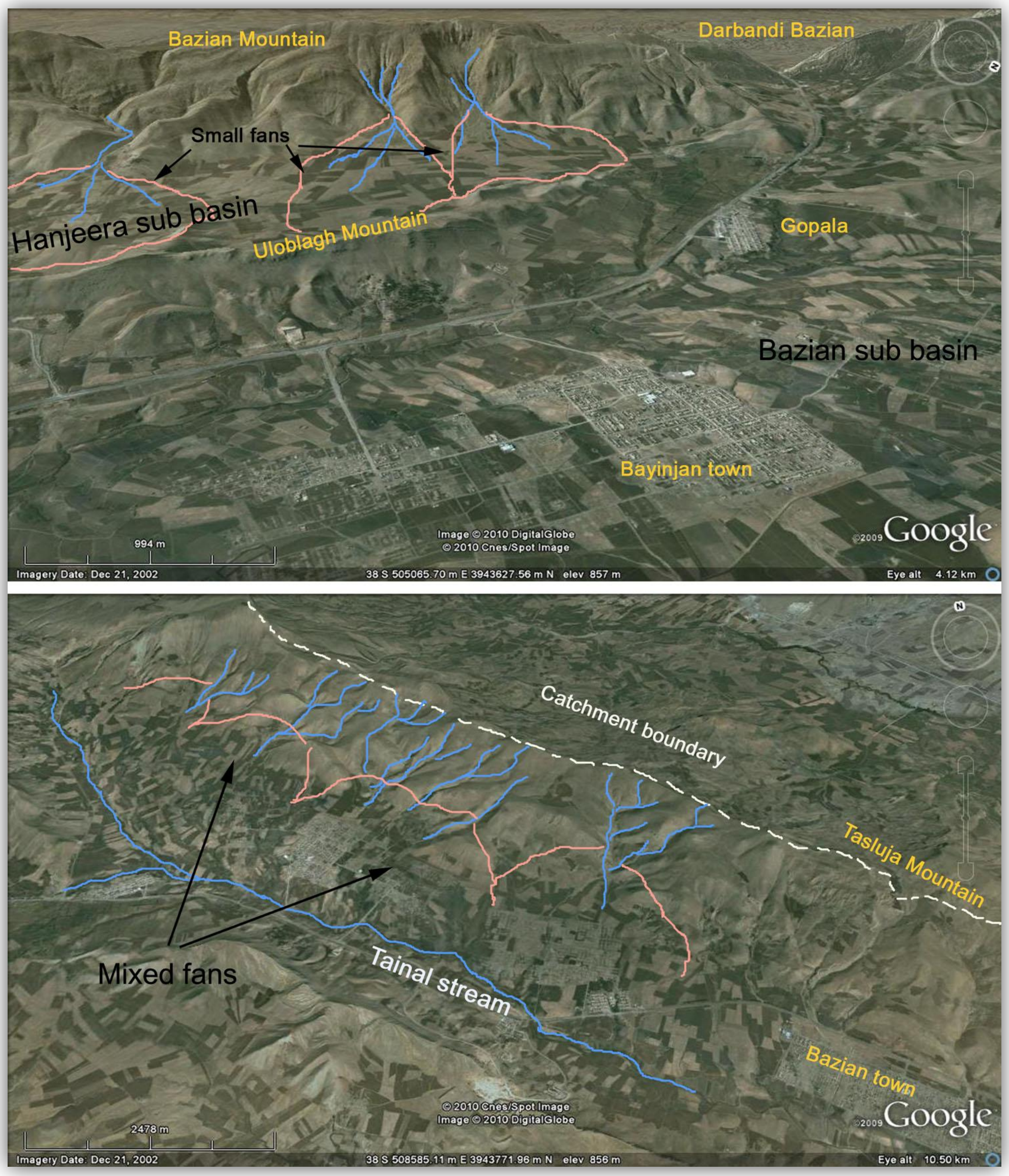

Fig (2.10) Mixed and small alluvial fans within the catchment area (From Google Earth - 2010)

CHAPTER THREE

HYDROCLIMATIC AND WATER BALANCE ANALYSIS

3.1 General Climate

The studied basin has a distinct continental interior of Mediterranean climatic type, it is characterized by cold and rainy winters with prevailling all types of precipitations (rainfall, hail and snow), as well as long, hot and dry summers. Nearly summer and winter comprise three fourth of the whole year, while spring and autumn comprise the other 3 months, so all seasons clearly could be felt throughout the year. The hottest months are June, July and August, while the coldest months are December, January and February.

Based on the classification of Thornthwaite, Lang factor and Emberger classification of defining climate, the studied area is classified under semi-arid climatic moisture type, Barzinji (2003).

According to Aziz (2001), during the summer "the region falls under the influence of Mediterranean anticyclones and sub-tropical high pressure belts moving from the west, south-west to north. Southerly wind blows over Arabian Peninsula developing dust storms, raising daily temperature to a maximum value of more than 45 C^0.

In the winter, the region is invaded by Mediterranean cyclones moving east to north-east over the region, Arabian Sea cyclones moving northward passing over the Gulf carrying a great amount of moisture which cause a large amount of precipitation in the region. The region is also exposed to the influence of very cold polar air mass immigrates with the polar jet streams downward to the Gulf, Aziz (2001).

Depending on the archives of Sulaimani meteorological station for the last 30 years, the maximum average monthly temperature was around 40 C^0 in July and August while the lowest average degree was around 2 C^0 recorded in January and February. The average wind velocity in the individual months of the year does not exceed 3 m/s. In summer, the total cloud cover is limited and clear weather predominates. The average annual air humidity is around 45%, and it exhibits a high seasonal diversity.

In January, humidity approaches the maximum rate, more than 70%, while it drops sharply from May to reach the lowest rate of 22% on July and August. Moreover, the relative humidity in this zone exhibits large 24-hour fluctuations, understandable in view of the high 24-hour air temperature amplitude. In the climatic zone under discussion, fog occurs rarely, depending on the distance from the hydrographic network and water-logged areas. Foggy days usually occur in December and January. According to Polservice (1980), the area is located at the boundary of major deserts of the Middle East; therefore both the weather and the climate are variable. The climate is greatly affected by the dusty and warm wind that blows from the southern and western desert of Iraq, Jordan and Saudi Arabia. Dust storms raise the daily temperature to a maximum value of more than 45º C.

The only meteorological station found inside the area is the Bazian meteorological station which was installed during the FAO project in Kurdistan by the end of 2004. Because of the recently installed of this station, and due to the lack and incomplete meteorological record for a long time, measurements for the years of 1980-2009 from Sulaimani meteorological station (where it locates far by 25-45 km from the studied area) is used for studying and analyzing meteorological data with some modification for both temperature and rainfall, while for other parameters, data of Sulaimani station is applied.

The Sulaimani meteorological station could be considered relatively representative of most of the entire basin, this can be clearly inferred from Fig (3.1), which indicates ***low*** and ***high*** *precipitation rate (Years 1983 and 1988 respectively)* inside and around the studied basin, the orientation of all the isohyetal lines in both maps are nearly parallel with the orientation of the longest dimension of the catchment area. It can be also concluded that the area is located in the isohyet line which is close to the Sulaimani station and it is less than the annual rainfall of it by 10% in both low and high precipitation rate.

To make consistency of this result, data for the last few years were used in both stations to show the relation between them, and to find a suitable equation for analyzing meteorological data at Bazian station.

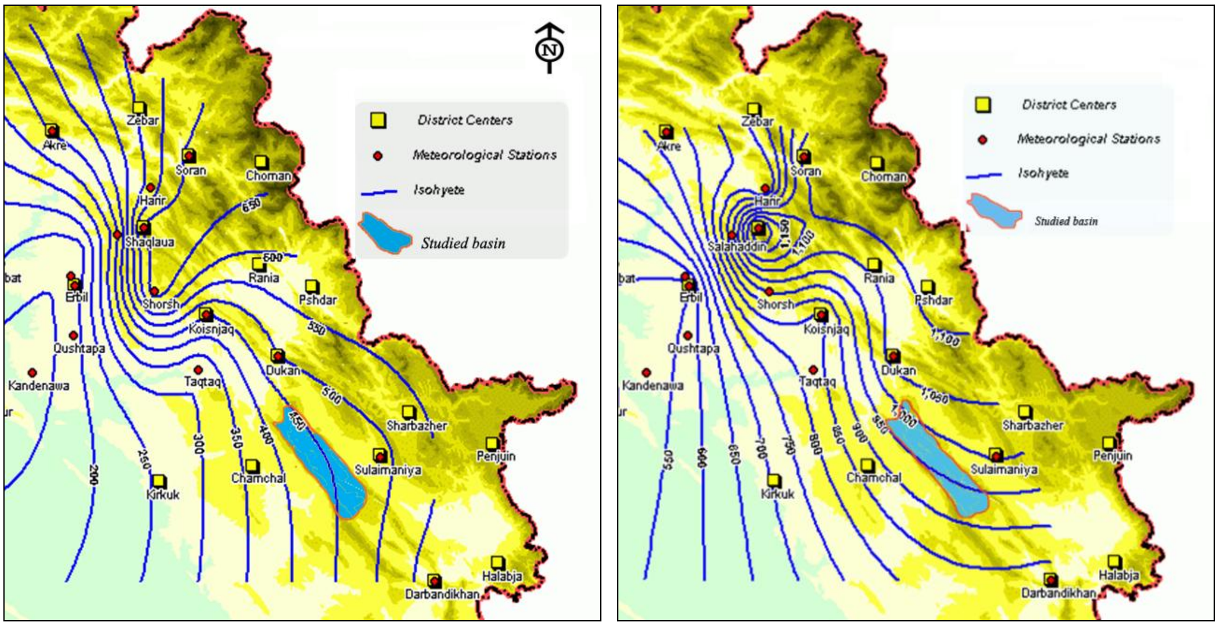

A- Low precipitation rate, 1983 *B- High precipitation rate, 1988*

Fig (3.1) Isohyetal map for the typical year with low and high precipitation rate based on average annual rainfall throughout the period of 1978-1990, modified from (stevanovic et al., 2003)

3.1.1 Rainfall

The annual rainfall in the region is not much less than that in most European countries, but its distribution is different, Stevanovic and Markovic (2003). Absence of precipitation during the summer is the main characteristic of rainfall period in the area.

Rainy season starts on October and ends at the last of May. The topography has a great influence on the rainfall distribution. The amount of precipitation increases from SW to NE direction, reaching the maximum rate towards Iranian border (Fig 3.1). Most of the annual rainfall occurs in the eight months starting from the beginning of the rainy season, while the four remaining months are regularly dry.

Due to the unavailability of gauging and recently operated meteorological stations in the studied area, data from adjacent stations (Sulaimani Station) for the period of 1980-2009 were used in the calculation of hydrological parameters.

In order to give a logical and accurate interpretation of climatic data, a correlation between cumulative average monthly precipitations at Bazian with that of Sulaimani stations for the periods between 2005-2006 and 2009-2010 were used (Fig 3.2). From this figure, excellent correlation coefficient is found between them, and the extrapolated equation was used to calculate the expected monthly rainfall for the catchment basin (Fig 3.3).

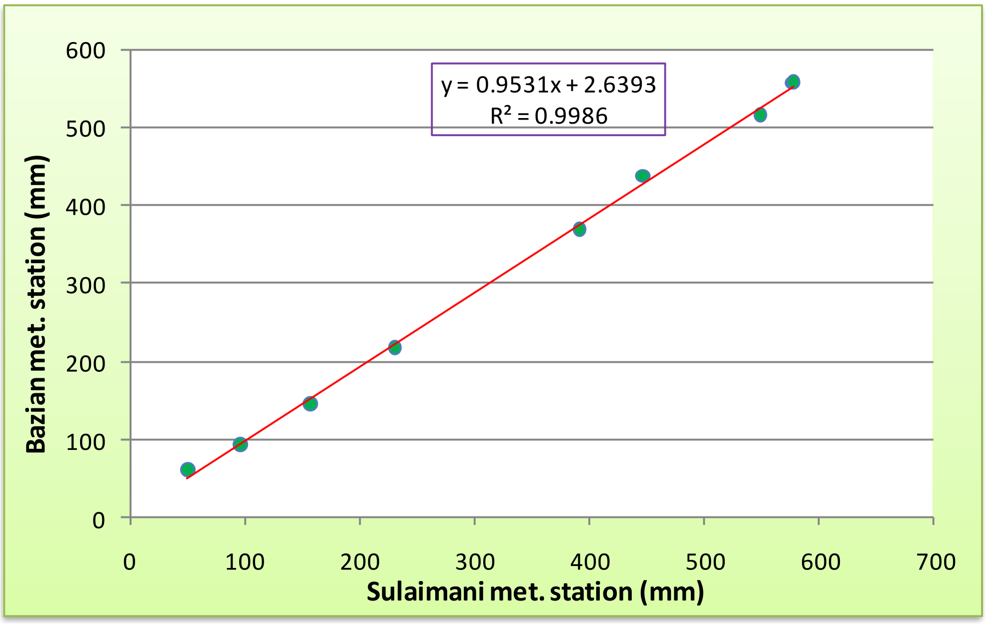

Fig (3.2) Correlation between cumulative average monthly precipitations at Bazian station with that of Sulaimani station for the year 2005-2006 and 2009-2010

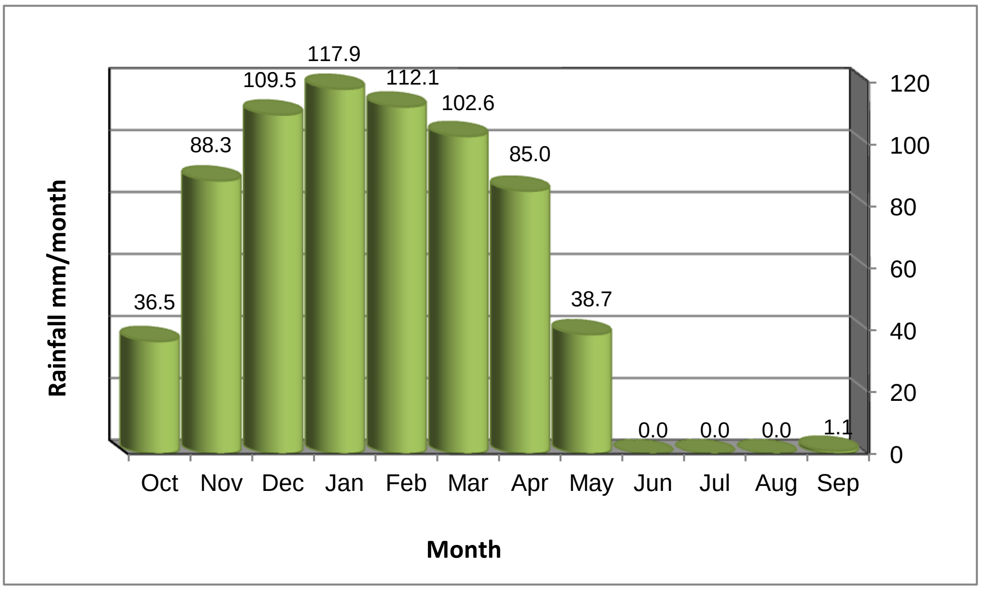

Fig (3.3) Average monthly rainfall for the period (1980-2009) of the study area, after correction based on equation presented in Fig (3.2)

During the last 30 years, the maximum monthly rainfall recorded was 364 mm which was in December-1991, while the minimum rainfall for the same month recorded in 1998 and it was 3.8 mm. However, the maximum average monthly rainfall for the years 1980-2009 for the same month was 112.2 mm. The mean annual rainfall was 710 mm, and more than a half of the recorded annual rainfall was more than the annual average.

A five-year moving average is used to minimize the random variability of the average annual rainfall, and the result is shown in Fig (3.4). As can be depicted from this figure, throughout 30 years of recorded rainfall, the most severe drought started in 1998 and ended in 2001, while another recent drought cycle started in 2006 and lasted 3 years to end in 2009.

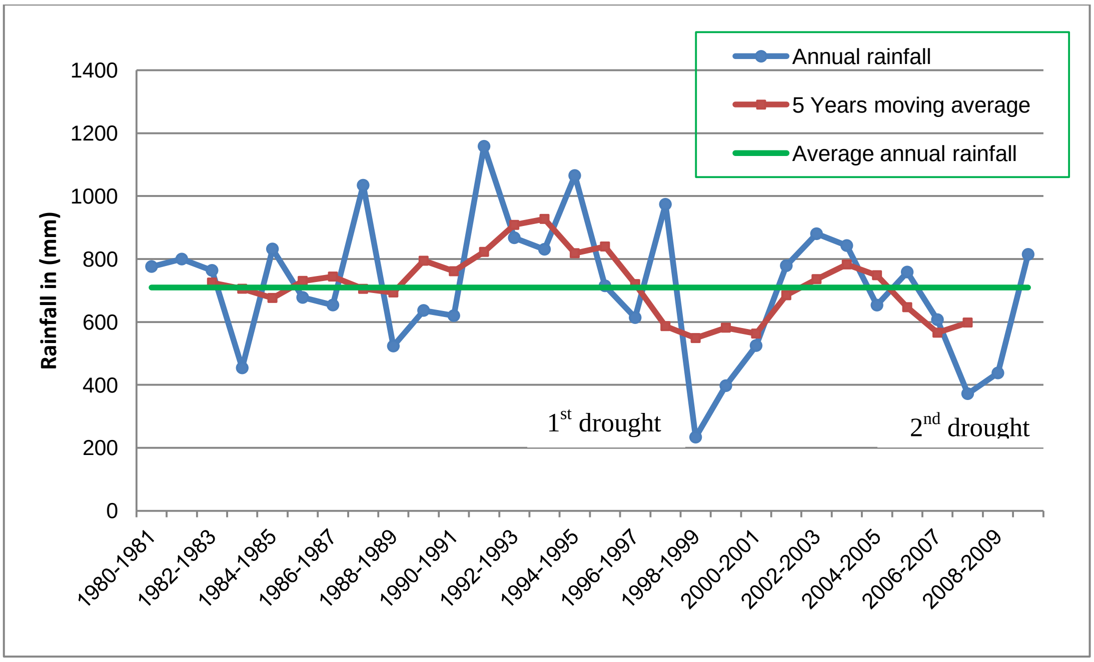

Fig (3.4) Trend of average annual rainfall and 5 years moving average at Sulaimani station for the period of (1980-1981 and 2009-2010)

3.1.2 Temperature

The maximum, minimum and the average mean monthly recorded temperature drgrees for the period (1980-2009) are presented in Fig (3.5).

The maximum mean monthly temperature is 39.3 C^o and 39.1 C^o in July and August respectively, while the minimum is 1.9 C^o recorded in January.

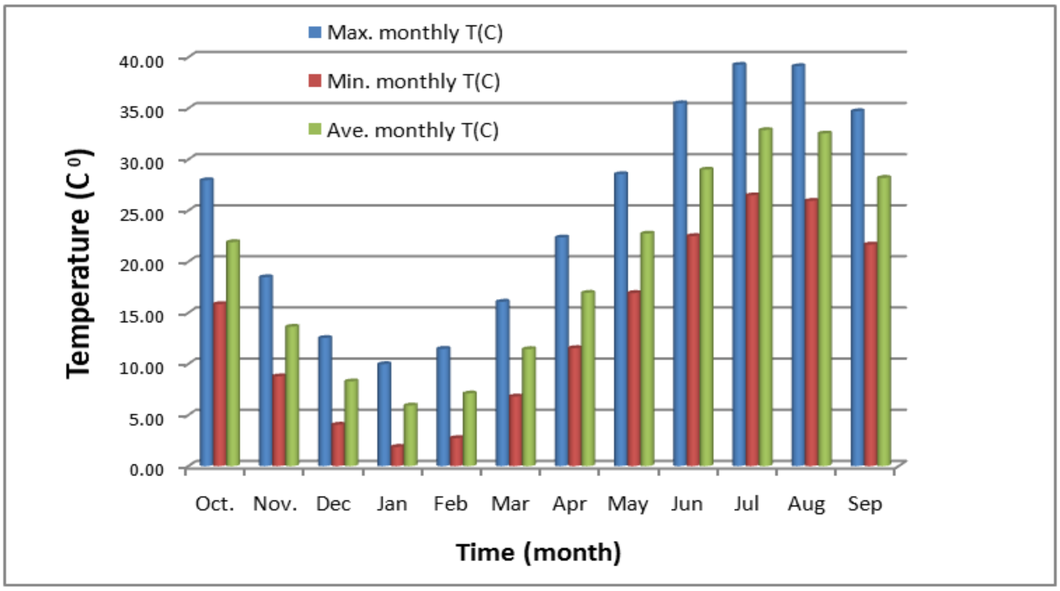

Fig (3.5) Maximum, minimum and average mean monthly temperature for the periods (1980-2009) recorded at Sulaimani meteorological station

A correlation between minimum, maximum and average monthly temperature in (C^0) at Bazian station with that of Sulaimani station for the year 2007-2009 were used, and the average monthly temperature is presented in Fig (3.6). As can be seen, excellent correlation coefficient is found between them, and the extrapolated equation was used in estimating evapotranspiration for the catchment basin.

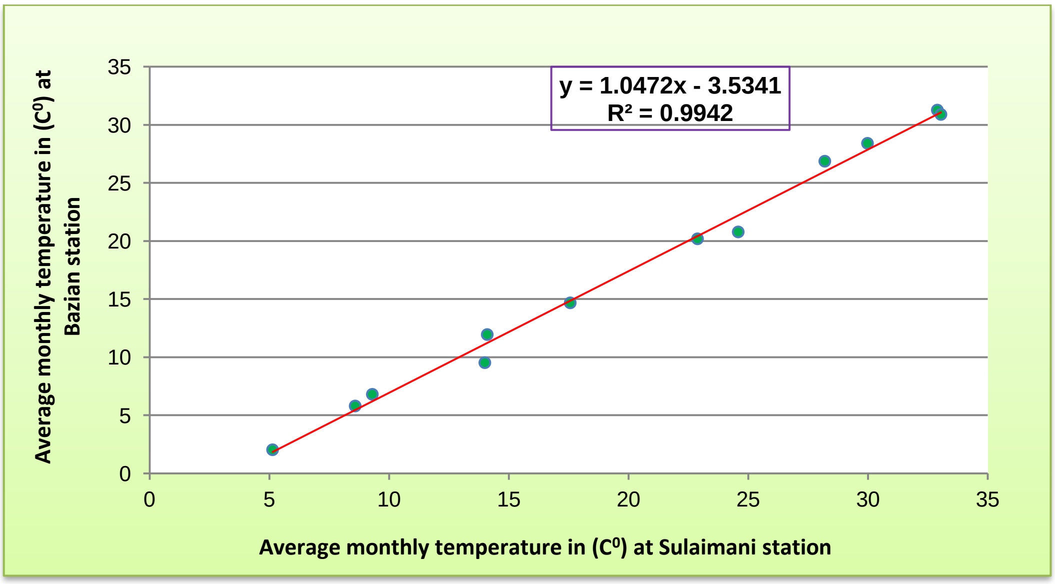

Fig (3.6) Correlation between average monthly temperatures at Bazian station with that of Sulaimani station for the years 2007-2009

3.1.3 Wind Speed

Jabbar (2007) estimated monthly wind directions using the data from Sulaimani meteorological station for the period of (1995 to 2004) to estimate the prevailing wind directions in the studied basin. The result was as follows:

1- Prevailing of southwestern wind direction on May, June, August, September and October, in addition to it's prevailing during April also with 6.2, while the northeastern wind direction prevails during July with 8.3 % of the monthly wind directions.

2- Prevailing of southeastern wind direction on December, January, February and March.

3- The northern and southern wind direction is the less prevailing wind direction (0.9 % and 0.6 %) respectively.

Generally, the minimum mean average wind speed was 1.3 m/sec recorded in December and January, in contrast June and July are the months with the highest average wind speeds (2.3 and 2.35 m/sec) respectively, Fig (3.7).

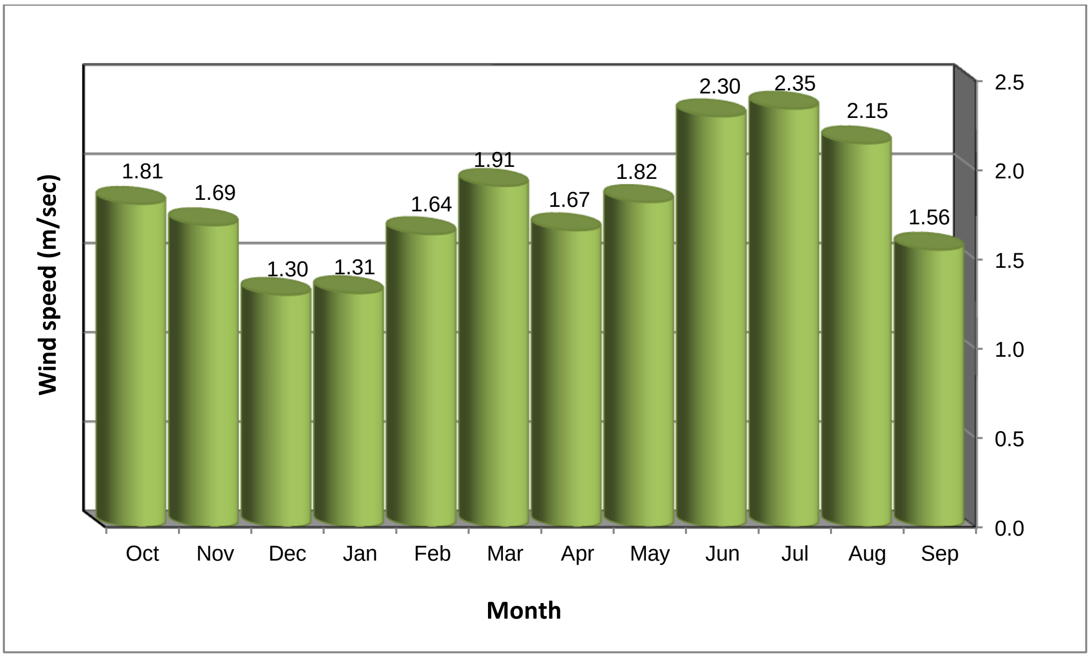

Fig (3.7) Average monthly wind speed in m/sec for the period of (1980-2009) recorded at Sulaimani meteorological station

3.1.4 Sunshine

According to Ali (2007), the maximum sunshine duration occurred in July with an absolute value of 13.2 hr / day in June 2001, and the minimum duration occurred in December with an absolute value of 3.5 hr /day in 2002. The mean maximum monthly sunshine is 11.6 hr/ day in August, while the mean minimum monthly is 4.6 hr / day which were recorded in December.

As can be inferred from Fig (3.8), the maximum average monthly sunshine duration was recorded on June, July and August while the minimum was in winter season especially on December and January.

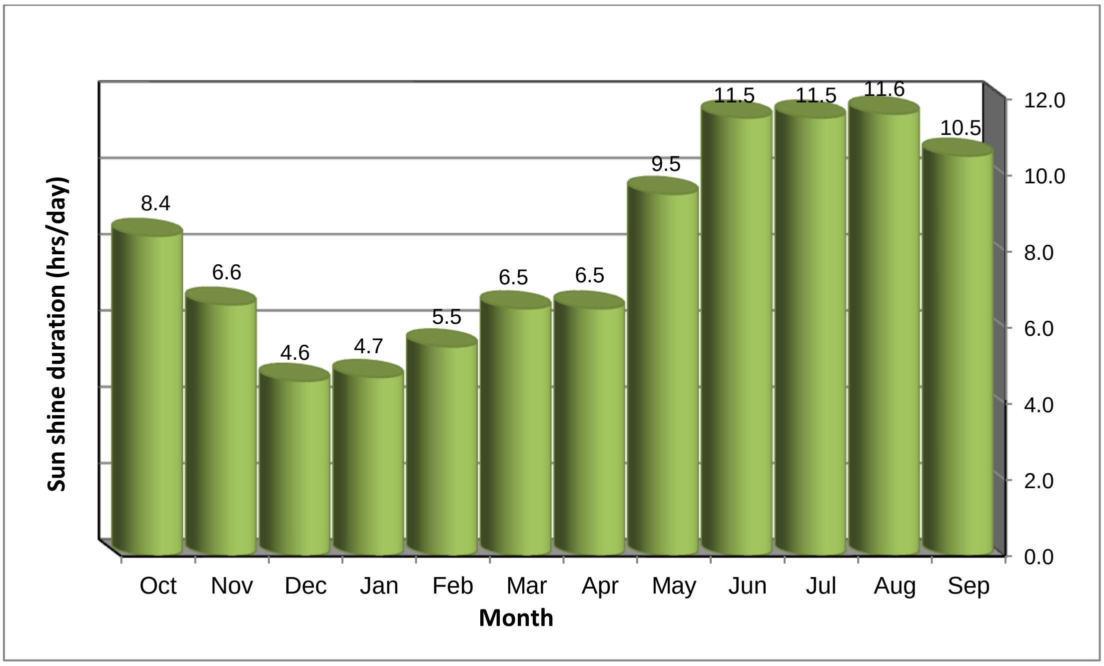

Fig (3.8) Average monthly sunshine duration for the period of (1994-2006) recorded at Sulaimani meteorological station

3.1.5 Relative Humidity

Relative humidity is a measure of the water vapor content of the air at a given temperature; it is related reversely to temperature and evaporation. The average monthly relative humidity varies from 22.33% in July to 70.26% in January as shown in Fig (3.9).

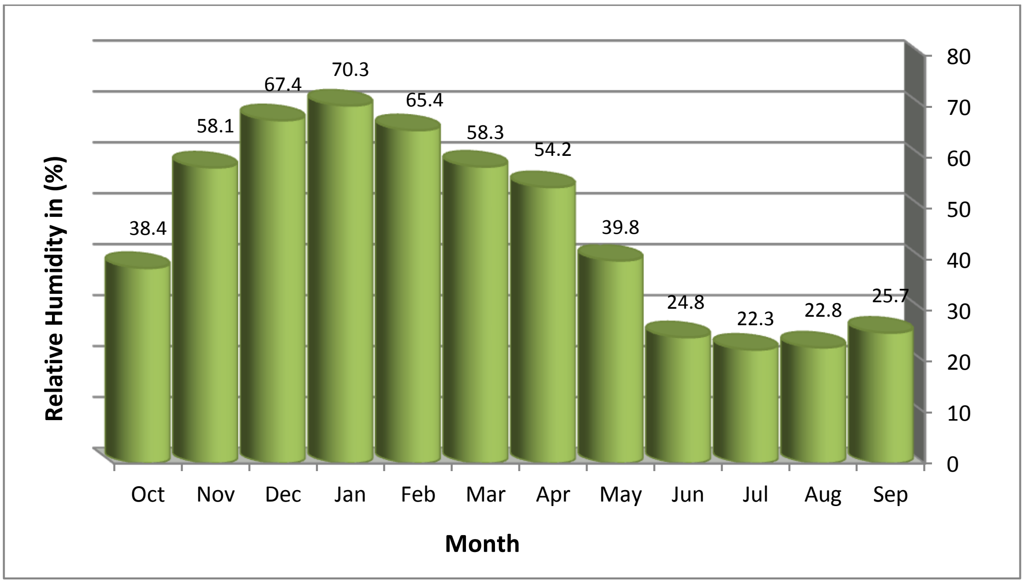

Fig (3.9) Average monthly relative humidity in (%) for the period of (1980-2009) recorded at Sulaimani meteorological station

3.2 Evaporation and evapotranspiration

Shaw (1994) claims that the several phases in the hydrological cycle that of evaporation; is one of the most difficult processes to quantify. The combination of two separate processes, whereby water is lost from the soil surface by evaporation on the one hand, and from the crop by transpiration on the other hand, is referred to as evapotranspiration, (Allen et al, 1998). Thus evaporation and transpiration occur simultaneously and there is no easy way for distinguishing between them. Several attempts were carried out inside and closer to the studied area to estimate evapotranspiration, among them Barzinji (2003), Jabbar (2007), Ali (2007) and Al Manmi (2007), but most of them used the Thornthwait method (1948), except Al Manmi (2007) who used FAO Penman-Monteith. Thornthwait and William (1945) assumed that the amount of water lost through evapotranspiration from a soil surface covered with vegetation is governed by climatic factors, accordingly the potential evapotranspiration for a given month is based on the mean monthly air temperature of that month and on the annual air temperature (Serrano, 1997).

The FAO Penman-Monteith method is considered to be the most convenient method for determining evapotranspiration. It uses more parameters than other methods such as solar radiation, air temperature, air humidity and wind speed data. In order to use this method in the present study, most of the required parameters from Sulaimani meteorological station were used (some data like temperature was corrected according to the fitting equations constructed between Bazian and Sulaimani station), (Fig 3.6).

- **FAO Penman – Monteith**

The FAO Penman-Monteith equation is a close, simple representation of the physical and physiological factors governing the evapotranspiration process, Allen et.al (1998). The equation is expressed as:

$$ET_0 = \frac{0.408\,\Delta\,(R_n - G) + \gamma \frac{900}{T+273} U_2\,(e_s - e_a)}{\Delta + \gamma\,(1 + 0.34\,U_2)} \quad \ldots\ldots\ldots\ldots\ldots\ldots\ldots (1)$$

Where;

ET_o: Reference evapotranspiration [mm day^{-1}]

R_n: Net radiation at the crop surface [MJ m^{-2} day^{-1}]

G: Soil heat flux density [MJ m^{-2} day^{-1}]

T: Mean daily air temperature at 2 m height [C°]

U_2: Wind speed at 2 m height [m s^{-1}]

e_s: Saturation vapor pressure [kPa]

e_a: Actual vapor pressure [kPa]

$e_s - e_a$; Saturation vapor pressure deficit [kPa]

Δ: Slope vapor pressure curve [kPa °C^{-1}]

γ: Psychrometric constant [kPa °C^{-1}]

The required meteorological parameters for estimating reference evapotranspiration (ET_0) were prepared in this study, along with factors to convert common units to the standard unit. Altitude of the Sulaimani station above sea level in (m) and latitude degrees of the location are specified, and then these data were adjusted for the local average value of atmospheric pressure. Preparing each of these parameters was briefly explained below:

1) **Air temperature**

Monthly maximum, minimum and average temperature were prepared by using the relation between Bazian and Sulaimani stations, results of each month were put into the equation.

2) **Air humidity**

Relative humidity record covering (1980-2009) at Sulaimani meteorological station and averaged into monthly time scale was used in the calculation of evaporation and reference crop evapotranspiration of the catchment.

3) **Wind speed:**

The average monthly wind speed in meters per second ($m\ s^{-1}$) once measured at 10 m above the ground level at the Sulaimani station, but it is adjusted to the standard height of 2 m which is required for this method depending on the calculation procedure provided by the FAO, Allen et.al (1998).

4) **Radiation:**

Monthly average net radiation (R_n) computed from the mean monthly measured duration of daily sunshine hours recorded at Sulaimani meteorological station. The mean monthly values of the required parameters for calculating reference evapotranspiration (ET_0) and effective rainfall were measured for the period 1980 - 2009 using CROPWAT ver. 8 software programs. Results are tabulated in Table (3.1) and presented in Fig (3.10).

Table (3.1) Mean monthly values of effective rainfall and reference evapotranspiration in (mm) for the Basara basin

Month	Oct	Nov	Dec	Jan	Feb	Mar	Apr	May	Jun	Jul	Aug	Sep	Total
ET_0 (mm)	114.7	59.4	35	31.9	41.7	75.3	101.1	157.5	209.1	233.7	217.9	153.9	1431.4
Effective rain (mm)	34.4	75.8	90.3	95.7	92.0	85.8	73.4	36.3	0.0	0.0	0.0	1.1	584.8

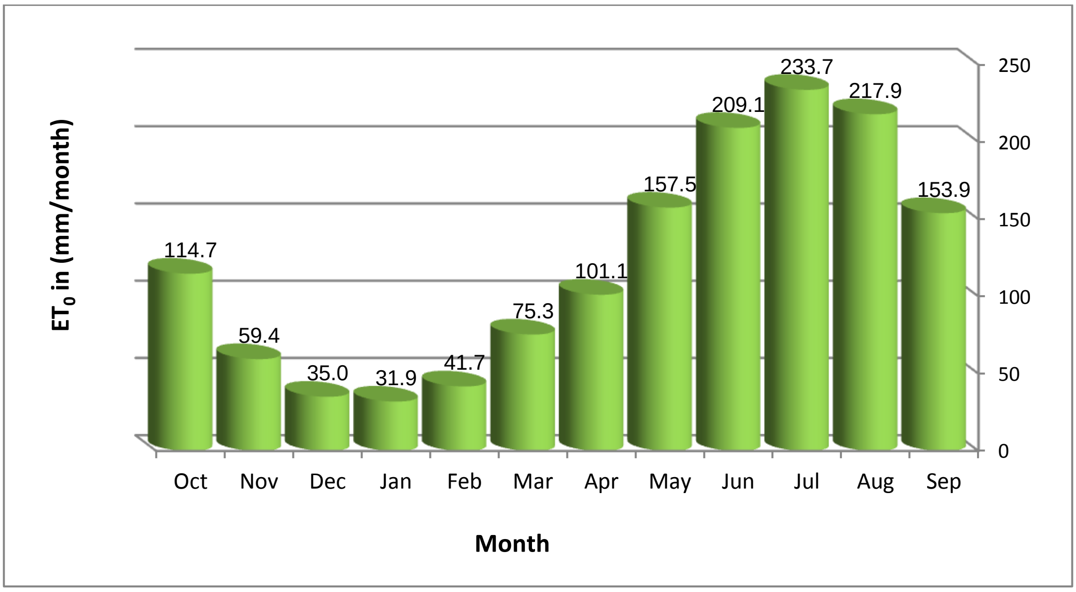

Fig (3.10) Average monthly reference evapotranspiration (ET_0) in (mm/month) for the period of (1980-2009) using FAO Penman-Monteith method

As can be inferred from the results of the FAO Penman-Monteith method, a very high evapotranspiration rate during the summer was confirmed (209.1, 233.7 and 217.9 on June, July and August respectively), while the rates decrease to reach the lowest amount on January (31.9 mm), where the average monthly temperature was around 5 C^0. Thus, with the starting of the dry season from June to the beginning of the wet season (October), the losses by evapotranspiration will be higher than the total amount of precipitation fall into the basin (815 mm is expected to be loss, while the total amount of annual rainfall is around 700 mm). Accordingly, temperature has a great effect on the evaporation rate in the area.

3.3 Soil classification

Generally, the soils of the study area formed from the processes of weathering, erosion and sedimentation during the Quaternary period. According to Berding (2002), plain area and most parts of the depressions are generally permeable and well-to moderately well drains. Soils in mountain regions are variable due to the differences in exposure, rate of runoff, topography and soil depth.

Based on Barzinji (2003), most parts of the area have soils with a brownish to yellow surface layers; this color of soils is due to iron oxides and indicates a somewhat more moist soil climate than do red colors. The soil organic matter of the surface layer ranges between (1.5 - 2.0 %), and the dominant soils of the bottom land and in the plains are Chromoxererts and Calcixerolls, while Xerorthents and Rendolls are dominant on the mountains and hilly area.

In order to assess the soil infiltration capacity of the studied area, 19 sites which underlaying by different geological units and covering most of the area were selected for making infiltration test throughout the basin Fig (3.11). Details about the infiltration test sites and iteration by SPSS program is given in Appendix (3.A & 3.B). Double ring infiltrometer was used. Once an area of about 50 x 50 cm was selected, the debris removed from the top layer, and then the infiltrometer was installed to a depth of 10cm. The accumulated volume of infiltration at each 1.025 liter was recorded using a timer watch. This process is continuous until the infiltration reached a more or less constant value. Finally the SPSS software program is used in analyzing and estimating infiltration capacity rate using Horton's equation (1940), eq. (2)

$\mathcal{F}_{\mathcal{P}} = \mathcal{F}_c + (\mathcal{F}_0 - \mathcal{F}_c)\, e^{-kt} \ldots\ldots\ldots\ldots\ldots\ldots\ldots\ldots\ldots \text{eq.}(2)$ Where;

$\mathcal{F}_{\mathcal{P}}$; is the infiltration capacity, t; is the total duration test time

$\mathcal{F}_c$; *is* the minimum or ultimate infiltration capacity

$\mathcal{F}_0$; is the initial or maximum infiltration rate at the beginning of the test

K; is the rate of decrease in the infiltration capacity

Numerous field experiments have found this relationship to be the most likely to occur where bare soils are exposed to rainfall as happens in arid and semi-arid areas (Ward and Robinson, 2000).

Based on Nikolov (1983) for soil classification, Table (3.2), nine locations of the test sites, showed a moderate infiltration type, most of these sites are located in the Quaternary deposits and partly underlined by Sinjar Formation. Seven locations were slow – moderate type, and mostly underlined by Pilaspi and Kolosh formations. Results of the remaing 3 sites

(sites no. 7, 11 and 13) showed that no or a very slow infiltration occurred because the upper layer was comprised totally of impermeable clayey layers and they underlined by Gercus and Kolosh formations (Table 3.3).

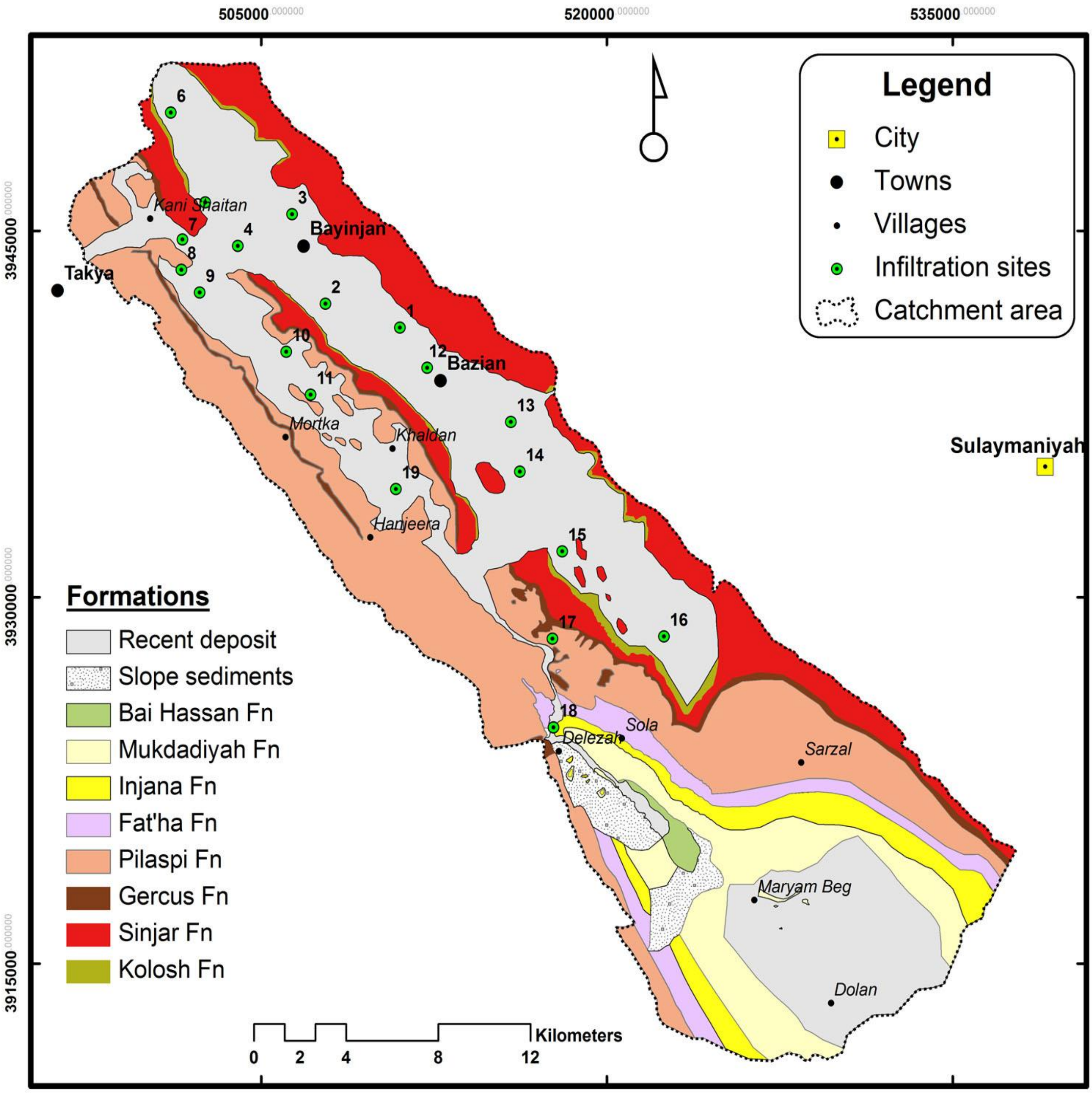

Fig (3.11) Location sites for infiltration test in the Basara basin

Table (3.2) Soil classification according to Nikolov, 1983

Infiltration rate	Type
>160 mm/hour	Rapid
60 - 160 mm/hour	Moderate – Rapid
20 – 60 mm/hour	Moderate
5 -20 mm/hour	Slow - moderate
1.5 - 5 mm/hour	Slow
<1.2 mm/hour	Very slow

Table (3.3) Results of infiltration test by double ring infiltrometer

Location	F_P (mm/hr.)	Type	Underneath geological units
Site_ 1	32.8	Moderate	Sinjar Fn
Site_ 2	36.5	Moderate	Quaternary deposits
Site_ 3	14.7	Slow - moderate	Sinjar Fn
Site_ 4	30.5	Moderate	Quaternary deposits
Site_ 5	18.3	Slow - moderate	Kolosh Fn
Site_ 6	45.1	Moderate	Quaternary deposits
Site_ 7	3.0	Slow	Gercus Fn
Site_ 8	6.7	Slow - moderate	Pilaspi Fn
Site_ 9	55.1	Moderate	Quaternary deposits
Site_ 10	16.55	Slow - moderate	Pilaspi Fn
Site_ 11	3.0	Slow	Gercus Fn
Site_ 12	51.16	Moderate	Quaternary deposits
Site_ 13	3.0	Slow	Kolosh Fn
Site_ 14	19.51	Slow - moderate	Quaternary deposits
Site_ 15	25.68	Moderate	Sinjar Fn
Site_ 16	18.17	Slow - moderate	Kolosh Fn
Site_ 17	43.96	Moderate	Pilaspi Fn
Site_ 18	31.63	Moderate	Fat'ha Fn
Site_ 19	14.50	Slow - moderate	Pilaspi Fn

3.4 Land use and Vegetal cover

The studied catchment is considered as one of the most fertile plains in Kurdistan region with guaranteed annual rainfall for cropping. According to the archives of directorate of statistics in Sulaimaniyah and Barzinji (2003), arable area occupy 97975 donum (about % 42.8 of the whole catchment) in which wheat and barley comprise 45% of the cultivated crops while both chickpea and lentil comprise 25%, the remainder is occupied by summer and winter vegetable in addition to the fallow area. Non arable area occupies 18765 donum, Orchards occupy 3817 donum. Forest area covers 45489 donum, while approximately 56836 donum is covered by natural pasture (Table 3.6).

Based on Barzinji (2003), the basin is located in low and medium oak forest zone. The dominant tree species is *Quercus aegilops*; *Quercus infectoria*, *Pinus halepensis and Cupressus sempervirens.*

Overgrazing becomes especially apparent near villages with an almost complete disappearance of vegetation cover. Grazing of stubbles after harvest is a common practice in the cropland areas (Berding, 2003). The growing period for most crops continues beyond the rainy season and, to a large extent, crops mature on moisture stored in the soil profile. The agricultural potential of the upland of the entire area is limited; reasons may refer to soil depth, slope steepness, and rockiness outcrop, while low lands in the center parts of most of the basin which occupied by alluvial and recent deposits are very important for agriculture.

Results of the previous climatic data and shading the light on both characteristics of soil, land use and vegetal cover simplify evaluating and studying the water surplus and water deficit periods, which in turn indicates and affects the water balance model of the basin.

3.5 Water Balance methods of the catchment area

Constructing a water balance is one of the first task in understanding the water regime of a specific area, (Mehta et al, 2006). Simply, water balance is a budgeting exercise that assesses the proportion of rainfall that becomes runoff, evapotranspiration and groundwater recharge. The water balance model is a necessary concept in water resources management; it can be employed successfully if the meteorological conditions and climatic elements of the basin are known. The first issue in the effort to achieve sustainable water management is to understand the annual water balance in the basin; this means finding out how much water comes into the system and find out where water goes (Fikos et al, 2005).

As explained earlier, the annual evapotranspiration rates are much greater than the mean annual precipitation; therefore the annual could not be used for modeling water balance in such environment, accordingly, the mean monthly calculations is required to construct a water balance model.

There are several methods to calculate such model on the basis of monthly calculation; most of them depend upon the meteorological conditions and climatic elements, as well as details on the land use, vegetal cover, cropping pattern and soil map are necessary for water management and development.

3.5.1 Crop Water Balance method

According to Allen et al. (1998), in arid and semi-arid climatic condition, irrigation is necessary to compensate for the evaporation deficit due to insufficient or erratic precipitation, thus estimating crop water requirement in such environment is of vital importance in assessing water balance method especially where the dry season of the area is regularly dry. Several software programs have been created for running such a kind of model, among them CROPWAT 8.0 which is developed by FAO for planning and management of irrigation is the most widely used nowadays.

CROPWAT 8.0 for Windows is a computer programme for the calculation of crop water requirements and irrigation requirements from existing or new climatic and crop data. According to Swennenhuis (2009), the program allows the development of irrigation schedules for different management conditions and the calculation of scheme water supply for varying crop patterns.

Allen et al (1998), claim that all calculation procedures as used by this program are based on the FAO guidelines as lay down in the publication No. 56 of the Irrigation and Drainage Series of FAO "Crop Evapotranspiration - Guidelines for computing crop water requirements".

In order to estimate the crop water requirement, the following parameters are required:

1) Climate / Reference crop evapotranspiration (ET_0)

The Climate/ET_0 module is primary for data input, requiring basic information on the meteorological station, such as (altitude, latitude and longitude) together with climatic data, that can be input on a monthly, decade or daily basis. Concerning the present study, a monthly basic measurement of ET_0 was used.

2) Rainfall data

Rainfall data is another requires information on the precipitation values on a monthly, decade or daily basis used to calculate the effective rainfall, in this study the monthly measurements was used also.

3) Cropping pattern

The Crop module is an essentially data input, requiring the following compulsory parameters as proposed for running this method: (Planting data, crop coefficient Kc, rooting depth, critical depletion fraction and planted area).

Concerning the first required two parameters, results for both ET_0 and effective rainfall is presented in Table (3.1), while for the last parameter (cropping pattern), essential information was collected and analyzed getting benefited from previous study and archives for the related directorate, some details about this point is presented under the section (Land use and vegetal cover).

In this study, arable area with non-arable, orchard, forest, natural pasture and residential area are considered as the major land covers in terms of the area they cover and their relative importance in estimating of evapotranspiration. Computational convenience land cover types of similar rooting depth and growth stage is combined to one and when there is a considerable difference in rooting depth or if the area covered for a specific type of vegetation is considered to be large disaggregating of land cover type is made. However, variables like crop coefficient and water capacity in the root zone were assigned by an average value weighted by the area covered with particular land use. Additionally, assumptions are introduced where there are no published values for variables of a certain land cover type in a specific environment similar to the study area.

After preparing and entering all the necessary data, the program (CROPWAT 8.0) was designed to run on the monthly basis, and the output for different cultivated crops in the studied area is tabulated and summarized in table (3.4).

Table (3.4) Results of main cultivated crops in the area using CROPWAT 8.0

Crop type	*Barley*	*Wheat*	*Chickpea & lentil*	*Winter Veg.*	*Summer Veg.*	*Fallow*
Total rainfall (mm)	653.7	653.7	226.4	691.7	123.9	338.4
ETc (mm/dec)	386.4	442.1	405.5	1465.1	468.8	282
Effective rainfall (mm/dec)	276.6	332.2	133.1	409.9	83.3	177.8
Total rain loss (mm/dec)	377.1	321.6	93.4	281.9	40.6	160.6
Actual water use by crop in (mm)	384.2	439.9	400.8	1463.9	461.8	278.6
Actual Irrigation required(mm/dec)	114.3	107.7	267.8	1053.7	378.5	100.8
Moist deficit at harvest (mm)	107.5	107.7	32.7	134.7	42.7	100.8
Efficiency rain (%)	42.3	50.8	58.8	59.3	67.2	52.5

- **Errors of the model**

Due to the lack and incomplete details about the previous required data for crop water balance method, it was very hard to make calibration and to assess the validity of the output, because this model is very sensitive to the climatic changes and growth stages of the crop pattern in which for each stage there is different crop coefficient. Despite these, this model is considered to be the best method among other 20 methods used in this field all over the world, (Behmanesh, 2003).

3.5.2 Thornthwaite and Mather (T&M) soil water balance model

Thornthwaite and Mather (T&M) soil water balance procedure which was used in this study is complimented in literatures for its applicability in long term water balance estimation. This type of monthly water balance model is lumped into Combined topography, surface runoff and flow net map that can be used to simulate steady state seasonal (climatic average) or continuous values of watershed or regional water input, snow pack, soil moisture and evapotranspiration, (Dingman 2002).

Long term average monthly precipitation, potential evapotranspiration, soil and vegetation combined characteristics are necessary parameters in estimating the water balance by this model.

By this method, long term average monthly evapotranspiration is estimated by using long-term average monthly air temperature as an index of the available energy for evapotranspiration, by assuming that air temperature is correlated to the integrated effects of net radiation and other effects of evapotranspiration, and the available energy is shared in fixed proportion between heating the atmosphere and evapotranspiration, (Thornthwaite and Mather, 1957). Thus, for areas like the studied basin, where adequate daily meteorological data are insufficient or even unavailable this method of water balance could be applied successfully in terms of monthly average data.

Concerning the average precipitation which is required for this model, corrected average monthly rainfall was used (Fig 3.3). Instead of using the Thornthwaite method to calculate potential evapotranspiration, a more realistic result which takes into account more complete range of meteorological parameters was obtained by applying a reference potential evapotranspiration calculated by FAO Penman - Monteith method.

The broad divisions of soil types into different groups as used in calculation of available water capacity of the root zone and suggested in Thornthwaite and Mather model of soil texture and vegetation combination, fine sand, fine sandy loam, silt loam and clay loam are mentioned. Accordingly, the soil classification given in the previous work carried out by Jabbar (2007) and Stevanovic et al. (2003) was reclassified to this general soil family definition based on the previous study and from soil infiltration test carried out during this work (Fig 3.12). As can be inferred from this map, clay loam covers most central and southern part of the area and comprises about 40% of the total basin, silty loam occupies around 20%, while 25% of the total surface is covered by loam-sandy loam class and the remainder area (15%) is covered with thin or in other cases without soil cover.

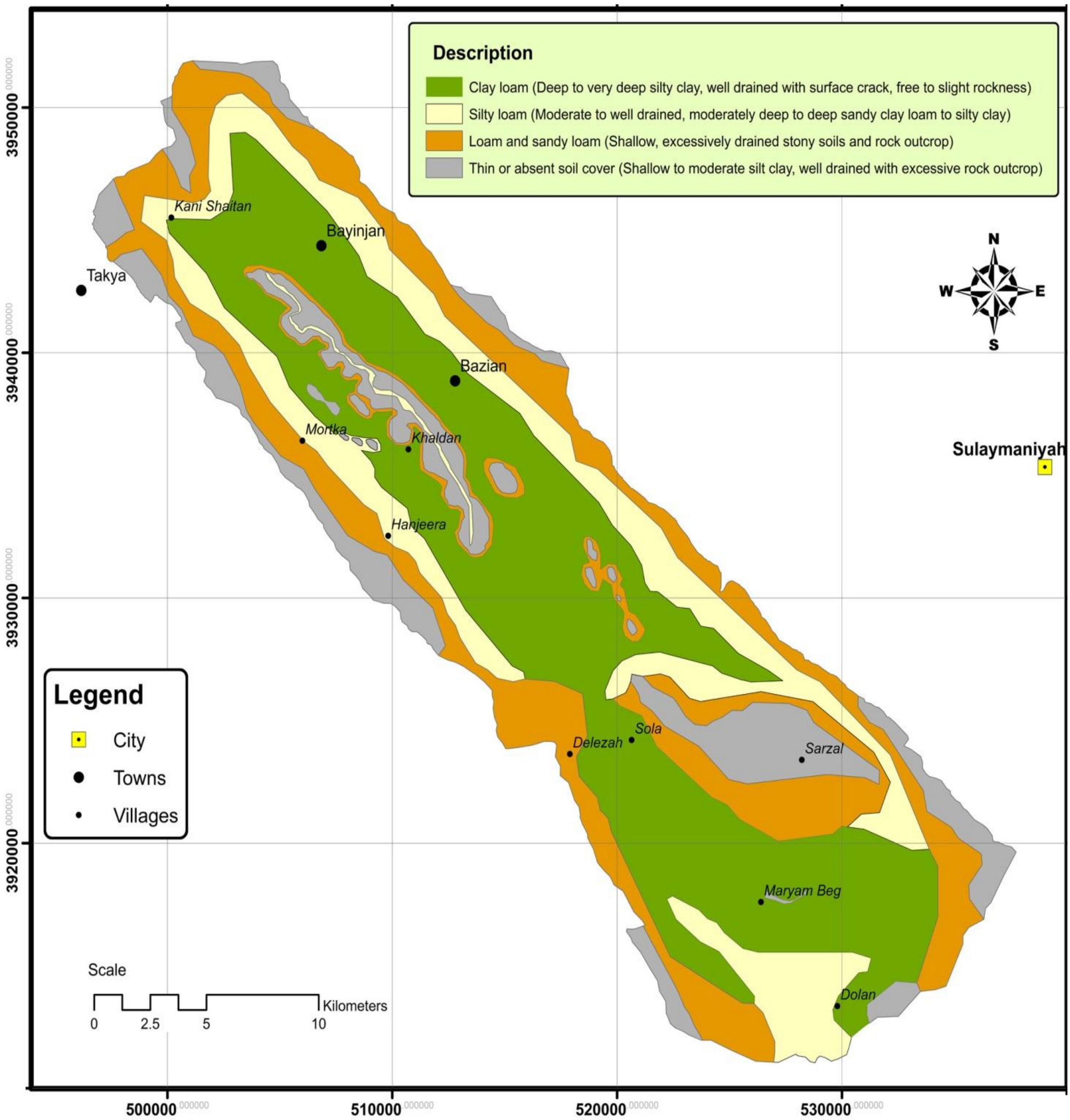

Fig (3.12) General soil map of the Basara basin (modified from Jabbar, 2007 and FAO, 2003)

Based on the table proposed by Thornthwaite and Mather (1957) for calculating Available Water Content (AWC), (Table 3.5) and benefiting from the ratios of each zone of the soil cover calculated from the soil map, the AWC of the studied area was estimated as 115 mm (Table 3.6), taking into account the weight of each zone with the area that each class occupied, then this result was put into the model in calculating soil water content (SW), and later in assessing the water balance method.

Table (3.5) Suggested available water capacity for combinations of soil texture and vegetation (Thornthwaite and Mather, 1957)

Vegetation	*Soil texture*	*AWC (% volume)*	*Rooting depth (m)*	*AWC (mm)*
Shallow rooted crops (spinach, peas, beans beets, carrots, etc)	Fine sand	10	0.5	50
	Fine sandy loam	15	0.5	75
	Silt loam	20	0.62	125
	Clay loam	25	0.4	100
	Clay	30	0.25	75
Moderately deep rooted crops (corn, cereals, cotton, tobacco)	Fine sand	10	0.75	75
	Fine sandy loam	15	1	150
	Silt loam	20	1	200
	Clay loam	25	0.8	200
	Clay	30	0.5	150
Deep rooted crops (alfalfa, pasture, grass, shrubs).	Fine sand	10	1	100
	Fine sandy loam	15	1	150
	Silt loam	20	1.25	250
	Clay loam	25	1	250
	Clay	30	0.67	200
Orchard	Fine sand	10	1.5	150
	Fine sandy loam	15	1.67	250
	Silt loam	20	1.5	300
	Clay loam	25	1	250
	Clay	30	0.67	200
Mature forest	Fine sand	10	2.5	250
	Fine sandy loam	15	2	300
	Silt loam	20	2	400
	Clay loam	25	1.6	400
	Clay	30	1.17	350

Table (3.6) Ratio and exposed area for the land use and vegetal cover zones (benefitting from archives of the directorate of statistics in Sulaimaniyah and Barzinji, (2003)

Arable area	Wheat	Barley	Chickpea	Lentil	Winter veget	Summer veg	Fallow	sum
In (Donum)	29240	14335	22034	1163	680	15944	14579	97975
In (Km^2)	73.10	35.84	55.09	2.91	1.70	39.86	36.45	244.9
% of the Arable area	29.84	14.63	22.49	1.19	0.69	16.27	14.88	100
% of basin	12.77	6.26	9.63	0.51	0.30	6.97	6.37	42.8

	Arable area	Non Arable area	Orchard	Forest	Natural pasture	Residential	sum
Donum	97975	18765	3817	45489	56836	6008	228890
(Km^2)	244.94	46.91	9.54	113.72	142.09	15.02	572
% of the basin	42.8	8.2	1.67	19.87	24.83	2.62	100
AWC	75	50	200	250	100	75	≈115

Accordingly, the average AWC of the whole basin was found to be equal to 115mm taking into consideration the land use cover type and percent weight of each class occupied relative to the whole catchment area.

The general equation for the soil water balance could be simply presented by table (3.7).

Table (3.7) Equations of the soil water balance model (Mehta et al., 2006)

Situation in the watershed	SW	APWL	Excess
Soil is drying $\Delta p < 0$	$=AWC \exp\left(\frac{APWLt}{AWC}\right)$	$= APWL_{t-1} + \Delta p$	$= 0$
Soil is wetting $\Delta p > 0$, but $SW_{t-1} + \Delta p \leq AWC$	$= SW_{t-1} + \Delta p$	$=AWC \ln\left(\frac{SWt}{AWC}\right)$	$= 0$
Soil is wetting above capacity $\Delta p > 0$; but $SW_{t-1} + \Delta p > AWC$	$= AWC$	$= 0$	$= SW_{t-1} + \Delta p - AWC$

When P > PET then AET = PET

When P < PET then AET = dSW + P

Where;

P is precipitation

PET is potential evapotranspiration

AET is actual evapotranspiration

dSW is the change in soil water content.

Calculations to determine both Soil Water Content (SW) and Accumulated Potential Water Loss (APWL) were performed for each month using monthly Precipitation (P) and Potential Evapotranspiration (PET).

After completing all the required data, excel spread sheet which prepared by Mehta et.al (2006) was used to run the model and the results was tabulated in Table (3.8).

The model as indicated in Fig (3.13), the predicted runoff has occurred by the beginning of November and continued until the middle of April, where the rate of both actual and potential evapotranspiration exceeding the amount of precipitation, and this effect continues during the dry season. Accordingly, the total amount of annual water surplus was estimated as 317 mm, which comprises 46% from the annual precipitation fall over the catchment area.

Table (3.8) Long term Basara catchment soil water balance

Months	Oct	Nov	Dec	Jan	Feb	Mar	Apr	May	Jun	Jul	Aug	Sep	Total
P	36.5	88.3	109.5	117.9	112.1	102.6	85.0	38.7	0.0	0.0	0.0	1.1	691.6
ET_0	114.7	59.4	35.0	31.9	41.7	75.3	101.1	157.5	209.1	233.7	217.9	153.9	1431.4
Kc	0.6	0.6	0.6	0.6	0.7	0.7	0.9	0.8	0.7	0.6	0.6	0.6	0.7
PET_{crop}	64.6	37.1	21.7	19.9	27.6	56.1	88.7	128.8	136.2	139.1	121.8	86.7	928.5
P-PET	-28.2	51.1	87.8	97.9	84.5	46.5	-3.7	-90.2	-136.2	-139.1	-121.8	-85.6	
APWL	-604.8	-91.9	0.0	0.0	0.0	0.0	-3.7	-93.9	-230.1	-369.2	-491.0	-576.6	
SW	0.6	51.7	115.0	115.0	115.0	115.0	111.4	50.8	15.6	4.6	1.6	0.8	
dSW	-0.2	51.1	0.0	0.0	0.0	0.0	-3.6	-60.5	-35.3	-10.9	-3.0	-0.8	
AET	36.6	37.1	21.7	19.9	27.6	56.1	88.6	99.2	35.3	10.9	3.0	1.9	438.2
Deficit	28.0	0.0	0.0	0.0	0.0	0.0	0.1	29.6	100.9	128.2	118.8	84.8	490.4
Surplus	0.0	0.0	87.8	97.9	84.5	46.5	0.0	0.0	0.0	0.0	0.0	0.0	***316.8***
Units	All units in mm												

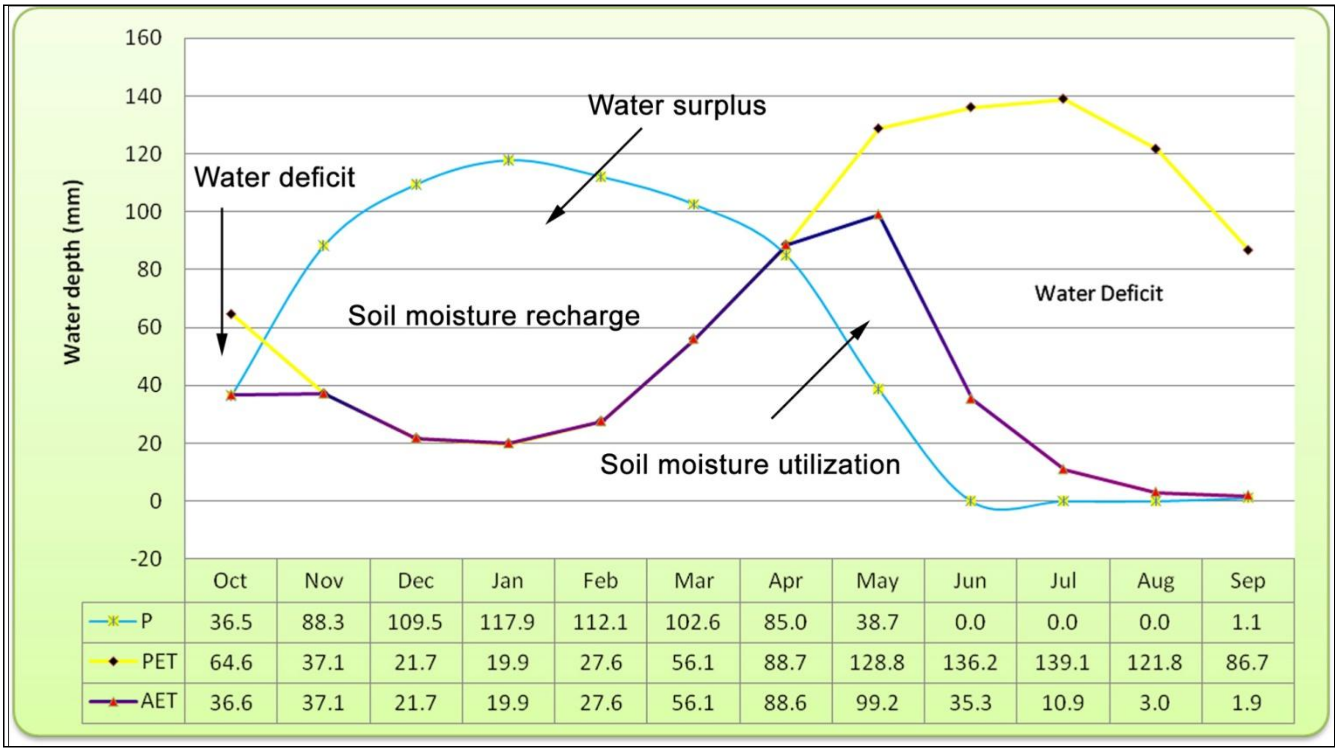

Fig (3.13) Basara catchment long term monthly soil water balance

- **Sensitivity analysis of the model**

Since most of the variables used in this model were derived from large scale map and from literature, therefore the catchment factors and behaviors were simplified as the studied basin that are too large to make a detail survey and studying full characteristics of the land use and soil cover. Thus, errors on assumed rates of each parameters, especially water surplus is expected. In order to make a comparison between the expected amounts of total runoff by this method with other well-known methods carried out in this field, an attempt was made to estimate runoff depth, and then percentage of runoff flowing over the catchment area from precipitation fall on the basin, a monthly average rainfall was correlated with runoff discharge using (SCS) method.

3.6 Soil Conservation Service method (SCS)

The Soil Conservation Service (SCS) Curve Number (CN) estimates precipitation excess as a function of cumulative precipitation, soil cover, land use, and antecedent moisture (USDA, 2004), using the following equation:

$$Q = \frac{(P - 0.2\,S)^2}{(P + 0.8\,S)} \qquad \text{For } P > 0.2S \qquad \text{.................... (eq. 3.1)}$$

$$S = \frac{25400}{CN} - 254 \qquad \text{.................... (eq. 3.2)}$$

Where:

Q = accumulated runoff excess at time t in (mm).

P = accumulated average monthly rainfall depth in (mm).

S = potential maximum retention which is assumed to be 0.2S, it could be estimated from eq. 3.2, and CN is curve number.

The SCS curve number method is a simple, widely-used method for determining the approximate amount of runoff from a rainfall event in a particular area. The CN for a watershed can be estimated as a function of land use, soil type and antecedent watershed moisture using tables published by the United States soil conservation service (USDA, 2004).

In order to construct a runoff percentage map of the studied basin, suitable topographical, geological and soil maps, with the assistance of the infiltration test results, as well as several field trips were achieved for dividing the basin into various zones with different curve numbers.

Regarding the infiltration rate, it can be concluded that the majority of the soils exhibited slow to moderate infiltration rates (Table 3. 3) and they can be placed under poor hydrologic condition. In respect to the soil texture, it varies from clay to silty loam. In contrast, most of the mountain areas exhibit high infiltration rates and soils could be classified under sandy loam, thin or absent soil cover type (Fig 3.12). These soil properties were used to place the soils of each sub-zone in different soil hydrologic groups as described by USAD, 2004.

The most challenging issue in using this method is to find a suitable curve number for areas where covered by limestone (such as Sinjar and Pilaspi formations), such sites are not given in the booklet of SCS of American Soil Service. These terrains represent significant part of the surface areas (about 40 % of the whole basin). With a few exceptions, those terrains put into hydrologic groups of B which has moderately low runoff or when thoroughly wet, while the soils of the most parts of the plain sites are placed under group ***C*** which characterized by high potential to yield runoff. Finally curve numbers for each zone are determined, and the basin is classified into different zones of runoff percentage, i.e. percentage of precipitation that becomes runoff (Fig 3.14).

As can be noted from this figure, the Basara watershed is divided into 8 subzones. The predicted lowest percentage of runoff is with locations dominated by Sinjar Formation (11%) and followed by Pilaspi Formation (14%) because those areas are characterized by joint and fracture networks system which provide excellent paths for percolating the precipitation, in addition to that, the undulated surfaces of the mountains lessen the opportunity for the flooded water flow downward the lower elevated lands before finding its way to the existing discontinuities. While urban areas and most formations that characterized by low infiltration rate (such as Kolosh, Gercus, Injana and Fat'ha formations) have high runoff potentials (44% and 39% respectively). Thus after computing the effect of each hydrologic zone with its own area, the expected monthly amount was calculated over the whole catchment, Table (3.9). Accordingly, the total rate of 149 mm or 21.5% from all fallen rainfalls over the whole catchment is predicted as an average runoff ratio based on the mean average monthly precipitation of the last 30 years ago.

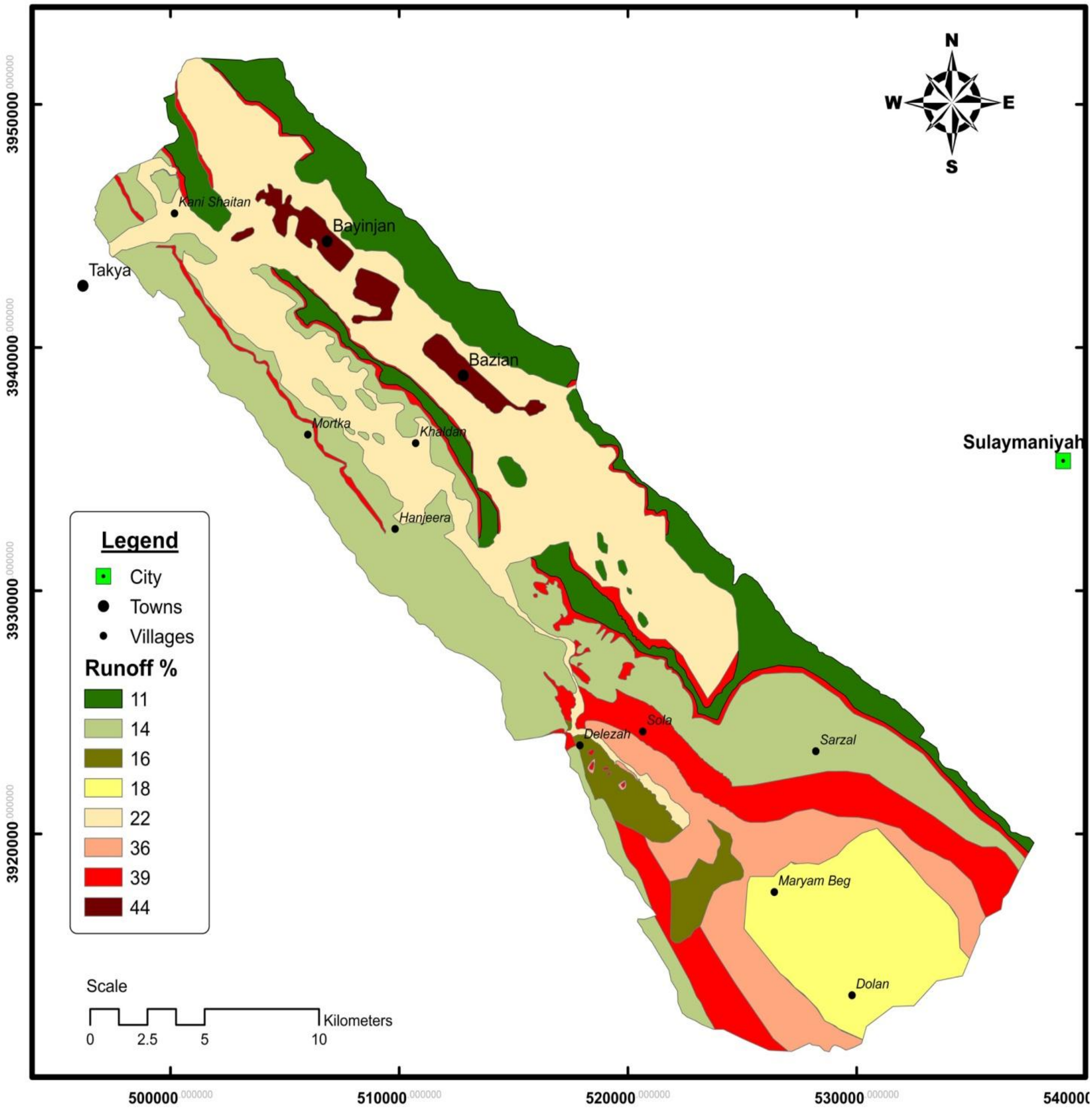

Fig (3.14) Runoff percentage of the Basara basin using SCS and soil water balance methods

Table (3.9) Expected amount of runoff for each month and for each geological formation zone, based on SCS method

Month	***Oct***	***Nov***	***Dec***	***Jan***	***Feb***	***Mar***	***Apr***	***May***	***Jun***		***Total***	
P	36.5	88.3	110	118	112	103	85	38.7	0.0		691.6	
Surplus	0.0	0.0	87.8	97.9	84.5	46.5	0.0	0.0	0.0		**316.8**	
CN	Runoff in (mm)								Enclosed area (km^2)	Volume (x 10^6 m^3)	Runoff in (mm)	Runoff %
90	0	0	81.7	89.7	84.2	46.5	0	0	12.39	3.74	302	**44**
86	0	0	71.9	79.6	74.3	46.5	0	0	64.77	17.6	272.3	**39**
83	0	0	65.0	72.4	67.3	46.5	0	0	45.76	11.5	251.2	**36**
69	0	0	37.4	43.2	39.2	32.8	0	0	156.5	23.9	152.7	**22**
65	0	0	30.9	36.0	32.4	26.7	0	0	50.9	6.42	126	**18**
62	0	0	26.3	31.0	27.7	22.5	0	0	14.33	1.54	107.5	**16**
60	0	0	23.4	27.9	24.7	19.9	0	0	144.6	13.9	95.8	**14**
57	0	0	19.3	23.3	20.5	16.2	0	0	81.97	6.5	79.3	**11**
									571.3	***85.1***		
T. runoff x10^6 m^3	0	0	21.4	24.6	22.4	16.7	0	0				***85.1***
T. runoff in mm	0	0	**37.5**	**43.0**	**39.2**	**29.3**	0	0				***149***

Where;

P; is monthly precipitation

Surplus**;** is calculated by soil water balance method

Runoff for each month and for each geological formations zone is calculated based on the SCS method, (equations 3.1 & 3.2).

CHAPTER FOUR

HYDROGEOLOGY

4.1 Preface

Basara basin is considered to be one of the important basins in Kurdistan from the adequate quantity and quality of groundwater as well as fertility of the land points of view. Groundwater is the major natural resources in the studied basin, and providing about 90% of drinking water supplies for the inhabitant inside the studied area. In most parts of the rural areas which were not served by public water schemes, groundwater is usually the only source of supply and also there are many hundredths of wells and tenth of springs in use.

Development of the Basara basin is attributed to the structural, stratigraphy and geomorphological setting of the area. The forming of numerous large anticlines and synclines with axis mainly oriented NW-SE parallel to the main structural setting with weathering most of the core of anticlines and orientation of drainage patterns to the regional fault system are good examples of Intensive uplifting and folding of geological formations during alpine Orogenic phases. This uplift has influenced the rates of recharge and discharge to and from the basin.

Geomorphologically, the studied basin lies between three major mountain series. The north and north-eastern parts of the catchment is bounded by Tasluja, Daragha, Chaqzih and Baranan mountains series. The southern boundary represented by Jabal Barze Dolan and Smaqa mountains which have lower elevation than northern boundary.

The main mountain series to the west and south-western boundary of the basin are Bazian, Hanjeera, Darbandi-Basara, Sagrma and Qala Mayman mountains. The last series represents a boundary between the low and high folded zones in the area. In addition to the series of Kuwaik and Uloblagh mountains which divided the catchment to the northern and central parts into two hydrologic sub-basins (Fig 2.2).

The above mentioned series of mountains have a large role on the directions of flow within the basin and in raising the groundwater level in the plain and recharging the aquifers annually through sets of fractured and joints within limestone beds of Eocene Karstic Fissure Aquifer "EKFA" and Miocene

Complex Aquifer "MCA". It is to be noted that these terms are used by Ali (2007).

Stratigraphically, the occurrence of relatively impermeable rocks represented by Kolosh, Gercus, Fat'ha and Injana formations and in some cases fine alluvium sediments which cover the central and southern parts of the basin have a great impact to impede percolating of the infiltration of rainfall and any other forms of surface runoff to the groundwater within the basin. Many springs such as "Kani Shaitan, Allaquli, Barika, Dargazen, Hayasee, Bibijak, Gomatagach, Mahmudia, Khewata, etc", emerge from the contact of these formations with karstic and fissured aquifers. These springs have the average rate of discharge in range of few liters to tenth of liters which are flowing even in low flow periods (Fig 4.1). Names, average discharge and other general information on each spring are presented in Appendix (4.A).

Structurally, as mentioned in chapter two, section (2.2), the majority of the joints within the studied area could be classified as the transversal joint sets, because most of the lineaments are perpendicular to the strike of the folds, in addition to that some sets of longitudinal joints are expected due to the presence of two main lineaments which are oriented NW-SE parallel to the main fold entire the area. Accordingly, some of the most important springs are flowing out, such as Warmziar and Kopala springs which characterized by high rate of discharge (more than 100 l/sec) as maximum flow period in May, in addition to other springs that issuing from groundwater but with low rate of discharge (2-5 l/sec) in low flow periods, such as Lazian, Zeyaka, Cholmak, Qushqaya etc. which are most probably flowing under the effect of the longitudinal fault sets. In contrast the transversal fault system may lead other springs to drain groundwater with relatively high amount of water (100 l/sec) in maximum flow period, such as in Hanjeera and Khaldan springs.

4.2 Classification of the hydrogeological units

As can be depicted from the geological map of the area (Fig 2.3), different lithostratigraphical units from various ages are cropping out. Based on the classification of Stevanovic & Iurkiewicz (2004), and depending on the hydrogeological properties, the water bearing layers in the studied area are rearranged and categorized into several subdivisions on the basis of hydrogeological and stratigraphical characteristics. The hydrogeological map is constructed and presented in Fig (4.1), and the classification of the main hydrogeological units is simply explained and presented in Table (4.1).

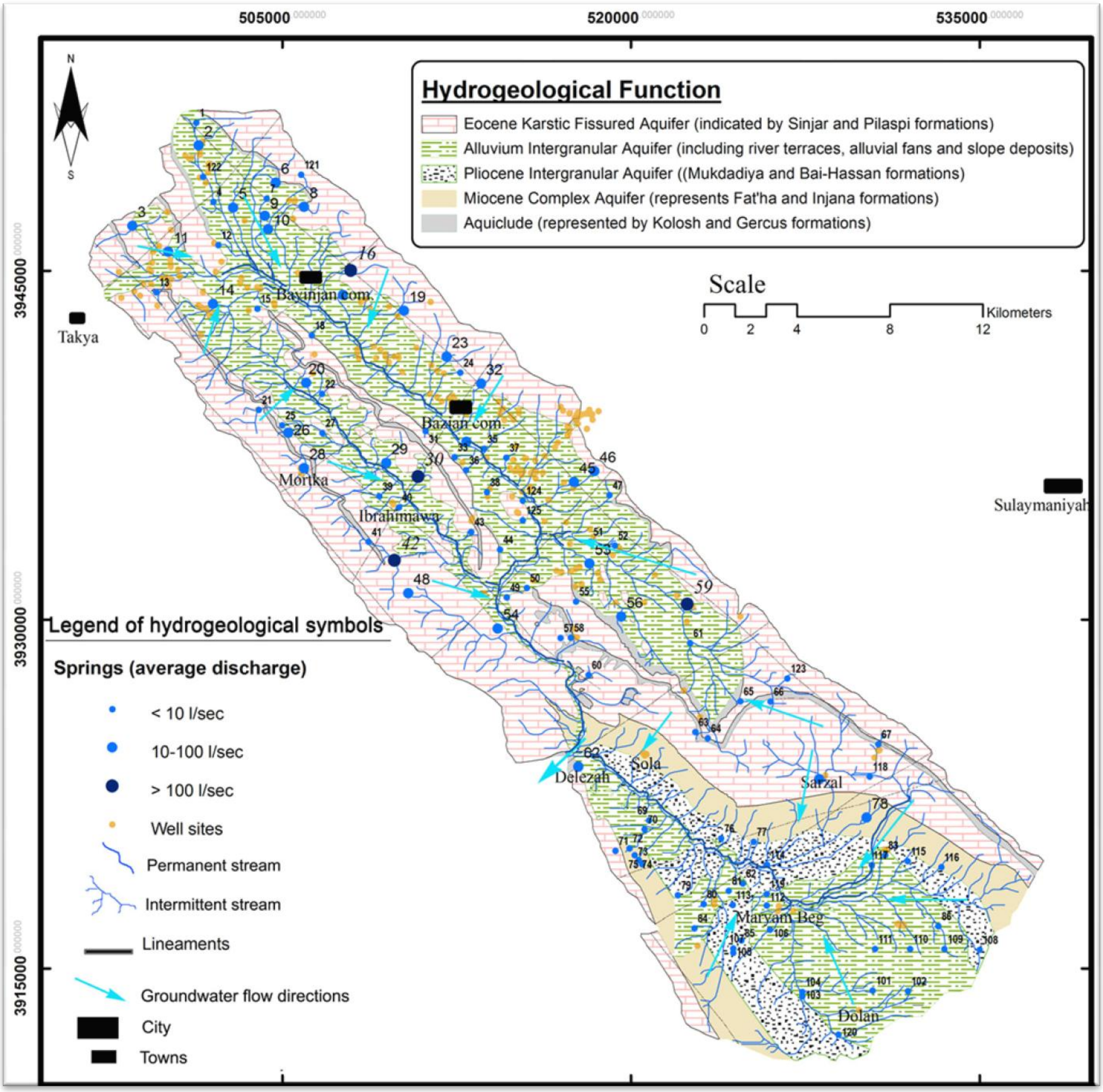

Fig (4.1) Hydrogeological map of the Basara basin

Table 4.1 Grouping of the formations and sediments according to some hydrologeologic and stratigraphic properties

Aquifer type	Geological Fn	Lithology	Porosity	Hydrogeological name	Abbreviation (as per Ali, 2007)
Karstic Fissured	Eocene Formations (Sinjar, Pilaspi)	Limestone, and Dolomitic chalky limestone	Fractures, joints and caverns	Eocene Karstic-Fissured Aquifer	EKFA
Intergranular	Recent deposits, including river terraces, flood plains, alluvial fans slope deposits, polysengenetic valley fillings	Gravel, Sand, Silt and Clay	Intergranular	Alluvium Intergranular Aquifer	AIA
	Pliocene Formations (Mukdadiya and Bai-Hassan)	Sandstones, Conglomerate, and Siltstones	Intergranular	Pliocene Intergranular Aquifer	PIA
Complex (CIFM)	Miocene Fat'ha and Injana Formations	Siltstone, Marl Sandstone, Lst Claystone and Gypsum	Intergranular _ fissured multi-layer	Miocene Complex Aquifer	MCA
Aquiclude	Kolosh and Gercus Formations	Shale, Marl, Mudstone, Siltstone and Conglomerate	No effective porosity	Aquiclude. Som time Gercus behave as aquitard where layers of conglomerate exist	-

4.2.1 Karstic Fissured Aquifers

The aquifers of this type consist of chemically deposited rocks from marine origin (algal reef and lagoon environments) and the outcrop of this aquifer occupying an area of 226 Km^2 or nearly 40% of the total area (Table 2.1). The chemical rocks include limestone, dolomitic limestone and chalky limestone. Most of the week zones (fractures, joints, and bedding planes) were enlarged by the dissolving effects of groundwater, forming canals and cavities in the massive limestone, and dolomitic limestone. Hydrogeologically, this type of water bearing beds is represented by the Eocene Sinjar and Pilaspi formations.

These formations act as a very good aquifer. This fact has been confirmed by drilling of two deep monitoring wells for pumping tests, the first one drilled in a plain area close to Kani Shaitan to the southeast and for a depth of 113m (named as piezometer well No.3), which penetrates Sinjar Formation, while the other one was drilled inside the Ala Cola company for a depth of 104m (named as piezometer well No. 2) and penetrating the Pilaspi Formation (Fig 4.2). It was observed that, these wells yield more than 7 l/s of water with relatively small drawdown (less than 1m), (Fig 4. 8 and 4.9).

It is worth mentioning that during the drilling of these monitoring wells, collapsing of the carbonate rocks in different levels of depth which may be attributed to relatively large cavities were struck in these aquifers as a result, the continuous drilling process for a deeper depth was prevented which may show more or less karstic aquifer characteristics.

In general, the porosities of these formations (Pilaspi and Sinjar formations) consist of cavities, solution channels and fractures. Large, small faults and sets of joints are frequent in all outcrops within these formations, in which good porosities and pathways for groundwater storing and percolation are created.

During preparation of this thesis, some new wells were drilled for governmental projects inside the area of the study; one was drilled in Tainal town for water supply for the inhabitant there. According to the previous electrical survey carrid out by Aziz (2005) and profiles of drilling wells around this area, it was believed that this place is totally composed of alluvial fan and weathered products of the surrounding formations, but after studying the lithology and fossils of samples, sliding blocks of Sinjar Formation with 15m thickness was observed (Fig 4.3). The depth of the formation ranged from few meters to around 40m within the Hanjeera sub basin (Fig 2.8), but the depth increases more to attain maximum depth of 200m towards southern studied catchment, inside the Tile sub basin (Fig 2.6).

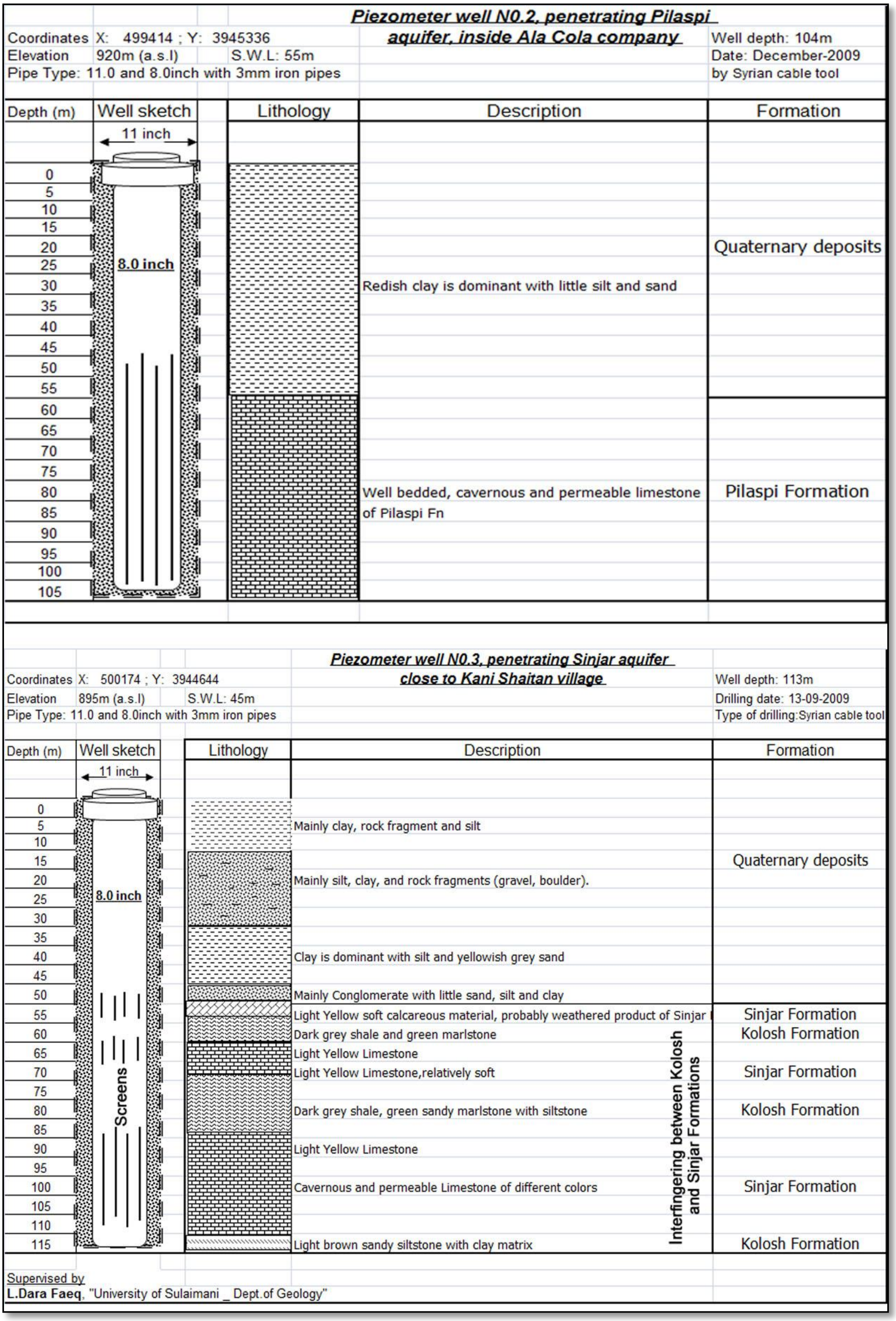

Fig (4.2) ***Hydrostratigraphic column of the two piezometer wells drilled in the Basara basin in 2009***

Fig (4.3) Drilling deep wells in (EKFA) in Tainal town (Bazian SB), photo was taken on February, 2009

Sinjar Formation is completely surrounded the Bazian sub basin, as well as the eastern part of the Tile sub basin. It forms a significant part of the recharging areas and aquifer of the large numbers of springs

Among 111 springs which is assigned in the hydrogeological map in Fig (4.1), a total number of 48 springs located within the Bazian sub basin and most probably fed by EKFA. Most of these springs could be classified as contact springs, because impervious layers of Kolosh, Gercus formations and recent deposits act as barriers or natural obstacles to the accumulation of groundwater and the predisposed position of the springs at the contact of the aquifers with impermeable rocks.

The joints and fractures in many cases transformed to fissures and caverns in the deeper part, especially within the Sinjar Formation. This is evident in the drilling of several deep wells (more than100m) through the western part of this formation, close to Kani Shaitan area. The porosity of Pilaspi Formation consists of fractures, fissures and joints like the Sinjar Formation. This unit occupies alone more than 25% of the total area and bounded the Hanjeera sub basin from all directions, as well as it bounded the eastern and western parts of the Tile sub basin.

Pilaspi Formation is somewhat similar to Sinjar Formation which regularly underlains by the impermeable layers of Gercus Formation, that acts as an aquiclude. This type of occurrence provides many villages by water, such as Sarzal, Mortka and Ibrahimawa etc.

4.2.2 Intergranular Aquifers

As can be noted from Table (4.1), this aquifer is formed within pores and spaces between grains and particles of various sizes (from boulders to silt). The hydraulic properties vary from place to place due to the vertical and lateral variation in lithology. Accordingly, the coarser deposits have higher values of transimissivity and the wells drilled through them have higher values of specific capacity. The intergranular aquifer can be classified into two major types:

4.2.2.1 AIA (Alluvial Intergranular Aquifer)

The most important accumulations of alluvial deposits are located in Bazian sub-basin which occupying a surface area of 133km^2 with variable thickness in range of few meters to more than 100m (as explained and shown in cross sections and geological map in chapter two). However, the geolectrical survey performed by Aziz (2005) near Baynjan town found the thickness of this layer to be 150m, while in Hanjeera and Tile sub basins, there is sporadic distribution and variable thickness.

Based on the archives of the Directorate of the Groundwater of Sulaimani (DGWS), more than 500 wells were drilled inside the studied area within the last few decades; approximately 80% of these wells were drilled inside this alluvium aquifer which taking water mainly from this aquifer, and partially from sliding blocks of Sinjar aquifer (Fig 4.1). It is mainly recharged by rainfall and sinking streams, that descend from the surrounding drainage patterns and from issuing of spring flows.

The relatively high production of wells within this aquifer is believed to be the result of the two main reasons:

- ***First / Nature of the underneath formation***

When the sediments of the fans, slope deposits and other forms of recent deposits cover the Kolosh Formation, it can store water in great quantities enough for exploitation by drilling wells. This is because of the underlying Kolosh Formation act as a barrier boundary for the percolating infiltrated water from the alluvial sediments, while the fine clastic acts as a lateral boundary, eventually provides a good medium for storing and moving groundwater. However, it is worthy to mention that this phenomena varies from one location to another, because these sediments formed multi-layer set in which the changes in depth and facies changes are abundant; this clearly confirmed by the geo-electrical survey which carried out in the area by Aziz (2005) (Fig 6.5).

- ***Second* / *Lithology***

The coarse sediments of the alluvial fans share a role in generating unconfined aquifer. These fans can be seen clearly on the Bazian plain as overlapped mixed fans (Fig 2.10). Although, these fans are recently developed by stream dissection and continual cultivation, their sediment can be easily identified. They consist of coarse fragments of poorly sorted and sub-angular flat clasts of limestone, derived from surrounding mountains.

In comparison, the grain size of this aquifer in Tile sub basin is characterized by finer clasticts (mostly silts and clays). This fact can be realized from the distribution of the drainage pattern in which the distribution of the stream pattern is more and denser as compared to the northern sub basins (Bazian and Hanjeera), this may attributed to the nature of the clastics, where the riverbed sediments has better sorting and roundness than those of the Bazian sub basin.

The main streams that cross the Tile sub basin are the Tile, Hurgena, Zayir, and Dolan streams. They are braided streams which have coarse sediments of gravels and little boulders. The continuous shifting of the route of these streams is very obvious from Fig (1.2). The existence of riverbed sediments several tenth of meters thick with an overlay of several meters thick of flood plain clay and mud is evidence of such shifts (Fig 2.6)

Aziz (2005) has classified the alluvial deposits aquifers in the Bazian and Hanjeera sub basins into two different horizons, named as shallow and deep aquifers:

(a) The shallow horizon (or aquifer as he named) within the Bazian sub basin is formed mainly of clay and gravel, in addition to rock fragments of Sinjar Formation in some limited locations. It is buried below a depth of (2-15 m) and has a thickness ranges between (4-35 m).

(b) The deeper horizon or deep aquifer is composed of gravel with clay, while in some locations the main constituent changes to Sinjar rocks.

This deep aquifer is mainly confined separated from the unconfined one by 10-40m of clay and underlained by impermeable layers of Kolosh Formation, it has a thickness ranges between (29-108 m), especially within the Bazian sub basin.

These sediments within the Hanjeera (or as he named as Pilaspi sub basin) are somewhat differ, they are characterized by more homogeneous and relatively thin recent sediments (10-30 m) and this was confirmed by constructing isopach map from electrical tomography survey.

The researcher believes that, in most cases these two aquifers alternate and forming one general multi intergranular aquifer with thickness of around 150 meters and at least in the area close to Gopala and Tainal towns. This fact was clearly seen from geoelectrical sections carried out by Aziz (2005) and from the chemical analysis of groundwater types taking from several drilling wells inside the area, (details about groundwater types and interpretation of samples will come in the next chapter). Accordingly, from the hydrogeological points of view, there is only one aquifer type represented by AIA, and there is hardly to separate it into shallow and deep aquifers as classified earlier.

4.2.2.2 PIA (Pliocene Intergranular Aquifer)

Pliocene intergranular aquifer represented by Mukdadiya and Bai-Hassan formations, is composed of sandstones, conglomerate, and siltstones. This aquifer type extends 46 km^2 in the southern part of the area, within the Tile sub basin.

The thickness varies from few meters in the foot hill zones of the mountain and reaches more than 100m in the depression area in the trough axis of the main syncline within the Tile sub basin (Fig 2.6). The main characteristics of this aquifer are the repetition of different grain sizes and variation in hydraulic conductivity from one place to another within the same aquifer horizon in addition to erosion and facial processes which alternate in the depositional environment that limit the extension of some lithological units. A good example was given in profile of Bai-Hassan Formation in Fig (2.7).

This aquifer has been tapped by many wells ranging in depth from (20-150 m), most of them provide local water supply for irrigation and in other cases for domestic uses, but the quantity is not sufficient due to the high degree of compactness of these layers and facies changes as mentioned earlier.

Most of the springs within this aquifer are issued potable water with limited rate of discharge (0.01-5 L/s in average) for villagers entire the sub basin (Fig 4.1).

4.2.3 CIFMA (Complex Intergranular-Fissured Multi-layered Aquifer)

This aquifer is represented by Fat'ha and Injana formations, it is characterized by low production, because it composed of very heterogeneous lithology (sandstone, siltstone, conglomerate, marl, gypsum, and clay) which contain insignificant amount of stored water, which is not sufficient for supplying water for big projects. Several tenths of wells (mostly hand dug and shallow wells) were drilled to meet household and irrigated demands for Homar aman, Qazanqaya and the surrounded villagers.

Among 50 wells which are recorded inside this sub basin, more than 60% of them are penetrating this aquifer type. Most of the drilled wells which were drilled in and around Solai Darband village are characterized by high salinity (1555 µs/cm), and this groundwater quality doesn't meet the standard even for irrigation purposes, thus people in this village brought water outside the area from other deep well (around 230m deep) which located north of the village penetrating Pilaspi Formation, but due to the high elevation, the static water level was more than 100m.

Generally, most of the stored water in this aquifer is believed to be within the siltstone and sandstone horizons, but they are mainly disconnected by clay horizon (Fig 2.6).

Many springs are draining water with various amounts ranging from (0.01-5 L/s), some of them are permanently issuing groundwater such as

Gurbaz and Mewli springs, while others are considered as intermittent springs.

4.2.4 Aquicludes

In the study area, aquicludes represented by Kolosh and Gercus formations. Since a relatively large thickness of Kolosh Formation (around 600m), as well as (about 80m) of the Gercus Formation would tend to impede flow downward, it might seem more appropriate to classify these formations as an aquiclude. However the upper part of the Gercus Formation is composed mainly of conglomerate, in some cases it may act as an aquitard.

Ali (2007) classified the conglomerate within the Gercus Formation as an Eocene Intergranular aquifer; he mentioned that due to the high degree of compactness of these layers, joints and fractures represent the other aspect of its effective porosity. When the layers start to become more saturated with water, the intergranular pores will be triggered, while the fractures work as an additional effective transmission zone for groundwater movement, accordingly he claims that, the term intergranular is preferable to fissured for this aquifer because it is more similar to conglomerate lithology.

As a whole, Gercus Formation separates the Sinjar from the overlying Pilaspi aquifers. These aquiclude beds vary considerably in their thickness and compaction due to the degree of subsidence and effects of weathering.

It is worth mentioning that in some locations (mainly in the Bazian sub basin), the slide blocks of Sinjar Formation remained coherent and unbroken but with secondary porosities, resulting from the joints and fractures which have finally been modified to karstic channel. Profiles of the drilling wells within this sub basin showed that these blocks are underlain by Kolosh aquiclude, may be surrounded totally by this formation in some cases, as a result of the presence of perched aquifer that may occur.

4.3 Flow net

Groundwater levels with reference to mean sea level (reduced level) have been used to prepare a static water level map with contour interval of 50m (Fig 4.4). This map is based on the collected data of water table in 270 wells, the water level updated during February to September (2009) by a team of the directorate of groundwater-Sulaimani, in addition to tenth of wells which were carried out by the researchers in 2009 and 2010.

It is clear from the flow net map that most of the mountain series which surround the basin are characterized by high equipotential lines; the higher values attain around 1050 m (a.s.l) in the eastern parts of the area. The central parts have lower static water level (around 700 m).

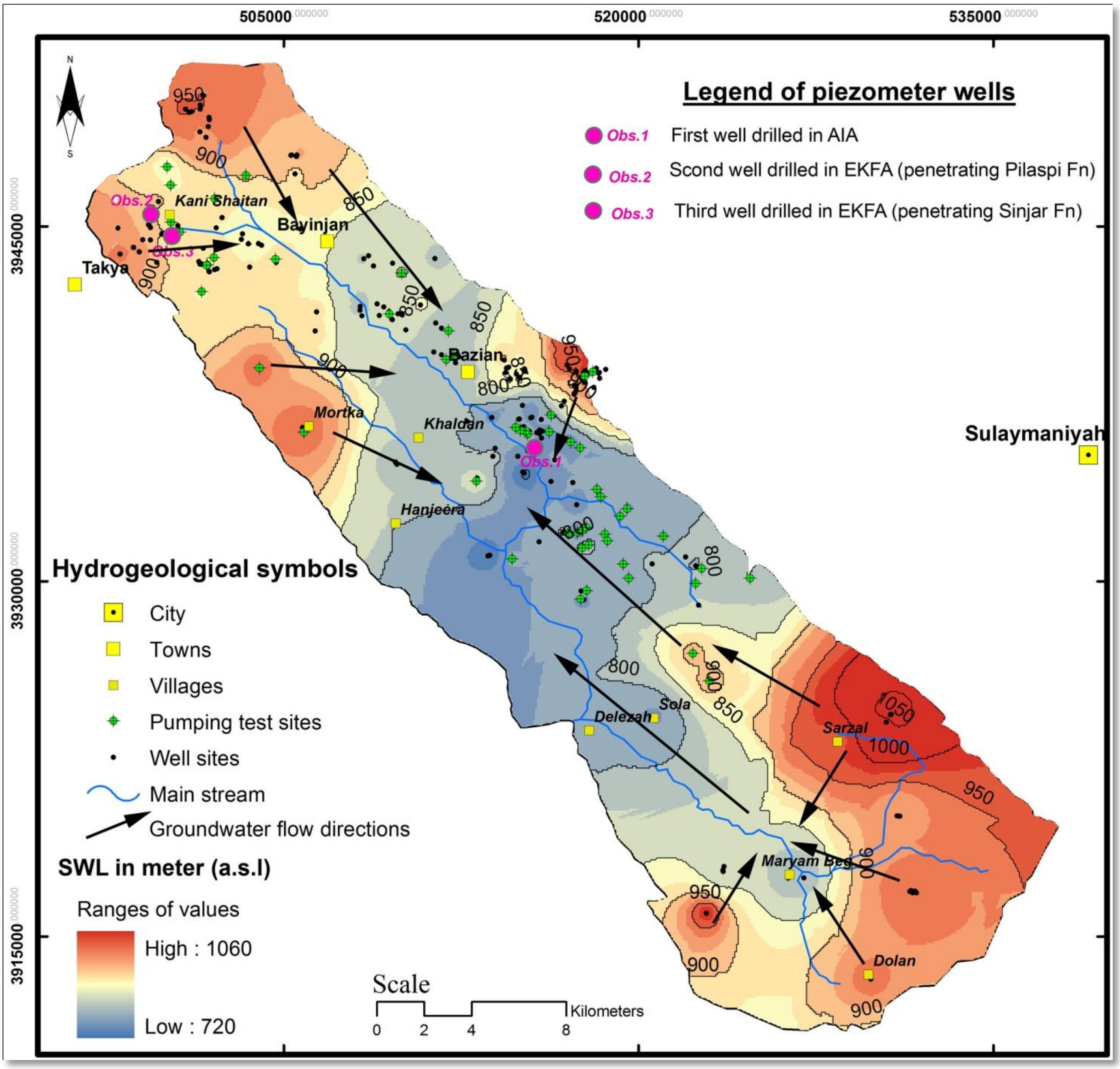

Fig (4.4) Flow net map of the Basara basin

The average hydraulic gradient within the Tile sub basin is around 0.03, this estimation is based on the calculation in three directions; the first is from the Qalasura village (2.5 km to the east of the Sarzal village) to the Maryam Beg village, the distance between these two sites is 8 km, while the differnce in equipotential line is 220m, thus the hydraulic gradient will be 0.0275. The second place is from Khawe village to Maryam beg too, the hydraulic gradient is 0.04, and the last calculated is 0.024, thus it can be concluded that the general hydraulic gradient within the Tile sub basin is around **0.03**. The same procedure was applied to other two sub basins by selecting several directions for estimating the hydraulic gradient within each sub basin, the result was as follows; **0.017** for Bazian sub basin and **0.027** for Hanjeera sub basin, thus it is clear that the hydraulic gradient for Tile and Hanjeera sub basins is more than the Bazian sub basin, and this may be attributed to the low transmissivity in addition to the less steepness of the water bearing beds within the Bazian sub basin.

4.4 Combined topography, surface runoff and flow net in the basin

The data for creating the model is based on topography map represented by digital elevation model (DEM), drilling wells (both deep and shallow), static water level (a.s.l) and springs. To determine the groundwater flow and confirm the absence of leakage to the other basins, the regional geology of the surrounding area is considered and combined maps also have been created (Fig 4.5 & 4.6). The delineation of the groundwater boundary is based mainly on the drainage pattern of the area, and this was prepared based on the DEM map using GIS tool, however, some places especially the northern part of the area was complicated to give a certain boundary because it has been deformed highly. In both combined maps, it can be noted that the mountainous area comprises the recharge area and almost all the groundwater flow is more or less resemble the direction of the drainage pattern towards the main stream which is finally oriented towards the Basara gorge. It can be also concluded that most of the streams inside the area can be classified as the effluent stream, since the elevation of the streams levels is less than the minimum equipotential lines of the groundwater flow.

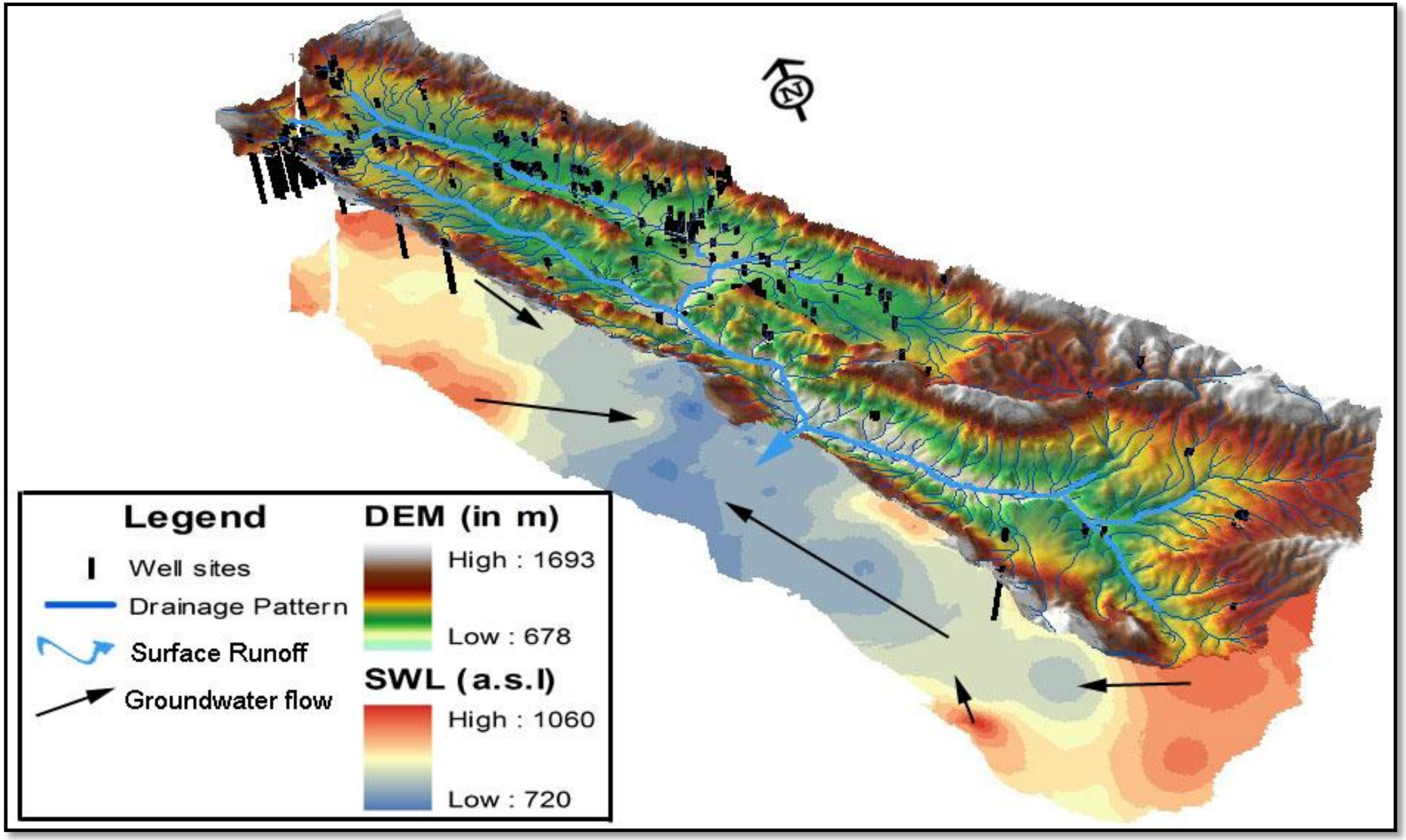

Fig (4.5) Combined topography, surface runoff and flow net directions of the Basara basin with changing view toward the North-West

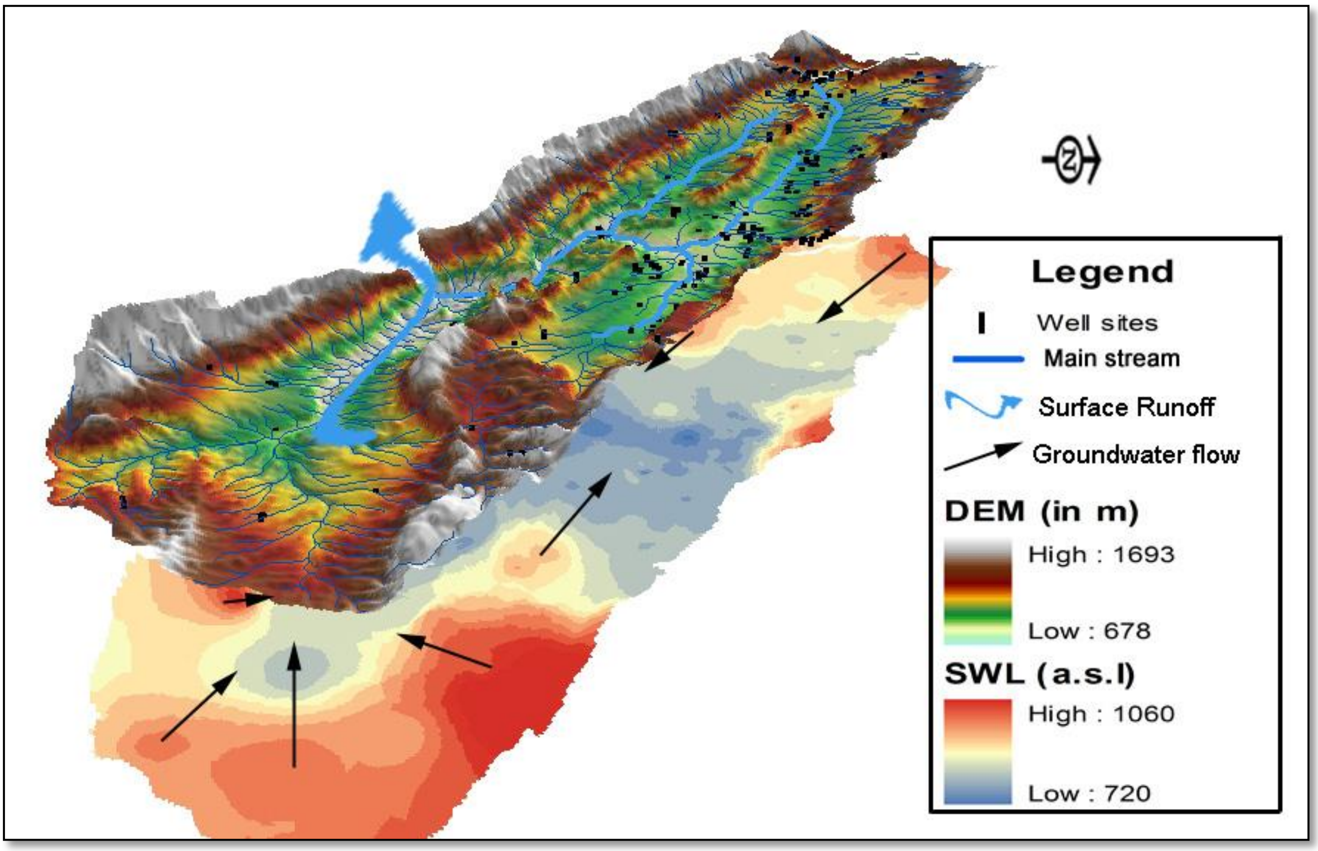

Fig (4.6) Combined topography, surface runoff and flow net directions of the Basara basin with changing view toward the East

4.5 Aquifer Characteristics

The hydraulic parameters of water bearing beds were obtained by pumping test, with assistance of drilling well profiles and electrical tomography sections, carried out in the area for estimating saturated thickness for the aquifers, within the selected sites. Those parameters comprise the Transmissivity (T) and storage coefficient (S) using the computer software programs namely AQTESOLVE version 4.02 which applied on the tested wells, it is capable of computing these parameters even for the single well and partially penetrating cases.

For the current study, well tests carried out on 58 wells which penetrating different aquifers. However, pumping data for more than 80 wells were collected, but due to the lack and doubtful record, only these numbers was applied. The pumping test methods are "Theis, Cooper - Jacob, Hantush-Jacob, Walton and Neuman methods". Each method is applicable under certain hydrogeological conditions. Among this number of pumping tests, 55 wells were single well test, and results of such tests may not give the real interpretation of aquifer characteristics, accordingly three locations were selected for performing pumping tests by using the principal of observation well.

The first selected site is located in a farming area, in which two previously drilling wells were penetrating the same aquifer (AIA) and they have depth of around 80m and the distance of 4.8m. One of the wells was used as a monitoring well and from the other well the process of pumping was started, both constant and recovery test were applied (Fig 4.7) and the results are tabulated in Appendix (4.B).

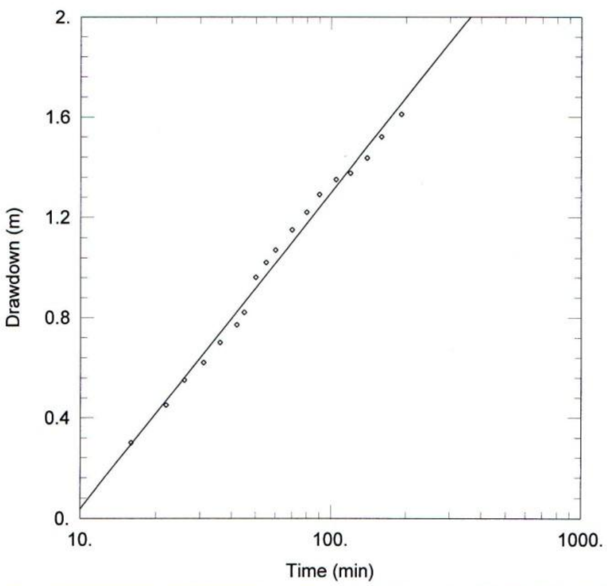

WELL TEST ANALYSIS

Data Set: D:\Others\Thesies\Excel data\Lithology\Bazian observation 1_136.aqt
Date: 09/22/10 Time: 23:39:34

PROJECT INFORMATION

Company: DOGW
Test Location: Bazian
Test Well: Bazian-Bahroz
Test Date: 9-8-2009

AQUIFER DATA

Saturated Thickness: 60. m Anisotropy Ratio (Kz/Kr): 1.

WELL DATA

Pumping Wells			Observation Wells		
Well Name	X (m)	Y (m)	Well Name	X (m)	Y (m)
1 Pizometer	0	0	◦ First Observ	4.8	0

SOLUTION

Aquifer Model: Confined Solution Method: Cooper-Jacob

T = 0.03763 m^2/min S = 0.03431

Fig (4.7) Pumping test analysis for the first observation well – AIA in Bazian subbsain

The latter two sites are selected for drilling two monitoring wells, for the purpose of evaluating EKFA and to estimate the hydrogeologic parameters for both Sinjar and Pilaspi formations. The first drilling piezometer well was in a plain area located close to Kani Shaitan, this place was selected because it was close to one of the deep and a highly productive governmental project well which supply water for Takya town. The distance between them is 58m, and both are penetrating Sinjar Formation. Duration of the pumping test lasted 420 minutes, the recorded drawdown was 0.05m with pumping discharge of 6.8 L/s (Fig 4.8).

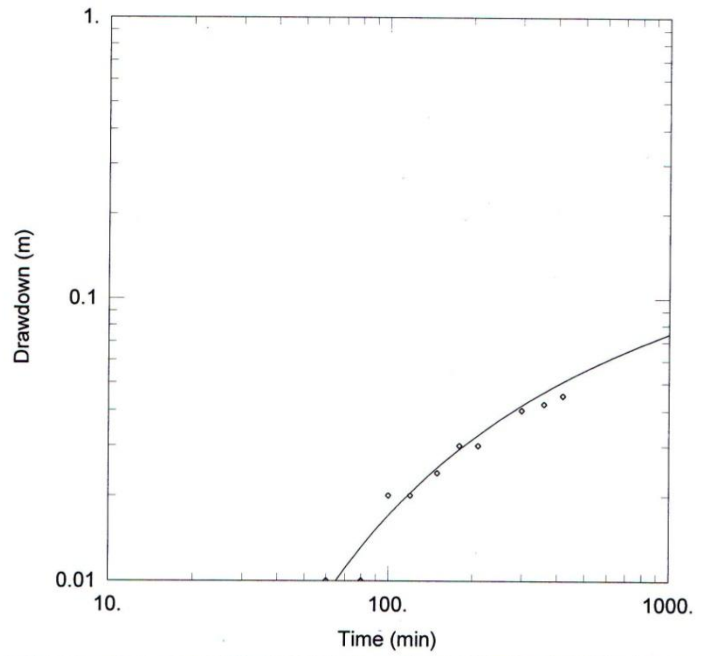

WELL TEST ANALYSIS

Data Set: D:\Others\Thesies\Excel data\Lithology\Bazian observation 3_144.aqt
Date: 09/22/10 Time: 23:41:39

PROJECT INFORMATION

Company: DOGW

WELL DATA

Pumping Wells

Well Name	X (m)	Y (m)
Bazian obs_3	0	0

Observation Wells

Well Name	X (m)	Y (m)
◦ Third Observ	58	0

SOLUTION

Aquifer Model: Confined Solution Method: Theis

T = 1.078 m^2/min S = 0.06384
Kz/Kr = 1. b = 36. m

Fig (4.8) Pumping test analysis for the third observation well – EKFA (Penetrating Sinjar aquifer) in the Bazian subbsain, (using Aqtesolve 4. 02)

The other piezometer was drilled inside Ala Cola water bottling factory for a depth of 104m similar to the productive wells that is used for water bottling by the company. After completion of the drilling process, screen pipes were inserted in permeable units to receive water from all horizons during the pumping test, in order to simulate a real case similar to the productive well. The distance between both wells is 34m, and pumping test continued 280 minutes. The recorded drawdown was 0.35m with pumping discharge of 12 l/s (Fig 4.9).

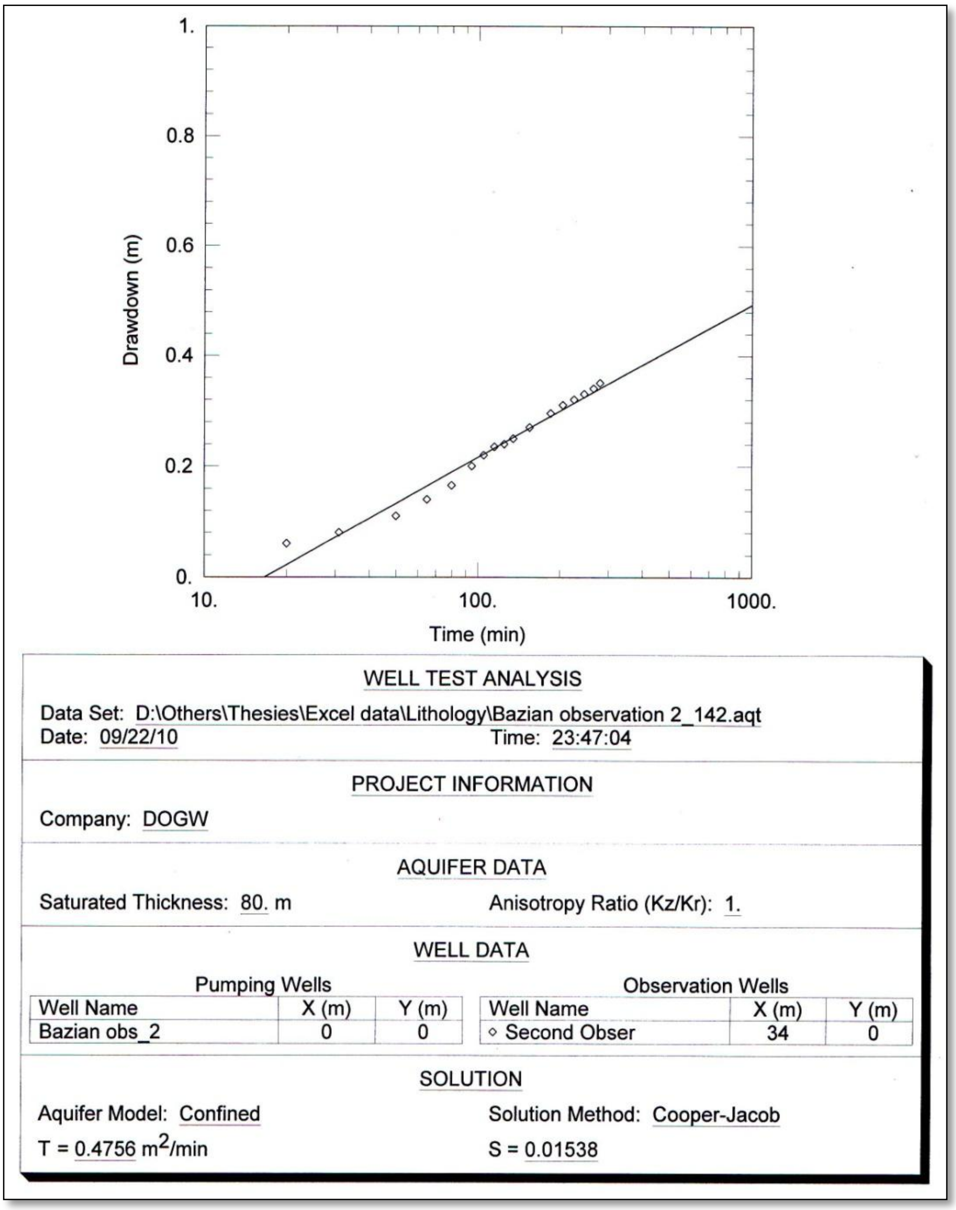

Fig (4.9) Pumping test analysis for the second observation well – EKFA (Penetrating Pilaspi aquifer) in Ala Cola company within the Bazian subbsain

A number of constraints are restricted to the comprehensive and detailed pumping test for the previously drilled wells, such as the duration of the pumping period in which the deficiency of electricity is one of these problems, and most of the Johnson's screen may not be at their appropriate locations and capacities. The duration of the tested wells ranges from (70 – 600 minutes), the wells were let to be recoverd after switching off the pump and recovery measurements were immediately done. All methods were applied, the steady and un-steady states flow condition for both constant and recovery tests analysis.

The computation of transmissivity from the resultant curve was carried out only in the initial drawdown measurements when the unsteady state conditions were prevailing, therefore T values obtained by the methods applying drawdown test measurements are lower when compared to those applying recovery test measurements especially for the EKFA, while the computation of transmissivity for the intergranular and complex aquifers, both by drawdown and recovery tests were close. In general, the transmissivity values obtained by the recovery test are of high accuracy as compared to these obtained by the constant pumping tests because in recovery test, water returns naturally to the well without the intervention of pumping.

Generally, results of the pumping tests for the wells penetrating inter-granular aquifers (AIA), and even the observation well test which was applied during this study have showed the transmissivity to be in a range between (4 x 10^{-6} to 2 x 10^{-3} m^2/sec), while the storage coefficient was 0.05 to 0.006. The specific capacity is at the range of 0.02 to 6.7 L/s/m (Appendix 4.B).

The results of nearly 45 single well tests which carried out mostly in Sinjar and partly in Pilaspi (EKFA), showed values of transmissivity between (2 x10^{-5} to 2 x10^{-2} m^2/sec), but when the observation well tests applied, the results of both Sinjar and Pilaspi were (1.8 x 10^{-2} and 7.9 x 10^{-3} m^2 /sec) respectively.

The storage coefficient was calculated to be in the range of (0.007 - 0.088), and the specific capacity is in the range of 0.1 to 13 L/s/m.

As a whole, the variation in aquifer parameters especially for the intergranular aquifers may refer to one or more of the following factors:

a) Lateral and vertical variation in the lithology of the water bearing beds.

b) Variation of the physical characteristics of the hydro-stratigraphic beds, such as grain size, compaction and cement material.

c) Unsuccessful well design which causes hydraulic loss and resistance for screen zones, particularly for the drilled old wells.

A well discharge is another factor affecting aquifer parameters. For the EKFA, the well yielding vary considerably from 0.6 L/s in W.110 to 19 L/s in W.54 in Bazian sub basin, while for AIA aquifer, it ranges between 0.5 L/s in W.106 in Bazian to 12 L/s in W.53. Many factors appeared to have affected the well yields in the study area, such as:

- Lithological properties of the aquifers.
- Variation in the well depth.
- Type of pumping equipments and the capacity of the pump.

In order to give more comprehensive explanation for this variation in aquifer characteristics, some relationship can be analyzed:

1. Some wells have low discharge or low rate of flow (less than 2 L/s) but they have high drawdown (more than 10m), such as (W.81, W.125) drilled in Dargazen and W.91 in Kani Shaitan. They are penetrating mostly AIA and partially EKFA. These wells are considered to be low yielding wells and need to be developed.
2. Other wells have discharges more than 7 L/s, but their drawdown is less than 1m, they are mostly penetrating EKFA, such as the two piezometers W.143 and W.144, in addition to W.87 in Tape Shuankara and W.92 in Halai mam Qadir which penetrates the AIA. Such wells have good yielding capacity and appear to be highly developed, thus it is possible to change pumps and increase the discharge rate because these wells have high potentials.
3. Some wells have low transmissivity (5×10^{-5} m^2/sec) but their discharge is relatively high (more than 4.5 L/s). The drawdown in these wells attains more than 25m, therefore the high rate of the discharge for these

wells will affect badly the productivity of the wells which can cause failure or even lead to the dryness in the future, for examples the wells (W.42, W.90, W.111, W.140, etc.). Details about each pumping test are given in Appendix (4.B).

4.6 Aquifer recharge

Groundwater recharge is one of the most difficult hydrogeological parameters that can be estimated (Chapmen & Sharma, 1987 and Darling et al, 1987). Estimation of the net groundwater recharge is necessary for both groundwater modeling and water resources management.

Nowadays, there are several methods applied for estimating the groundwater recharge from precipitation and other forms of surface runoff, each has its limitations and difficulties in application.

In general, the main sources of the recharge of the aquifers in the study area are from the precipitation during the rainy season. The main streams which are flowing inside the area are generated from rainfall and issuing springs that drained water from all kinds of the aquifers particularly from the EKFA inside the catchment area. This clearly felt from the layer of the drainage pattern and spreading of springs from the hydrogeological map in Fig (4.1).

For the estimation of the annual volume of recharge in the study basin, the simple water balance and SCS methods were applied. Part of this method was outlined in chapter three in which a total amount of runoff (using SCS method) and the rate of evapotranspiration using FAO Penman-Monteith method was calculated, the remainder represent amount of the net recharge percolated downward to reach the groundwater storage.

As outlined in the soil water balance method in chapter three (Fig 3.13), net recharge occurs during December to March. However, the rainy season starts from October and continues until the end of May even for some years until the beginning of June. The aquifer receives the percolated rainfall for these four months. The most probable reason for such limited percolation of net recharge to the aquifer during the rainy season may refer to the following facts:

- Most of the fallen rainfall in the starting of the rainy season (October and November) tends to replenish the soil moisture deficiency and part of it is consuming through evapotranspiration and surface runoff.
- Large amount of the rainfall during wet period (April and May) will consume by evapotranspiration as well as by runoff because the soil is saturated.
- It is also worth mentioning the impact of the topography of the area, as can be seen from Fig (6.9) in chapter six, most of the area has slopes of more than 6% which means that topography has a great impact in transforming most of the fallen rainfall into the form of runoff because rainfall does not have enough time for infiltration, in contrast most of the flat areas where associated in the central and southern parts of the area characterized by slow infiltration rate which led the process of evapotranspiration to be activated.
- The total average annual recharge to the aquifers inside the area is estimated to be at the range of 96 millions m^3 (Table 4.2), and this amount is calculated based on the average annual rainfall of 691 mm/year.

Net recharge has been calculated taking into consideration the variable geology of the area and the different response of each hydrostratigraphic layer for contributing and percolating water from rainfall, with regard to black box balance. In other words, the net recharge in each geological zone was calculated based on the water surplus minus the total runoff (including soil moisture) for each month separately as shown in table (4.2). Accordingly the net recharge map was created and shown in Fig (4.10).

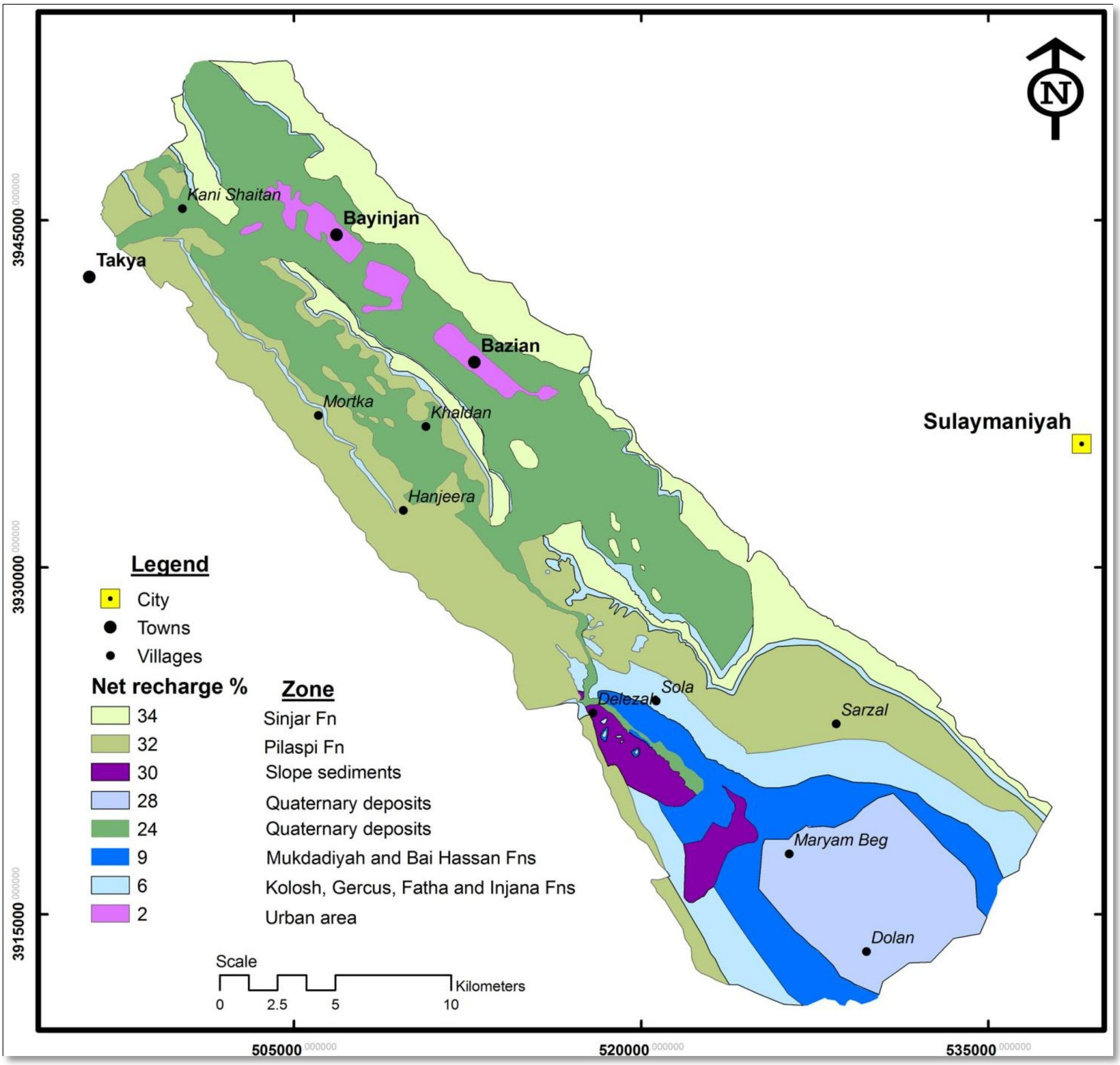

Fig (4.10) Annual net recharge to the groundwater in (%) from rainfall of the Basara basin, using SCS and soil water balance methods

As can be depicted from Fig (4.10), the watershed is divided into 8 subzones. The predicted highest rate of the net recharge is with locations dominated by EKFA represented by Sinjar and Pilaspi formations (34% & 32%) respectively, while the minimum is located in an Urban area, and in Aquiclude beds as well as Miocene Complex Aquifer (MCA), (2% and 6%) from the total annual rainfall, respectively.

Table (4.2) Expected amount of net recharge for each month and for each geological zones based on SCS and soil water balance methods

Month	***Oct***	***Nov***	***Dec***	***Jan***	***Feb***	***Mar***	***Apr***	***May***	***Jun***		***Total***	
P	36.5	88.3	110	118	112	103	85	38.7	0.0		691.6	
Surplus	0	0	*87.8*	*97.9*	*84.5*	*46.5*	0	0	0		**316.8**	
Runoff	0	0	***37.5***	***43.0***	***39.2***	***29.3***	0	0	0		**149**	
Proposed CN	Net recharge in (mm)								Enclosed area (km^2)	Volume ($X\ 10^6\ m^3$)	Net recharge in (mm)	Net recharge %
90	0	0	6.1	8.3	0.3	0.0	0	0	12.39	0.18	14.7	**2**
86	0	0	15.9	18.4	10.2	0.0	0	0	64.77	2.88	44.5	**6**
83	0	0	22.8	25.5	17.2	0.0	0	0	45.76	3.0	65.5	**9**
69	0	0	50.3	54.7	45.3	13.7	0	0	156.5	25.68	164.1	**24**
65	0	0	56.9	61.9	52.1	19.8	0	0	50.9	9.71	190.7	**28**
62	0	0	61.5	66.9	56.8	24.1	0	0	14.33	3.0	209.3	**30**
60	0	0	64.4	70.1	59.8	26.7	0	0	144.6	31.96	220.9	**32**
57	0	0	68.5	74.6	64.0	30.4	0	0	81.97	19.46	237.5	**34**
									571.3	***95.87***		
T. NR $x10^6\ m^3$	0	0	21.4	24.6	22.4	16.7	0	0				***95.87***
T. NR in mm	0	0	***50.3***	***54.9***	***45.3***	***17.3***	0	0				***167.8***

As explained in the beginning of this chapter, more than 400 wells were drilled inside this alluvium aquifer, mostly recharged from the percolated water from rainfall and streams seepage that descend from the surrounding drainage patterns and from issuing of spring flows. This may be attributed to the sediments of the fans accumulated in the plain area especially inside the Bazian and Hanjeera sub basins which consist mainly of silt, sand and clay in addition to the coarse fragments of poorly sorted and sub-angular flat clasts of limestone, derived from surrounding mountains. This fact may be one of the reasons for the highest amount of the net recharge within the basin; another fact is the activity of the irrigation and vegetal cover which facilitate downward movement of water through pathways penetrated by their roots which decrease the opportunity for the runoff.

The rate of recharge within the EKFA is at the range of 220 to 240 mm/year, if the total annual rainfall taken as 691 mm (Table 4.2). The reason for such relatively high net recharge rate within the EKFA zones compared to the other zones may refer to the nature of the joint and fracture network which provide excellent paths for percolating the precipitation. Moreover, the undulated nature for the surfaces of the mountains decreases the opportunity for the flooded water flow downward to the lower elevated lands before finding its way to the existing discontinuities. In contrast, most of the urban areas have the lowest amount of recharge (15 mm/year or 2% from the fallen annual rainfall), because it is mostly covered by building and paved road which transforms all the fallen rainfall to the form of runoff.

4.7 Aquifer discharge

The mechanism of the aquifer discharge is expected simply to be through the following ways:

1. Drainage through springs.
2. Artificial drainage through wells.

4.7.1 Aquifer discharge through springs

Spring discharge represents the main groundwater outflow, mostly in the case of EKFA and Intergranular aquifers.

The dominant factors which influenced the emergence of springs are:

- Locations of water bearing layers and impermeable rocks. Good examples are represented by a number of springs which are flowing in contact between EKFA with Aquiclude layers, such as springs which assigned as 3, 8, 12, 14, 15, 43, 49, etc (Fig 4.1).
- Influence of the tectonic elements, as a result, many springs are emerging continuously even in dry seasons. Khaldan, Qushqaya and Sarzal springs are best examples of these conditions (Fig 4.1). Some other springs are flowing until the dry season where the discharge gradually decreases or even drying out.

- Moreover, climatic conditions and resources of the aquifer system actually dictate the amount of water discharged through outlet points (Stevanovic and Iurkiewicz, 2004).

In order to register and geo-reference the main springs inside the catchment area, and to explain the impact of the tectonic elements on the distribution of them on one hand, and to find the influence of the hydrogeological zones in issuing the springs on the other hand.

More than 110 springs from field survey, previous work by FAO project during (2000-2003), as well as recorded springs by Aziz (2005), were used to establish the map showing locations of the main springs and average annual discharge in L/s (Fig 4.1).

The discharge of the spring is varying highly. Some of them have average discharge of more than 100 L/s such as Khaldan spring, others has very little discharge 0.05 L/s like Gawani spring.

The geo-referenced spring's layer in the hydrogeologic map in the studied area is categorized into three major groups based on their discharge rate:

1- Group of high discharge rate (more than 100 L/s). This group is represented by Kopala, Khaldan, Hanjeera and Warmziar springs. They are issuing from both EKFA and AIA, and most probably issuing under the effect of tectonic activity.
2- Medium discharge group springs. The discharge magnitude is at the range of (10-100 L/s).
3- Group of low discharge values, which include all the springs with very low discharge rate (less than 10 L/s).

Based on the distribution of the spring's layer in (Fig 4.1), the springs occur in the studied area with different hydrogeological zones. The number and relation of each zone are shown in table (4.3).

Table (4.3) Distribution of the springs with the hydrogeological units

Hydrogeological type	Number of springs distributed
EKFA	11
AIA	44
PIA	8
MCA	6
Contact between EKFA & IA	24
Contact between EKFA & Aquiclude	15
Contact between IA & Aquiclude	3

In general, the following comments from this table could be concluded:

A- Springs which discharge from Intergranular aquifer in both forms (AIA & PIA), relatively covering half the number of the springs appearing either under structural control or contact springs. Examples of these springs are Kani Sarchawa, Lazian, Qulka, Kani Pari, Hayasee, Kuchkena, Zekan, Ibrahimawa, *Kani Shaya, Warmziar*, Gawani, Gurbaz, Shilan, etc (Fig 4.11 - *B & D*).

B- Those discharging from EKFA, issuing in three forms:

First / a total number of 11 springs flowing inside this aquifer alone, most of them are issuing under the effect of tectonic lineaments and in some cases aquiclude beds corporate this situation. The average discharge of these springs is variable from as low as 0.1 L/s to 160 L/s. Examples of these springs are Kani Shaitan-3, Kopala, Klashkaran, Bibijaki Saru, Qushqaya springs within the Bazian sub basin, Khaldan, *Mortka and Cholmak* springs inside the Hanjeera sub basin, in addition to Kani Pan and Qala Sure springs within the Tile sub basin (Fig 4.11 - *A &C*).

***Second* /** those emerging in or close to the contact with intergranular aquifers and represented by 24 springs, mostly occupy the area comprising the Bazian and Hanjeera sub basins. Most of them are more likely to be discharged under the effect of structural control by longitudinal lineaments, the discharge of these springs are at the range of

10-100 L/s. Name of some of these springs are Kani Shaitan-1, Gomashin, Tepe Shuankara, Shekh Mand, Warmziar, etc.

Third **/** a total number of 15 springs within this aquifer can be classified as a contact spring type, because they are issuing when they contact Aquiclude beds of Kolosh and Gercus formations. This kind of spring is distributed mainly over the area of the Bazian and Hanjeera sub basins. Examples are Allaquli, Karezakan, Tainal, Kowaik-1, Hanjeera, Gomatagach, Mahmudia, SE-Khewata, Darikali, Barowi Gawra, etc (Fig 4.1).

Fig (4.11) some dominant springs in the studied area "A- Cholmak; B- Kani Shaya; C- Mortka; D- Warmziar", photo was taken on April, 2009

A small number of springs, which emerge from MCA, concentrated on the south western area, within the Tile sub basin such as Mewli-1, Mewli-2, and Kani Roshnai.

4.7.2 Spring flow regime

Analysis of the spring flow regime would give an estimation about storage capacity of the aquifers, which is considered to be an essential parameter for groundwater management.

Kresic (2007) defines the hydrograph of a spring, as the final results of various processes that govern the transformation of precipitation and other water inputs in the spring's drainage area into the flow at the point of discharge. Analysis of a spring hydrograph is mainly related to the falling hydrograph limb which corresponds to a period with no or limited amount of precipitation and it is mainly called recession analysis.

The philosophy of this analysis is that when the relation between spring discharge and time is established, it is possible to predict the rate of a spring flow after a given period without precipitation, in addition to estimate the volume of discharged and even a total volume of the stored water.

As explained earlier, more than 50 springs are issuing from and in contact of the EKFA, among this number only a few of them continue flowing throughout the year and the others are seasonally.

The most commonly used method in analyzing such flow regime is Maillet (1905) equation, who proposed an exponential mathematical formula eq (4.1) that describes the falling limb of hydrograph and spring base flow.

$$Q_t = Q_0 . e^{-\alpha(t-t0)} \quad \text{............ eq (4.1)}$$

Where;

Q_t; is the predicted flow at a given time in (l/sec)

Q_0; is the spring flow at the beginning of recession (l/sec)

α; is the recession coefficient or coefficient of discharge which depends on the aquifer parameters, such as transmissivity and specific yield.

t; is time (in days) since the beginning of recession for which the flow rate is calculated .

t_0; is time at the beginning of recession.

The Maillet equation when plotted on a semi log paper is a straight line with the recession coefficient as its slopes, the introduction of the conversion factor 0.4343 is a convenience for expressing discharge in cubic meter per second, and time in days, thus the equation is expressed as eq (4.2):

$$\alpha = \frac{\text{Log Q0} - \text{Log Qt}}{0.4343\ (t - t0)}$$ ....eq (4.2)

This method applied for analyzing flow on three springs (Khaldan, Hayasee and Kuchkena springs) which characterized by variable discharge rates. The daily discharge of these springs had been recorded earlier during January to October, 2002 by FAO project.

- **Khaldan spring**

This spring is one of the largest springs in the studied area; it is located in the Hanjeera sub basin and supplies water to several villages and provides water for large irrigated land area. The output of the Mailet method is shown in Fig (4.12), and the results are tabulated in table (4.4).

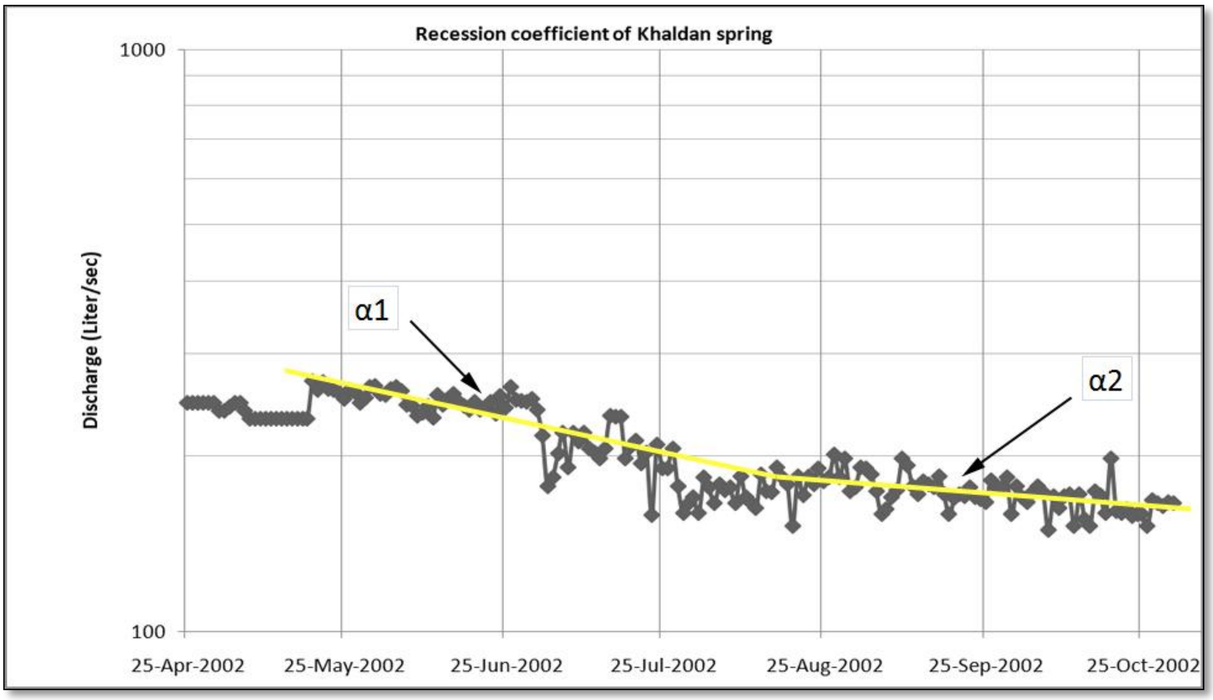

Fig (4.12) Recession coefficient of Khaldan spring discharge

Table (4.4) Recession coefficients and dynamic reserves of Khaldan spring

Spring Name	α_1	α_2	V total x 10^6 m^3
Khaldan	**0.00553** Per 77 days	**0.0018** Per 84 days	**0.93**

As can be depicted from this figure; two recession coefficients can be selected. The first recession period started from 19 May and continued until 9 August. This period coincides with the time when rainwater and snowmelt percolated downward to the aquifers and the discharge of the spring decreases gradually, but with higher rate compared to the second micro-regime which starts from 9 August. The first recession coefficient is calculated as 0.00553 which is continued for 77 days, while the second micro-regime is activated which has a coefficient of discharge 0.0018 and continued for 84 days until the beginning of the new wet period.

According to Kresic (2007), the variation of the coefficient of discharge has a physical explanation. It is accepted in practice that **α** of order 10^{-2} indicates rapid drainage of well interconnected large fissure and large karstic channel, while midler slopes of the recession curve (**α** of the order 10^{-3}) represent slow drainage of small voids or narrow fissures and aquifer matrix porosity aquifer. Accordingly, the main contribution to the Khaldan spring in both periods is from storage in small voids and narrow fissure of Pilaspi aquifer.

Considering the calculation of the volume of groundwater accumulated in the aquifer at the beginning of recession and the volume discharged during the first recession, the following equation can be used, eq (4.3), (after Maillet, 1905):

$$\alpha = \frac{Qt}{Vt} \qquad \text{............eq (4.3)}$$

Based on this equation, the volume of the dynamic groundwater is estimated as 928,642 m^3 per 77 days.

- **Hayasee spring**

Hayasee is one of the largest springs within the Hanjeera subbasin. At that spring a new intake structure and concrete channels were constructed under the FAO Programme, which is used mainly for irrigation purpose (Fig 4.13).

Aziz (2005), refers to issuing of this spring to the presence of a horst structure which has the vertical displacement that ranges between 80-100m, and it has width of 1100m with length more than 1000m extending from NE towards SW from Hayasee to Cholmak. It extends to underlain Kolosh Fn, above this horst, there is a large recent sediments which provide optimum reservoir for accumulating stored water (Fig 4.14). According to this conclusion, the groundwater of Hayasee most probably represents mixing water, part of its storage receives water from recent infiltrated rainfall to the overlain recent sediment, and a large portion is issued from Pilaspi Fn.

The Maillet recession curve, shows that the perennial Hayasee spring has two distinctive micro regimes of discharges with two recession coefficients, the first is most probably indicates rapid drainage of well interconnected large fissure and karstic channel, in which the discharge of the spring sharply fall from 156 L/s when the recession period is started to attain 57 L/s at the beginning of June, the second micro regime is activated and draining water mostly from the static reserve (Fig 4.15).

The dynamic reserve is estimated to be about 312,000 m^3 based on eq (4.3), (Table 4.5).

Table (4.5) Recession coefficients and dynamic reserves of Hayasee spring

Spring Name	α_1	α_2	V total x 10^6 m^3
Hayasee	**0.02638** Per 38 days	**0.00066** Per 100 days	**0.31**

Fig (4.13) Hayasee spring, showing Irrigation scheme constructed by FAO, (photo was taken in April, 2009)

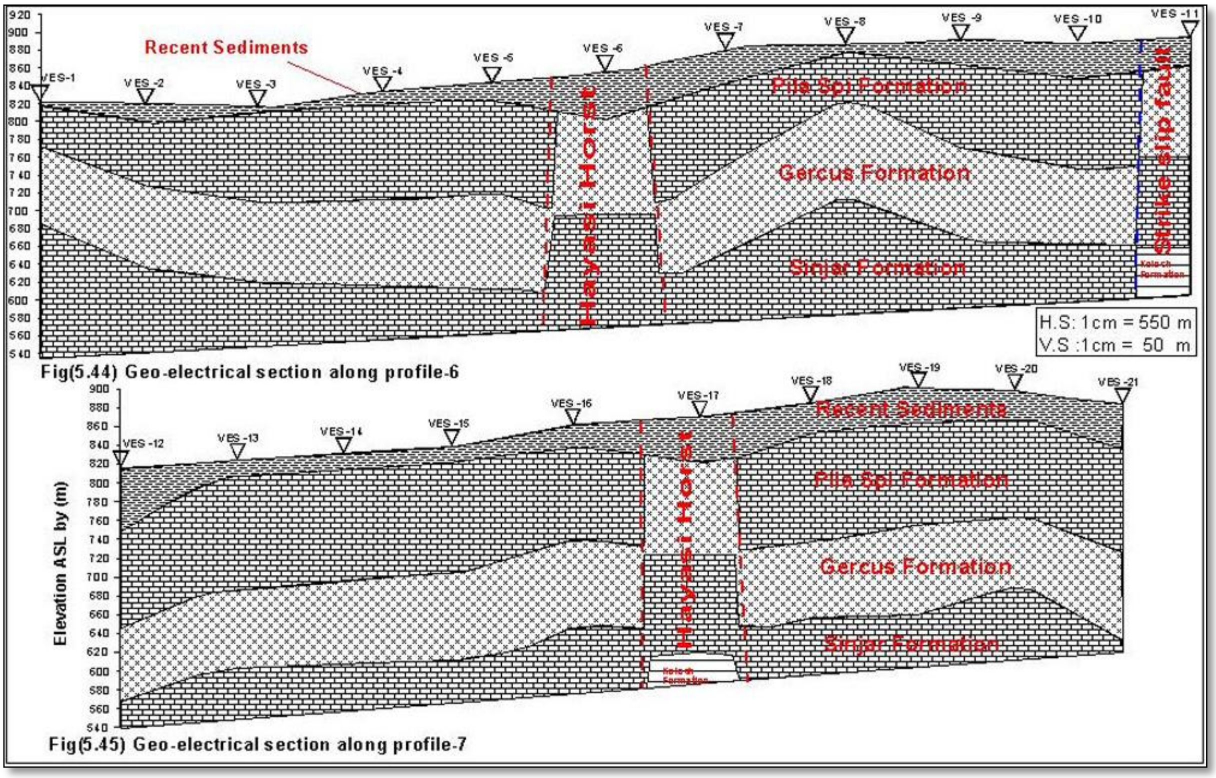

Fig (4.14) Horst structure beneath Hayasee spring (after Aziz, 2005)

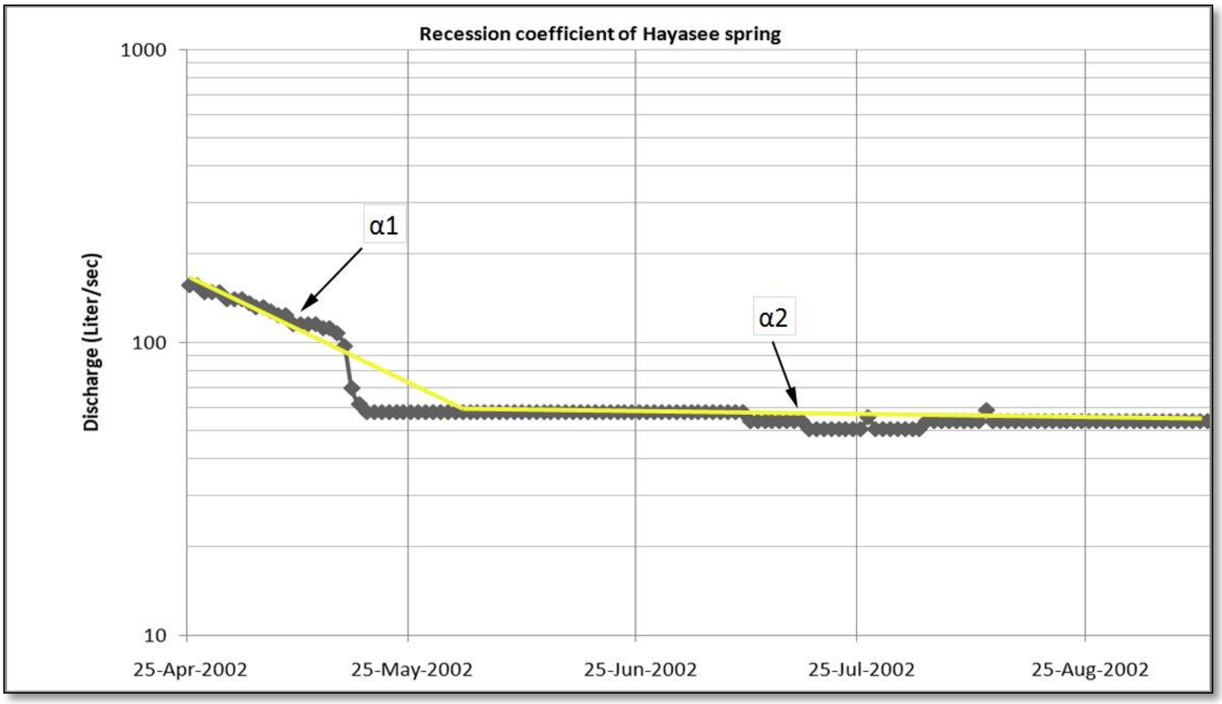

Fig (4.15) Recession coefficient of Hayasee spring discharge

- **Kuchkena spring**

Similar to Khaldan and Hayasee springs, this spring locates in Hanjeera subbasin and has two distinctive micro regimes of flowing (Fig 4.16). The first estimated recession coefficient **(0.03485)**, is most probably indicates rapid drainage of well interconnected large fissure and karstic channel in which the discharge of the spring observably decreases from 90 L/s when the recession period is started to attain 22 L/s at the beginning of June, whereby the second micro regime is activated and draining water mostly from storage in small voids and narrow fissure of the aquifer.

The dynamic reserve is estimated to be about 150000 m^3 (Table 4.6).

Table (4.6) Recession coefficients and dynamic reserves of Kuchkena spring

Spring Name	α_1	α_2	V total x 10^6 m^3
Kuchkena	**0.03485** Per 39 days	**0.004196** Per 150 days	**0.15**

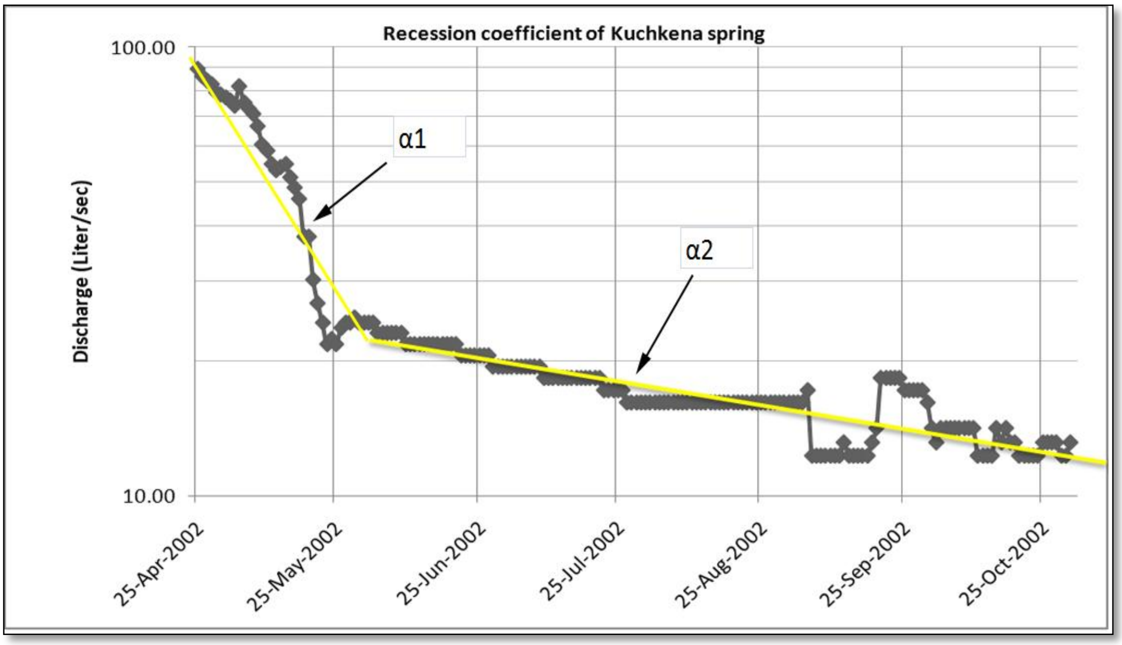

Fig (4.16) Recession coefficient of Kuchkena spring discharge

4.7.3 Artificial drainage

The total volume of water that is withdrawn from the hydrogeological system in the area is not precisely known. This is due to the lack of information that determines the number of the wells which are working and those which have not working. Lack of this information makes the estimation of the total volume of discharged water seems to be very difficult. However, most of the operating wells are characterized by very low discharge rates since they have been installed for local domestic use, with exception that, other wells are draining groundwater for more than16 hr / day with relatively high rate, (such as those wells which providing water for governmental and industrial projects).

Within the last few years, the studied catchment (especially the Bazian sub basin), became densely residential and rising of highly industrial activities, but the problem arises when there is little or even without any system of water distribution or sewage draining system. As a result, people started the drilling wells (both shallow and deep wells) in range of few meters to several tenths of meters, without any control to the local government. More than 500 wells were drilled inside the studied catchment, in addition to that many other wells without permision from the related governmental offices and by cheap traditional machines called Syrian drilling machines. The limited cost of drilling wells by these machines, (drilling 1 m not exceeding 15$) encouraged many owners of even the older houses and irrigated land to drill wells inside their areas, because the municipal tap water could not satisfy their real demand, especially during summer period. As a result, the overexploitation and pollution risk in this basin is expected, because most of these wells are neither properly drilled nor protected.

The main sources for supplying potable water in the studied catchment, is come from drilling wells, springs and streams. In order to assess the availability of water resources, annual production and total expected annual recharge for the area, it is more reasonable to classify and evaluate each sub-basin separately.

- **Annual groundwater recharge and discharge for Bazian sub basin**

The densely populated, highly industrial and irrigation activities are located in this sub basin. It is reported that before arriving the second water supply line of Dokan project to this sub basin in the middle of 2010, potable water for most of the towns (represented by Bazian, Tainal, Gopala, Baynjan, etc.) and some of the villages is supplied from drilling wells and springs for about 90 percent of the population.

For example, most of the daily demand for a densely populated town like Takya was supplied from several deep wells (70 – 150m) which were drilled inside this sub basin and provide potable water of 1750 m^3/day, but after completion of the new water system from Dokan project on June 2010, supplying water from these wells decreases to less than 500m^3/day, (personal communication with the manager of the Directorate of water of Takya).

As a whole, more than 450 wells were drilled and distributed throughout this sub basin, in addition to tenth of springs with variable rate. It is worth to mention that approximately 85% of these wells are working, while the remainder are failed and do not work properly, this fact based on the archive from a recent survey conducted by a team from Directorate of Groundwater in Sulaymaniyah in 2009, in addition to the field survey carried out by in the present study. Industrial activities, farming and irrigation in this area are relatively high. Many farmers practice regular cultivation and crop cycling during different seasons, while several factories for different purposes drilled tenth of deep wells which are working 24 hours per day to provide water for their produces.

The total annual natural and artificial groundwater discharge is shown in table (4.7).

Table (4.7) Annual groundwater production and estimated recharge in Bazian sub basin, based on the updated data of the year 2009-2010

Type of discharge	No. of wells or springs	Average daily operation hours	Estimated average discharge rate (l/s)	Annual production X 10^6 (m^3/year)	Estimated annual recharge X10^6 (m^3/year)	Percent of annual production (Q %) from annual recharge (R %)
Deep and shallow wells	340	4	4	7.15	≅ 43.34	71.5
Governmental projects	18	-	-	0.91		
Industrial activities	17	-	-	0.69		
Springs	48			22.3		
Total annual production				31		

According to the above table, the following information can be concluded:

1- Among 450 wells which were drilled in this sub basin, more than 50 wells are used for governmental projects and industrial activities, as follows:

- 27 wells were drilled between 2000 and 2008 to supply Takya (nowadays only 12 wells are working) and 9 wells for Chamchamal towns (only 6 wells are working now, the others even dried or shut down). Daily discharges from these wells are 20 l/s for Takya and 23 l/s for Chamchamal. Most of these wells are penetrating EKFA, and located close to Kani Shaitan village.

- 9 wells were drilled within the last few years to supply water for Mass Cement Factory and Oil Refinery. The daily discharges from these wells are estimated to be around 10 l/s, and most of them are penetrating EKFA.
- Three large water bottling factories delivering water for their production from 8 drilling wells which penetrating EKFA (mostly Pilaspi aquifer). Regular discharges from these wells are expected to be 18 l/s.

2- Approximately 85% from all reported wells inside this sub basin is properly working, if the daily operation of 4 hours with 4 l/s of discharge is assumed, the total expected annual production will be around 7 million m^3.

3- Based on the interview with managers of the Directorate of Waters of Takya and Chamchamal, the total annual expected extracted water from all these projects is calculated as 1.6 million m^3.

4- Among 48 springs which geo-referenced inside this sub basin, some of them are characterized by relatively high discharge 100 l/s, such as Warmziar, Kopala and Halay sarwchawa, the others have few liters of discharge. Based on the calculation of the average spring discharge in three times throughout the year which carried out by Aziz (2005) and weekly calculation of inventory points conducted by a team of FAO project in 2001, as well as calculation of some springs in two different seasons by the researcher during preparation of present work, the total expected discharge from whole springs is estimated to be around 22.3 million m^3, and this rate comprises 44% of the annual recharge to the groundwater storage to this sub basin.

5- Based on the calculation of soil water balance and SCS methods, the total expected annual recharge for this sub basin is around 43 million m^3. This is based on the annual precipitation of 690 mm.

6- However, the groundwater exploitation in this sub-basin compared to the existing reserve is low and the annual estimated recharge is higher than the estimated exploited volume. But, if the safe yield is taken into consideration, the groundwater resources in this area could be considered to be under stress due to the excessive groundwater abstraction.

Ali (2007) used the rate of 45% as safe yield in (Sharazoor – Piramagroon basin) which is located adjacent to the eastern part of the present study, accordingly, if the safe yield is considered to be 45% of the total annual recharge, exploitation of the groundwater in this sub-basin should not exceed 19.5 million m^3. Therefore, avoiding the devastation of the aquifers by suitable groundwater management is the necessary solution for the sustainable development of the entire region for the few next decades which most likely to keep growing irrigation and other industrial activities.

- **Annual groundwater recharge and discharge for Hanjeera sub basin**

The total annual natural and artificial groundwater discharge is calculated and presented in table (4.8).

Information of this table is attained based on the following criteria:

1- Among 30 wells which were drilled and documented in the DGWS, about 10 wells are used mainly for industrial activities, such as those drilled to provide water for the Bazian Cement factory, while the other wells are used mainly for irrigation and livestock purposes. The expected total annual discharge from these wells is around 0.45 million m^3.

2- It is believed that the annual discharge from nearly 24 springs recorded inside this sub basin is around 16.2 million m^3, and this comprises 66% of the total expected recharge from precipitation fall over the area, because some of the largest springs inside the studied catchment is located within this sub basin such as Khaldan and Hanjeera springs.

3- The total estimated annual recharge is approximately 24.6 million m^3, if the total annual precipitation is 690 mm.

4- The present ground water withdrawal from the existing wells and emerging springs comprises 68% of the total annual recharge. If 45% of annual recharge is considered the safe yield, the maximum current exploited volume should not exceed 11 million m^3. Accordingly, groundwater resource is now under severe stress and groundwater management is the necessary solution to avoid further overexploitation of the groundwater storage.

Table (4.8) Annual groundwater recharge and production in Hanjeera sub basin

Type of discharge	No. of wells or springs	Average daily operation hours	Estimated average discharge rate (l/s)	Annual production X 10^6 (m^3/year)	Estimated annual recharge X10^6 (m^3/year)	Percent of annual production (Q %) from annual recharge (R %)
Deep and shallow wells	20	3	4	0.32	24.6	68
Industrial activities	10	-	-	0.13		
Springs	24			16.2		
Total annual production				16.65		

- **<u>Annual groundwater recharge and discharge for Tile sub basin</u>**

However this sub basin is occupying an area more than the Hanjeera sub basin, but the total expected discharge is less than the previous one. Based on the tabulated table (4.9), the total expected artificial discharge from a number of 40 shallow and deep wells which drilled inside the area is calculated to be around 0.315 million m^3, while the expected annual discharged groundwater via 39 springs is around 4 million m^3. Thus, the whole discharge from this sub basin is expected to be 4.42 million m^3, but the total estimated recharge is believed to be around 28 million m^3 (Table 4.9).

Table (4.9) Annual groundwater recharge and production in Tile sub basin

Type of discharge	No. of wells or springs	Average daily operation hours	Estimated average discharge rate (l/s)	Annual production X 10^6 (m^3/year)	Estimated annual recharge X10^6 (m^3/year)	Percent of annual production (Q %) from annual recharge (R %)
Deep and shallow wells	40	2	3	0.315	28	16
Springs	39			4.1		
Total annual production				4.42		

It is obvious from this table that, in this sub basin the present ground water withdrawal from the existing wells and whole springs is quite limited. If 45% of annual recharge is considered to be the safe yield as Ali (2007) suggested, the maximum current exploited volume will comprises 35% of the safe yield. Accordingly, this area could be considered the area of low population stress as compared to other sub basins and more wells could be drilled without any harmful impact on the aquifer, but not necessarily the wells getting successful.

Finally, it is worth mentioning that the above mentioned calculation of annual discharge and annual recharge are fairly accurate and care should be taken when they are taken for any future hydrogeologic assessment. For example, details about most of the shallow and deep wells in the study area from well archives and during field survey for preparing this thesis. For a large number of the drilling wells, including well pumping rate and duration of pumping work as well as location of well slots, are either missing or incomplete, accordingly, accurate analysis details about aquifer balance parameters is impossible, and it could be improved if a full investigation has been carried out.

4.8 Basara dam project

Generally, this project is considered to be a medium size dam planned to be constructed near Delaizha village, at the outlet of Basara gorge (Table 4.10). Most parts of the dam reservoir are located within a synclinal structure (New Sola – Qazanqaya syncline) which gives a suitable structural configuration in collecting water, especially collecting larger amount of groundwater into the basin (Hamasur, 2009).

As previously mentioned in chapter one under previous study section, the proposed Basara dam site was assessed by both Agrocomplet (1979) and Sogreah (1983) (as cited from ITSC, 2006) and recently by ITSC Hydroengineering (2006). According to these studies, the primary aim of this project is to provide the storage, regulating the irrigation and hydropower generation purposes.

As can be noted from table (4.10), it is planned that Bassara dam should support irrigation on 2,600 ha and generate hydropower within range of 2 Mw.

Table (4.10) the main characteristics of the proposed Basara dam and irrigation area, (from ITSC, 2006)

❖	CATCHMENT AREA	F=574 km^2
❖	APPROXIMATE ALTITUDE	Hm=944 m
❖	MEAN FLOW (YEAR)	Qm=8 m^3/s
❖	SPECIFIC DISCHARGE	q=13.9 l/s/km^2
❖	PROJECT FLOOD	Q_{PMF}=2870 m^3/s
❖	IRRIGATION AREA	F=2600ha (net)
❖	NWL	715 m
❖	min WL	701 m
❖	max WL	719.3 m
❖	CREST LEVEL	720.8 m
❖	DAM HEIGHT	50 m
❖	BOTTOM LEVEL	673.8 m
❖	CREST LENGTH	268m
❖	CREST WIDTH	10 m
❖	DEAD STORAGE CAPACITY	18×10^6 m^3
❖	USEFUL STORAGE CAPACITY	35×10^6 m^3
❖	DEAD STORAGE LEVEL	687.8 m
❖	QUANTITY OF FILL IN DAM	0.57×10^6 m^3
❖	HP POTENTIAL (energy producible)	18 GWh/year
❖	VOLUME OF WATER SUPPLIED TO THE IRRIGATION (annual)	V=28×10^6 m^3
❖	SPILLWAY	L=130 m
❖	TOTAL DISCHARGE	2420 m^3/s

Beside these great benefits after completion of this project, many negative impacts may affect the environment of the area. For example, to convert river into lake will cause profoundly changes of existing environment of the river system and affects the water quality, climate, biodiversity and natural and cultural geo heritage as ITSC (2006) mentioned. Another negative disadvantage of this project is the impact on groundwater in the area especially within the Tile sub basin in which the groundwater table will follow the reservoir level and later will has the impact on the fluctuation of the water table. In other word, the accumulated lake water will flow from the reservoir and infiltrate into the aquifers which may influence the quality of the groundwater nearby the proposed dam site.

CHAPTER FIVE

HYDROCHEMISTRY

5.1 Preface

The quality of groundwater and its suitability for domestic, irrigation and industrial purposes is of high importance as it affects human life, influences water management and future planning. Thus, the quality is considered to be more important than the quantity especially for the studied basin where the fast development from all kinds of activity, particularly industrial sector will provide opportunities for pollution from various sources to contaminate air, surface and groundwater resources.

A number of 65 samples collected during wet and dry season, and analyzed for major, minor and heavy metals as well as to assess the seasonal variation. 40 samples in wet period and 25 samples in dry period from deep and shallow wells as well as springs were taken. Temperature, pH and electrical conductivity were measured instantaneously in the field by using multi-parameter portable device model (TPS/90FL-T Field Lab Analyzer), because these parameters considerably change with time. Sample collection from the drilled wells was often conducted after continuous pumping of 5 -10 minutes. For the chemical analysis, a 250 ml plastic bottle was filled at each locality (Fig 1.3).

The major cations "Ca^{2+}, Mg^{2+}, Na^{+}, K^{+}" were measured by the Ion Chromatography (model 4110B) and Inductive Coupled plasma (Optima 2100 Perkin Elmer), whereas anions "F^{-}, Cl^{-}, Br, $NO_2^{=}$, NO_3^{-}, PO_4^{3-}, SO_4^{2-} " were measured by Ion Chromatography and " HCO_3^{-}, CO_3^{2-} " by titration. These analyses were conducted from the Laboratories division in the Twin River Institute, the American University of Iraq _ Sulaimani, as well as the laboratory of Chemistry department of college of Science, University of Sulaimani and laboratory of Kurdistan Institute for Strategic studies and Scientific Research (KISSR) in Sulaimani (Tables 1.2 & 1.3). The results of the chemical analysis are tabulated in the Appendix (5.A & 5.B).

5.2 Physico-chemical properties of the groundwater

Results of each parameter analyses are briefly explained and tabulated in the following sections:

5.2.1 Temperature

Temperature measurements of the groundwater samples were taken immediately in the field after sample collection. The maximum, minimum, average temperatures and homogeneity index for the springs and water well samples are tabulated in table (5.1).

Table (5.1) Range of temperature values of the groundwater samples in Basara basin, taking on April, 2009.

Item	Median T (C^o)	Max. T (C^O)	Min. T (C^o)	Homogeneity Index(IH)
Springs	18.3	26.5	16.5	0.62
Wells	18.9	21.2	17	0.80

Significant differences are observed between samples taken from springs and those taken from wells. An extreme higher value (26.5 C^0) was recorded in Shekh Mand spring, while the value of (16.5 C^0) with minimum variability is recorded in Delezha, Hanjeera and Mortka springs. In contrast, the highest value of water temperature of the wells (21 C^0) was recorded in Tainal and Bazian towns, and the minimum was located in Allai, Dargazen Baba Ali and Zeiaka villages.

Relatively high homogeneity index (HI) for the wells indicates low spatial variation in the temperature of water samples, due to the variation of groundwater table depth. But the phenomena for low homogeneity index (HI) for the spring samples (0.62) may imply an increase in groundwater temperature with the depth as the majority of the permanent well known springs issuing from EKFA.

5.2.2 Hydrogen ion concentration (pH)

The pH values of the groundwater samples indicated that the pH of the springs ranges from 7.0 to 8.2, while the well samples have the values of 6.23 and 8.1 (Table 5.2).

Table (5.2) Range of pH values of groundwater samples for both wet and dry seasons

Wet season				**Dry season**			
Springs		Well		Springs		Well	
Range	Median	Range	Median	Range	Median	Range	Median
7.55 - 8.2	7.75	6.94 – 8.1	7.69	6.97 – 7.02	7.02	6.23 – 8.1	7.1

As can be depicted from this table, the pH values in the wet season for the spring and well samples is slightly greater than the values in the dry seasons. Mechanism of recharge by precipitation during wet seasons may be the reason for such cases.

5.2.3 Total dissolved solids (TDS)

Like water temperature, TDS was measured in the field immediately during sample collection in both periods. The TDS values vary considerably in the area from less than 200ppm to more than 1550 ppm (Table 5.3).

In general, the TDS values in the wet season for all the samples are slightly greater than the values in dry seasons. This could be attributed to the errors resulted from the carelessness of the staff who achieved the analysis and storing the samples in a non convenient condition.

Concerning the spring samples, the maximum TDS value was 327 ppm recorded in Aligoran spring (issuing from EKFA - Pilaspi aquifer) which is located in the Hanjeera sub basin, and the minimum is 126 ppm recorded in the Qushqaya spring (EKFA - Sinjar aquifer) which is located in Bazian sub basin. Approximately the dominant TDS values in both seasons show the values less than 300 ppm (Appendix 5.A).

It is worth mentioning that the highest values (1555 ppm) for the well samples recorded in the Sollai Darband village where the enrichment of the groundwater by the sulfate from Fat'ha Formation seems to be the result for such concentration. The values less than (200 ppm) recorded in Bazian and Gopala towns as well as in Khewata village within the Bazian sub basin.

Table 5.3 Range of TDS values of groundwater samples for wet and dry seasons

Wet season				**Dry season**			
Springs		Well		Springs		Well	
Range	Median	Range	Median	Range	Median	Range	Median
126 - 327	225	172 – 1555	282	127 – 252	200	174 – 1540	218

As a whole, all groundwater samples are classified as a fresh water type, because the TDS value is less than 1000ppm, except the sample from the Sollai Darband village which is located in the Tile sub basin, is considered to be slightly brackish water based on the classification of Todd (1980).

- **Groundwater salinity**

The total dissolved solids (TDS) and electrical conductivity (EC) usually measure the salinity in groundwater. A total number of 62 locations were used for creating TDS map, 40 of these locations were selected during present study and 22 sites from previous surveys by a team of DGWS during February to August- 2009, they compiled to plot the salinity map (Fig 5.1).

High saline zone is recorded in the southern part of the study area within the Tile sub basin at Solai Darband and Maryam Beg villages. In general, the salinity pockets at those mentioned sites may attribute to the following factors:

1- The lithologies of the formations occupying the southern basin have been formed under prevailing saline conditions in lagoon depositional environment, especially in the case of Fat'ha and Injana formations, (detail about these formations are explained in chapter two). Hence, favorable conditions for the formation of evaporates were existed and dominating during the Miocene, where the lagoonal environment was progressively changed into fluvio-lacustrine toward overlying Mukdadiya Formation as Buday (1980) mentioned.

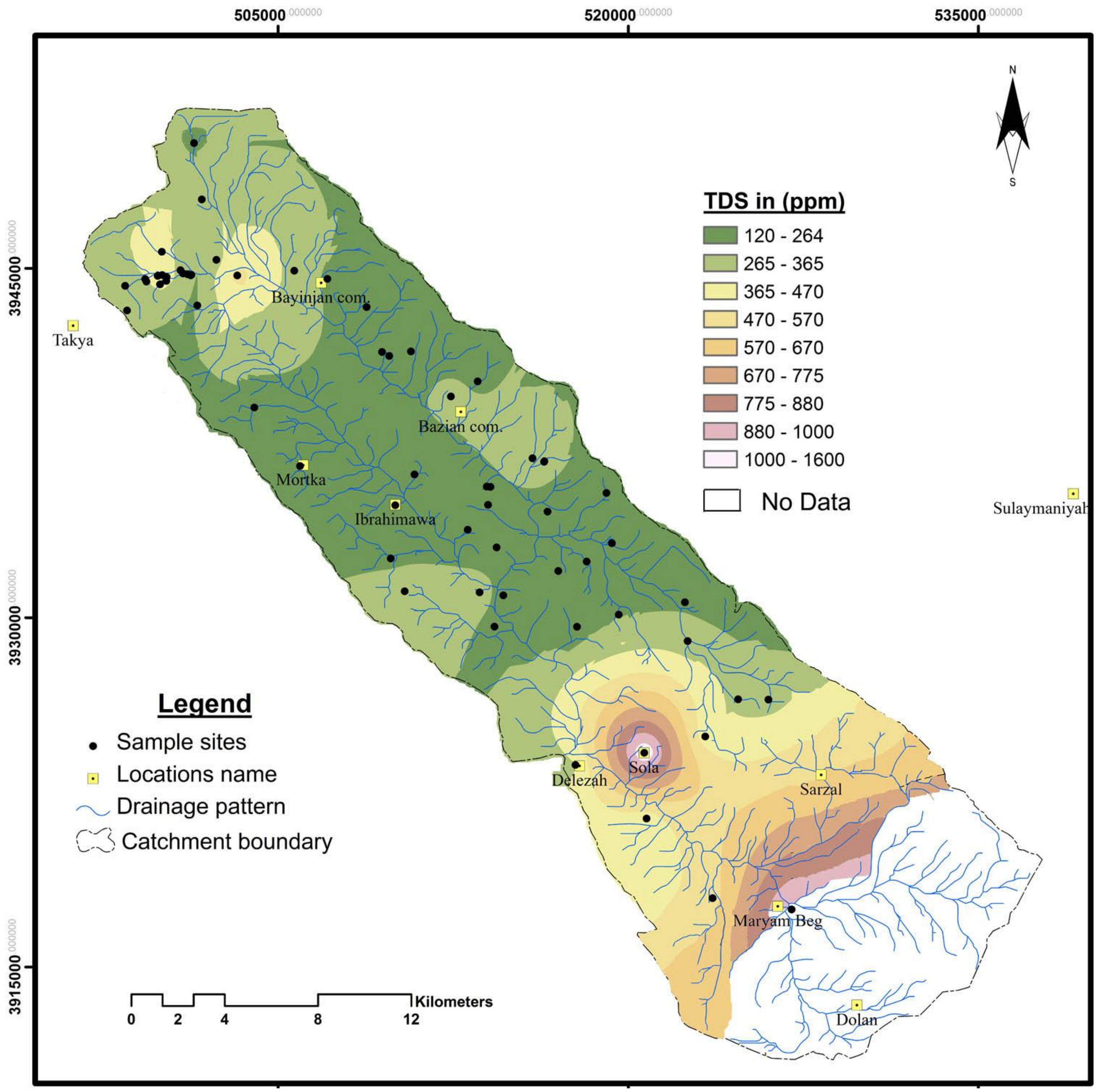

Fig (5.1) salinity zones for the Basara basin on the basis of the TDS during wet period. Two pockets of saline zones are encountered within the Tile sub basin. Due to the lack of TDS values, the southern area assigned as No Data.

2- Low infiltration rate, as clays dominate the lithology of the southern area compared to that of the other sub basins that characterized by relatively higher infiltration. These areas with clay dominant provide sufficient time for the evaporation process which led the TDS to be accumulated especially in summer seasons. The distribution of denser drainage pattern within the Tile sub basin particularly around these areas may prove this statement.

3- The groundwater mechanisms by evapotranspiration in the Maryam Beg could lead to notable salts increment within the saturated and unsaturated zones, especially where the groundwater level is some meters in depth, in and around this location, which most probably enriches the concentration of TDS.

To solve salinity problems in these areas, selection of the less saline units should be conducted during well drilling and the more saline units should be sealed.

5.2.4 Ionic Balance (I_B)

The calculation of the ionic balance (I_B) tests the accuracy of the chemical analysis. In order to evaluate the analyzed samples, concentration of the ions which was recorded in ppm has converted to epm and I_B, and assessing each samples based on the following formula (5.1), (WHO, 2008):

$$I_B = \frac{\Sigma\, Cations - \Sigma\, Anions}{\Sigma\, Cations + \Sigma\, Anions} \times 100 \quad \text{............ (5.1)}$$

In general, the acceptable limit for I_B is in the range of 0-5%, and the range of 5-10% should be carefully used in hydrochemical interpretation. After application of the I_B formula for the analyzed groundwater samples in both seasons, the calculated I_B for wet season samples indicates reliable analytical results than the dry period samples. As a result, the analyzed wet period samples are considered in interpreting the distribution of the ion concentration in most of the tested sites. The accuracy of (I_B) of the analyzed samples in the wet period is tabulated in (Table 5.4).

5.3 Chemical properties of the groundwater

Ranges and median values of chemical analysis for the groundwater samples are tabulated in table (5.5).

Table (5.4) Accuracy of the hydrochemical analysis based on the I_B% formula

Sites	Location	I_B %	Sites	Location	I_B %
1	Direc. of Bazian Health	*3.08*	21	Warmziar spring	*8.11*
2	Primary school of Tainal	*-2.71*	22	Zeika village	*8.51*
3	Gopala community	*2.31*	23	Gawani village	*-4.20*
4	Gomashin spring	*0.37*	24	Barowi Gawra spring	*-4.19*
5	Ardi Bazian factory	*-4.12*	25	Barowi Bichuk spring	*9.85*
6	Mass Cement factory	*2.09*	26	Darikali spring	*-2.85*
7	Bardaqaraman com.	*-1.80*	27	Halai Sarchawa spring	*1.45*
8	Gopala dawajin	*9.37*	28	Halai Mam qadir village	*6.59*
9	Bazian oil refinery	*5.27*	29	Balulan village	*9.02*
10	Kani Sarchawa spring	*-0.40*	30	Shekh Mand spring	*1.31*
11	Dargazen_ Baba Ali	*2.42*	31	Gomatagach spring	*9.77*
12	Cholmak spring	*7.44*	32	Hanjeera spring	*9.55*
13	Mortka spring	*1.77*	33	Aligoran spring	*4.31*
14	Zekan spring	*1.90*	34	Khewata village	*9.85*
15	Khaldan spring	*2.47*	35	Delezha spring	*9.91*
16	Alibzaw spring	*4.05*	36	Solai Darband village	*-0.72*
17	Allai dawajin	*9.93*	37	Gurbaz spring	*9.67*
18	Asia storage	*6.53*	38	Qazanqaya village	*9.30*
19	Qushqaya spring	*5.72*	39	Mariam beg village	*9.84*
20	Kani shaya spring	*6.01*	40	Agriculture field	-0.38

Table (5.5) Ranges of the major hydrochemical ions for the wet period in Basara basin in ppm

Ions	Wells			Springs		
	Maximum (ppm)	*Minimum (ppm)*	*Median (ppm)*	*Maximum (ppm)*	*Minimum (ppm)*	*Median (ppm)*
Ca^{2+}	336.72	32.73	72.59	107.73	38.97	52.29
Mg^{2+}	70.72	7.65	16.5	43.3	2.96	16.92
Na^{+}	301	1.37	9.67	70.01	1.53	3.8
K^{+}	5.68	0.25	0.56	0.86	0.11	0.39
(HCO_3^-)	335	141.6	201.8	160.2	49.6	96
SO_4^{2-}	1244	5.11	18.03	47.35	8.17	14.6
Cl^-	161.98	4.54	9.79	12.14	2.79	5.85
NO_3^-	192.7	0.73	21.5	55.5	2.73	10.1
CO_3^{2-}	14	2	5.165	6.67	1.6	4

5.3.1 Cations

- ***Alkaline earth metals (Ca^{2+} and Mg^{2+})***

Calcium and Magnesium are the most abundant cations in the studied area; this may refer to the impact of lithology, in which both carbonate rocks represented by limestone and quaternary deposits which are composed mostly of eroded fragments of the surrounding limestone, and both occupying more than 80% of the studied area. These lithologies have great impact to the interaction between the lithology and moved groundwater through them; as a result, greater amounts of calcium concentrate on the flowing water. The calcium concentration ranges between 32.73 ppm and 336.72 ppm in the wells with median 72.59 ppm. Spring samples possess the lower concentration of Ca^{2+} that ranges between 38.97 ppm and 107.73 ppm and median 52.29 ppm. As a whole, the concentration of Ca^{2+} increases towards the Basara gorge which implies solubility impact of the carbonate rocks where the surface and groundwater flowing through them.

Mg^{2+} concentrations in different aquifer types vary considerably along the flow direction. Most of the spring issuing from Sinjar aquifer "such as Qushqaya, Warmziar, Kani shaya, Gomashin, etc and majority of the wells drilling in Tainal, Bardaqaraman, mass cement, etc." have Mg^{2+} concentration less than 10 ppm, while most of the springs issuing from Pilaspi aquifer within the Hanjeera sub basin such as "Aligoran, Hanjeera, Shekh mand, etc. have the Mg^{2+} concentration of more than 20 ppm. This high amount of Mg^{2+} concentrations within the fissured Pilaspi Fn. might be attributed to the high residence time of groundwater flow as compared to that of relatively karstified Sinjar Fn. As a result more chance supposed to be available for ionic exchange to take place.

- ***Alkali metals (Na^+ and K^+)***

The sodium varies in its concentration between 1.37 to 300 ppm in the wells and from 1.5 to 70 ppm in the spring samples in the whole area (Table 5.5). Most of the lower values are recorded in the EKFA while the highest values are found within the MCA and AIA especially within the Tile sub basin. This high concentration of sodium most probably related to the lithology in which these wells penetrating Fat'ha Formation, the later contains the bed of gypsum, and this may contribute the higher concentration of this ion. Similar to the TDS, Na^{+} concentration in groundwater increases with flow direction towards the Basara gorge.

Conserve to the sodium, concentration of K^{+} ranges between less than 1ppm in most location occupied by EKFA to attain maximum value of 5.68 ppm in MCA especially at Solai Darband village as well as in Maryam Beg and Qazanqaya villages, the concentration are around 3 ppm and mostly occupied by AIA.

It is worthy mentioning that the impact of urbanization, pesticide and sewage outlets on magnesium and sodium ion concentrations has vital roles in increasing such concentrations, especially close and toward the southern Bazian town where many irrigated fields are activated.

5.3.2 Anions

- ***Bicarbonates (HCO_3^-)***

Since the pH of the water ranges between 7 and 8 particularly in the wet seasons, all of the carbonate hardness calculated by titration is regarded as HCO_3^- and for some samples CO_3^{2-} is estimated too. The concentration of the HCO_3^- in the spring samples ranges between 99.2 to 320.4 and median value of 192 ppm. While for the wells, it varies from 141 to 335 ppm with median value of 201.8 ppm. The higher concentration of this ion in the study area is found within the Tile sub basin which ranges between 230 to 335 ppm, except in Solai Darband where the concentration decreases to 175 ppm.

It can also be concluded that the majority of the springs issuing from Pilaspi aquifer is relatively higher in HCO_3^- content than those flowing from Sinjar aquifer. This might be attributed to the difference in residence time of groundwater flow in the two aquifers; due to the karstic nature of Sinjar aquifer the flow rate is relatively higher than that in Pilaspi aquifer which consequently increases HCO_3^- content in the later one. This fact clearly seen from the Qushqaya and Kani Shaya springs which issuing from Sinjar aquifer, the concentration of this ion recorded as 99 and 109 ppm respectively, and this is represented as the lowest concentration overall the area.

- ***Sulfates (SO_4^{2-})***

The high concentration of the sulphate is recorded in the MCA especially at Solai Darband village (1244 ppm). The oxidation of these sulfides results in the increase of the (SO_4^{2-}) concentration within the area occupied by Fat'ha Fn. Another reason for the increment of sulphate in the Gopala town, Maryam beg and Qazanqaya villages where the concentrations are 155, 395 and 66.24 ppm respectively, this may attribute to the emission of the sulfides from sewage infiltration. On the other hand, most of the irrigated lands have concentration less than the urban area, the reason may refer to the low permeability, in which finer material of the AIA impede the percolation of the irrigated water downward over these areas. Finally, the concentration of this ion in the study area is within the permissible limits (less than 250 ppm) except in the Solai Darband and Maryam beg villages.

- ***Chloride (Cl^-)***

The ionic concentration of the (Cl^-) in the whole area shows comparatively lower values that range between 4.5 and 162 with 9.8 ppm median values in the well samples, as well as from 2.8 to 12.1 and 5.85 ppm median in the analyzed spring samples. The relatively extreme higher values are recorded in the Solai Darband, Maryam beg villages and Gopala, Bardaqaraman towns where the concentrations are 162, 87, 56.6 and 45.6 ppm respectively. On the other hand, most of the spring samples have the value less than 10 ppm.

As a whole, lower groundwater enrichment in both sulphate and chloride in almost all the aquifer types within the study area, led to the maintaining of the better groundwater quality in the area. Most of the sites where the samples were taken from the EKFA and the AIA, groundwater recharge by precipitation influence the process of new waters intrusion (recent age, as proved by Tritium isotope analyses) that contain less Cl^- and Na^+ newly reform the chemistry of groundwater and consequently dilute the concentration of these anions. Moreover, ionic exchange seems to take place in the AIA and MCA within the Tile sub basin, due to a prolonged contact with rocks represented by Neogene formations especially clays and Gypsum units within the Fat'ha, Injana and Mukdadiya formations that are dominating in the southern basin. This ionic exchange may increase the concentration of these anions with the groundwater flow direction.

- **Nitrate (NO_3^-)**

The nitrate presents in all of the springs and well samples. It ranged between 0.7 and 193 ppm with median value of 21.5 ppm in the well samples and 10 ppm in spring samples, (Table 5.5). Extremely higher concentrations are found in well samples from Gopala, Allai and Bardaqaraman towns which lie in Bazian sub basin where livestock population is comparatively higher and people are mostly dependable on water from the shallow wells (15-30 m depth). Solai Darband village which is located in Tile sub basin also has higher concentration of this anion (146 ppm). Almost all the spring samples showed nitrate concentration within the permissible limit based on the WHO (2008) and Iraqi standard (1996), except samples from Warmziar spring (55.5 ppm) and this may attribute to the anthropogenic activities in the area that is well cultivated and the accumulation of trees and grass on and around the spring may be the reason beyond this abnormal concentration (Fig 4.11 D).

5.3.3 Heavy metals

A total number of 10 samples for analyzing (Cd, Cu, Zn, Pb, Mn, and Ni) were taken and analyzed at Twin River Institute and 25 samples for analyzing (F and Br) were analyzed at the laboratory of Chemistry in College of Science, University of Sulaimani. Highly urbanized and more industrially and agriculturally active areas have been selected for analyzing heavy metals, such as Bazian, Tainal, Gopala and Bardaqaraman towns, as well as in industrial factories, like Mass Cement and Bazian Oil Refinery (Fig 5.4). The concentration of these analyses is shown in tables (5.6). Brief descriptions of some of the above heavy metals are presented in the following section:

- ***Cd***; Cadmium, is released to the environment in wastewater, and diffuse pollution is caused by contamination from fertilizers and local air pollution (WHO, 2008).

Table (5.6) WHO guidance levels and concentration of some Heavy metals in the groundwater samples taken mostly from wells and main springs sites in the Basara basin on April and September -2009

Sites	*Cd _mg/L*	*Cu_ mg/L*	*Zn_mg/L*	*Pb _mg/L*	*Mn _mg/L*	*Ni _mg/L*	*F_mg/L*	*Br_mg/L*
Site-1	ND	ND	0.032	ND	0.064	0.06		
Site-2	ND	ND	0.168	0.003	0.044	0.048	0.0486	0.0749
Site-3	0.003	0.003	0.042	0.1	0.054	0.136	0.0197	0.1154
Site-4							0.0054	ND
Site-5							0.0328	ND
Site-6	0.007	0.005	0.163	ND	0.014	0.022		
Site-7	0.008	0.002	0.024	ND	0.011	0.022	0.0467	ND
Site-8							0.021	ND
Site-9	0.005	0.003	0.012	ND	ND	0.083		
Site-10	ND	0.009	0.009	ND	0.062	0.012	0.032	ND
Site-11							0.106	ND
Site-12							0.089	ND
Site-13							0.075	ND
Site-15							0.006	ND
Site-16							0.0324	ND
Site-17	ND	0.023	0.023	ND	0.086	0.085	0.037	0.116
Site-18	ND	0.008	0.126	ND	0.217	0.023	0.026	ND
Site-19							0.134	ND
Site-20							0.1428	ND
Site-21						0.023	0.042	ND
Site-22							0.029	ND
Site-23							0.058	0.043
Site-24							0.051	ND
Site-31							0.027	ND
Site-32							0.0316	ND
Site-34			0.022				0.065	ND
Site-35							0.082	ND
Site-36	0.01	0.031	0.065	0.026	0.103	0.171		
Site-40							0.1899	ND
Maximum permissible level per:								
WHO, (2008)	***0.003***	***2.0***	***1.1***	***0.01***	***0.1***	***0.07***	**1.5**	**0.01**
Iraqi st. (1996)	***0.004***	***1.0***	***3.0***	-	***0.05***	***0.02***	**-**	**-**

ND: means not detected

Nearly half of the measured concentrations of cadmium in the analyzed groundwater samples show values in range between 0.003 - 0.01 ppm, and in most cases undetectable. Almost all the analyzed measured samples show a slightly higher concentration than the permissible level of 0.003 ppm as proposed by the WHO (2008). Two of these samples which have higher concentration of this element are located in the industrial area (Mass cement factory "site.6" and Bazian Oil Refinery "site.9"); the other two samples are situated in Bardaqaraman town "site.7" and Solai Darband village "site.36". Pollution of groundwater in these locations may result of the leakage from sewage waste water.

- ***Cu;*** Results of the analyzed Cu element showed the concentration in the range of 0.002 to 0.031 with median value of 0.006 ppm. This implies that all groundwater samples fall under the permissible limit of Cu concentration based on WHO (2008) and Iraqi standard (1996) which give 2ppm and 1ppm respectively, and there is no hazards associated with this element.
- ***Zn;*** Based on WHO (2008), surface water and groundwater normally do not exceed 0.01 and 0.05 ppm respectively, concentrations in tap water can be much higher as a result of dissolution of zinc from pipes.

  The concentration of this metal in groundwater samples was in the range of 0.009 to 0.168 and 0.032 ppm median values. Some of them exceeding the recommended concentration in groundwater of 0.05 ppm, such as well samples in Tainal, Mass cement factory and Asia storage wells. Dissolution of zinc from well pipes as well as percolation of sewage may be the reasons for zinc pollution in these localities. While the remainder samples are under the permissible standard limit.
- ***Pb;*** Most of the analyzed groundwater samples show undetectable concentration of this metal; only two samples which located in Gopala and Solai Darband village have the concentration of 0.1 and 0.026 ppm respectively, and these values exceeding the standard permissible limit of this element in drinking water (0.01 ppm).

- ***<u>Mn and Ni;</u>*** The measured concentration of these elements in groundwater samples was in the range of 0.011 to 0.217 with the median value of 0.062 ppm for the Mn, and 0.012 to 0.171 ppm for Ni element.

  Only two analyzed samples exceeding the recommended concentration for Mn (site 18 and site 36), while for Ni, four samples exceeding the permissible limit based on WHO (2008). Generally, most of the contaminant samples from these sites restricted to the wells located in the highly urbanized and active industrial areas as well as agricultural fields. In general, pollution of groundwater in these locations may result from an industrial disposal and leakage of sewages.

5.3.4 Total Hardness (TH)

Hardness is a property of water which causes difficulty of lathering with soap. It is caused primarily by calcium and magnesium ions. Total hardness for the analyzed samples was calculated based on equation (5.2) proposed by Faure (1998), and the results is presented in Appendix (5.C).

Hardness $_{\text{equivalent } CaCO_3}$ = 2.497 (Ca^{2+}) + 4.115 (Mg^{2+}) ………….. (5.2)

Where, all the units should be in (ppm).

The hardness varies from 140 to 1131 ppm in the analyzed well samples, but it ranges from 365.5 to 1115.2 in the spring samples. As can be inferred from table (5.7), only 10% of the spring sample exhibit very hard water while, 28.5% of the well samples can be classified as very hard water according to the classification of water which is based on TH as suggested by Sawyer & Mc catry (1967), (Table 5.7).

Table (5.7) Water classes and range of the TH of the groundwater samples of the Basara basin based on TH values as suggested by Sawyer & Mc Catry, (1967)

Range of TH as $CaCO_3$ (ppm)	Water class	Springs %	Wells %
< 75	Soft	-	-
75-150	Moderately hard	10.5 %	14 %
150-300	Hard	79 %	57.5 %
➢ 300	Very hard	10.5 %	28.5 %

5.3.5 Alkalinity

Alkalinity is the ability of water to neutralize acids. Carbonate and bicarbonate are the main sources of alkalinity in groundwater. The range and description of alkalinity in the area is presented in Appendix (5.C).

In the studied area, the range of total alkalinity concentration is between 40 to 137 ppm, in both well and spring samples, and this implies that all the groundwater samples could be classified as slightly alkaline since the concentration is less than 150 ppm, especially during the wet period.

5.4 Classification of groundwater

The groundwater samples of the study area are classified according to the Piper, Durov and Pie charts classifications.

5.4.1 Piper diagram

Based on the abundance of the different ions, groundwater in the study area has been classified into 3 different hydrochemical groups. These groups have been termed A, B and C and their distributions are reflected by the Piper diagram (Fig 5.2).

- ***Group A***

In general, all springs and most of the well samples are represented by this group which is dominated by alkaline earth metals and bicarbonate. This type shows the freshest groundwater in the study area. The impact of the carbonate rocks on the composition of the groundwater type of this group clearly felt. Therefore, high content of the alkaline earth metals could be attributed to the groundwater recharge from the carbonate rock represented by Sinjar and Pilaspi formations that surrounding the studied catchment.

- ***Group B***

The samples of group ***B*** are characterized by the dominance of the alkaline earth metals and salts (chloride and sulphate). This hydrochemical group includes two samples from drilling well, lie in Gopala and Solai Darband village.

- ***Group C***: The high content of salts with alkali metals marks this group. One sample from deep well is form this group and it lies in the southern basin at Mariam Beg village.

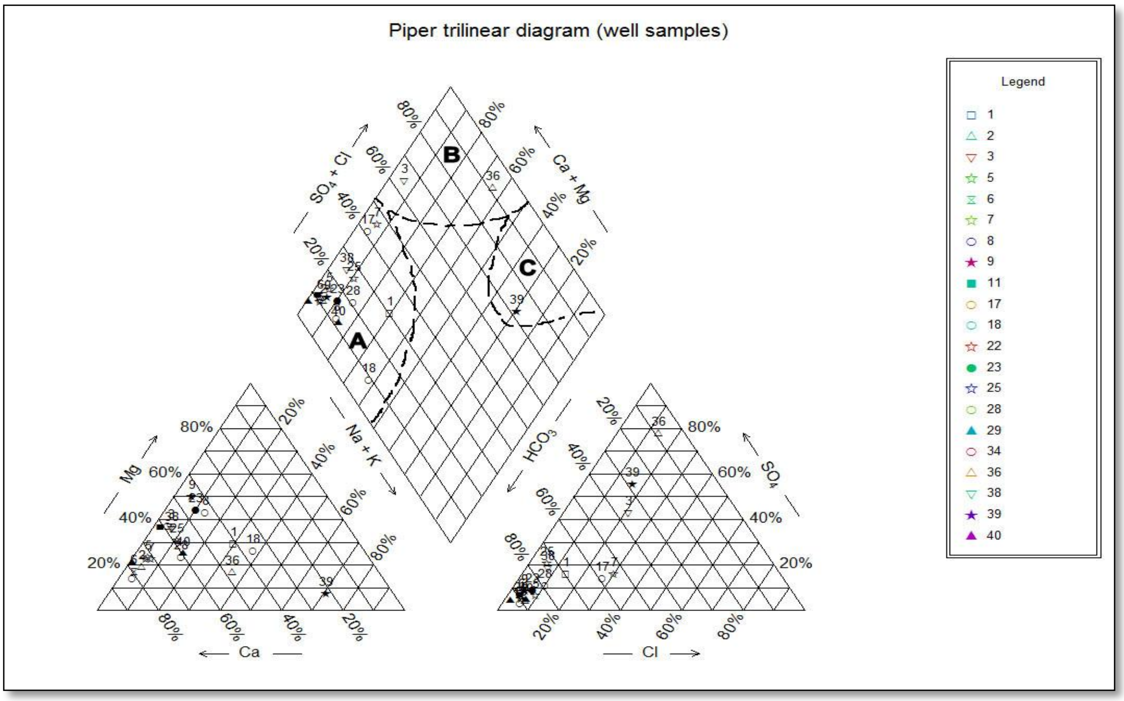

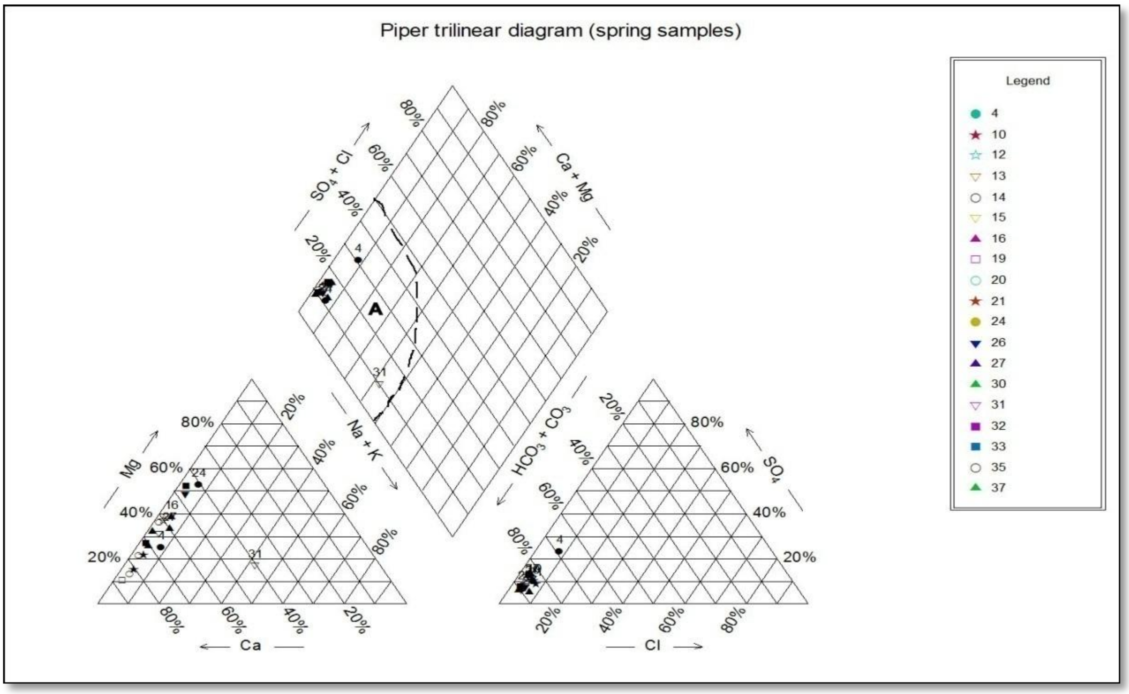

*Fig (5.2) Piper diagram shows the hydrochemical composition of the groundwater samples (in %meq/l) from the study area in wet season. Three different hydrochemical groups are distinguished: Group **A** represents the sample with high alkaline earth metals and bicarbonate, Group **B** with high content of alkaline earth metals and salts, and Group **C** with high alkali earth metals and salts. The diagrams show also the distribution of the wells and springs samples related to different hydrochemical groups separately.*

5.4.2 Durov diagram

Figure (5.3) shows the water classification according to Durov's classification and the complete similarities with the results of the Piper classification for both well and spring samples

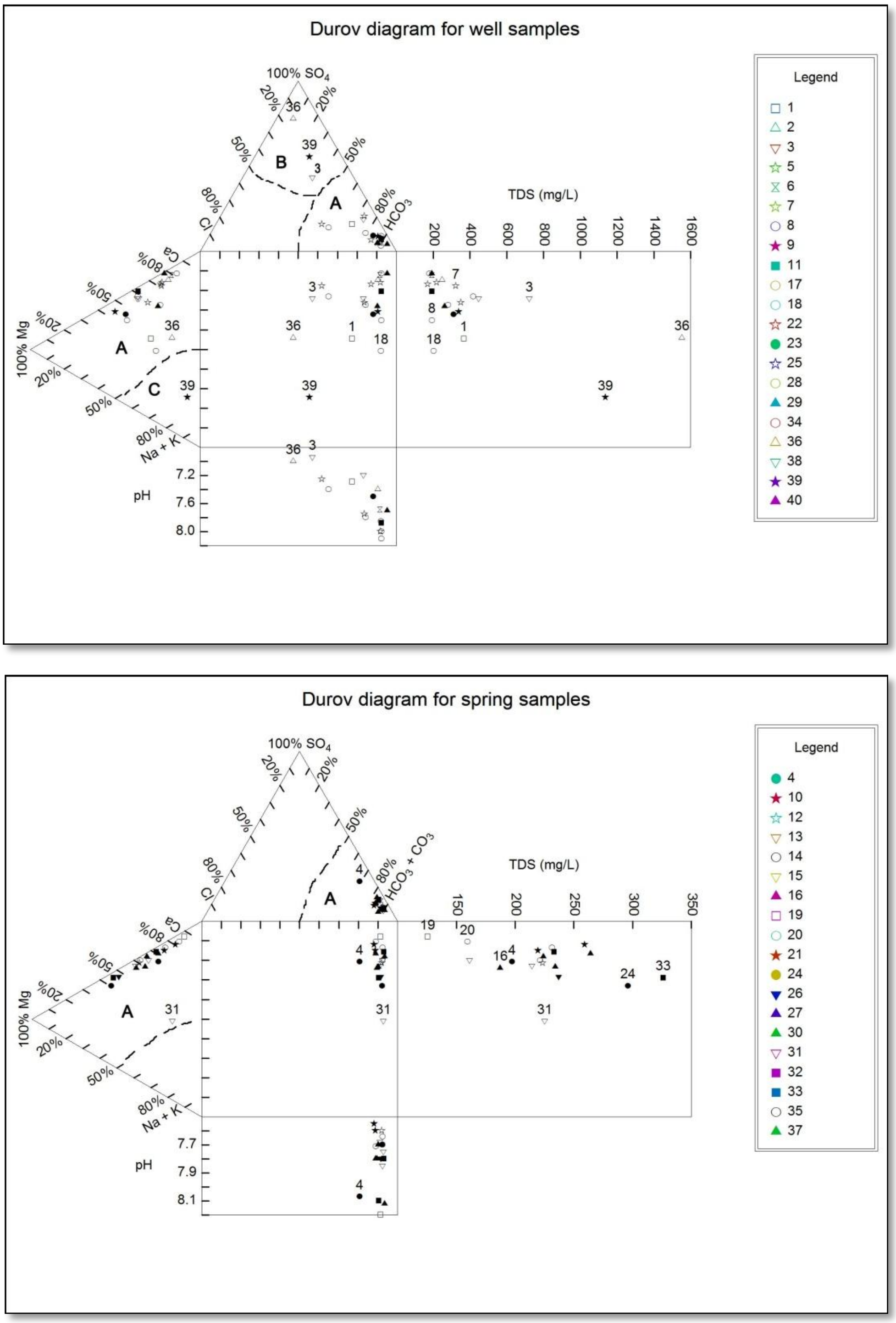

Fig (5.3) Durov diagram representing the dominant groundwater chemistry types of well and spring samples for wet season, in the Basara basin

5.4.3 Pie charts

Unlike Piper and Durov diagram, Pie chart diagram is used for presenting spacial distribution of water type for each sample separately. Accordingly, almost all the groundwater samples are dominated by Ca then by Mg HCO_3^- water type, and these two cations collectively assigned as group ***A*** in Piper and Durov diagrams. Some analyzed samples in the study area from wells and spring samples which were analyzed in April, (2009) are presented in Fig (5.4).

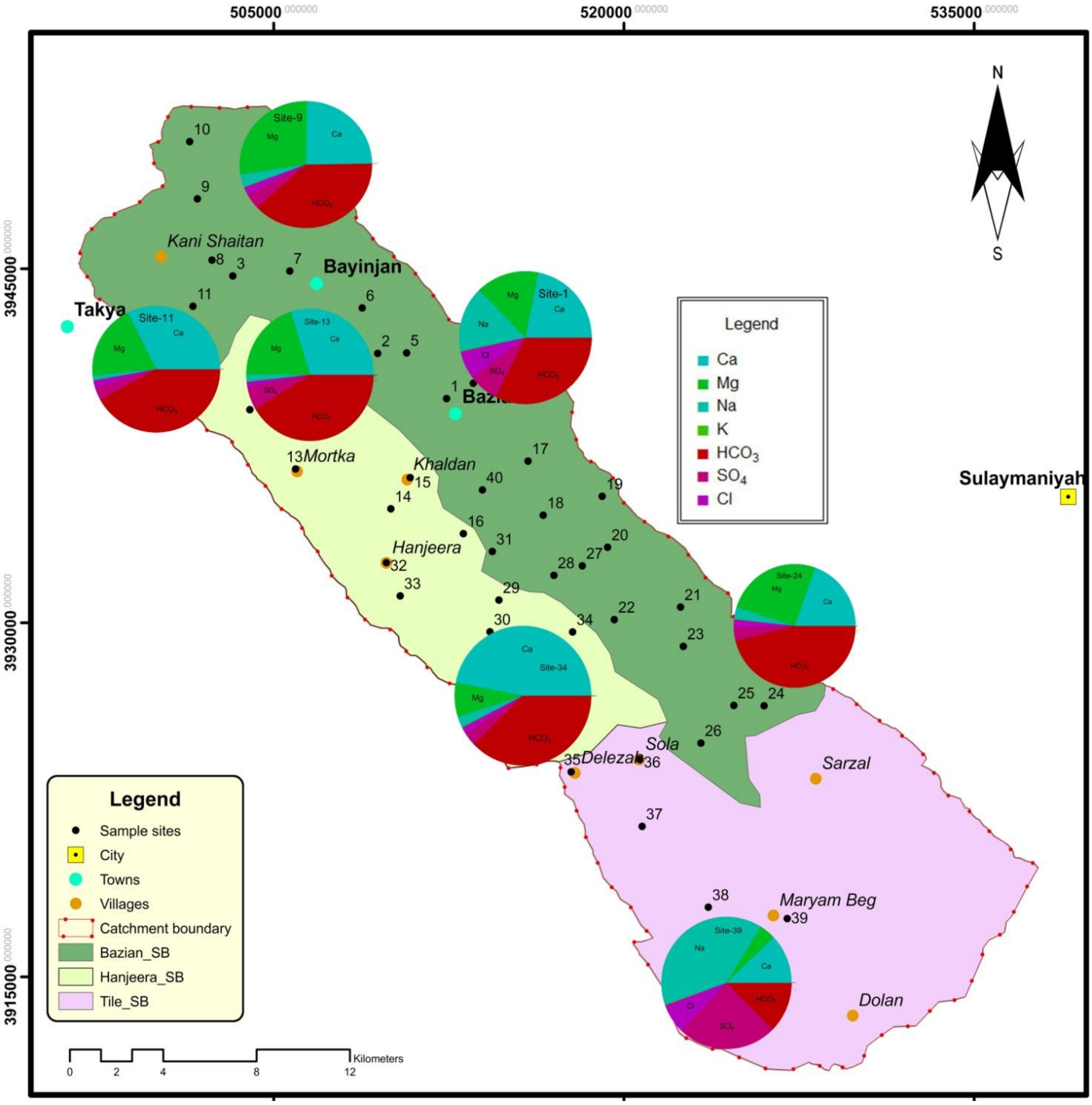

Fig (5.4) Sample sites and Pie chart diagram, showing main groundwater chemistry type in the Basara basin of some analyzed well and spring samples in epm %.

5.5 Groundwater suitability

The hydrochemical investigations of groundwater normally aim to the assessment of groundwater suitability for drinking, irrigation, industrial and other purposes. Due to climatic changes and high demand of fresh water in the study area where the semi arid condition is prevailing, groundwater availability with a good quality probably may be precarious in the next few decades. However, groundwater quality remains an important issue as geological and hydrogeological circumstances as well as human impacts highly affects water quality. In the following section, the groundwater suitability is discussed based on several categories:

5.5.1 Drinking water purpose

The sub division of the groundwater into three hydrochemical groups as discussed earlier, facilitates the assessment of the potability of groundwater. Most of the analyzed samples which located in the zone of ***A*** are found to be suitable for domestic use. This is because the classification was based mainly on the concentration of the major cations, and anions as long as each ion was found to be within the permissible limit with some exception as tabulated in table (5. 8). On the other hand, the exploitation of groundwater from group ***B*** and ***C*** should always be cautiously treated since the salts content is high. This implies that high attention should be paid for its exploitation, particularly in the areas where Fat'ha Formation is exposed or it is believed to have impact on the interaction with the groundwater flow direction, and this is true for the southern area close to Solai Darband and Maryam Beg villages where the concentration of different elements in the drilling well samples of these pockets is far beyond the permissible limits and too harmful for human health (Fig 5.1). Therefore, groundwater in these saline areas should be exploited to cover only the higher demands. Another sources for water, mainly surface water collected after rainy seasons (especially in the case for Maryam beg and Qazanqaya) as well as bringing water from Tile stream close to Solai Darband village to provide their demands should be highly considered, established and developed in these area.

Table (5.8) Evaluation of the groundwater samples of the Basara basin with respect to WHO and Iraqi standards

Parameter	Range of water samples	WHO recommendations 2008		Iraqi Standard 1996	Suitability of taken samples (from chemical point of view)
		Range limits	Max. permissible	Range limits	
Temp.(C^0)	16.5-26.5	8-25	-	-	Suitable except Shekh mand spring
PH	6.9 - 8.2	6.5-9.5	6.5-9.2	6.5-8.5	Suitable
Ca^{2+}	33 - 337	75	200	50	Suitable except Sollai Darband well
Mg^{2+}	8 - 71	50	125	50	Suitable
Na^+	1.4 - 300	200	250	200	Suitable except Sollai Darband and Maryam beg wells
K^+	0.11 – 5.7	10	12	-	Suitable
Cl^-	2.8 - 162	250	-	250	Suitable
SO_4^{2-}	5.1 - 1244	250	-	250	Suitable except Sollai Darband and Maryam beg wells
NO_3^{--}	0.7 - 193	50	-	50	Suitable except Gopala, Allai, Bardaqaraman, Sollai Darband wells and Warmziar spring
Ni	0.01-0.17	0.07	-	0.02	All analyzed samples were contaminated except Kani sarchawa spring, based on Iraqi standard
Cd	0.003-0.01	0.003	-	0.004	Suitable except Bardaqaraman, Mass cement, Oil refinery and Solai ndarband wells
Cu	0.002-0.03	2		1	all suitable
Zn	0.009-0.17	1.1	3	3	all suitable
Mn	0.01-0.217	0.1	-	0.05	suitable except Bazian health dir., Allai, Asia storage and Sola wells, as well as Kani sarchaw spring based on Iraqi standard
TH	115 - 1131	-	-	500	Suitable except Gopala and Solai Darband wells
TDS	126 - 1555	1000		1000	Suitable except Maryam beg and Sollai Daeband wells

It is worth mentioning that, this conclusion of suitability of most of the groundwater for domestic uses are based on the chemical analysis only, as no biological and bacteriological tests performed, due to limited fund, therefore attention should be paid toward this issue in future.

5.5.2 Irrigation purpose

The assessment of groundwater suitability for irrigation purpose has been achieved based on the basis of the relation between adjusted sodium adsorption ratio (SAR) and the electrical conductivity (EC). The EC more or less measures the salinity while the SAR measures the tendency of the replacement or exchange of the calcium and magnesium on the soil particles with sodium adsorbed in groundwater.

The United States Salinity Diagram (Richards, 1954) classifies irrigation water into sixteen classes depending on electrical conductance (µS/cm) at 25°C and sodium adsorption ratio (SAR). Later, Al Manmi (2007) has proposed an excel program and presented a table for irrigation quality class rating to describe the calculated adjusted sodium adsorption ratio (SAR) and its suitability of groundwater for irrigation (Table 5.9). It is represented by the formula (5.3)

$$\mathrm{SAR} = \frac{\mathrm{Na}}{0.5\sqrt{\mathrm{Ca+Mg}}}\ \mathrm{x}\ (1+ (8.4 - \mathrm{pHc}))\ \mathrm{in\ meq/l}\ \ldots\ldots.. \quad (5.3)$$

Where, pHc is a theoretical, calculated pH of the irrigation water in contact with lime and in equilibrium with soil CO_2.

According to the calculated adjusted SAR, the values are in the range of 0.08 and 18.07, Appendix (5.C). This relation was plotted in Fig (5.5) which represents the alkali hazard chart that begins out the alkali distribution of the waters; the latter is of high agricultural importance according to the U.S. salinity laboratory (1954). In addition to water composition, water suitability for irrigation depends on many other factors, such as climate, system of irrigation and drainage.

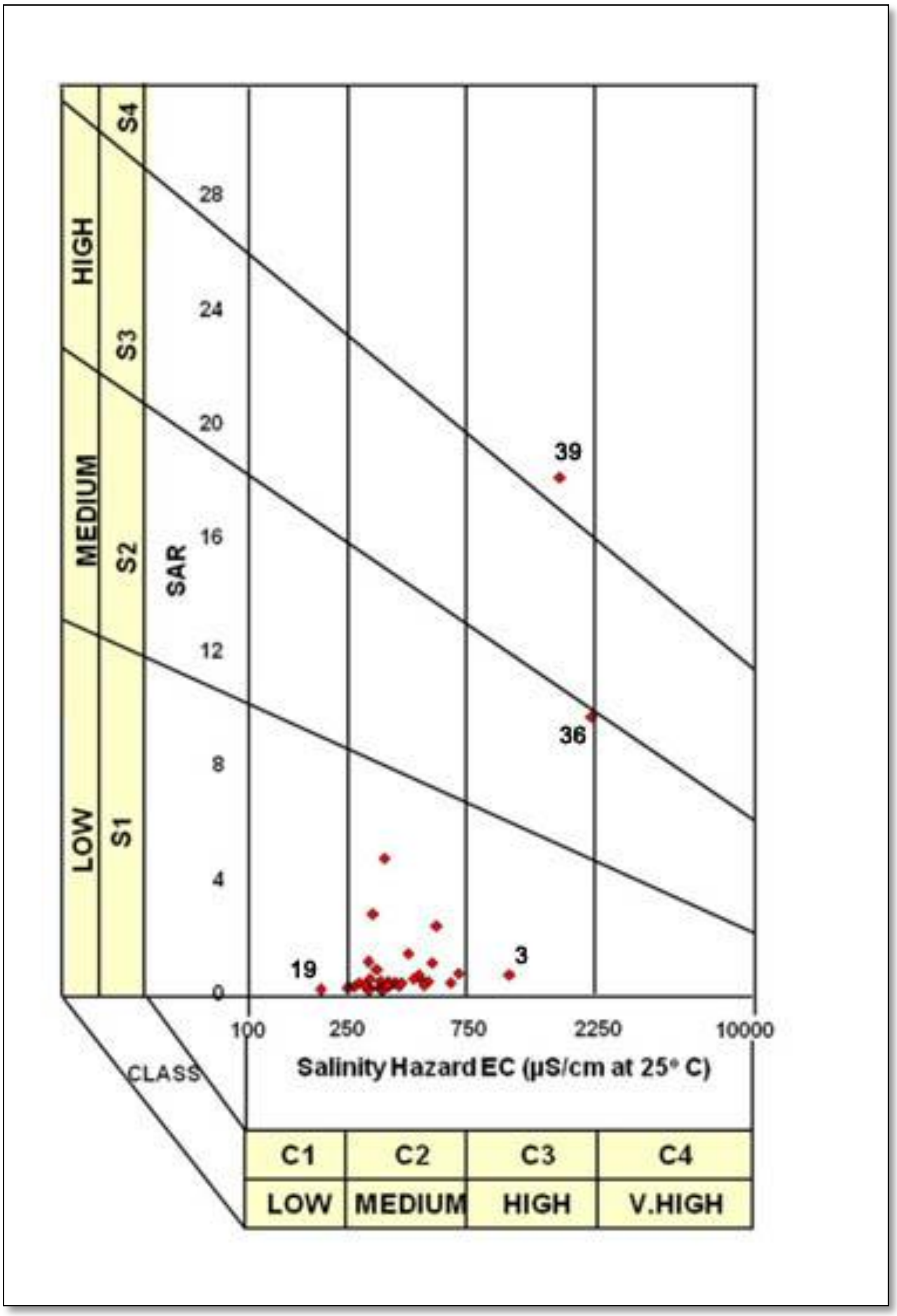

Fig (5.5) Wilcox diagram showing the relation between salinity and alkalinity hazards and their significance in detecting groundwater suitability for irrigation in the analyzed springs and well samples

Based on this figure, almost all the water of group ***A*** locates as cluster points in class (C2S1), while two spring samples which is assigned as site 19 and 20 located at Qushqaya and Kani Shaya springs respectively, and they are classified as class (C1S1) indicating low salinity and low sodium hazard waters. One sample of group ***B*** (site 3) is located in field C3S1 while the other sample (site 36) is located in C4S2 which indicating high salinity and low sodium hazard waters for the first site and very high salinity with medium sodium hazard water for the other sites as shown by Wilcox diagram (Fig 5.5). Group ***C*** which is indicated by (site 39) represents the Maryam Beg village, and locates in field C3S4 which implies high salinity and very high sodium hazard waters.

Finally, it could be concluded that all the groundwater issuing from springs as well as water that taking from wells in the studied area, indicates a good suitability of groundwater for irrigation purpose except site 39 where it locates in the field C3S4, it is doubtful and may harmful and far beyond the permissible limits.

Table (5.9) Interpretation of the quality class ratings of water for irrigation purposes based on the adjusted SAR and EC, from Al Manmi (2007)

Class	*Irrigation Quality Class Rating*
C1S1	Good
C1S2	Suitable
C1S3	Doubtful
C1S4	Doubtful
C2S1	Good
C2S2	Suitable
C2S3	Doubtful
C2S4	Doubtful
C3S1	Suitable
C3S2	Suitable
C3S3	Doubtful
C3S4	Doubtful
C4S1	Doubtful
C4S2	Doubtful
C4S3	Unsuitable
C4S4	Unsuitable

5.5.3 Industrial uses

The quality requirements for the industrial vary widely according to the potential uses. For example, salty and brackish water are commonly used for cooling purposes, particularly when they are used only once (not recycled) and can be disposed without polluting the environment (Driscoll, 1995). Many industrial factories are found in the study area located mainly in the Bazian and partially in the Hanjeera sub basins. These factories are supplied by water from private wells in each factory. The majority of the analyzed groundwater samples which are located in or close to these industrial sites are quite safe and suitable for the existing types of industry which include water bottling and other kinds of drinking, food productions and cement products.

Recently, Bazian Oil Refinery factory which is located in the northern Bazian sub basin, start working and according to some reports, some of their industrial disposal are dump and spreading over the plain area close to this site. Such practices will cause negative impacts on the environment and may pose a possible source of contamination to the groundwater. However, a big treatment plan is constructed inside this factory, but it seems to either not completed or not worked properly, thus its highly recommended to impede disposing these waste products, because they may contain heavy and many toxic metals which may need a very long time for retarding or even might not be solved by natural bio-degradation process.

Based on the water quality guide proposed by Hem (1991), the groundwater samples of the area are suitable for some industries but not for others (Table 5.10).

- ***Building and construction***

As mentioned previously, all the groundwater in the studied area is considered to be suitable for building and constructing purposes based on the permissible limits of the major ions proposed by Altoviski (1962) (Table 5.11).

Table (5.10) Water quality requirements for different industries, concentrations in ppm (Hem, 1991)

Type of Industry	Ca^{2+}	Mg^{2+}	Cl^-	HCO_3^-	SO_4^{2-}	TH	TDS	pH	Suitability of analyzed groundwater samples
Cement manufacture	-	-	250	-	250	-	600	6.5-8.5	All samples are suitable except Gopala, Sollai Darband and Maryam beg wells
Leather tanning	-	-	250	-	250	350	-	6.5-8.3	All samples are suitable except well sites (3, 25, 36, 38 and 37)
Bottling and drinks	100	-	500	-	500				All samples are suitable except well sites (3, 34, 36, 38, and spring site 37)
Freeze fruits			300		250	250	500	6.5-8.5	All samples are suitable except sites (3, 17, 24, 25, 28, 29, and from 32 to 39)
Petroleum products	75	30	300			350	1000	6-9	All water samples are suitable except sites (3, 17, 22, 24, 25, 28, 29, and from 32 to 39)
Textile	100	50	500	250	100	900	1000	6.5-8	All water samples are suitable except sites (3, 34, 36, 37 and 38)
Paper industry	20	12	200			100		6-10	Almost all samples are not suitable for paper industry because of high Ca content and high TH

Table (5.11) Suitability of groundwater for building and construction (Altovisky, 1962)

Major Ions	Na^+	Ca^{2+}	Mg^{2+}	Cl^-	SO_4^{2-}	HCO_3^-
permissible limit (ppm)	1160	437	271	2187	1460	350

- ***Livestock***

Based on the Altoviski (1962), almost all the groundwater of the study area have ranged from very good and excellent for livestock and poultry uses, except Solai Darband well sample where the sulfate concentration is recorded to be 1244 ppm, and this can be classified also as a good water type according to table (5.12).

Table (5.12) Groundwater utilization for livestock and poultry as suggested by Altoviski (1962)

Elements	Very good water	Good water	Allowable	Could be used	Max. permissible
Na^{+}	800	1500	2000	2500	4000
Ca^{2+}	350	700	800	900	1000
Mg^{2+}	150	350	500	600	700
Cl^{-}	900	2000	3000	4000	6000
SO_4^{2-}	1000	2500	3000	4000	6000
TDS	3000	5000	7000	10000	15000
TH	1500	3200	4000	4700	5400

CHAPTER SIX

GROUNDWATER VULNERABILITY MAPPING

6.1 Preface

Nowadays, aquifer vulnerability assessments are carried out in almost all developed countries in areas where water resources are under stresses originating from urbanization, industrial and agricultural activities. The vulnerability studies can provide valuable information for stakeholder working on preventing further deterioration of the environment (Mendoza & Barmen, 2006). Aquifer vulnerability studies are useful in the evaluation of the economic impacts of the waste disposal in highly vulnerable areas. Moreover, they are providing preliminary information and criteria for decision making in such areas as designation of land use controls, delineation of monitoring networks, and management of water resources in the context of regional planning as related to protection of groundwater quality (Bachmat & Collin, 1990). Yet internationally, vulnerability maps were becoming an essential part of groundwater protection schemes and a valuable tool in environmental management (Warren et al 1998).

The first attempt to the concept of groundwater vulnerability to contamination was applied by Margat (1968) in France. Then there were several approaches for developing aquifer vulnerability assessment maps, such as DRASTIC (Aller et al, 1987), GOD (Foster, 1987), AVI (Van stempvoort et al, 1993), SINTACS (Civita, 1994), etc. A thorough overview of existing methods is given in Vrba and Zaporozec (1994) and in Gogu and Dassargues (2000). These methods have been mainly applied to groundwater protection in porous aquifers, except the EPIK (Doerfliger and Zwahlen, 1998; Doerfliger et al, 1999), PI (Goldscheider et al, 2000) and COP (Vias et al, 2006) methods which were specifically developed for the assessment of vulnerability in karstic area (Hamza, et al, 2007).

Recently, the concept VURAAS (Vulnerability and Risk assessment for Alpine Aquifer System) was developed in Alpine karst area in Austria, by Cichocki (2003) and Zojer (2003), in which the final result of this system is the risk map which shows areas at varying degree of potential groundwater contamination risks. The map of vulnerability and the map of Hazards are the basis for the risk map.

6.2 DRASTIC method

The best known and probably the most widely applied scheme of vulnerability assessment was developed by the US Environmental Protection Agency (USEPA) and is known as the DRASTIC methodology, Aller et al (1987), applied later in several regions by different researchers where they modified this system to meet a wide range of application such as land use index, lineaments, aquifer thickness and impact of contaminant. Thirumalaivasan et al (2003) developed a software package AHP-DRASTIC to derive rating and weights for modified DRASTIC model parameters (Sener et al, 2009).

In general, the DRASTIC system is composed of two major parts: (1) the designation of mappable units, termed hydrogeological settings; and (2) the application of a numerical scheme of relative ranking of hydrogeological factors (Lee, 2003). Hydrogeological factors help to evaluate the relative groundwater pollution potential of any hydrogeological setting.

Hydrogeological setting is a composite description of all the geological and hydrological factors controlling groundwater flow into, through and out of an area (Kim & Hamm, 1999). Recently, geographic information system (GIS) techniques have been widely used in aquifer vulnerability mapping. The major advantage of GIS-based mapping is the combination of data layers and rapid change in the data parameters used in vulnerability classification (Wang et al, 2007).

A DRASTIC method was derived from rating and weights associated with the seven parameters. These are:

Depth to groundwater (D), Net recharge (R), Aquifer media (A), Soil media (S), Topography (T), Impact of the vadose zone (I) and Hydraulic conductivity (C) (Fig 6.1).

Each parameter is subdivided into ranges and is assigned different ratings in a scale of **1** least contaminant potential to **10** highest contaminations potential.

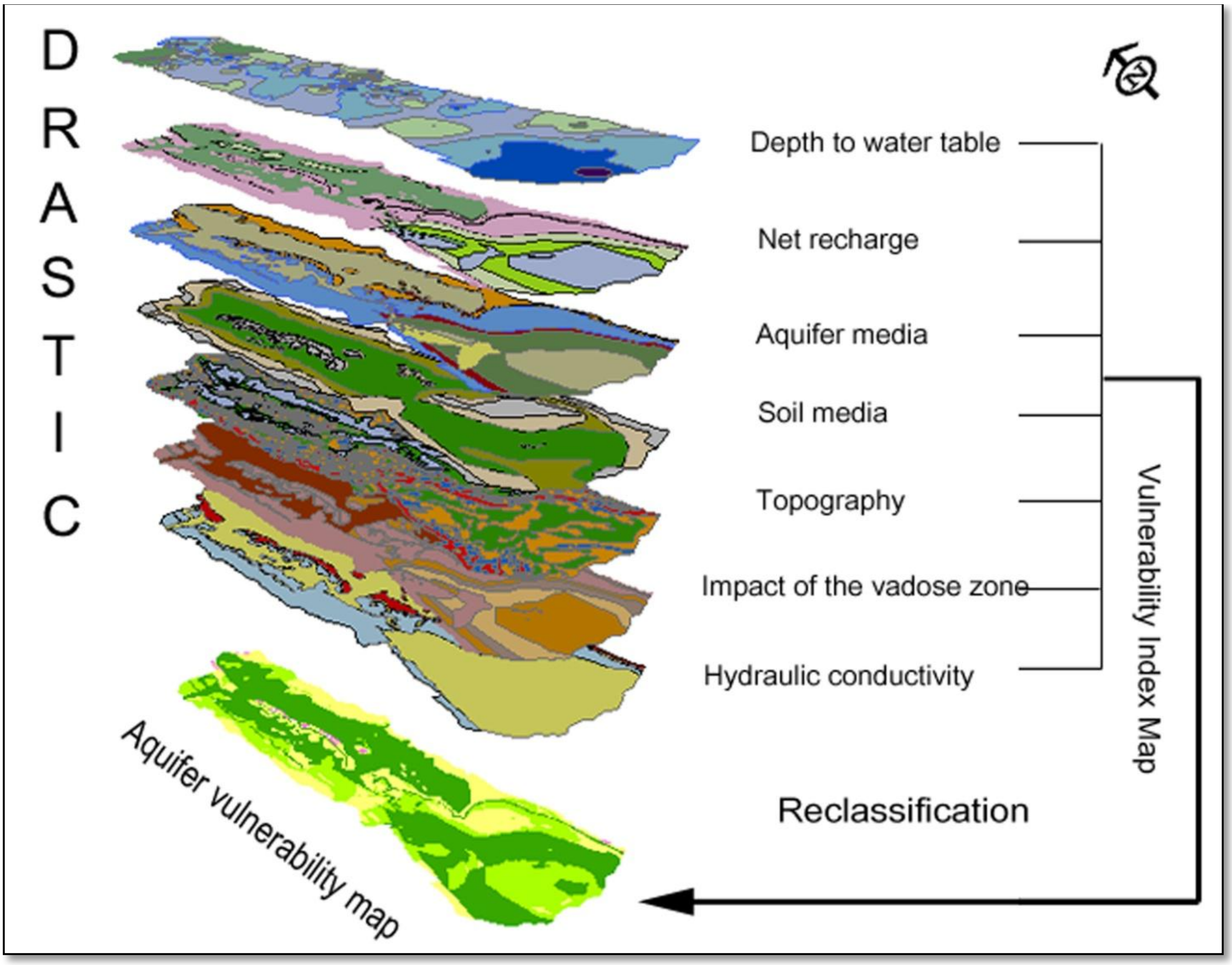

Fig (6.1) Methodology flowchart for DRASTIC method

6.2.1 Depth to water table map (D_MAP)

This factor deals with the duration of contaminant in liquid phase to travel through the unsaturated zone to reach the water table in the aquifer. In general the deeper the water table, the longer the pollutant material in liquid phase takes to reach the groundwater which gives a chance for attenuation of contaminant material by degradation or natural retention.

Generally, Depth of water is computed from water table surface topography, then water table contours are digitized, geo-referenced and rasterized. Water table elevations is actually represent the static water level, and they are subtracted from land surface elevation on a pixel by pixel basis to compute depth of water using profiles from the archives of the DGWS and other private company which drilled these wells inside the study area.

For this study, groundwater head measurements were made in 283 wells. These data were recorded in the GIS environment to construct depth to water table map (Fig 6.2). The layer was converted to raster format with 80m cell size. Most of the data were collected on August and September, 2009 by the team from directorate of groundwater of Sulaimaniyah (DGWS) and partly by the researcher during field works. The rating for this parameter presents a wide range of variation from the occurrence at ground level at the zones of natural discharge represented by springs to greater depths exceeding 110m close to the Bazian Oil Refinery site.

The rating for depth to water table varies from 9 (for 1.5-4.5 m water table depth) to 1 (for more than 30 m depth), based on the ranges and rating for depth to groundwater table proposed by Aller et al (1987) (Table 6.1).

As can be depicted from the depth to water table map (Fig 6.2), the southern part and some sites in the central area are the shallowest location in the basin; therefore the highest rating value belongs to these areas. In contrast, northern and northwestern part have water table more than 30m, this probably related to overexploited withdrawal groundwater at these locations, especially nowadays some of the densely settlement towns (like Takya and Chamchamal cities where they are located several kilometers to the west of the area) provide all or most of their consumption of potable water on the groundwater through drilling wells percolating both Sinjar and Pilaspi formations close to Kani shaitan area) in addition to that several big factories of water bottling (such as Ala Cola and Ice Water were built inside these areas), as well as the two big cement factories (Bazian and Mass Cement) have their own drilling wells where they are draying water for their production. All these activities make groundwater to be depleting more in comparison to the surrounding area.

It is necessary to mention that, the sharp topography in the area may cause great values of groundwater depth; at the end, all these factors depleted the groundwater table make the area less vulnerable and have rating of 1 and 2.

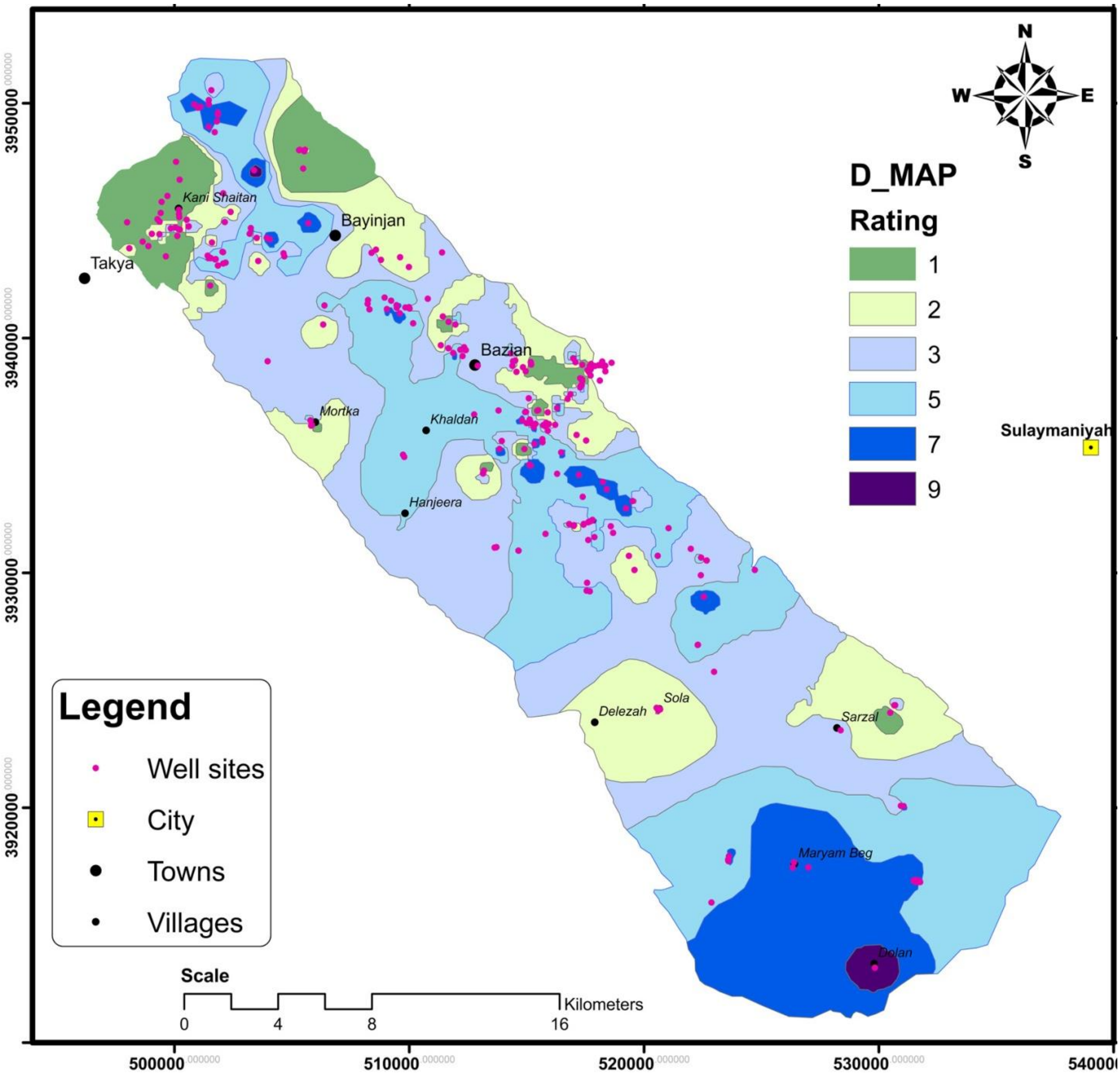

Fig (6.2) Rating map of (depth to water table) (D_map) of the Basara basin

Table (6.1) Ranges and rating for depth to groundwater table proposed by Aller et al (1987)

Depth to water (m)	*Rating*
Between 0 and 1.5	10
1.5 - 4.5	9
4.5 - 9	7
9 - 15	5
15 - 23	3
23 - 30	2
More than 30	1

6.2.2 Net recharge (R_MAP)

According to Mohammadi et al (2008), net recharge; is the total depth of water which infiltrates into the aquifer on an annual basis. Contaminant can move with groundwater easily depending on water quantity. Therefore, net recharge is a very important factor for assessment of aquifer vulnerability. Net recharge includes the average annual amount of infiltration and does not take into consideration the distribution, intensity or duration of recharge events (Al-Zabet, 2002). Thus, the more the recharge, the greater the contamination of groundwater will occur.

In order to evaluate the net recharge percolated to the basin, the simple groundwater balance has been used, eq (6.1).

$NR = P – ET – R_0$ ………………. (6.1)

Where;

NR: is the net recharge in mm/year, P: is the annual precipitation in mm; ET is the evapotranspiration in mm/year calculated by FAO Penman Monteith method and R_0 is the total runoff in mm.

Total runoff for each month is calculated using SCS method, accordingly the annual runoff was 149 mm/year (approximately 21.5 % of the annual precipitation), while the expected evapotranspiration for the wet season (October to May) was 387 mm. Accordingly, the total expected average net recharge is estimated in 96 million cubic meters per year or 168 mm/year on average or 24 % of the total annual rainfall (when recharges from surface runoff are not considered in this calculation) with sharp variations, ranging from hardly 15 mm/year to 238 mm/year, as explained in chapter four and the results is given in Table (4.2).

The rating of net recharge varies from low vulnerability **1** (for 15 to 45 mm/year), such as that of urban area, aquiclude or aquifers with very low to low permeable rocks, (Kolosh, Gercus, Fat'ha and Injana formations fall within this rate) to high vulnerability **8** (for 220 to 238 mm/year) in the karstic fissured aquifer represented by both Sinjar and Pilaspi formations, based on the proposed table given by Aller et al (1987) (Table 6.2).

Table (6.2) Ranges and rating for the net recharge in (mm/year) based on Aller et al (1987)

Factors	Range (mm/year)	Rating
Net Recharge	Less than 50	1
	50 - 100	3
	100 - 175	6
	175 - 250	8
	More than 250	9

The net recharge map was prepared using the inverse distance weight (IDW) interpolation method of ArcGIs spatial analyst (Fig 6.4).

Generally, IDW interpolation explicitly implements the assumption that things that are close to one another are more alike than those that are farther apart. To predict a value for any unmeasured location, IDW will use the measured values surrounding the prediction location. Those measured values closest to the prediction location will have more influence on the predicted value than those farther away. Thus, IDW assumes that each measured point has a local influence that diminishes with distance. It weights the points closer to the prediction location greater than those farther away, hence the name inverse distance weighted (Fig 6.3), "from ArcGIS help topics".

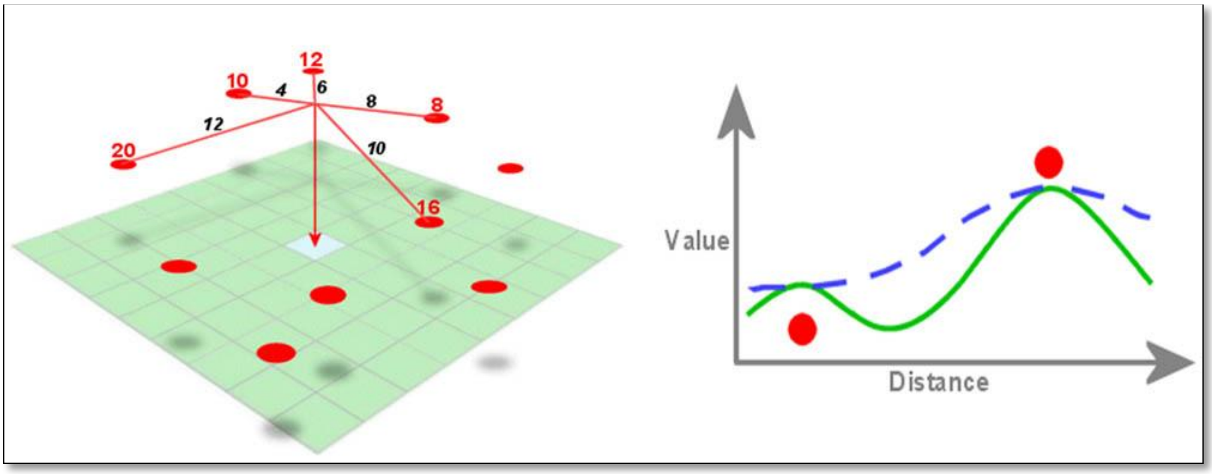

Fig (6.3) Principal of Inverse Distance Weight (IDW) interpolation method "from ArcGIS help topics"

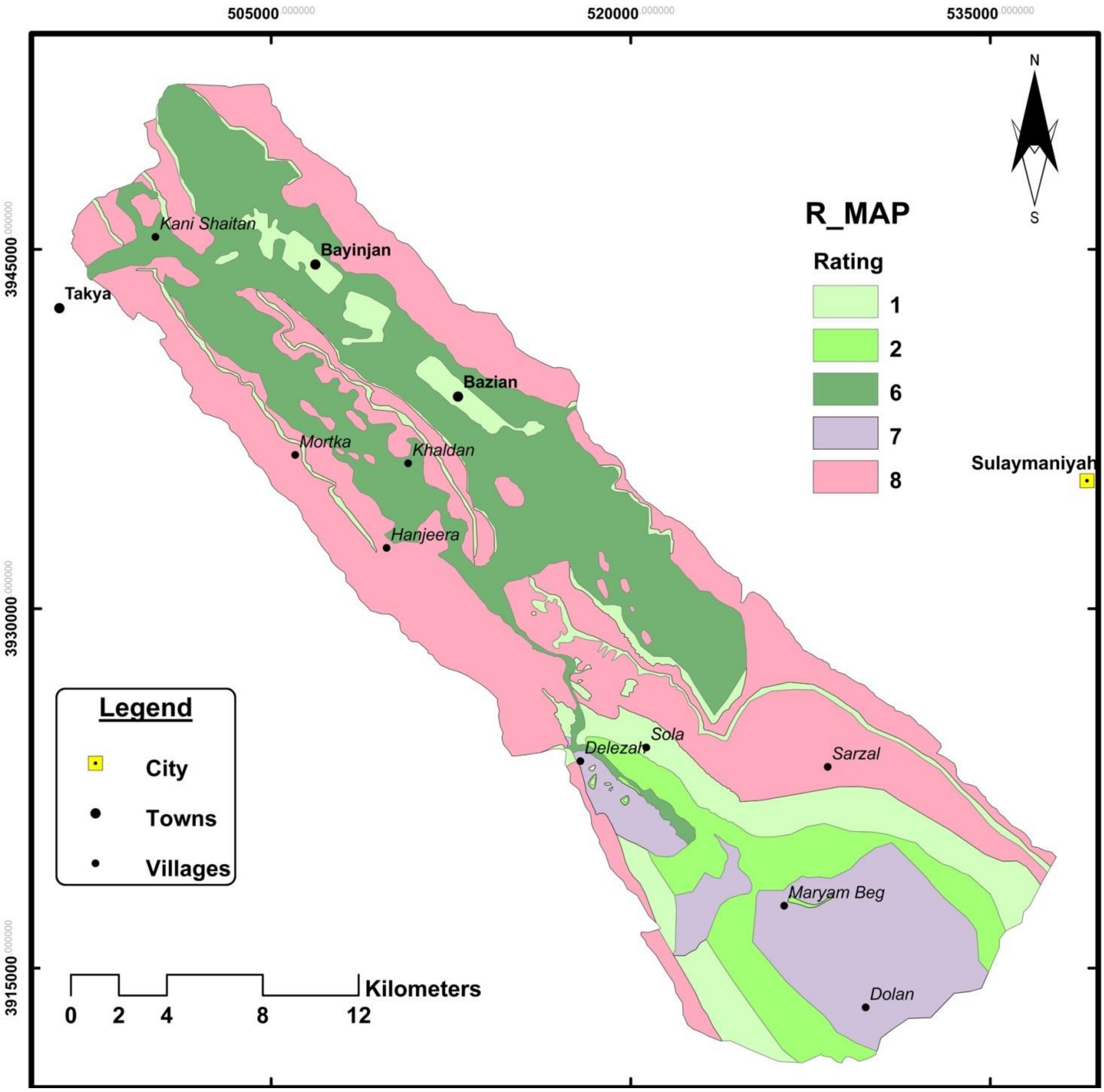

Fig (6.4) Rating map of net recharge (R_map) of the Basara basin

6.2.3 Aquifer media (A_MAP)

This factor refers to the consolidated or unconsolidated rocks through which water circulate in the aquifer. In those rocks with inter-granular porosity, or secondary (inter-granular dissolution and dolomitization in carbonate rocks), the dispersive component is controlled by the size and lithology of the walls. In fractured or karstified rocks, the advective component of transport is prevailing, thus aquifer media is responsible for the system flow control, which defines the path and length the contaminant has the cross (Hernandez et al, 2004). This parameter is highly related to the geological setting of the area. Accordingly, geological map of the basin was prepared from the field studies, benefiting from previous investigation done by Aziz (2005), Hamasur (2009) and directorate of geological survey of Baghdad (2007). The main aquifer which is being exploited in the central part of the basin is the Quaternary alluvial aquifer, in which the hydrologic condition changes according to the overlying layers, in most cases it is unconfined and it changes to semi-confined and even to the confined aquifer. The thickness was mapped using a previous geo-electrical survey done in the area by Aziz (2005), in addition to the archives of the drilling well; it ranges between 50m in most central part to 100m at Dargazen village. This aquifer is mostly sand, silt and gravel with inter-beds of sliding part of Sinjar Formation (Chapter four).

The two other most important aquifers are Pilaspi and Singar aquifers; they are classified as karstic fissured aquifer. However, fracture and fissured network system of Sinjar aquifer believed to be slightly more developed than the Pilaspi as the pumping test showed the transmissivity of this aquifer is more than the previous one.

The DRASTIC ratings were assigned according to the permeability of each aquifer medium (Table 6.3).

Table (6.3) Ranges and rating for the Aquifer media, based on Aller et al (1987)

Factors	***Range***	***Rating***	***Typical rating***
Aquifer media	Massive shale	1 - 3	2
	Metamorphic/ Igneous	2 - 5	3
	Weathered metamorphic/ Igneous	3 - 5	4
	Glacial Till	4 - 6	5
	Bedded sandstone, limestone, shale	5 - 9	6
	Massive sandstone ,massive limestone	4 - 9	6
	Sand and gravel	4 - 9	8
	Basalt	2 - 10	9
	Karst limestone	9 - 10	10

The fracture and fissured aquifer are most vulnerable medium with respect to contamination and it was assigned with rating of 7 and 8 respectively. Furthermore, most of the clastic formations identified as semi permeable to impermeable and assigned a rating of 2 and 3 at the southern part, where clay is more predominant, which implies low values of vulnerability for this area, while most of the central part is particularly difficult to classify, because it is composed of multi-layer set in which the changes in depth and facies changes are abundant, this clearly felt from the geo-electrical survey carried out in the area by Aziz (2005) (Fig 6.5). Finally the aquifer media of the basin was obtained and the rating was between 2 and 8, based on Aller et al (1987) (Fig 6.6).

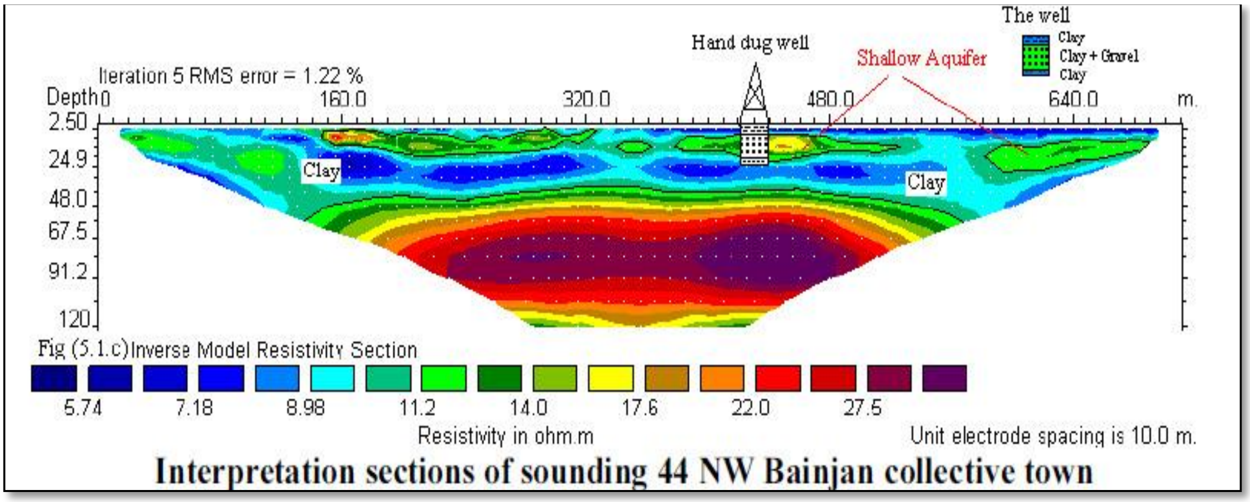

Fig (6.5) 2D electrical tomography inside the studied area (From Aziz, 2005)

6.2.4 Soil media (S_MAP)

Soil has a significant impact on the amount of recharge that can infiltrate into the ground, and hence on the ability of a contaminant to move vertically into the vadose zone (Lee, 2003). In general, the presence of fine textured material decreases infiltration, and therefore pollution potential; if the soil is thick the filtration, biodegradation, sorption and volatilization process may become important. Also, the organic matter content has the great impact on the contaminant attenuation.

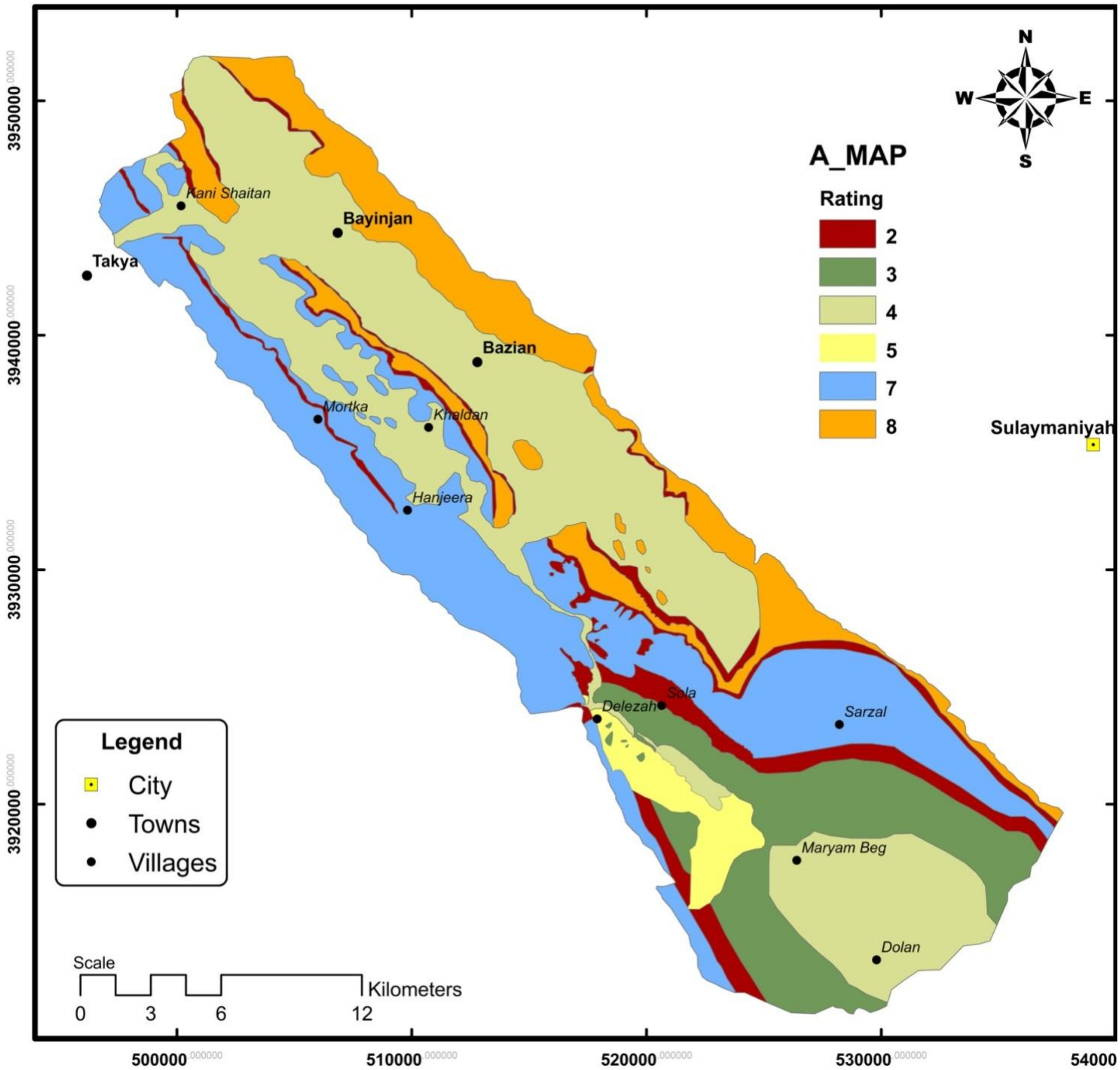

Fig (6.6) Rating map of aquifer media (A_map) of the Basara basin

For this study, the soil media of the basin was taken from soil map (Fig 3.12), and reclassified in order to meet the new classification of the DRASTIC system. Each class was assigned with rating from **10** (Thin or absent soil cover) to **2** (for Muck and clay loam), according to table proposed by Aller et al (1987) (Table 6.4).

Table (6.4) Ranges and rating for soil media, based on Aller et al (1987)

Factors	Range	Rating
Soil media	Thin or Absent ,Gravel	10
	Sand	9
	Peat	8
	Shrinking and/or aggregated clay	7
	Sandy loam	6
	Loam	5
	Silty loam	4
	Clay loam	3
	Muck	2
	Non shrinking and non-aggregated clay	1

According to the present map, 4 main classes were identified. The predominant soils are clay loam, silty loam and sandy loam. Extension and types of each soil in the studied area is presented in soil media (Fig 6.8) and tabulated in Table (6.5).

Fig (6.7) Soil cover of the area; A Thin or absent soil cover in the mountain area close to Tille village (photo was taken in March, 2010); B Thickness of soil, close to Dargazen village (photo was taken in April, 2009)

The highest vulnerability values for this factor (10) are located within the mountains area (Fig 6-7A), where no soil or thin layer of weathered soil covers is predominant. On the contrary, the lower values (3 and 4) are related to the Quaternary and clastic formations where clay and silty loam are more frequently found (Fig 6-7B).

Table (6.5) Extension and rating of soil type in the studied area

Soil type	*Rating*	*Extension area (km^2)*	*Extension area (%)*
Clay Loam	3	230	40.3
Silty loam	4	112	19.5
Loam and sandy loam	5	145	25.4
Thin or soil absent	10	84	14.8

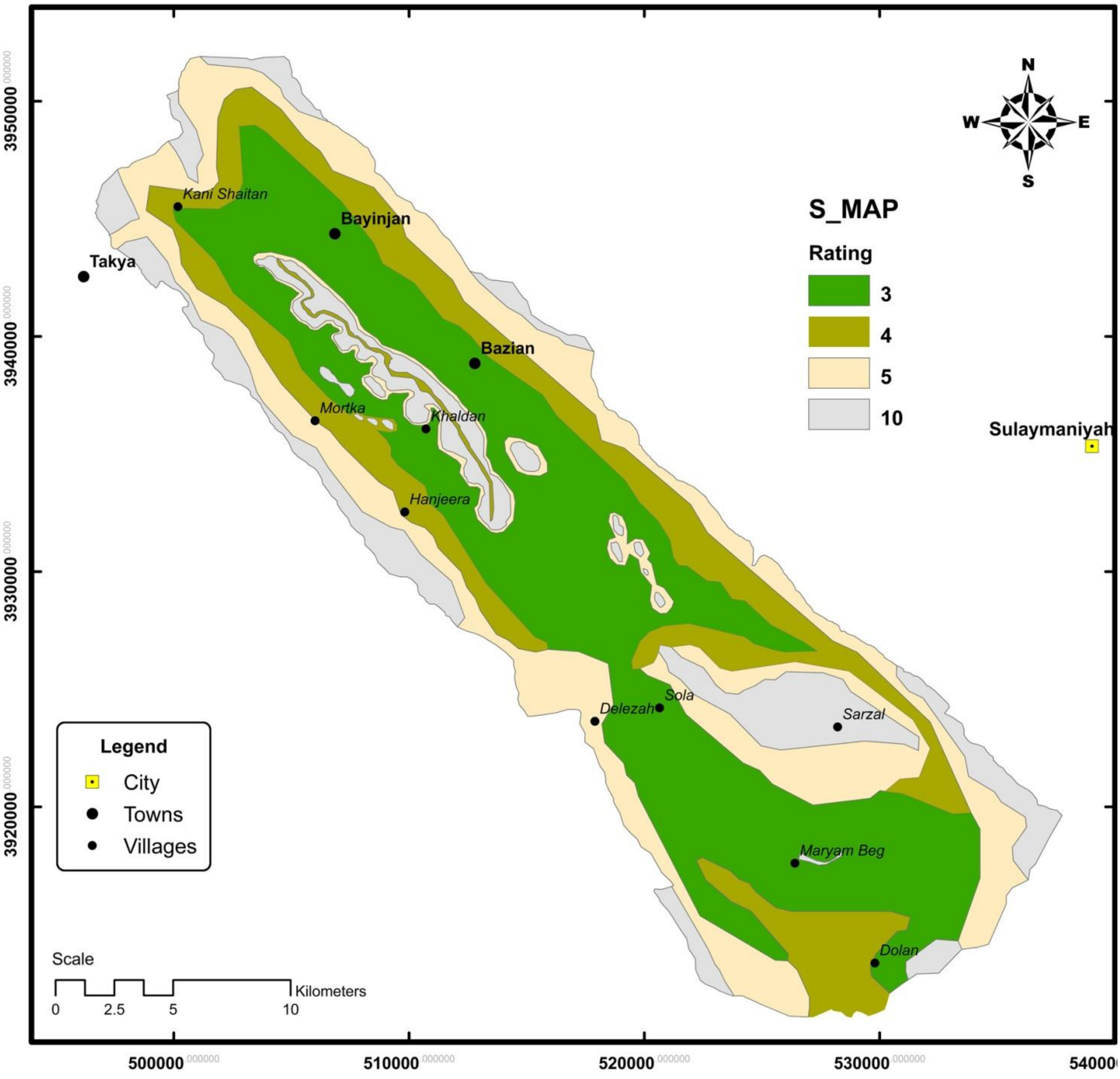

Fig (6.8) Rating map of soil media (S-map) of the Basara basin

6.2.5 Topography (T_MAP)

Topography refers to slope and slope variability over the land surface. It controls the likelihood of a pollutant to be evacuated by runoff or to remain on the ground time enough to infiltrate. When slopes are under 2%, the velocity of direct runoff is quite small, thus favoring infiltration and evapotranspiration. Conversely, when slopes are over 18%, rainwater easily runoff and can evacuate greater amounts of substances either dissolved or suspended (Hernandez et al, 2004).

The digital elevation model (DEM) from NASA srtm satellite image with resolution of 80m is used to construct the topography map layer from elevation points and the topography map by interpolation. The slope aspect was then calculated from the topography map in Arc GIS 9.3. It was sliced into ranges and assigned a rating ranging from 1 to 10 based on standard table prepared for this purpose (Table 6.6). Flat areas were assigned high rates because they slow down the runoff and allowing more time for the contaminants to percolate down to reach the groundwater, whereas steep areas increase the runoff washing out the contaminants hence are assigned low rates (Babiker et al, 2005).

Table (6.6) Ranges and rating for topography based on Aller et al (1987)

Factors	*Range (percent slope)*	*Rating*
	0 - 2	10
	2 - 6	9
Topography (%)	6 - 12	5
	12 - 18	3
	More than 18	1

Topographically, the studied area is diverted and conditioned by the geology and the deformation phase that took place during the tectonic activity during Cretaceous in the area, trending structures towards NW-SE direction.

The highest peaks frequently reach heights over 1600m, being the most outstanding the ranges in the south western part of the area, while the lowest elevation (680m) recorded close to Basara gorges.

For the evaluation of vulnerability of this factor, slopes have been smoothed and slope ranges were assigned with a rating from 10 to 1, based on the proposed table recommended by Aller et al (1987) (Fig 6.9).

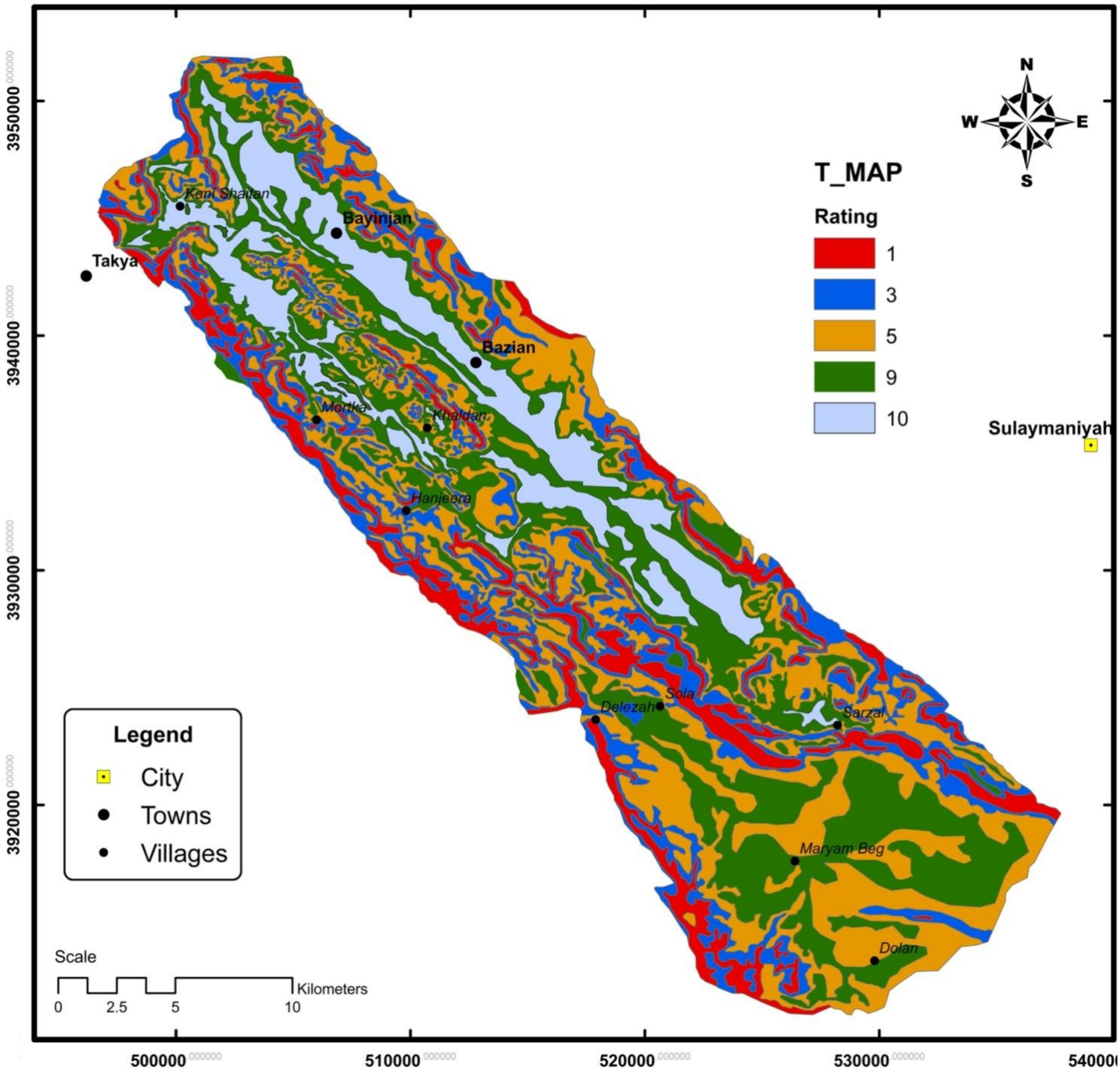

Fig (6.9) Rating topography map (T_map) of the Basara basin

6.2.6 Impact of the vadose zone (I_MAP)

The vadose zone is defined as the zone above the water table or unsaturated zone. Percolation of precipitation and any kind of surface water is occurred within this zone, so it has an important role in attenuating the pollutant materials. Based on Hernandez et al (2004), in a stratified sedimentary media with strong variations in the hydraulic conductivity, a pollutant can reach an aquifer even when the horizontal distance from its location at the ground surface is large, while open fractures and karstic cavities enable a strong concentration of infiltration water and decrease the attenuation potential of the vadose zone.

This parameter was obtained using drilling profiles from private drilling company and from directorate of groundwater aided by geo-electrical section carried out by previous study. These profiles were used to encode the geological units according to the DRASTIC model rating system. Coarse media was assigned a high rating value compared to the fine media types (Table 6.7).

Table (6.7) Ranges and rating for impact of the vadose zone based on Aller et al (1987)

Factors	*Range*	*Rating*	*Typical rating*
Impact of the vadose zone media	Confining layer	1	1
	Silt/ clay	2 – 6	3
	Shale	2 – 5	3
	Limestone	2 – 7	6
	Sandstone, Bedded limestone, sandstone, shale, sand and gravel	4 – 8	6
	Metamorphic/ Igneous	2 - 8	4
	Sand and gravel	6 – 9	8
	Basalt	2 - 10	9
	Karst limestone	8 - 10	10

The most vulnerable areas are related to the unsaturated zone of limestone lithology, with higher values (rate with 8). Generally, these zones are located at the ranges where the permeable formations that constitute the aquifers Sinjar and Pilaspi in addition to clastic and un-consolidated material from Bai Hassan and slope deposits formations among other outcrop. The recent deposits in the central part of the basin use to have vadose zones where gravel and sand levels alternate with clay and silt that considerably decreased the vulnerability values (rate with 2). Nevertheless, in other cases these lithologies present lower contents in fine materials, which can result in medium vulnerability values (3 to 5) such as the case of Kolosh, Gercus, Injana and Fatha formations (Fig 6.10).

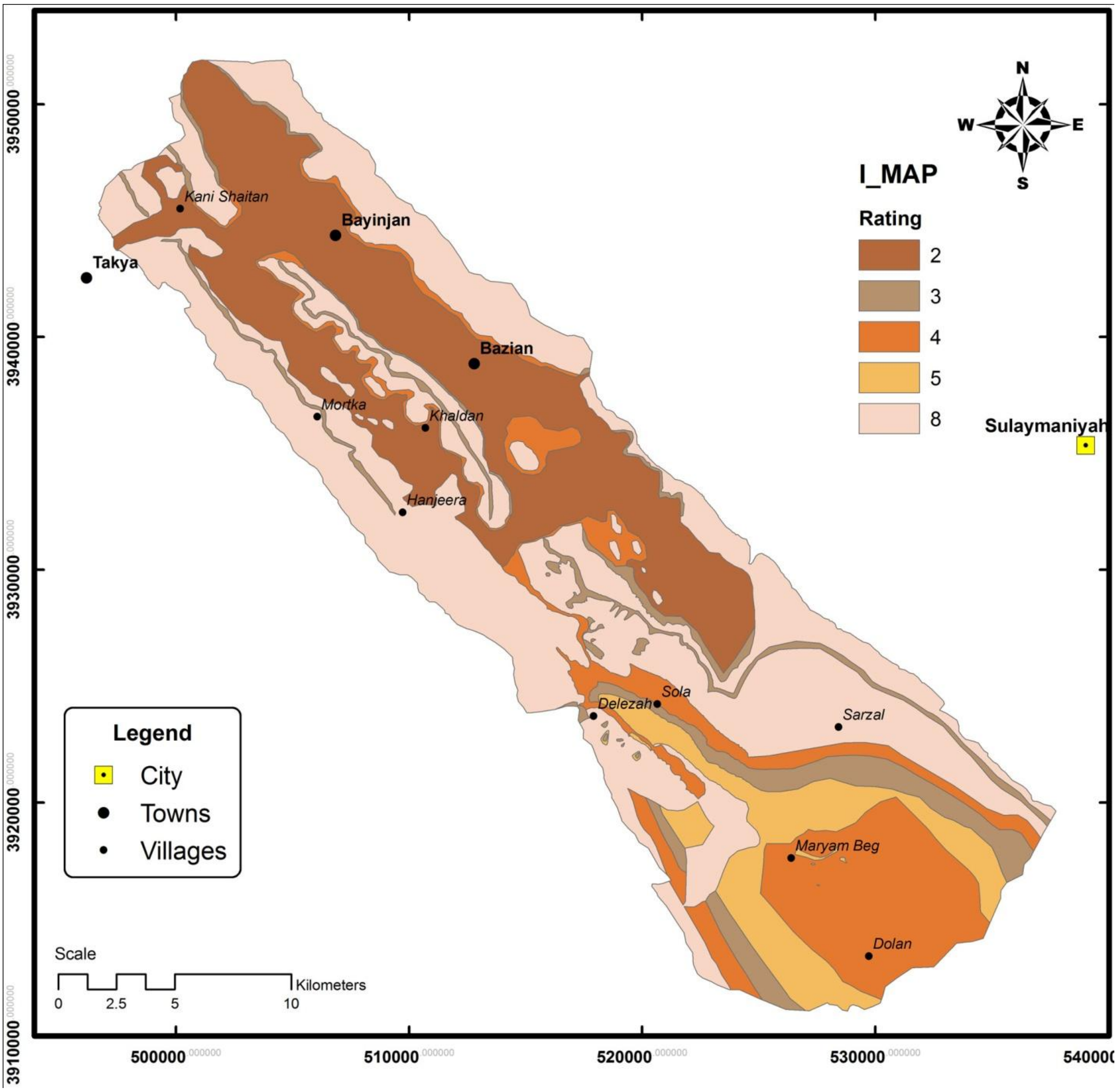

Fig (6.10) Rating map of the impact of the vadose zone (I_map) of the Basara basin

6.2.7 Hydraulic conductivity (C_MAP)

Hydraulic conductivity controls the rate of groundwater movement in the saturated zone, thus, contaminant migration is limited depending on the permeability of the medium (Sener et al, 2009).

For assessing the hydraulic conductivity, the scaled values based on pumping tests data, drilling wells profiles and electrical tomography sections have been used (Fig 6.11). Accordingly, 58 wells were selected for calculating the transmissivity by pumping test, then hydraulic conductivity is estimated based on the following equation:

C = T / b; where <u>C</u> is the hydraulic conductivity in (m/day), <u>T</u> is the transmissivity in (m^2/day) and <u>b</u> is the aquifer saturated thickness in (m).

The different hydraulic conductivity zones in the area were defined and assigned ratings according to table (6.8).

Table (6.8) ranges and rating for the hydraulic conductivity based on Aller et al (1987)

Factors	*C (m/day)*	*Rating*
Hydraulic conductivity	Less than 4.0	1
	4.0 – 12.0	2
	12.0 – 30.0	4
	30.0 – 40.0	6
	40.0 – 80.0	8
	More than 80.0	10

Most of the pumping tests carried out in the area were single well test. Thus results of such tests may not reflect the real case of hydraulic conductivity, accordingly 3 wells were selected for analyzing the pumping test, both constant and recovery test were applied using the principal of observation well, each tests carried out in a different aquifer in the area.

Generally, results of the hydraulic conductivity calculated for the wells penetrating Alluvium Intergranular Aquifer (AIA), and even the observation well test which was applied during this study, as well as some wells which are penetrating complex and other inter-granular aquifers in the area, have showed the hydraulic conductivity less and around 1.0 m/day, this might be attributed to the repetition of the fine, medium and coarse grained textures, as well as variations in permeability from one site to another.

The results of nearly 45 single well tests carried out mostly in Sinjar and partly in Pilaspi karstic-fissured aquifers, showed values between (0.1 – 35) and (0.5 – 2) m/day respectively. But, when the observation well tests applied, the results of both Sinjar and Pilaspi were (43 m/day) and (8.5 m/day) respectively. The fissures and general aquifer’s anisotropy may contribute occasionally to this better permeability as cited by Stevanovic & Iurkiewicz (2004). Thus, a result of the present study was applied to all outcrops exposed by karstic-fissured aquifers, i.e. all areas where Sinjar is exposed; a hydraulic conductivity of 43 m/day, while for the outcrop of Pilaspi an 8.5 m/day was applied. Accordingly, the central and most southern zone of the basin has the lowest hydraulic conductivity rating value (1). In contrast, high rating C value is assigned to the Sinjar aquifer where the outcrop is exposed, (rating with 6). The Pilaspi aquifer in the basin show low vulnerability (3). The positions of the test wells and rating distribution are shown in Fig (6.12).

Fig (6.11) pumping test at boreholes, (Photo A was taken during a drilling well in Gopala for domestic use in 18/2/2009, while photo B was taken in 21/1/2010 for pumping test analysis at Ala Cola company)

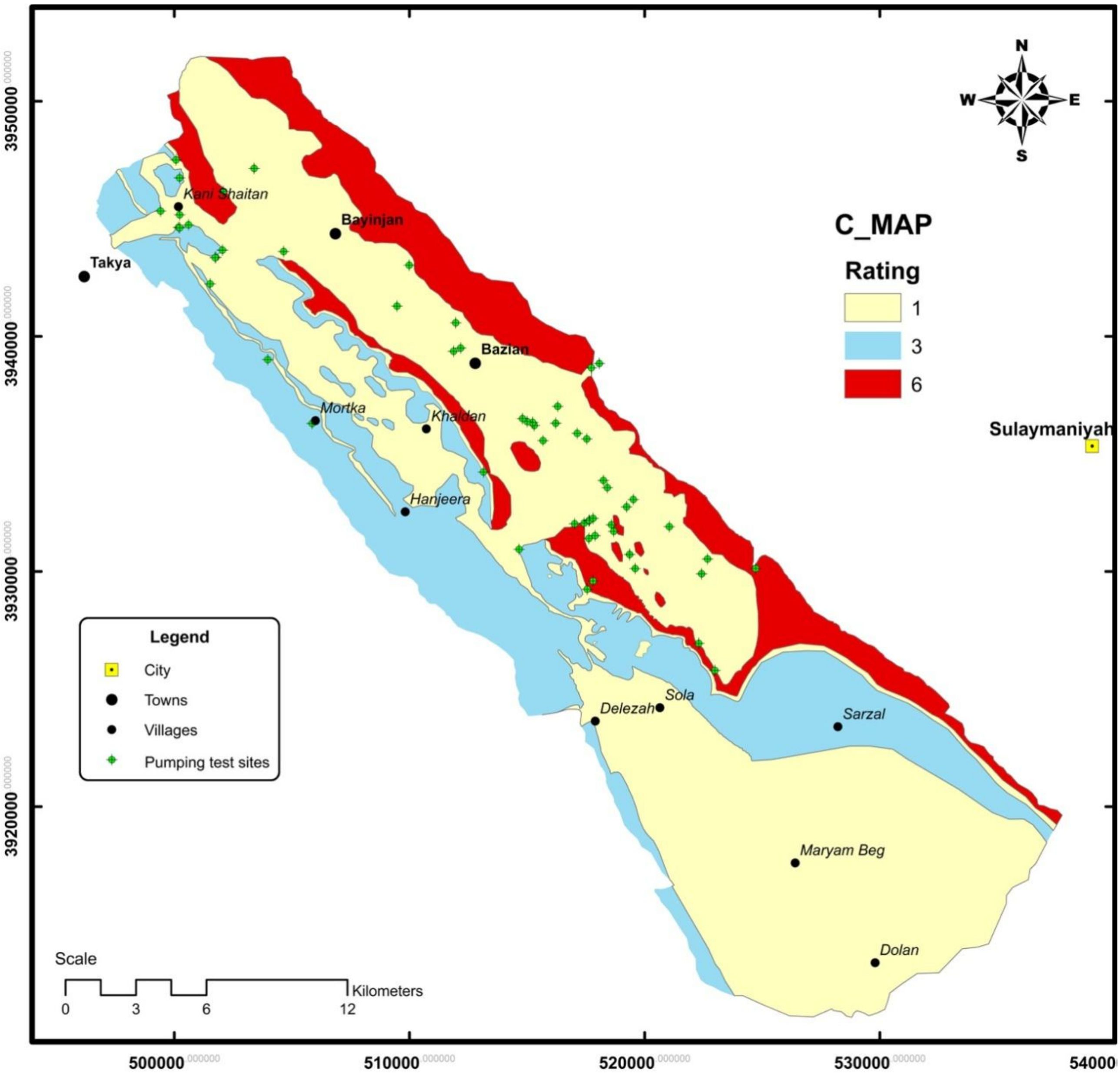

Fig (6.12) Rating hydraulic conductivity map (C_map) of the Basara basin

6.3 Vulnerability map

Vulnerability maps nowadays have been produced for a number of purposes. For example, they provide a measure of the likelihood of contamination, assist in ensuring that protection schemes are not unnecessarily restrictive for human economic activity, help in the choice of engineering preventative measures, and enable major developments, which have a significant potential to contaminate, to be located in areas of relatively low vulnerability and therefore, of relatively low risk from a groundwater perspective (Warren et al, 1998).

The linear additive combination of the prepared previous seven parameter maps with ratings and weights was used to calculate the DRASTIC vulnerability index ($\boldsymbol{DVI}$) as given bellow:

$$\boldsymbol{DVI} = (\boldsymbol{Dr} \times \boldsymbol{Dw}) + (\boldsymbol{Rr} \times \boldsymbol{Rw}) + (\boldsymbol{Ar} \times \boldsymbol{Aw}) + (\boldsymbol{Sr} \times \boldsymbol{Sw}) + (\boldsymbol{Tr} \times \boldsymbol{Tw}) + (\boldsymbol{Ir} \times \boldsymbol{Iw}) + (\boldsymbol{Cr} \times \boldsymbol{Cw}).$$

Where; D, R, A, S, T, I, and C are the seven factors of the DRASTIC method, $\boldsymbol{w}$ the weight of the factor, and $\boldsymbol{r}$ the rating associated.

The weighting represents an attempt to define the relative importance of each factor in its ability to affect pollution transport and it varies from 1 to 5 (Table 6.9). The higher the value for the ($\boldsymbol{DVI}$) the greater the vulnerability of that location of the basin will occur.

Table (6.9) Weights of the factors in the DRASTIC method, based on Aller et al (1987)

Factor	DRASTIC method
D: ***D***epth to Water	5
R: Net ***R***echarge	4
A: ***A***quifer Media	3
S: **S**oil Media	2
T: ***T***opography	1
I: ***I***mpact of the vadose zone	5
C: Hydraulic ***C***onductivity	3

The final groundwater vulnerability map was obtained at a scale of (1:250,000) using the seven hydrogeological data layers in GIS environment (Fig 6.13). All parameter maps were converted into raster format and multiplied by their respective weights. The range of the DRASTIC vulnerability index in the studied basin was between ***37*** and ***168***. Accordingly, vulnerability classes of the study area were reclassified into four classes based on the proposed table recommended by Aller et al (1987) (Table 6.10).

Table (6.10) Ranges of vulnerability using DRASTIC method based on Aller et al (1987)

Index of vulnerability	Vulnerability degree
Less than 100	Very low
100 – 125	Low
125 – 150	Medium
150 – 200	High
More than 200	Very High

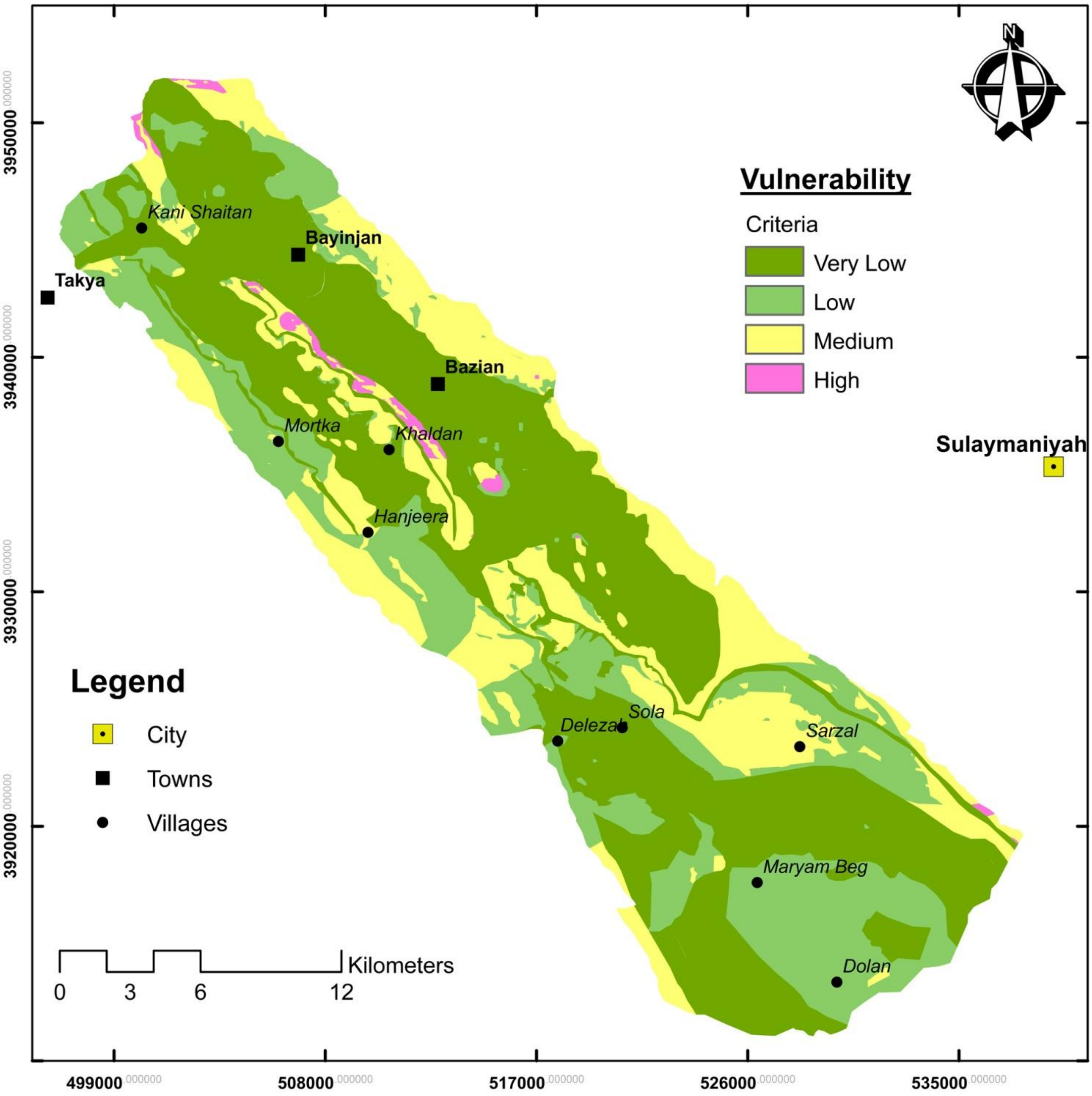

Fig (6.13) Groundwater vulnerability map of the Basara basin

6.4 Groundwater Hazards

Based on the prepared vulnerability map of the groundwater to pollution in the Basara basin by DRASTIC method, most of the basin show the highest extension of the zones with very low and low vulnerability zones which occupying an area of 281 Km^2 or 49 % and 151 km^2 or 26.5 % of the studied basin respectively comparing to the other zones of the catchment area. The zones with medium vulnerability occupy 131 km^2 or 23 % of the basin, while the zones with high vulnerability occupy only 8 km^2 or 1.3 % of the total surface of the basin.

The zones with high vulnerability are distributed mainly in the mountain areas, solely in the eastern Uloblagh and Kuwaik Mountains, in addition to the small zones in the farthest northern corner and south eastern corner of the area with scarce of human activity. The high vulnerability in these zones are probably related to the shallowness of the water table, the high infiltration rate as well as the high permeability of the vadose zone materials, which are mainly constituted by karstic fissured outcrops of Sinjar Formation. Most of the medium vulnerability zones are located within the Sinjar and pilaspi formations. In contrast, the areas with very low and Low vulnerability zones are located in the central and southern part of the basin, frequently at plain and over clastic formations with greater occupation and activity. The reasons for such low vulnerability especially in the central and southern part is related to the confining layers and low permeability which impede movement of groundwater downward, and the greater depth of the water table in those locations. However, in future, such areas could be vulnerable to conservative pollutants in long term when continuously and widely discharged and leached materials occur. Despite this suitable disposition, any activities that implies the generation of waste disposal must be accompanied by a study about the impact on groundwater especially for the physical and chemical properties of the soil. Local studies must assess the pollution risk of the activity particularly in sites where industrial projects are active, such as Bazian Oil Refinery project where it is close to the Pilaspi aquifer and most of its waste which composed of heavy metal and other pollutant sources are disposed over the plain area, if such cases continued without treatment plant and finding suitable solution for this plume pollution source, a great risk to the quality of groundwater will happen in the future.

Since both Bazian Cement and Mass Cement factories are directly located on the outcrop of Sinjar Formation, activities for such factories probably influence the quality of groundwater; especially where they are located directly on the outcrop of Sinjar aquifer, the later has a large hydraulic conductivity, in case if the pollutant material drained into the aquifer, the flow of groundwater will spread-out over most of the area within a short time, thus monitoring their actions and taking samples for sureness the quality of groundwater at such sites are highly recommended.

CHAPTER SEVEN

CONCLUSIONS AND RECOMMENDATIONS

7.1 Conclusions

The present study evaluates the Basara basin from the climatic, geologic, hydrogeological and environmental points of view. The overall conclusion led to consider this basin as one of the important basins from economic and social importance for the Iraqi Kurdistan region. The results and conclusions of the present work are briefly outlined in the following points:

- The total amount of ***annual water surplus*** was estimated as 317 mm, which comprise 46% from the average annual precipitation fall over the catchment area.
- Results of the ***SCS method*** have shown that the lowest percentage of runoff is with locations dominated by Sinjar and Pilaspi formations (11%, 14%) respectively, while Kolosh, Gercus, Injana and Fatha formations have high runoff potentials (ranged between 44% and 39% of the precipitation respectively). The total rate of 149 mm/year from all fallen rainfall over the whole basin is predicted as runoff.
- ***The aquifers*** of the Basara basin are grouped as Karstic-fissured aquifers for Eocene formations represented by Sinjar and Pilaspi; intergranular aquifers (AIA) and (PIA) for Alluvium and Pliocene intergranular aquifers respectively; Miocene Complex Aquifer (MCA) indicated by Fat'ha and Injana formations, and finally Aquiclude of Kolosh and Gercus formations.
- Results of the pumping tests reveal great variation in the ***transimissivity (T)*** and **storage coefficient (S)** values. For the AIA, it was in the range of (4×10^{-6} to 2×10^{-3} m^2/sec); while the storage coefficient was 0.05 to 0.006. For EKFA, T values was between (1.8×10^{-2} and 7.9×10^{-3} m^2/sec) for both Sinjar and Pilaspi respectively. The storage coefficient was calculated to be in range of (0.007 - 0.088).
- The total expected ***annual recharge*** to the aquifers in the area is estimated to be around 96 million m^3 based on the average rainfall of 691 mm/year.

- Conclusions from ***Recession Coefficients technique*** of three springs in the basin (Khaldan, Hayasee and Kuchkena springs) have revealed two recession coefficients. The first micro-regime of Hayasee and Kuchkena springs indicates rapid drainage of well interconnected large fissure and large karstic channel, while the second coefficient of discharge represents slow drainage of small voids or narrow fissures and aquifer matrix porosity aquifer. In contrast, the main contribution to the Khaldan spring in both periods is from storage in small voids and narrow fissure of Pilaspi aquifer.
- The complete exhaustion of the ***dynamic reserve*** of the springs is estimated to be 0.93, 0.31 and 0.15 million m^3 for Khaldan, Hayasee and Kuchkena springs respectively.
- The total ***annual groundwater recharge and discharge*** for each sub basin is calculated to be as follows:

For Bazian sub basin, the total annual recharge is believed to be around 43 million m^3, while the volume of exploited groundwater is about 9 million m^3. If the natural annual discharge from springs entered into this calculation, 71.5% of total annual production from average annual recharge is expected.

For Hanjeera sub basin, the total annual recharge and the volume of exploited groundwater is estimated as 25 million and 0.5 million m^3 respectively. The 68% of total annual production from average annual recharge is expected when the natural average annual discharge from all springs inside this sub basin is considered.

For Tile sub basin, the total volume of groundwater exploited is expected to be 0.3 million m^3, while the total recharge is believed to be around 28 million m^3. 16% of total annual production from average annual recharge is expected when discharge from issuing springs is considered in this calculation.

- All the analyzed groundwater samples are classified as a fresh water type (from chemical points of view), except the sample from the Sollai

Darband village which is located in the Tile sub basin, is considered to be slightly brackish water.

- A total number of 10 samples for analyzing ***heavy metals*** (Cd, Cu, Zn, Pb, Mn, and Ni) and 25 samples for (F and Br) were analyzed. Results showed that most of the groundwater samples are not contaminated with Cu based on the permissible level proposed by W.H.O, (2008). In general, some of the analyzed samples are contaminated with Zn, Pb, Mn and Ni. Of 9 shallow wells tested, 5 are slightly contaminated with cadmium and the later were undetectable. In most cases, pollution of groundwater in these locations may result from an industrial disposal and leakage of sewages and in other cases fertilizers for irrigation purposes may be responsible in other groundwater samples.
- For the first time in Iraq, the ***groundwater vulnerability map*** using DRASTIC system was constructed using GIS techniques by this study. Based on this map, most of the basin shows the highest extension of the zones with very low and low vulnerability zones. In contrast the zones with high vulnerability is distributed mainly in the mountain areas, solely in the eastern Uloblagh and Kuwaik Mountains, in addition to that, small zones in the farthest northern corner and south western corner of the area have less or no human activity.

7.2 Recommendations

In the light of this study, the following points are recommended:

1- Implementation of distributed rainfall-runoff models of the basin is necessary to get more reliable estimation of the water balance of the catchment.

2- The amount of water infiltrated to the groundwater in the form of sewage and abstraction from springs and streams for irrigation and domestic water supply have not been accounted in the water balance, so details about these sectors are crucial.

3- Installation of piezometer wells in different aquifer types and a continuous monitoring program are necessary especially in Bazian sub basin to avoid the devastation of the aquifers. Suitable groundwater management is the necessary solution for the sustainable development of the entire region.
4- Since the basin has many perennial streams and several large springs which providing water for the inhabitant entire the basin, it is necessary to install many gauging stations to measure continuous runoff and to have a clear view about the spring flow regime.
5- Groundwater flow modeling is required to simulate aquifer behavior using different senarios to predict the effects of pumping on the drawdown.
6- Attention toward the Isotopic analysis is highly recommended to define the origin, storage properties, water dynamic, mixing rate, tracing the movement and defining the recharge areas for the groundwater inside and outside the study area.
7- Creating a Local Meteoric Water Line (LMWL) for the study area by taking precipitation on the monthly basis is highly recommended.
8- The anthropogenic pollution may endanger water resources within the few next decades, particularly in Bazian sub basin where agriculture and industrial activities is very high. Accordingly, attention should be paid for environmental protection in this area.
9- Preparation of a vulnerability map for the other basins in Kurdistan is highly recommended to provide information and criteria for decision making and management of water resources to protect the groundwater quality.
10- Application of other methods of vulnerability methodology like EPIK, GOD and VURAS is also necessary which is more frequently used in karstic medium.

REFERENCES

1- **Ali S. S., (2007):** Geology and hydrogeology of Sharazoor - Piramagroon basin in Sulaimani area, northeastern Iraq. Unpublished PhD thesis, Faculty of Mining and Geology, University of Belgrade, Serbia. 330p.

2- **Allen R. G., Pereira L. S., Raes D, and Smith M. M., (1998):** Crop evapotranspiration - Guidelines for computing crop water requirements - FAO Irrigation and drainage paper No. 56, 307p.

3- **Aller L., Bennett T., Lehr JH., Petty RH, and Hackett G (1987):** DRASTIC: a standardized system for evaluating groundwater pollution potential using hydrogeologic setting. USEPA report 600/2-87/035, Robert S. Kerr Environmental Research Laboratory, Ada, Oklahoma, 622 p.

4- **Al Manmi, D. A., (2007):** Water resources management in Rania area, Sulaimaniyah NE-Iraq. Unpublished PhD thesis, University of Baghdad, 225p.

5- **Altoviski M. E., (1962):** Hand book of Hydrogeology. Gosgeolitzdat, Moscow, USSR (In Russian), 614p.

6- **Al-Zabet T., (2002):** Evaluation of aquifer vulnerability to contamination potential using the DRASTIC method. Env Geol 43: 203-208.

7- **APHA, (2005):** Standard methods of the examination of water and wastewater. Washington D.C., American Public Health Association.

8- **Aziz, B.Q., (2005):** Two dimension resistivity imaging tomography for hydrogeological study in Bazian basin, west Sulaimani city, NE-Iraq. Unpublished PhD thesis, University of Sulaimani, 183p.

9- **Aziz, M., (2001):** Climate of north Iraq, Brief – note (unpublished working document of FAO AM SS, FAO documentation Fund, Erbil.

10- **Babiker IS., Mohamed MAA., Hiyama T, and Kato K., (2005):** A GIS-based DRASTIC model for assessing aquifer vulnerability in Kakami-gahara Heights, Gifu Prefecture, Central Japan. Sci Total Environ 345:127–140.

11- **Barzinji Kh. T., 2003:** Hydrologic studies for Goizha-Dabashan and other watersheds in Sulaimani governorate. Msc. Thesis, College of Agriculture, Univ. of Sulaimani. 224 p.

12- **Behmanesh, O., (2003):** The aspects of water balance in the irrigated area (southwest part of Urumieh lake), M.Sc. Thesis, international institute for geo-information science and earth observation, Netherlands, 75p.

13- **Bellen R. C., Dunnington H. V., Wetzel R., and Morton D., (1959):** Lexique Stratigraphique International. Asie, Iraq. vol. 3C, 10a, 333p.

14- **Berding F., (2002):** Soil management consultancy, FAO Agricultural Rehabilitation Programme, Mission Report, No. 1, Erbil, Iraq.

15- **Berding F., (2003):** Agro-ecological zoning of the three northern governorates of Iraq, FAO Agricultural Rehabilitation Programme, Plant production SS, Erbil, Iraq.

16- **Beydoun, Z. R., (1993):** Evolution of the northeastern Arabian plate margin and shelf hydrocarbon habitat and conceptual future potential. Revue de institute. Francais, du petrole, v.48, p. 311-345.

17- **Buday T., (1980):** Regional Geology of Iraq: Vol. 1, Stratigraphy, I.I. Kassab and S.Z. Jassim (Eds) D. G. Geo Survey. Min. Invest. Publication. 445p.

18- **Chapman, T. G. & Sharma, M. L., 1987**: Summary of symposium on groundwater recharge. Mandurah, Balkema, Roterdam, p 311-321.

19- **Cichocki G., (2003):** Wassertransport als Grundlage fur eine Vulnerabilitastsbewertung und Risikoanalyse in Karbonatgesteinen. Testgebiet Nassfeld, Karnische Alpen. Diss. an der TU Graz.

20- **Civita M., (1994):** Contamination Vulnerability mapping of the aquifer: theory and practice. Quaderni di Techniche di protezione Ambientale, Pitagora, Italy.

21- **Clark I. D., & Fritz, P., (1997):** Environmental isotopes in hydrogeology. Lewis Publishers, boca Raton, New York, 311p.

22- **Darling, W. G., Edmunds, W. M, and Kinniburgh, D. K., (1987):** Source of recharge to the basal Nubian sandstone aquifer, Butana region, Sudan. In: isotope techniques in water resources development. IAEA, Vienna, p. 205-224.

23- **Dingman, S. L., (2002):** Physical hydrology, second edition. Printice Hall, New Jersey.

24- **Doerfliger, N, Jeannin PY, and Zwahlen F., (1999):** Water vulnerability assessment in karstic environments: a new method for defining protection areas using a multi-attribute approach and GIS tools (EPIK method). Env Geol 39(2):165-176.

25- **Doerfliger, N, and Zwahlen F., (1998):** Groundwater vulnerability mapping in karstic regions (EPIK): application to groundwater protection zones. Swiss Agency for the Environment, Forests and landscape (SAEFL), Bern, Switzerland.

26- **Driscoll, F. G., (1995):** Groundwater and wells (2^{nd} edition). US Filter Johnson Screens.

27- **Dubertret, L., (1959):** Lexique stratigraphique international. Asie. Fascicule 10a, Iraq. Center National Recherche Scientifique, Paris.

28- **Faure, G., (1998):** Principles and application of geochemistry (2^{nd} edition). Prentice Hall Inc., USA, 600p.

29- **Fikos I., Ziankas G., Rizopulou A. and Famellos S., (2005):** Water balance estimation in Anthemountas river Basin and correlation with underground water level. Global NEST Journal, Vol.7, No.3, .354-359.

30- **Fontes, J. Ch., (1980):** Environmental isotopes in groundwater hydrology. In: Fritz P and Fontes J CH (Ed.), Handbook of Environmental Isotope Geochemistry, Vol. 1. The Terrestrial Environment, A: 49-74.

31- **Foster, S., (1987):** Fundamental concepts in aquifer vulnerability, pollution risk and protection strategy. In: Van Duijvenbooden W, Van Waegeningh HG (eds) Vulnerability of soil and groundwater to pollutants. Committee on Hydrological Research, The Hague, 69-86.

32- **Gebreegziabher, Y., 2004:** Assessment of the water balance of Lake Awassa catchment, Ethiopia.

33- **Gogu, R, and Dassargues, A., (2000):** Current trends and future challenges in groundwater vulnerability assessment using overlay and index methods. Env Geol 39(6):549-559.

34- **Goldscheider, N., Klute M., Sturm S, and Hotzl, H., (2000):** The PI method: a GIS based approach to mapping groundwater vulnerability with special consideration of karst aquifer. Z Angew Geol 46(3):157-166.

35- **Hamasur, G. A., (2009):** Rock mass engineering of the proposed Basara dam site, Sulaimani, Kurdistan region, NE Iraq. Unpublished PhD thesis, University of Sulaimani, 183p.

36- **Hamza, M. H., Added A., Rodríguez R, and Abdel jaoued S., (2007):** A GIS-based DRASTIC vulnerability assessment in the coastal alluvial aquifer of Metline-Ras Jebel-Raf Raf (Northeastern part of Tunisia). IAH selected papers, Taylor & Francis Group, London, UK.

37- **Hem, J. D., (1991):** Study and interpretation of the chemical characteristics of natural water (3rd edition). USGS Water supply. Paper 2254, 263p.

38- **Hernandez L. R., Bravo J. A, and Mejuo M. F., (2004):** Map of vulnerability to groundwater contamination. Excelentisima Diputacion Provincial de Alicante, Espana. A-1029-2004.

39- **Horton, R. E., (1940):** An approach toward a physical interpretation of infiltration capacity. J. Soil Sci. Amer., 5, 399–417.

40- **International Atomic Energy Agency (IAEA), (1993):** Mathematical models and their applications to isotope studies in groundwater hydrology, proceedings of a final research co-ordination meeting held in Vienna, 1-4 June 1993, TECDOC-777, 279p.

41- **ITSC. (2006):** Bassara Dam Planning Report, Environmental Impact Assessment Study. General Directorate for Engineering Design, Ministry of Water Resources, Baghdad Iraq. 191p.

42- **Jabbar, M. Q., (2007):** The Catchments area of Basara Rivers: A study in physical geography. M.Sc. thesis (in Arabic). College of Arts, Geography Department, University of Baghdad, 197p.

43- **Jassim, S. Z, and Goff, J. C., (2006):** Geology of Iraq (First edition). Published by Dolin, Prague and Moravian Museum, Brno, Czech Republic, 341p.

44- **Kattan, Z., (1997):** Chemical and environmental isotope study of precipitation in Syria. J. Arid Environments, Elsevier, V. 35, p 601-615.

45- **Kim, Y., Hamm, S., (1999):** Assessment of the potential for groundwater contamination using the DRASTIC /EGIS technique, Cheongju area, South Korea. Hydrogeo1 J 7:227-235.

46- **Kresic, N., (2007):** Hydrogeology and groundwater modeling (Second edition). Published by CRC Press, Taylor and Francis group, LLC, USA, 807p.

47- **Lawa F. A., Ali, S. S, and Kareem, K. H., (2003):** Geological & Hydrogeological Study of Qaradagh- Kalar Basin (NE- Iraq), FAO Coordination office for Northern Iraq, FAO Suliamaniyah Sub- office, Published report.

48- **Lawa, F. A., (2004):** Sequence stratigraphic analysis of the Middle Paleocene – Middle Eocene in the Sulaimani district (Kurdistan region). Unpublished PhD thesis, University of Sulaimani, 258p.

49- **Lawa, F.A., Kareem, K. H, and Ali, S. S., (2002):** Hydrogeological study of Sulaimaniyah and part of Kirkuk areas, NE Iraq. Part two: Bazian-Sangaw Basin, Surdash-Koya Basin, Qaradagh-Kalar Basin. Report, FAO GWU documentation Fund, Erbil

50- **Lee S., (2003)**: Evaluation of waste disposal site using the DRASTIC system in southern Korea. Env Geol 44: 654-664.

51- **Leibundgut, C., Maloszewski, P., and Kulls, C., (2009):** Tracer in hydrology (1st edition). John Wiley & Sons Ltd. Germany, 415p.

52- **Maillet, E., editor, (1905):** Essais dihydraulique souterraine et fluvial. Herman et Cie, Paris, vol.1, 218p.

53- **Margat, J., (1968):** Vulnerabilite de nappes d eau souterraine a la pollution [Groundwater vulnerability to contamination]. Bases de al cartographie, (Doc.) 68 SGC 198 HYD, BRGM, Orleans, France.

54- **Markovic, M, and Iurkiewicz, A., (2002):** Basara Gorge, FAO Coordination office, UNSCR\ FAO Agricultural Program, Erbil - Suliamaniyah, February, Unpublished report.

55- **Mazor E., (2004):** Chemical and isotopic groundwater hydrology (3rd edition). Marcel Dekker Inc, New York. Basel. 453p.

56- **Mehta, V. K., Walter, M. T., and DeGloria, D. S., (2006):** A simple water balance model. Cornell University, technical report No.5, 9p.

57- **Mendoza JA, and Barmen G., (2006):** Assessment of groundwater vulnerability in the Rio Artiguas Basin, Nicaragua. Environmental Geology 50: 569_580.

58- **Mohammadi K., Niknam R, and Majd V. J., (2008):** Aquifer vulnerability assessment using GIS and fuzzy system: a case study in Tehran–Karaj aquifer, Iran. J. Environ Geol (2009) 58:437–446.

59- **Mook, W. G., (2001):** Environmental isotopes in the hydrological cycle, Principles and applications. IHP-V I Technical Documents in Hydrology I No. 39, Vol. II UNESCO, Paris, 2001.

60- **Moser, H., Rauert, W. (eds.) 1980:** Isotopenmethoden in der Hydrologie. Lehrbuch der Hydrogeologie, 8, 400p. Geburder Borntraeger, Berlin / Stuttgart.

61- **Nikolov, S. P., (1983):** Rainfall erosion in northern Iraq. An aid to soil conservation. Ministry of Agriculture and Agrarian Reform. Baghdad, Iraq.

62- **Numan N.M.S., and Ameen, M.S., (1983):** Regional Alpine Geoflextures in the folded zone of Iraq. Second geological congress of the Middle East, GEOCOM II, Baghdad.

63- **Parsons M. R., (1957):** Groundwater resource of Iraq, Sulaimanyia Liwa and area of north of Khaniqin. Engineering Company, Ministry of Development Board, Govt. of Iraq, V. 12, 93 p.

64- **Piper, A.M., 1944:** A graphic procedure in the geochemical interpretation of water analyses. American Geophysical Union Transactions, 25, 914-923.

65- **Polservice (1980):** Sharazoor irrigation project. Feasibility report, Annex 1, Climate and water resources, Ministry of Irrigation, Baghdad, 76 p.

66- **Richard L.A., (1954):** Diagnosis and improvement of saline and alkali soils, Agric. Handbook No.60, U.S. Dept. Agric., Washington D.C., 160p.

67- **Sawyer, C.N. and P.L. MacCarty, (1967):** Chemistry of Sanitary Engineers. 2nd Edn., McGraw-Hill Publishing Co. Ltd., New York, USA

68- **Sener E., Sener S, and Davraz A., (2009):** Assessment of aquifer vulnerability based on GIS and DRASTIC methods: a case study of the Senirkent-Uluorlu Basin (Isparta, Turkey). Hydrogeology Journal v.17: 2023-2037.

69- **Serrano S.E., (1997):** Hydrology for engineers, geologists, and environmental professionals. Hydro science Inc. U.S.A., 452p.

70- **Shaw E. M., (1994):** "Hydrology in Practice", third edition_UK..

71- **Stevanovic. Z, and Iurkiewicz A., (2004):** Hydrogeology of Northern Iraq, General hydrogeology and aquifer system. Vol.2, (1st edition), FAO.

72- **Stevanovic, Z, and Markovic, M., (2003):** Hydrogeology of Northern Iraq, Climate, Hydrology, Geomorphology & Geology., Vol.1, 2nd edition, FAO.

73- **Surdashy, A. M, and Lawa, F. A., (1993):** Microfacies and depositional environment of Sinjar Formation in selected sections from NE-Iraq. Journal of Zanko – Salahaddin, Special issue of the 2nd Scientific Conference. University of Salahaddin.

74- **Surdashy, A. M., (1988):** Stratigraphy, microfacies and depositional environment of the Sinjar Formation in selected sections, Northeastern Iraq. M.Sc. thesis (in Arabic). College of Science, Salahaddin University, Erbil.

75- **Swennenhuis, J., (2009):** CROPWAT Version 8.0. Water Resources Development and Management Service, FAO, Rome.

76- **Thirumalaivasan D., Karmegam M, and Venugopal K., (2003):** AHP-DRASTIC: software for specific aquifer vulnerability assessment using DRASTIC model and GIS. Environ Model Softw 18:645-656.

77- **Thornthwaite, C. W. (1948):** An approach toward a rational classification of climate. Geogr. Rev., 38, 55–94.

78- **Thornthwaite, C. W, and Mather J. R., (1957):** Instructions and tables for computing potential evapotranspiration and the water balance. 3, New Jersey.

79- **Thornthwaite, C. W. with H. G. Wilm and others (1945):** Report of the committee on transpiration and evaporation, 1943–1944. Trans. Amer. Geophys. Union, 25, 686–93.

80- **Todd D. K., (1980):** Groundwater hydrology, 2nd ed., John Wiley, NY, 535p.

81- **USDA NRCS, (2004):** National engineering handbook, Part 630 hydrology, Chapters 9, 20p, and Chapter 10, 79p.

82- **U.S. Salinity Laboratory Staff, (1954):** Diagnosis and improvement of saline and alkali soils. U.S. Department of Agriculture Handbook, 60,160p.

83- **Van Stempvoort D., Ewert L, and Wassenaar L., (1993):** Aquifer vulnerability index (AVI): a GIS compatible method for groundwater vulnerability mapping. Can Water Resource J 18:25-37.

84- **Vias JM., Andreo B., Perles MJ., Carrasco F., Vadillo I, and Jimenez P., (2006):** Proposed method for groundwater vulnerability mapping in carbonate (karstic) aquifers: the COP method. Application in two pilot sites in southern Spain. Hydrogeol J 14:912-925.

85- **Vrba J., Zaporozec A., (1994):** Guidebook on mapping groundwater vulnerability. IAH, Heise, Hanover, Germany.

86- **Wang Y., Merkel BJ., Le Y., Ye H., Fu S. and Ihm D., (2007):** Vulnerability of groundwater in Quaternary aquifers to organic contaminants: a case study in Wuhan city, China. Env Geol 53: 479-484.

87- **Ward, R. C, and Robinson, M., (2000):** Principles of Hydrology. 4th ed. London: McGraw-Hill.

88- **Warren P. W, and Daly D., (1998):** Mapping Groundwater Vulnerability, Geological Society Special Publication, London; No. 130.

89- **WHO, (2008):** Guidelines for drinking-water quality. 3rd edition. Vol.1, Recommendations, Geneva, 515 p.

90- **Zojer, Ht., (2003):** Stoffransport als Grundlage fur eine Vulnerabilitastsbewertung und Risikoanalyse in Karbonatgesteinen. Testgebiet Nassfeld, Karnische Alpen. Diss. an der TU Graz.

- http://www.fao.org/nr/water/infores_databases_cropwat.html
- http://www. Quran explorer.com
- http://www. Google.com
- http://www. landsat.com

LIST OF APPENDICES

Appendix (3.A) Names and coordinates of infiltration test sites

Infiltration site	Location	Longitude	Latitude	Elevation_m
Site_ 1	Bazian Wheat Factory	511024	3941045	860
Site_ 2	Mass Cement Factory	507790	3942024	832
Site_ 3	Bardaqaraman town	506339	3945692	873
Site_ 4	Gopala- Agriculture field	503986	3944388	868
Site_ 5	Gopala- Bazian Oil Refinery	502572	3946168	870
Site_ 6	Kani Sarwchawa village	501078	3949852	945
Site_ 7	Kani Shaitan-	501582	3944655	873
Site_ 8	Dargazen - Baba Ali	501534	3943414	873
SITE_ 9	Soil field (Bazian Cement)	502334	3942486	889
Site_ 10	Bazian Cement Factory	506089	3940061	869
Site_ 11	Mortka village	507147	3938302	847
Site_ 12	Bazian town	512201	3939401	818
Site_ 13	Allai town	515838	3937183	810
Site_ 14	Agriculture (paved road)	516227	3935150	786
Site_ 15	Zeka village	518069	3931885	802
Site_ 16	Orchard area	522477	3928405	835
Site_ 17	Khewata village	517643	3928308	807
Site_ 18	Delezha (agriculture land)	517683	3924675	694
Site_ 19	Electric tower (3)	510851	3934434	799

Appendix (3.B) Iteration and results of the infiltration test of the studied area by SPSS Program

Iteration	Residual SS	FC	FO	K
1	274466.6047	14.6300000	825.820000	5.00000000
1.1	124912.8069	84.0269352	836.832328	9.89679611
2	124912.8069	84.0269352	836.832328	9.89679611
2.1	15415.12809	39.8929236	1037.96465	17.5031023
3	15415.12809	39.8929236	1037.96465	17.5031023
3.1	3936.595289	32.7173936	1209.30520	22.9717998
4	3936.595289	32.7173936	1209.30520	22.9717998
4.1	3313.559222	32.5681340	1268.52805	24.8507217
5	3313.559222	32.5681340	1268.52805	24.8507217
5.1	3299.004944	32.7873269	1278.37457	25.1971479
6	3299.004944	32.7873269	1278.37457	25.1971479
6.1	3298.771964	32.8345401	1279.55084	25.2431833
7	3298.771964	32.8345401	1279.55084	25.2431833
7.1	3298.768499	32.8409347	1279.69149	25.2488205
8	3298.768499	32.8409347	1279.69149	25.2488205
8.1	3298.768448	32.8417196	1279.70846	25.2495023
9	3298.768448	32.8417196	1279.70846	25.2495023
9.1	3298.768448	32.8418146	1279.71051	25.2495846

Run stopped after 18 model evaluations and 9 derivative evaluations.
Iterations have been stopped because the relative reduction between successive
residual sums of squares is at most SSCON = 1.000E-08

Nonlinear Regression Summary Statistics   Dependent Variable I

Source	DF	Sum of Squares	Mean Square
Regression	3	731920.92585	243973.64195
Residual	8	3298.76845	412.34606
Uncorrected Total	11	735219.69430	
(Corrected Total)	10	571180.78302	

R squared = 1 - Residual SS / Corrected SS = .99422

Parameter	Estimate	Asymptotic Std. Error	Asymptotic 95 % Confidence Interval Lower	Upper
FC	32.841814584	6.994148786	16.713278560	48.970350608
FO	1279.7105062	60.300486926	1140.6573340	1418.7636784
K	25.249584614	2.059577567	20.500190228	29.998979000

Asymptotic Correlation Matrix of the Parameter Estimates

	FC	FO	K
FC	1.0000	.1996	.3397
FO	.1996	1.0000	.8498
K	.3397	.8498	1.0000

$$f(t) = 32.84 + (1279.71 - 32.48)\, e^{-25.25 * t}$$

$$r^2 = 0.994$$

```
All the derivatives will be calculated numerically.
 Iteration  Residual SS         FC          FO           K
     1      2916534.568  15.0300000  2040.40000  5.00000000
     1.1    1393188.031  217.529830  1764.97370  10.1920691
     2      1393188.031  217.529830  1764.97370  10.1920691
     2.1    179551.0460  79.1272210  2179.38565  21.8347924
     3      179551.0460  79.1272210  2179.38565  21.8347924
     3.1    15754.06572  40.2133265  2524.48919  32.8931502
     4      15754.06572  40.2133265  2524.48919  32.8931502
     4.1    6099.822936  36.3643054  2652.19839  38.3023820
     5      6099.822936  36.3643054  2652.19839  38.3023820
     5.1    5833.343174  36.4053887  2679.42020  39.5757297
     6      5833.343174  36.4053887  2679.42020  39.5757297
     6.1    5831.807422  36.4603695  2681.61422  39.6829799
     7      5831.807422  36.4603695  2681.61422  39.6829799
     7.1    5831.804077  36.4654024  2681.71467  39.6880840
     8      5831.804077  36.4654024  2681.71467  39.6880840
     8.1    5831.804071  36.4656432  2681.71911  39.6883110

Run stopped after 16 model evaluations and 8 derivative evaluations.
Iterations have been stopped because the relative reduction between
successive
residual sums of squares is at most SSCON = 1.000E-08


Nonlinear Regression Summary Statistics     Dependent Variable I

  Source                  DF  Sum of Squares  Mean Square

  Regression               3  4231984.26283  1410661.42094
  Residual                 9     5831.80407      647.97823
  Uncorrected Total       12  4237816.06690

  (Corrected Total)       11  3652744.64223

  R squared = 1 - Residual SS / Corrected SS =     .99840

                                                Asymptotic 95 %
                           Asymptotic     Confidence Interval
  Parameter   Estimate    Std. Error     Lower          Upper

  FC         36.465643232  8.125375874 18.084765997 54.846520467
  FO         2681.7191142 56.133830302 2554.7355679 2808.7026605
  K          39.688311028  2.297001854 34.492131831 44.884490225

  Asymptotic Correlation Matrix of the Parameter Estimates

                  FC         FO          K

  FC          1.0000      .1828      .3011
  FO           .1828     1.0000      .8009
  K            .3011      .8009     1.0000
```

$$\mathbf{f(t) = 36.46 + (2681.72 - 36.46\ )\ e^{-39.39*t}}$$

$$\mathbf{r^2 = 0.998}$$

```
All the derivatives will be calculated numerically.

 Iteration  Residual SS          FC          FO           K
     1      2266.148089  13.0300000  94.5200000  5.00000000
     1.1    9.158898216  14.1534958  191.891662  5.02083984
     2      9.158898216  14.1534958  191.891662  5.02083984
     2.1    9.122564270  14.1577758  191.935649  5.01113529
     3      9.122564270  14.1577758  191.935649  5.01113529
     3.1    9.122552363  14.1557496  191.915664  5.01042379
     4      9.122552363  14.1557496  191.915664  5.01042379
     4.1    9.122552295  14.1556033  191.914165  5.01036979

Run stopped after 8 model evaluations and 4 derivative evaluations.
Iterations have been stopped because the relative reduction between
successive
residual sums of squares is at most SSCON = 1.000E-08


Nonlinear Regression Summary Statistics     Dependent Variable I

  Source                  DF  Sum of Squares  Mean Square

  Regression               3    11529.43815     3843.14605
  Residual                 2        9.12255        4.56128
  Uncorrected Total        5    11538.56070

  (Corrected Total)        4     4476.52708

  R squared = 1 - Residual SS / Corrected SS =     .99796

                                                Asymptotic 95 %
                                 Asymptotic     Confidence Interval
  Parameter   Estimate           Std. Error     Lower         Upper

  FC        14.155603302  1.733668893  6.696228105 21.614978498
  FO        191.91416491 13.685306627 133.03104299 250.79728683
  K          5.010369787   .458096741  3.039338592  6.981400982

  Asymptotic Correlation Matrix of the Parameter Estimates

                 FC         FO          K

  FC          1.0000      .5472      .7142
  FO           .5472     1.0000      .9302
  K            .7142      .9302     1.0000
```

$$f(t) = 14.15 + (191.91 - 14.15)\, e^{-5.01*t}$$

$$r^2 = 0.998$$

```
All the derivatives will be calculated numerically.
 Iteration  Residual SS          FC          FO           K
     1      44775.49739  16.6200000  453.770000  5.00000000
     1.1    23025.98964  58.5099929  537.316652  9.95225244
     2      23025.98964  58.5099929  537.316652  9.95225244
     2.1    2618.304832  31.0297041  675.849374  14.9762477
     3      2618.304832  31.0297041  675.849374  14.9762477
     3.1    1650.905346  29.8977668  759.274752  17.0504707
     4      1650.905346  29.8977668  759.274752  17.0504707
     4.1    1616.605455  30.3415959  778.412795  17.5573320
     5      1616.605455  30.3415959  778.412795  17.5573320
     5.1    1615.513292  30.4770076  781.660782  17.6629553
     6      1615.513292  30.4770076  781.660782  17.6629553
     6.1    1615.472212  30.5061558  782.264000  17.6837300
     7      1615.472212  30.5061558  782.264000  17.6837300
     7.1    1615.470684  30.5119239  782.379622  17.6877438
     8      1615.470684  30.5119239  782.379622  17.6877438
     8.1    1615.470627  30.5130396  782.401847  17.6885164
     9      1615.470627  30.5130396  782.401847  17.6885164
     9.1    1615.470625  30.5132544  782.406122  17.6886650

Run stopped after 18 model evaluations and 9 derivative evaluations.
Iterations have been stopped because the relative reduction between
successive
residual sums of squares is at most SSCON = 1.000E-08

Nonlinear Regression Summary Statistics     Dependent Variable I

  Source                   DF   Sum of Squares   Mean Square

  Regression                3    248406.13768    82802.04589
  Residual                  7      1615.47062      230.78152
  Uncorrected Total        10    250021.60830

  (Corrected Total)         9    163815.95421

  R squared = 1 - Residual SS / Corrected SS =      .99014

                                              Asymptotic 95 %
                           Asymptotic     Confidence Interval
  Parameter    Estimate    Std. Error     Lower          Upper

  FC        30.513254428  5.888353022 16.589512069 44.436996786
  FO        782.40612164 55.671434763 650.76409688 914.04814640
  K         17.688665024  1.703415304 13.660727885 21.716602163

  Asymptotic Correlation Matrix of the Parameter Estimates

 FC        FO          K

  FC          1.0000      .2519      .4183
  FO           .2519     1.0000      .8799
  K            .4183      .8799     1.0000
```

$$\mathbf{f(t) = 30.51 + (782.41 - 30.51)\, e^{-17.69 * t}}$$

$$\mathbf{r^2 = 0.99}$$

```
All the derivatives will be calculated numerically.
 Iteration  Residual SS        FC          FO           K
     1      3252.861096  12.9200000  179.820000  5.00000000
     1.1    393.8824982  19.2785069  293.654884  7.72162468
     2      393.8824982  19.2785069  293.654884  7.72162468
     2.1    165.4926310  18.2091767  325.584764  7.88466705
     3      165.4926310  18.2091767  325.584764  7.88466705
     3.1    165.3928293  18.2576142  326.441771  7.89791802
     4      165.3928293  18.2576142  326.441771  7.89791802
     4.1    165.3924971  18.2617443  326.505381  7.90010022
     5      165.3924971  18.2617443  326.505381  7.90010022
     5.1    165.3924880  18.2624270  326.515768  7.90046071
     6      165.3924880  18.2624270  326.515768  7.90046071
     6.1    165.3924878  18.2625398  326.517480  7.90052017

Run stopped after 12 model evaluations and 6 derivative evaluations.
Iterations have been stopped because the relative reduction between
successive
residual sums of squares is at most SSCON = 1.000E-08


Nonlinear Regression Summary Statistics     Dependent Variable I

  Source                 DF  Sum of Squares  Mean Square

  Regression              3    42420.84721    14140.28240
  Residual                6      165.39249       27.56541
  Uncorrected Total       9    42586.23970

  (Corrected Total)       8    22940.47969

  R squared = 1 - Residual SS / Corrected SS =     .99279

                                              Asymptotic 95 %
                          Asymptotic      Confidence Interval
  Parameter   Estimate    Std. Error      Lower          Upper

  FC        18.262539802  2.388062046 12.419162479 24.105917124
  FO        326.51748037 21.910831338 272.90360750 380.13135324
  K          7.900520174   .678923046  6.239255326  9.561785022

  Asymptotic Correlation Matrix of the Parameter Estimates

                  FC        FO         K

  FC          1.0000     .3557     .5395
  FO           .3557    1.0000     .8923
  K            .5395     .8923    1.0000
```

$$f(t) = 18.26 + (326.52 - 18.26)\, e^{-7.9*t}$$

$$r^2 = 0.993$$

```
All the derivatives will be calculated numerically.
 Iteration  Residual SS         FC          FO           K
     1      14511.48920  12.3500000  128.180000  5.00000000
     1.1    9196.385120  44.9540000  128.180000  5.00000000
     2      9196.385120  44.9540000  128.180000  5.00000000

Run stopped after 3 model evaluations and 2 derivative evaluations.
Iterations have been stopped because the magnitude of the largest
correlation
between the residuals and any derivative column is at most RCON =
1.000E-08


Nonlinear Regression Summary Statistics     Dependent Variable I

  Source                 DF  Sum of Squares  Mean Square

  Regression              3    10104.31058     3368.10353
  Residual                2     9196.38512     4598.19256
  Uncorrected Total       5    19300.69570

  (Corrected Total)       4     9196.38512

  R squared = 1 - Residual SS / Corrected SS =     .00000

                                         Asymptotic 95 %
                          Asymptotic     Confidence Interval
  Parameter   Estimate    Std. Error     Lower         Upper

  FC        44.954000000 30.325542238 -85.52627709 175.43427709
  FO        128.18000000   .000000000 128.18000000 128.18000000
  K          5.000000000   .000000000  5.000000000  5.000000000

  Asymptotic Correlation Matrix of the Parameter Estimates

                  FC         FO          K

  FC          1.0000     .          .
  FO             .       1.0000     .
  K              .        .       1.0000
```

$f(t) = 44.95 + (128.18 - 44.95)\ e^{-5.0*t}$

r^2 = --

```
All the derivatives will be calculated numerically.

>Error # 16649.  Command name: NLR
>There are fewer cases than parameters to be estimated.
>This command not executed.
```

Error

```
All the derivatives will be calculated numerically.
 Iteration  Residual SS          FC          FO           K
     1      3887.842428  6.72000000  229.570000  5.00000000
     1.1    85.62188925  6.70602540  294.818081  3.59591552
     2      85.62188925  6.70602540  294.818081  3.59591552
     2.1    1.450927461  6.73074010  297.674646  4.09940827
     3      1.450927461  6.73074010  297.674646  4.09940827
     3.1    .0018797944  6.69698802  299.822585  4.21579986
     4      .0018797944  6.69698802  299.822585  4.21579986
     4.1     3.9484E-09  6.69632285  299.918406  4.22038768
     5       3.9484E-09  6.69632285  299.918406  4.22038768
     5.1     1.6860E-20  6.69632202  299.918549  4.22039433
     6       1.6860E-20  6.69632202  299.918549  4.22039433
     6.1     3.2312E-27  6.69632202  299.918549  4.22039433

Run stopped after 12 model evaluations and 6 derivative evaluations.
Iterations have been stopped because the relative difference between
successive parameter estimates is at most PCON = 1.000E-08


Nonlinear Regression Summary Statistics     Dependent Variable I

  Source                   DF   Sum of Squares  Mean Square

  Regression                3    53185.18970    17728.39657
  Residual                  0   3.231174E-27
  Uncorrected Total         3    53185.18970

  (Corrected Total)         2    31132.86167

  R squared = 1 - Residual SS / Corrected SS =    1.00000

                                                Asymptotic 95 %
                           Asymptotic     Confidence Interval
  Parameter    Estimate    Std. Error     Lower          Upper

  FC          6.696322020   .
  FO         299.91854922   .
  K           4.220394333   .

  Asymptotic Correlation Matrix of the Parameter Estimates

                     FC         FO          K

  FC          1.0000      .5438      .6868
  FO           .5438     1.0000      .8936
  K            .6868      .8936     1.0000
```

$f(t) = 6.696 + (299.91 – 6.696)\ e^{-4.22*t}$

$r^2 = 1$

```
All the derivatives will be calculated numerically.
 Iteration  Residual SS         FC           FO           K
     1      2250110.093  11.4500000  1854.70000  5.00000000
     1.1    918983.5886  230.500060  2017.40721  16.0643807
     2      918983.5886  230.500060  2017.40721  16.0643807
     2.1    192772.7371  59.5697001  3102.00568  37.2198105
     3      192772.7371  59.5697001  3102.00568  37.2198105
     3.1    75207.29719  62.5803701  5253.14170  60.8645119
     4      75207.29719  62.5803701  5253.14170  60.8645119
     4.1    12704.31706  54.5599358  6967.40431  68.9047555
     5      12704.31706  54.5599358  6967.40431  68.9047555
     5.1    9342.668040  55.0086961  7193.12094  68.9023556
     6      9342.668040  55.0086961  7193.12094  68.9023556
     6.1    9342.668032  55.0085165  7193.10650  68.9023289

Run stopped after 12 model evaluations and 6 derivative evaluations.
Iterations have been stopped because the relative reduction between
successive
residual sums of squares is at most SSCON = 1.000E-08


Nonlinear Regression Summary Statistics     Dependent Variable I

  Source                 DF  Sum of Squares  Mean Square

  Regression              3  3548117.34147  1182705.78049
  Residual                2     9342.66803     4671.33402
  Uncorrected Total       5  3557460.00950

  (Corrected Total)       4  2462442.96708

  R squared = 1 - Residual SS / Corrected SS =     .99621

                                           Asymptotic 95 %
                         Asymptotic     Confidence Interval
  Parameter   Estimate    Std. Error     Lower          Upper

  FC        55.008516482 40.072514641 -117.4095980 227.42663099
  FO        7193.1064992 1528.0210808 618.56242473 13767.650574
  K         68.902328889 10.644770746 23.101576981 114.70308080

  Asymptotic Correlation Matrix of the Parameter Estimates

                  FC         FO          K

  FC           1.0000      .3848      .4647
  FO            .3848     1.0000      .9812
  K             .4647      .9812     1.0000
```

$$f(t) = 55.09 + (7193.11 - 55.09)\, e^{-68.9*t}$$

$$r^2 = 0.996$$

```
All the derivatives will be calculated numerically.
 Iteration  Residual SS         FC          FO           K
     1      3254.793277  13.3100000  179.250000  5.00000000
     1.1    152.5907908  17.1758871  293.035684  7.14205119
     2      152.5907908  17.1758871  293.035684  7.14205119
     2.1    30.78296562  16.4842433  306.448979  6.86817545
     3      30.78296562  16.4842433  306.448979  6.86817545
     3.1    30.68871611  16.4236669  306.235751  6.87493594
     4      30.68871611  16.4236669  306.235751  6.87493594
     4.1    30.68870604  16.4249327  306.247530  6.87543016
     5      30.68870604  16.4249327  306.247530  6.87543016
     5.1    30.68870598  16.4250257  306.248378  6.87546540
Run stopped after 10 model evaluations and 5 derivative evaluations.
Iterations have been stopped because the relative reduction between
successive
residual sums of squares is at most SSCON = 1.000E-08

Nonlinear Regression Summary Statistics     Dependent Variable I

  Source                 DF  Sum of Squares  Mean Square

  Regression              3    35463.05799    11821.01933
  Residual                2       30.68871       15.34435
  Uncorrected Total       5    35493.74670

  (Corrected Total)       4    19427.23372

  R squared = 1 - Residual SS / Corrected SS =     .99842
                                                Asymptotic 95 %
                         Asymptotic     Confidence Interval
  Parameter   Estimate    Std. Error     Lower         Upper

  FC        16.425025704  2.672560134  4.925927548 27.924123861
  FO        306.24837847 16.847282099 233.76037416 378.73638279
  K          6.875465396   .631806838  4.157019980  9.593910812

  Asymptotic Correlation Matrix of the Parameter Estimates

                  FC         FO         K

  FC          1.0000      .4562      .6251
  FO           .4562     1.0000      .9031
  K            .6251      .9031     1.0000
```

$f(t) = 16.43 + (306.25 – 16.43)\, e^{-6.88*t}$

$r^2 = 0.998$

```
All the derivatives will be calculated numerically.
>Error # 16649.  Command name: NLR
>There are fewer cases than parameters to be estimated.
>This command not executed.
```

Error

```
All the derivatives will be calculated numerically.
 Iteration  Residual SS          FC          FO          K
     1      1378771.248  20.5000000  1133.90000  5.00000000
     1.1    744407.9636  201.470585  936.805528  10.4622419
     2      744407.9636  201.470585  936.805528  10.4622419
     2.1    87329.46317  72.6250108  1224.00072  22.9059543
     3      87329.46317  72.6250108  1224.00072  22.9059543
     3.1    18600.48656  50.2380453  1621.03843  33.6045199
     4      18600.48656  50.2380453  1621.03843  33.6045199
     4.1    13673.12781  50.1384784  1790.72400  37.7087031
     5      13673.12781  50.1384784  1790.72400  37.7087031
     5.1    13500.46844  50.8908404  1826.04949  38.7245517
     6      13500.46844  50.8908404  1826.04949  38.7245517
     6.1    13494.19413  51.1036163  1832.25202  38.9375371
     7      13494.19413  51.1036163  1832.25202  38.9375371
     7.1    13493.95736  51.1491871  1833.42082  38.9793059
     8      13493.95736  51.1491871  1833.42082  38.9793059
     8.1    13493.94860  51.1581609  1833.64464  38.9873502
     9      13493.94860  51.1581609  1833.64464  38.9873502
     9.1    13493.94828  51.1598896  1833.68754  38.9888935
    10      13493.94828  51.1598896  1833.68754  38.9888935
    10.1    13493.94827  51.1602213  1833.69576  38.9891894
Run stopped after 20 model evaluations and 10 derivative
evaluations.
Iterations have been stopped because the relative reduction between
successive
residual sums of squares is at most SSCON = 1.000E-08
Nonlinear Regression Summary Statistics     Dependent Variable I
  Source                 DF  Sum of Squares  Mean Square
  Regression              3  1489117.79343   496372.59781
  Residual               11    13493.94827     1226.72257
  Uncorrected Total      14  1502611.74170
  (Corrected Total)      13  1133531.74192
  R squared = 1 - Residual SS / Corrected SS =     .98810
                                               Asymptotic 95 %
                          Asymptotic     Confidence Interval
  Parameter   Estimate    Std. Error     Lower          Upper
  FC        51.160221322 10.713042772 27.580973162 74.739469482
  FO        1833.6957582 107.21081198 1597.7263521 2069.6651644
  K         38.989189407  3.287699282 31.753012077 46.225366736
  Asymptotic Correlation Matrix of the Parameter Estimates
                FC         FO         K
  FC          1.0000     .1924     .3443
  FO           .1924    1.0000     .8522
  K            .3443     .8522    1.0000
```

$$f(t) = 51.16 + (1833.70 - 51.16)\, e^{-38.99 * t}$$

$$r^2 = 0.988$$

```
All the derivatives will be calculated numerically.
>Error # 16649.  Command name: NLR
>There are fewer cases than parameters to be estimated.
```

Error

```
All the derivatives will be calculated numerically.
 Iteration  Residual SS          FC          FO           K
     1      10754.95220  14.5500000  181.650000  10.0000000
     1.1    2617.450428  20.1397615  332.259624  5.87933713
     2      2617.450428  20.1397615  332.259624  5.87933713
     2.1    183.0525123  19.8455310  315.990998  7.25392964
     3      183.0525123  19.8455310  315.990998  7.25392964
     3.1    102.9732479  19.2905955  331.078471  7.95901839
     4      102.9732479  19.2905955  331.078471  7.95901839
     4.1    101.6119144  19.3923497  335.589562  8.10383838
     5      101.6119144  19.3923497  335.589562  8.10383838
     5.1    101.5891931  19.4293085  336.204835  8.12461585
     6      101.5891931  19.4293085  336.204835  8.12461585
     6.1    101.5887894  19.4349525  336.283877  8.12741505
     7      101.5887894  19.4349525  336.283877  8.12741505
     7.1    101.5887823  19.4357192  336.294347  8.12778818
     8      101.5887823  19.4357192  336.294347  8.12778818
     8.1    101.5887821  19.4358216  336.295740  8.12783785

Run stopped after 16 model evaluations and 8 derivative evaluations.
Iterations have been stopped because the relative reduction between
successive
residual sums of squares is at most SSCON = 1.000E-08

Nonlinear Regression Summary Statistics     Dependent Variable I

  Source                 DF  Sum of Squares  Mean Square

  Regression              3    40801.05992    13600.35331
  Residual                4      101.58878       25.39720
  Uncorrected Total       7    40902.64870

  (Corrected Total)       6    21369.81257

  R squared = 1 - Residual SS / Corrected SS =     .99525

                                          Asymptotic 95 %
                          Asymptotic     Confidence Interval
  Parameter   Estimate    Std. Error     Lower         Upper

  FC        19.435821554  2.708331632 11.916287451 26.955355657
  FO        336.29573954 23.221012255 271.82387373 400.76760536
  K          8.127837847   .747869133  6.051420253 10.204255441

  Asymptotic Correlation Matrix of the Parameter Estimates

                    FC         FO          K

  FC            1.0000     .3919     .5691
  FO             .3919    1.0000     .9029
  K              .5691     .9029    1.0000
```

$$f(t) = 19.44 + (336.295 - 19.44)\, e^{-8.127*t}$$

$$r^2 = 0.995$$

```
All the derivatives will be calculated numerically.

 Iteration  Residual SS          FC          FO           K

     1      12434.50916  20.4400000  289.610000  10.0000000
     1.1    162.0898955  25.4793808  489.409014  11.4380282
     2      162.0898955  25.4793808  489.409014  11.4380282
     2.1    75.00315406  25.6112491  493.210472  10.9979150
     3      75.00315406  25.6112491  493.210472  10.9979150
     3.1    74.95720269  25.5293377  492.984253  10.9962630
     4      74.95720269  25.5293377  492.984253  10.9962630
     4.1    74.95720223  25.5290829  492.981728  10.9961585

Run stopped after 8 model evaluations and 4 derivative evaluations.
Iterations have been stopped because the relative reduction between
successive
residual sums of squares is at most SSCON = 1.000E-08


Nonlinear Regression Summary Statistics     Dependent Variable I

  Source                 DF  Sum of Squares  Mean Square

  Regression              3    91977.55170    30659.18390
  Residual                2       74.95720       37.47860
  Uncorrected Total       5    92052.50890

  (Corrected Total)       4    51521.90312

  R squared = 1 - Residual SS / Corrected SS =     .99855

                                                Asymptotic 95 %
                          Asymptotic     Confidence Interval
  Parameter   Estimate    Std. Error     Lower          Upper

  FC        25.529082945  4.015605929  8.251325131 42.806840758
  FO        492.98172793 26.069022758 380.81577600 605.14767986
  K         10.996158491   .970230824  6.821592186 15.170724795

  Asymptotic Correlation Matrix of the Parameter Estimates

                  FC        FO         K

  FC          1.0000     .4226     .5892
  FO           .4226    1.0000     .9027
  K            .5892     .9027    1.0000
```

$$f(t) = 25.53 + (492.98 - 25.53)\ e^{-10.996*t}$$

$$r^2 = 0.9985$$

```
All the derivatives will be calculated numerically.

 Iteration  Residual SS          FC          FO           K

     1      9233.122525  15.7800000  179.660000  10.0000000
     1.1    34926.89280  18.8617952  271.661486  1.47914407
     1.2    5358.998678  18.2395163  201.242898  8.49128548
     2      5358.998678  18.2395163  201.242898  8.49128548
     2.1    780.1815259  21.1004910  242.395566  6.26351537
     3      780.1815259  21.1004910  242.395566  6.26351537
     3.1    24.79231557  17.8559737  306.439514  7.17237786
     4      24.79231557  17.8559737  306.439514  7.17237786
     4.1    17.26336697  17.8429953  309.738869  7.11335561
     5      17.26336697  17.8429953  309.738869  7.11335561
     5.1    17.26303866  17.8324536  309.678520  7.11150876
     6      17.26303866  17.8324536  309.678520  7.11150876
     6.1    17.26303836  17.8321422  309.676250  7.11141038
     7      17.26303836  17.8321422  309.676250  7.11141038
     7.1    17.26303836  17.8321256  309.676128  7.11140512
Run stopped after 15 model evaluations and 7 derivative evaluations.
Iterations have been stopped because the relative reduction between
successive
residual sums of squares is at most SSCON = 1.000E-08

Nonlinear Regression Summary Statistics     Dependent Variable I

  Source                  DF  Sum of Squares  Mean Square

  Regression               3    35386.04996    11795.34999
  Residual                 1       17.26304       17.26304
  Uncorrected Total        4    35403.31300

  (Corrected Total)        3    17417.82090

  R squared = 1 - Residual SS / Corrected SS =     .99901

                                         Asymptotic 95 %
                          Asymptotic     Confidence Interval
  Parameter   Estimate    Std. Error     Lower          Upper

  FC        17.832125565  3.556642811 -27.35930621 63.023557342
  FO        309.67612837 19.563843138 61.093931750 558.25832500
  K          7.111405116   .773498692 -2.716827640 16.939637873

  Asymptotic Correlation Matrix of the Parameter Estimates

                  FC        FO         K

  FC          1.0000     .5178     .6847
  FO           .5178    1.0000     .9144
  K            .6847     .9144    1.0000
```

$$f(t) = 17.83 + (309.68 - 17.83)\, e^{-7.11*t}$$

$$r^2 = 0.999$$

```
All the derivatives will be calculated numerically.
 Iteration  Residual SS          FC           FO            K
     1      28046.53287  26.6200000  575.330000  10.0000000
     1.1    7708.354993  55.6401126  804.545694  17.7353233
     2      7708.354993  55.6401126  804.545694  17.7353233
     2.1    2182.098066  43.1614399  951.721514  21.6527052
     3      2182.098066  43.1614399  951.721514  21.6527052
     3.1    2031.234985  43.6527154  991.064108  22.5646014
     4      2031.234985  43.6527154  991.064108  22.5646014
     4.1    2028.507926  43.8989511  996.556402  22.7360036
     5      2028.507926  43.8989511  996.556402  22.7360036
     5.1    2028.428155  43.9484510  997.422566  22.7664870
     6      2028.428155  43.9484510  997.422566  22.7664870
     6.1    2028.425758  43.9573492  997.570993  22.7717822
     7      2028.425758  43.9573492  997.570993  22.7717822
     7.1    2028.425687  43.9588977  997.596603  22.7726975
     8      2028.425687  43.9588977  997.596603  22.7726975
     8.1    2028.425685  43.9591655  997.601024  22.7728556

Run stopped after 16 model evaluations and 8 derivative evaluations.
Iterations have been stopped because the relative reduction between
successive
residual sums of squares is at most SSCON = 1.000E-08


Nonlinear Regression Summary Statistics     Dependent Variable I

  Source                 DF  Sum of Squares  Mean Square

  Regression              3   397331.80772   132443.93591
  Residual                6     2028.42568      338.07095
  Uncorrected Total       9   399360.23340

  (Corrected Total)       8   248412.44300

  R squared = 1 - Residual SS / Corrected SS =     .99183

                                            Asymptotic 95 %
                          Asymptotic     Confidence Interval
  Parameter   Estimate    Std. Error     Lower          Upper

  FC         43.959165502  7.805609623 24.859526810 63.058804194
  FO         997.60102403 68.571423773 829.81279455 1165.3892535
  K          22.772855592  2.154254051 17.501585824 28.044125359

  Asymptotic Correlation Matrix of the Parameter Estimates

                  FC         FO          K

  FC           1.0000      .2907      .4676
  FO            .2907     1.0000      .8787
  K             .4676      .8787     1.0000
```

$$f(t) = 43.96 + (997.60 - 43.96)\, e^{-22.77*t}$$

$$r^2 = 0.992$$

```
All the derivatives will be calculated numerically.
 Iteration  Residual SS        FC           FO           K
     1      14962.97512  17.9000000  413.140000  10.0000000
     1.1    2245.008367  31.9109467  631.432621  15.1215714
     2      2245.008367  31.9109467  631.432621  15.1215714
     2.1    1371.844485  31.1790224  710.675989  16.5165335
     3      1371.844485  31.1790224  710.675989  16.5165335
     3.1    1360.010647  31.5289048  722.499073  16.7992820
     4      1360.010647  31.5289048  722.499073  16.7992820
     4.1    1359.689538  31.6095062  724.352220  16.8604884
     5      1359.689538  31.6095062  724.352220  16.8604884
     5.1    1359.675388  31.6272826  724.728556  16.8734354
     6      1359.675388  31.6272826  724.728556  16.8734354
     6.1    1359.674768  31.6310572  724.807025  16.8761469
     7      1359.674768  31.6310572  724.807025  16.8761469
     7.1    1359.674741  31.6318484  724.823408  16.8767135
     8      1359.674741  31.6318484  724.823408  16.8767135
     8.1    1359.674740  31.6320136  724.826828  16.8768318

Run stopped after 16 model evaluations and 8 derivative evaluations.
Iterations have been stopped because the relative reduction between
successive
residual sums of squares is at most SSCON = 1.000E-08


Nonlinear Regression Summary Statistics     Dependent Variable I

  Source                  DF  Sum of Squares  Mean Square

  Regression               3   211721.67646    70573.89215
  Residual                 7     1359.67474      194.23925
  Uncorrected Total       10   213081.35120

  (Corrected Total)        9   134134.57216

  R squared = 1 - Residual SS / Corrected SS =     .98986

                                           Asymptotic 95 %
                          Asymptotic     Confidence Interval
  Parameter   Estimate    Std. Error     Lower         Upper

  FC         31.632013599  5.445873089 18.754570021 44.509457177
  FO         724.82682820 54.230131136 596.59294495 853.06071145
  K          16.876831828  1.669679931 12.928666172 20.824997484

  Asymptotic Correlation Matrix of the Parameter Estimates

                FC         FO          K

  FC          1.0000      .2668      .4284
  FO           .2668     1.0000      .8901
  K            .4284      .8901     1.0000
```

$$f(t) = 31.63 + (724.83 - 31.63)\, e^{-16.877*t}$$

$$r^2 = 0.9899$$

```
All the derivatives will be calculated numerically.

 Iteration  Residual SS          FC           FO           K

     1      12911.28177  11.8300000  250.470000  10.0000000
     1.1    215.8437815  18.6841296  423.810274  8.83161889
     2      215.8437815  18.6841296  423.810274  8.83161889
     2.1    128.3989385  18.3992304  421.727552  9.23502304
     3      128.3989385  18.3992304  421.727552  9.23502304
     3.1    128.0976074  18.4806209  423.217814  9.30145511
     4      128.0976074  18.4806209  423.217814  9.30145511
     4.1    128.0950168  18.4960739  423.389155  9.30823554
     5      128.0950168  18.4960739  423.389155  9.30823554
     5.1    128.0949929  18.4976797  423.405426  9.30888817
     6      128.0949929  18.4976797  423.405426  9.30888817
     6.1    128.0949927  18.4978346  423.406980  9.30895063

Run stopped after 12 model evaluations and 6 derivative evaluations.
Iterations have been stopped because the relative reduction between
successive
residual sums of squares is at most SSCON = 1.000E-08


Nonlinear Regression Summary Statistics     Dependent Variable I

  Source                  DF  Sum of Squares  Mean Square

  Regression               3    68949.37781    22983.12594
  Residual                 2      128.09499       64.04750
  Uncorrected Total        5    69077.47280

  (Corrected Total)        4    39659.95472

  R squared = 1 - Residual SS / Corrected SS =     .99677

                                           Asymptotic 95 %
                          Asymptotic     Confidence Interval
  Parameter   Estimate    Std. Error     Lower         Upper

  FC        18.497834622  5.099710680 -3.444449456 40.440118699
  FO        423.40698026 31.344436535 288.54275484 558.27120568
  K          9.308950627  1.118822257  4.495046989 14.122854266

  Asymptotic Correlation Matrix of the Parameter Estimates

                FC         FO          K

  FC          1.0000      .3591      .5444
  FO           .3591     1.0000      .8881
  K            .5444      .8881     1.0000
```

$$f(t) = 14.50 + (423.41 - 18.50)\, e^{-9.308*t}$$

$$r^2 = 0.9967$$

Appendix (4.A) Names and coordinates of the dominant springs

Spring ID	Name	Av. annual discharge (l/sec))	Elevation in m (a.s.l)	Longitude	Latitude
1	Kani Sarchawa	3.0	989	501289	3951371
2	Kani Sarchawa	17.5	939	501402	3950379
3	Kani_Shaitan1	10.7		498548	3946922
4	Lazian_3	9.2		502028	3947962
5	Lazian_2	14.7		502889	3947711
6	Awee Gawra	18.3		504718	3948787
7	Kalak_Eastr	9.8		504324	3948106
8	Allaquli	14.2		505938	3947747
9	lazian_1	18.7		504252	3947352
10	Qulka	11.2		504395	3946778
11	Kani_Shaitan2	12.8		500090	3945810
12	Barika	6.5		502244	3946105
13	Kani_Shaitan3	9.0		499562	3944082
14	Dargazen	40.0		502025	3943570
15	Kani_Spee	2.0		503926	3943375
16	Kopala Village	100.0		507950	3945008
17	Kani Pari	41.7		507608	3943960
18	Karezakan	3.6		506267	3942229
19	KlashKaran Vilage	11.6		510242	3943277
20	Hayasee Saru	78.7		506023	3940180
21	Cholmak	2.0	925	503981	3939024
22	Hayasee Khwaru	2.0		506706	3939717
23	Bibijaki Saru	16.0		512070	3941302
24	Bibijaki_Khwaru	6.5		512655	3940619
25	Cholmak	2.0		504986	3938351
26	Cholmak2	21.4		505258	3938033
27	NE_Mortka	8.0		506722	3938027
28	Mortka	12.0	935	505940	3936511
29	Kuchkena	41.8		509472	3936731
30	Gakali	161.3	823	510846	3936146
31	Tainal	1.5		511165	3938110
32	Gomashin	35.7	889	513551	3940143
33	Kowaik_2	1.0		512408	3936989
34	Kolaka	13.6		512924	3937645
35	Kurra	5.7		513680	3937352
36	Kowaik_1	1.0		512899	3936426
37	Kuzhaka	7.8		514630	3936962
38	-	2.0		513801	3935475
39	Karez_Ibrahimawa	6.2		509169	3935304
40	Zekan	2.0	811	510020	3934824

Appendix (4.A) Continued...

Spring ID	Name	Av. annual discharge (l/sec)	Elevation in m (a.s.l)	Longitude	Latitude
41	-	5.0		508706	3933353
42	Hanjeera	103.3	890	509826	3932541
43	AliBzaw	2.0	826	513125	3933774
44	Gomatagach	1.0	810	514365	3933015
45	Kani_Gawra	41.7		517556	3935914
46	Tepe_Shuankara	16.0		518434	3936377
47	Qushqaya	1.5	827	519069	3935353
48	AliGoran	20.0	989	510422	3931134
49	Balulan	7.9	797	514650	3930958
50	East Balulan	5.0		515520	3931362
51	-	2.0		518244	3933349
52	Kani Shaya	2.0	783	519303	3933194
53	Halai Sarwcahawa	84.0	793	518219	3932409
54	Shekh Mand	12.0	815	514267	3929614
55	Mahmudia	1.2		517635	3930786
56	Zeka	11.9	824	519591	3930129
57	Khewata	1.0		516973	3929211
58	East Khewata	0.5		517418	3929226
59	Warmziar	99.0	805	522429	3930660
60	SE_Xewata	2.0	777	518176	3927631
61	Gawani	0.1	829	522546	3928996
62	Delezha	30.0	791	517743	3923677
63	-	1.5		522763	3925172
64	Darikali	2.0	957	523300	3924898
65	Barwi Bichuk	2.0	893	524709	3926494
66	Barwi Gawra	1.0	937	526007	3926479
67	Qala Sura	4.0		530645	3924642
68	Sarzal Spring	30.0		528104	3923138
69	Gurbaz	1.2	803	520783	3921370
70	-	1.0		520586	3920990
71	-	3.0		519333	3920060
72	-	2.0		519941	3920167
73	Sari Milalan	3.0		520156	3919881
74	Mewli_2	2.5		520335	3919666
75	Mewli_1	2.0		520478	3919487
76	Girda Sur	1.0		523879	3920597
77	-	1.0		525276	3920453
78	Ibrahimawa	15.0		530144	3921492
79	W. of Qazanqaya	4.0		522018	3918162
80	Qazanqaya	0.1		523128	3917768

Appendix (4.A) Continued...

Spring ID	Name	Av. annual discharge (l/sec)	Elevation in m (a.s.l)	Longitude	Latitude
81	Grde Shekh Husain	2.0	-	524202	3918341
82	-	6.0	-	524810	3918663
83	Hargena spring	2.5	-	530932	3919881
84	Girda Sur	1.5	-	522732	3916731
85	Haldera vilage	2.0	-	524751	3916218
86	Karez_ Bakhi Saru	2.0	-	533228	3916827
101	Piran Spring	0.2	1030	530403	3914056
102	Mekail Pasha	0.6	1010	531923	3914031
103	Dolan Qul	7.0	861	527366	3913813
104	Khwshki spring	0.2	854	527371	3914001
105	Kani Zana	0.4	830	524401	3915684
106	Khwby spring	1.5	825	525983	3916670
107	Rostam Agah	1.5	832	524399	3915866
108	Qula Rashaka	0.2	1024	535001	3915814
109	Cham spring	0.2	1028	533485	3915841
110	Shilan spring	0.4	1010	532012	3915839
111	Naw dey spring	0.3	985	530506	3915846
112	Afratan Spring	5.0	821	525846	3917717
113	Peawan spring	0.4	822	524384	3917735
114	Pirakhan spring	0.8	815	525851	3919466
115	Kalaki Jawza	1.0	910	531912	3919616
116	Kani Roshnai	1.0	914	533355	3919367
117	Wakash spring	2.0	937	530357	3919428
118	Qala sure	0.2	1030	530276	3923250
119	Shatoo spring	0.4	827	525840	3918210
120	Blak jar	0.5	873	528930	3912162
121	Gormaka spring	1.5	908	505806	3949136
122	Sarchaw spring	3.0	958	501583	3949042
123	Kani pan spring	0.8	942	526732	3927474
124	Naw Dey spring	1.0	814	515346	3935121
125	Gawaa spring	5.0	791	515340	3934277

Appendix (4.B) Pumping test analysis of the Basara basin

Well_ID	*Location*	*Longitude*	*Latitude*	*b (m)*	*Q (l/s)*	*Duartion (min)*	*T_ m^2/sec*	*C (m/day)*
W.40	Khewata	517806	3929605	30	3.5	323	2.6E-04	0.74
W.41	Warmziar	522418	3929908	50	3.4	540	3.6E-04	0.63
W.42	Aalibzaw	513147	3934239	50	4.5	200	5.4E-05	0.09
W.53	Orchard Bazian- 7	512173	3939510	60	12.1	450	2.7E-04	0.40
W.54	Orchard Bazian- 8	511871	3939373	65	18.9	360	8.5E-04	1.13
W.60	Tainal- (Comunity)	509465	3941293	60	7.8	600	1.2E-04	0.17
W.69	Dari kali/ sq16	522985	3925797	36	4.5	120	1.1E-03	2.64
W.70	Kani shaya/ sq 8	519515	3933067	40	3.0	120	9.3E-05	0.20
W.71	Dargazen/ sq 10	504645	3943615	100	5.3	220	1.5E-04	0.13
W.72	Kani shaya/ sq 8	519230	3932756	40	4.5	120	8.1E-05	0.18
W.73	Dari kali/ sq 9	522298	3926947	40	5.3	200	1.1E-03	2.38
W.74	Tapa shuanka /sq6	517127	3935882	80	4.5	150	1.2E-04	0.13
W.75	Tapa shuanka /sq6	518242	3933881	70	3.8	100	8.7E-05	0.11
W.78	Tapa shuanka /sq6	518411	3933572	70	3.7	120	9.5E-05	0.12
W.81	Dargazen/ sq 10	502044	3943677	30	1.7	130	1.7E-05	0.05
W.83	Allahi_Mahabad Ra	517730	3938672	18	1.0	75	2.1E-04	1.01
W.84	Tapa shuanka /sq6	515677	3935571	45	7.6	75	6.9E-04	1.33
W.86	Tapa shuanka /sq6	517535	3935644	80	4.9	360	3.6E-04	0.39
W.87	Tapa shuanka /sq6	516217	3936312	60	7.9	240	1.4E-02	19.45
W.89	Tapa shuanka /sq6	516299	3937028	54	5.2	90	2.5E-04	0.41
W.90	Warmziar /sq 6	522672	3930538	50	4.5	95	9.6E-05	0.17
W.91	Kani Shaitan- 25	500222	3945175	140	2.3	*160*	4.5E-04	0.28
W.92	Halai mam qadir	517023	3932036	36	7.3	300	1.6E-03	3.72
W.93	Halau mahmudia/ 15	517426	3932063	50	3.8	120	1.0E-04	0.18
W.94	Halau mahmudia/ 15	517626	3932163	60	4.0	120	1.1E-04	0.16
W.95	Halau mahmudia/ 15	517626	3932163	30	2.6	90	8.4E-05	0.24
W.96	Halau mahmudia/ 15	517646	3932183	40	3.0	100	9.8E-05	0.21
W.97	Halau mahmudia/ 15	518584	3931994	45	4.5	70	1.2E-04	0.24
W.98	Halau mahmudia/ 15	519357	3930732	40	3.0	240	5.7E-05	0.12
W.99	Halau mahmu/ 15	517625	3931410	85	5.0	200	2.2E-04	0.22
W.102	Warmziar	521046	3931913	50	4.5	80	6.5E-05	0.11
W.104	Balolan_Adnan Sadi	514659	3930952	60	3.8	70	1.9E-04	0.27
W.106	Agriculture rese. cen	511963	3940582	50	0.5	75	4.6E-06	0.01
W.109	Cholmak village	503969	3939020	60	1.8	90	1.3E-03	1.80
W.110	Allai / sq 4	518069	3938852	50	0.6	143	4.6E-05	0.08
W.111	Barika /sq 26	502077	3946170	50	4.5	120	9.0E-05	0.16
W.113	Khewata-Usm.Kari	517555	3929250	60	9.1	160	4.7E-04	0.68
W.117	Tapa shuanka /sq6	515305	3936218	60	6.5	100	8.9E-04	1.28
W.118	Tapa shuanka /sq6	515235	3936347	60	4.5	240	1.6E-04	0.23
W.119	Halau mahmu/ 15	518683	3931714	40	4.5	85	3.4E-04	0.73
W.120	Mortka /sq 35	505856	3936302	60	3.4	170	1.9E-05	0.03

Appendix (4.B) Continued...

Well_ID	*Location*	*Longitude*	*Latitude*	*b (m)*	*Q (l/s)*	*Duartion (min)*	*T_ m^2/sec*	*C (m/day)*
W.122	Dargazen /sq 10	501521	3942240	100	4.1	100	1.7E-04	0.15
W.123	Dargazen /sq 10	501760	3943367	100	3.8	180	1.1E-04	0.09
W.124	Klashkaran /sq 3	509985	3943031	70	17.0	70	1.1E-03	1.35
W.125	Dargazen_Fatah qadir	501730	3943357	100	2.0	140	2.2E-04	0.19
W.127	Halau mahmu/ 15	517887	3931532	55	5.3	85	7.1E-05	0.11
W.128	Halau mahmu/ 15	517804	3932266	40	5.2	120	8.7E-05	0.19
W.129	Lazian /sq 28	503392	3947150	60	3.6	240	3.2E-05	0.05
W.136	Bazian obs_1 Pizomet	515001	3936384	60	4.3	192	7.2E-04	1.04
W.137	Bazian Oil Refinery_1	500068	3947512	30	3.4	180	2.4E-04	0.68
W.139	Bazian Oil Refinery_2	500220	3946749	50	1.4	240	1.9E-04	0.32
W.140	Baroi Bichuk	524719	3930133	40	5.6	270	5.2E-05	0.11
W.141	Zeika village	519593	3930133	45	3.8	300	1.8E-02	34.44
W.142	Bazian resear. center	514806	3936508	50	6.8	360	2.4E-04	0.41
W.143	Bazian obs_2 Pizomet	499414	3945336	80	12.0	280	7.9E-03	8.56
W.144	Bazian obs_3 Pizomet	500174	3944644	36	6.8	420	1.8E-02	43.11
W.202	Takya /18_ No-3	500601	3944753	45	12.8	360	9.3E-03	17.93
W.204	Takya /14_ No-5	500227	3944628	55	3.8	360	1.2E-02	18.73

Well_ID	*S*	*s (m)*	*Sp.Capacity (L/s/m)*	*Type of Aquifer*	*Condition*	*Penetration*	*Method of test*
W.40	0.0010	16.2	*0.21*	Unconfined aquifer	Steady state	Fully penetrate	Neuman
W.41		10.6	*0.32*	Confined aquifer	Steady state	Fully penetrate	Theis
W.42		49.9	*0.09*	Leaky aquifer	Unsteady state	Fully penetrate	Walton
W.53		37	*0.33*	Leaky aquifer	Steady state	Fully penetrate	Hantush-Jacob
W.54		8.7	*2.18*	Confined aquifer	Steady state	Fully penetrate	Cooper&Jacob
W.60		25.7	*0.30*	Leaky aquifer	Unsteady state	Fully penetrate	Walton
W.69		20.75	*0.22*	Confined aquifer	Unsteady state	Fully penetrate	Theis
W.70		16.2	*0.19*	Confined aquifer	Steady state	Fully penetrate	Theis_recovery
W.71		16	*0.33*	Unconfined aquifer	Steady state	Partial pentrate	Theis_recovery
W.72		17.5	*0.26*	Confined aquifer	Steady state	Fully pentrate	Theis_recovery
W.73		23	*0.23*	Leaky aquifer	Steady state	Fully penetrate	Hantush-Jacob
W.74		18.2	*0.25*	Unconfined aquifer	Steady state	Partial pentrate	Theis_recovery
W.75		19.4	*0.19*	Confined aquifer	Steady state	Fully pentrate	Theis_recovery
W.78		20.7	*0.18*	Confined aquifer	Steady state	Fully pentrate	Theis_recovery
W.81		19.5	*0.09*	Confined aquifer	Unsteady state	Fully pentrate	Theis/ step test
W.83		2.3	*0.44*	Unconfined aquifer	Unsteady state	Fully pentrate	Cooper&Jacob
W.84	0.0060	3	*2.53*	Unconfined aquifer	Steady state	Fully pentrate	Theis
W.86		6.5	*0.76*	Confined aquifer	Unsteady state	Partial pentrate	Theis
W.87		0.6	*13.13*	Confined aquifer	Steady state	Fully pentrate	Theis_recovery
W.89		11.5	*0.46*	Confined aquifer	Steady state	Fully pentrate	Theis
W.90		31.2	*0.15*	Confined to semi confined	Un-steady state	Partial pentrate	Neuman

Appendix (4.B) Continued...

Well_ID	***S***	***s (m)***	***Sp.Capacity (L/s/m)***	***Type of Aquifer***	***Condition***	***Penetration***	***Method of test***
W.91		*13*	0.17	Confined aquifer	Steady state	Partial pentrate	Theis
W.92		1.1	6.68	Confined aquifer	Steady state	Fully pentrate	Theis_recovery
W.93		14.5	0.26	Unonfined aquifer	Steady state	Fully pentrate	Neuman
W.94		12	0.33	Unconfined aquifer	Steady state	Fully pentrate	Cooper&Jacob
W.95		8.5	0.30	Unconfined aquifer	Steady state	Fully pentrate	Cooper&Jacob
W.96		10.5	0.29	Unconfined aquifer	Steady state	Fully pentrate	Cooper&Jacob
W.97		7	0.65	Unconfined aquifer	Steady state	Fully pentrate	Cooper&Jacob
W.98		23	0.13	Unconfined aquifer	Steady state	Fully pentrate	Neuman
W.99		9	0.56	Unconfined aquifer	Steady state	Fully pentrate	Cooper&Jacob
W.102		13	0.35	Leaky aquifer	Steady state	Fully penetrate	Hantush-Jacob
W.104		8	0.47	Unconfined aquifer	Steady state	Partial pentrate	Cooper&Jacob
W.106		25.5	0.02	Leaky aquifer	Unsteady state	Fully penetrate	Walton
W.109		0.8	2.27	Unconfined aquifer	Unsteady state	Fully pentrate	Theis
W.110		5.4	0.11	Unconfined aquifer	Unsteady state	Fully pentrate	Cooper&Jacob
W.111		25	0.18	Confined aquifer	Steady state	Fully pentrate	Theis
W.113		4	2.27	Confined aquifer	Steady state	Fully pentrate	Theis_recovery
W.117		2.5	2.60	Unconfined aquifer	Steady state	Fully pentrate	Theis_recovery
W.118		14.5	0.31	Unconfined aquifer	Steady state	Fully pentrate	Neuman
W.119		2	2.27	Unconfined aquifer	Steady state	Partial pentrate	Theis
W.120		41	0.08	Confined aquifer	Unsteady state	Fully pentrate	Theis_recovery
W.122		11.3	0.37	Confined aquifer	Unsteady state	Partial pentrate	Theis_recovery
W.123		30	0.13	Confined aquifer	Steady state	Partial pentrate	Theis_recovery
W.124		4	6.25	Confined aquifer	Unsteady state	Fully pentrate	Theis
W.125		10.05	0.20	Confined aquifer	Unsteady state	Partial pentrate	Theis
W.127		15	0.35	Leaky aquifer	Unsteady state	Fully penetrate	Walton
W.128		14.6	0.36	Leaky aquifer	Unsteady state	Fully penetrate	Walton
W.129		54	0.07	Leaky aquifer	Unsteady state	Fully penetrate	Walton
W.136	0.034	1.61	2.68	Confined aquifer	Unsteady state	Fully pentrate	Cooper&Jacob
W.137		6	0.57	Confined aquifer	Unsteady state	Fully pentrate	Theis
W.139	0.0065	7.5	0.19	Leaky aquifer	Unsteady state	Fully penetrate	Walton
W.140		46.1	0.12	Confined aquifer	Unsteady state	Fully pentrate	Theis_recovery
W.141	0.0065	0.3	12.61	Confined aquifer	Unsteady state	Fully pentrate	Theis_recovery
W.142	0.0065	26.7	0.26	Confined aquifer	Unsteady state	Fully pentrate	Theis
W.143	0.0154	0.35	34.29	Confined aquifer	Unsteady state	Partial pentrate	Cooper&Jacob
W.144	0.0630	0.05	136.33	Confined aquifer	Steady state	Fully pentrate	Theis
W.202	0.0065	1.5	8.52	Confined aquifer	Steady state	Fully pentrate	Theis
W.204		0.5	7.57	Confined aquifer	Steady state	Partial pentrate	Theis_recovery

Where;

b is the saturated thickness in (m); ***S*** is the storage coefficient

s is the drawdown in (m) ; ***C*** is the hydraulic conductivity in (m/day)

T is the transmissivity in (m^2/sec); ***Sp.Capacity*** is the specific capacity in ***L/s/m***

Appendix (5.A) locations and chemical analysis of the groundwater samples in the wet period of the Basara basin

sites	location	longitude	latitude	Elevation in m (a.s.l)	TDS (ppm)	ph	Temp in (C^0)
S.1	Dir. of Bazian health	512407	3939494	840	368	7.29	20.9
S.2	Tainal. Primary school	509456	3941407	826	250	7.4	21.2
S.3	Gopala	503251	3944690	853	725	6.94	20
S.4	Gomashin spring	513551	3940143	889	198	8.07	17.8
S.5	Bazian	510694	3941430	853	172	_	18.7
S.6	Mass cement factory	508793	3943335	858	195	7.69	19.7
S.7	Bardaqaraman	505693	3944897	861	325	7.25	18.9
S.8	Gopala_dawajin	502359	3945361	882	195	8.1	19.5
S.9	Bazian Oil Refinery	501734	3947958	898	340	_	18.8
S.10	Kanisarwchawa spring	501402	3950379	939	220	7.6	19.4
S.11	Dargazen Baba Ali	501542	3943404	887	195	7.88	17
S.12	Cholmak spring	503981	3939024	925	224	7.6	17
S.13	Mortka spring	505940	3936511	935	215	7.68	16.7
S.14	Zekan spring	510020	3934824	811	222	7.64	17.2
S.15	Khaldan spring	510846	3936146	823	162	7.85	18.7
S.16	Alibzaw spring	513125	3933774	826	188	7.8	18.5
S.17	Allai_dawajin	515897	3936844	816	420	7.4	17.2
S.18	Asia storage	516545	3934553	780	204	7.85	18.9
S.19	Qushqaya spring	519069	3935353	827	126	8.2	18.8
S.20	Kani shaya spring	519303	3933194	783	160	7.71	19
S.21	Warmziar spring	522429	3930660	805	260	7.55	19.6
S.22	Zeika village	519591	3930129	824	220	8	17.4
S.23	Gawani village	522546	3928996	829	312	7.5	17.5
S.24	Barowi gawra spring	526007	3926479	937	297	7.7	17.6
S.25	Barowi bchuk	524709	3926494	893	352	7.75	19.3
S.26	Darikali spring	523300	3924898	957	238	7.8	17.6
S.27	Halai sarwchawa spring	518219	3932409	793	235	7.7	18.3
S.28	Halai mamqadir	517003	3932006	815	282	7.8	18.9
S.29	Balulan village	514650	3930958	797	195	7.7	18.7
S.30	Shekhmand spring	514267	3929614	815	225	8.12	26.5
S.31	Gomatagach spring	514365	3933015	810	226	7.75	19
S.32	Hanjeera spring	509826	3932541	890	234	7.8	16.6
S.33	Aligoran spring	510422	3931134	989	327	8.1	20.5
S.34	Khewata village	517806	3929605	827	180	8	19.2
S.35	Delezha spring	517743	3923677	791	232	7.7	16.5
S.36	Solai Darband	520686	3924198	804	1555	7	19.8
S.37	Gurbaz spring	520783	3921370	803	265	7.8	21
S.38	Qazanqaya village	523616	3917945	827	450	7.2	18.4
S.39	Mariambag village	526997	3917465	815	_	_	_
S.40	Agriculture field	513941	3935624	799	212		18

Appendix (5.B) Concentrations of the major ions of the groundwater samples in the wet season for the Basara basin

sites	Unit	Na^{+}	K^{+}	Mg^{2+}	Ca^{2+}	SO_4^{2-}	Cl^{-}	HCO_3^{-}	CO_3^{2-}
S.1	ppm	37.19	0.77	19.16	44.69	35.94	24.64	201.8	ND
	epm	1.62	0.02	1.60	2.19	0.75	0.68	3.31	
S.2	ppm	5.28	0.36	9.99	66.64	7.46	9.54	201	4.93
	epm	0.23	0.01	0.83	3.27	0.16	0.26	3.30	0.16
S.3	ppm	14.78	0.26	50.14	127.93	155.06	56.63	164.2	ND
	epm	0.64	0.01	4.18	6.27	3.23	1.57	2.69	
S.4	ppm	8.11	0.63	13.81	59.78	47.35	11.49	180.6	ND
	epm	0.35	0.02	1.15	2.93	0.98	0.32	2.96	
S.5	ppm	3.29	0.42	8.33	42.34	8.94	9.79	148	ND
	epm	0.14	0.01	0.69	2.07	0.19	0.27	2.43	
S.6	ppm	3.19	0.31	7.65	59.54	9.35	5.23	160.2	5
	epm	0.14	0.01	0.64	2.92	0.19	0.14	2.63	0.17
S.7	ppm	7.46	0.36	14.05	72.59	32.61	45.56	141.6	ND
	epm	0.32	0.01	1.17	3.56	0.68	1.26	2.32	
S.8	ppm	17.78	0.56	29.7	49.3	18.03	4.86	230	8
	epm	0.77	0.01	2.47	2.42	0.38	0.13	3.77	0.27
S.9	ppm	6.86	0.34	30.48	44.41	16.41	7.25	211.4	4
	epm	0.30	0.01	2.54	2.18	0.34	0.20	3.47	0.13
S.10	ppm	2.75	0.63	8.38	46.86	13.27	5.85	144.8	ND
	epm	0.12	0.02	0.70	2.30	0.28	0.16	2.37	
S.11	ppm	1.89	0.25	15.62	43.39	10.51	4.54	170.8	2
	epm	0.08	0.01	1.30	2.13	0.22	0.13	2.80	0.07
S.12	ppm	2.85	0.3	19.33	52.29	12.64	4.97	192	2
	epm	0.12	0.01	1.61	2.56	0.26	0.14	3.15	0.07
S.13	ppm	2.94	0.41	18.63	45.49	20.32	3.63	192	ND
	epm	0.13	0.01	1.55	2.23	0.42	0.10	3.15	
S.14	ppm	1.62	0.21	15.9	44.86	11.42	3.74	167.6	4
	epm	0.07	0.01	1.32	2.20	0.24	0.10	2.75	0.13
S.15	ppm	3.14	0.39	11.94	40.59	8.27	3.98	146.4	4
	epm	0.14	0.01	0.99	1.99	0.17	0.11	2.40	0.13
S.16	ppm	3.8	0.31	16.92	41.06	19.89	3.73	156.2	4
	epm	0.17	0.01	1.41	2.01	0.41	0.10	2.56	0.13
S.17	ppm	7.4	0.63	31.48	82.68	27.45	40.89	150	ND
	epm	0.32	0.02	2.62	4.05	0.57	1.13	2.46	
S.18	ppm	38.92	1.12	14.29	32.73	5.11	8.09	201.8	9.33
	epm	1.69	0.03	1.19	1.60	0.11	0.22	3.31	0.31

Appendix (5.B) continued...

sites	Unit	Na^{+}	K^{+}	Mg^{2+}	Ca^{2+}	SO_4^{2-}	Cl	HCO_3^{-}	CO_3^{2-}
S.19	ppm	1.53	0.19	2.96	41.25	8.17	2.79	99.2	ND
	epm	0.07	0.00	0.25	2.02	0.17	0.08	1.63	
S.20	ppm	2.33	0.43	4.3	44.9	9.8	4.35	109	ND
	epm	0.10	0.01	0.36	2.20	0.20	0.12	1.79	
S.21	ppm	4.09	0.35	8.07	69.21	11.11	6.86	140	ND
	epm	0.18	0.01	0.67	3.39	0.23	0.19	2.30	
S.22	ppm	6.44	0.41	16.19	86.38	10.58	9.35	255	3.33
	epm	0.28	0.01	1.35	4.23	0.22	0.26	4.18	0.11
S.23	ppm	9.67	1.5	23.43	40.4	19.56	11.95	234.2	ND
	epm	0.42	0.04	1.95	1.98	0.41	0.33	3.84	
S.24	ppm	7.89	0.46	35.02	43.87	18.23	8.87	315.6	ND
	epm	0.34	0.01	2.92	2.15	0.38	0.25	5.18	
S.25	ppm	19	3.49	31.56	99	63.09	14.02	288	14
	epm	0.83	0.09	2.63	4.85	1.31	0.39	4.72	0.47
S.26	ppm	3.95	0.33	24.44	38.97	14.6	7.2	231	ND
	epm	0.17	0.01	2.04	1.91	0.30	0.20	3.79	
S.27	ppm	6.62	0.49	17.93	53.38	10.24	10.15	221.2	ND
	epm	0.29	0.01	1.49	2.62	0.21	0.28	3.63	
S.28	ppm	23.62	1	18.77	80.68	26.69	19.22	253.8	3.33
	epm	1.03	0.03	1.56	3.95	0.56	0.53	4.16	0.11
S.29	ppm	1.37	0.38	15.61	95.84	9.43	4.55	280	ND
	epm	0.06	0.01	1.30	4.70	0.20	0.13	4.59	
S.30	ppm	2.23	0.11	19.08	64.18	12.51	5.1	235.8	6.67
	epm	0.10	0.00	1.59	3.14	0.26	0.14	3.87	0.22
S.31	ppm	70.01	0.38	14.81	57.64	15.28	7.94	305	1.6
	epm	3.05	0.01	1.23	2.82	0.32	0.22	5.00	0.05
S.32	ppm	3.66	0.86	22.4	98.3	18.86	5.9	295	4
	epm	0.16	0.02	1.87	4.82	0.39	0.16	4.84	0.13
S.33	ppm	4.51	0.41	43.3	61.75	37.29	7.26	320.4	ND
	epm	0.20	0.01	3.61	3.03	0.78	0.20	5.25	
S.34	ppm	6.3	0.56	10.46	102.41	15.85	6.48	250	5.33
	epm	0.27	0.01	0.87	5.02	0.33	0.18	4.10	0.18
S.35	ppm	4.03	0.31	15.64	90.83	17.54	5.81	260	ND
	epm	0.18	0.01	1.30	4.45	0.36	0.16	4.26	
S.36	ppm	288.58	5.68	70.72	336.72	1244.1	161.98	175.6	ND
	epm	12.55	0.15	5.89	16.50	25.88	4.49	2.88	
S.37	ppm	6.39	0.84	23.46	107.73	28.14	12.14	305	2
	epm	0.28	0.02	1.95	5.28	0.59	0.34	5.00	0.07
S.38	ppm	13.17	2.58	43.31	115	66.24	19.52	335	10
	epm	0.57	0.07	3.61	5.64	1.38	0.54	5.49	0.33
S.39	ppm	301	3.58	16.5	81	395	87	255	8.67
	epm	13.09	0.09	1.37	3.97	8.22	2.41	4.18	0.29
S.40	ppm	12.34	1.818	11.04	43.77	7.412	8.5	180	ND
	epm	0.54	0.05	0.92	2.14	0.15	0.23545	2.95	

Appendix (5.C) Results of some other calculated chemical components

Sites	EC (µS/cm)	T. Hardness (ppm)	Alkalinty (ppm)	SAR	NO_3^-
1	574.1	190.4	82.7	1.66	22.3
2	390.0	207.5	87.3	0.23	43.3
3	1131.0	525.8	67.3	0.40	192.7
4	308.9	206.1	74.0	0.35	9.4
5	268.3	140.0	60.7	0.17	17.9
6	304.2	180.2	70.7	0.15	25.9
7	507.0	239.1	58.0	0.30	61.1
8	304.2	245.3	86.7	0.70	9.8
9	530.4	236.3	90.7	0.27	23.4
10	343.2	151.5	59.3	0.14	21.2
11	304.2	172.6	72.0	0.09	8.56
12	349.4	210.1	80.7	0.12	5.7
13	335.4	190.3	78.7	0.13	6.9
14	346.3	177.4	72.7	0.08	14.9
15	252.7	150.5	64.0	0.16	10.1
16	293.3	172.2	68.0	0.18	6.4
17	655.2	336.0	53.3	0.25	98.1
18	318.2	140.5	92.0	2.03	0.7
19	196.6	115.2	40.7	0.09	13.2
20	249.6	129.8	44.7	0.13	15.9
21	405.6	206.0	50.0	0.18	55.6
22	343.2	282.3	102.7	0.24	11.1
23	486.7	197.3	96.0	0.42	12.3
24	463.3	253.7	129.3	0.30	6
25	549.1	377.1	127.3	0.60	ND
26	371.3	197.9	94.7	0.17	4.8
27	366.6	207.1	90.7	0.28	10.1
28	439.9	278.7	107.3	0.87	24.7
29	304.2	303.5	90.7	0.05	9.2
30	351.0	238.8	103.3	0.09	13.5
31	352.6	204.9	93.3	3.02	15.7
32	365.0	337.6	98.0	0.12	8.7
33	510.1	332.4	131.3	0.15	2.7
34	280.8	298.8	66.7	0.23	17.6
35	361.9	291.2	82.0	0.15	4.8
36	2425.8	1131.8	72.0	5.31	146.2
37	413.4	365.5	102.7	0.21	13.3
38	702.0	465.4	137.3	0.38	28.3
39	1801.3	270.2	90.0	11.33	6.9
40	330.7	154.7		0.61	*20.7*

التقيم الهايدروجيولوجي وخريطة عرضة المياه الجوفية لحوض باسرة، محافظة السليمانية، إقليم كردستان العراق

رسالة

مقدمة الى مجلس كلية العلوم - جامعة السليمانية كجزء من متطلبات درجة دكتوراه فلسفة في علم الأرض

من قبل

دارا فائق حمةمين

ماجستير في الهايدروجيولوجي-٢٠٠4

بإشراف

أ.م. د. صلاح الدين سعيد علي

جمادي الثاني- ١٤٣2 هـ   مايس - ٢٠١١ م

ألمستخلص

يقع حوض باسرة شمال شرق العراق،25 كم غرب مدينة السليمانية، بين خطي طول (496652 و 537752 شرقا) و خطي عرض (3911038 و 3951906 شمالا). هذا الحوض له شكل مستطيل و يغطي مساحة مقدارها 571 كم^2. من الناحية التكتونية، يقع الحوض في منطقة معقدة في الرصيف القاري الغير المستقر من الصفيحة العربية ضمن حزام طيات وفوالق زاكروس الزاحفة، وتحديدا على طول حدود الامتداد الجنوب الغربي للطيات العالية مع نطاق اقدام الجبال لهذا الحزام والذي يمتاز بشدة عمليات الطي والتكسر التي نتجت من عدة مراحل من التشوه اثناء فترة بناء الألباين.

ان مسار تصريف المياه السطحية والجوفية لهذا الحوض هو باتجاه مضيق باسرة عن طريق ثلاثة انهر رئيسة و عدة انهار فرعية.

لحساب التبخر النتحي المصدري في معادلة (FAO - Penman Monteith)، الساقط المؤثر و كمية مياه الري الحقيقية المطلوبة للمحاصيل الزراعية المختلفة في منطقة الدراسة، تم اتباع طريقة الموازنة المائية للمحاصيل مستخدما برنامج (CROPWAT 8.0) على قاعدة البيانات الشهرية للفترة بين (1980-2009).

اظهرت نتائج كل من طريقتي الموازنة المائية للتربة و (SCS) بأن كمية مياه السيولة (runoff) المتوقعة من مجموع الساقط المطري السنوي هي 149 ملم او مايعادل 21.5٪ و كمية المياه المغذية (recharge) هي 168 ملم او مايعادل 24٪ من مجموع الساقط السنوي على منطقة الدراسة.

ان جميع الوحدات الصخرية المتواجدة والمنكشفة على السطح في المنطقة هي وحدات ترسيبية عائدة الى حقبة الحياة الحديثة حيث يمثل كولوش التكوين الأقدم و تمثل ترسبات زمن الهولوسين الأحدث عمرا.

اظهرت الدراسة الهيدروجيولوجية الحالية وجود ثلاثة وحدات طباقية حاملة للمياه والتي تمتاز بعدم التناظر والتجانس لوحداتها. الوحدة الأولى عرفت بالمكامن المائية الكارستية المتشققة الإيوسينية، الوحدة الثانية تمثلت بمكامن المائية الفتاتية البينية والمتمثلة بالترسبات النهرية والترسبات البلايوسينية، بينما الوحدة الأخيرة والأقل شيوعا سميت بالمكامن المائية المعقدة العائدة الى زمن المايوسين.

لغرض إجراء إختبارات الضخ للمكامن المائية الرئيسة الثلاث،تم حفر بئري مراقبة مخترقا تكويني سنجار والبيلاسبي والإستعانة ببئر آخر موجود خارقاً المكامن المائية الفتاتية البينية (AIA) قريب من بئر انتاجي وذلك للحصول على المعاملات الهيدروليكية الاساسية لهذه المكامن المائية الثلاث على حدة.

إن حجم المياه المتوقعة المترشحة الى المكامن المائية الجوفية من الساقط السنوي خمنت ب 96 مليون م^3، حوالي 10 مليون م^3 من هذه الكمية تستهلك عن طريق الإستخدام المنزلي والزراعي وكذلك الصناعي. ان النسبة المئوية المتوقعة من الإنتاج السنوي مقارنة بالتغذية السنوية للأحواض الصغيرة والمتمثلة ب "بازيان وهنجيرة و تلي" كانت 71.5٪، 68٪ و 16٪ على التوالي.

اعتمادا على نتائج التحليلات الكيميائية ل 65 نموذج مائي مأخوذ من العيون والآبار الضحلة والعميقة تبين بأن معظم مياه المنطقة هي مياه كلسية بيكاربونية ويمكن تصنيفها بانها مياه عذبة ذات جودة عالية حسب مقاييس منظمة الصحة العالمية وكذلك حسب المقاييس العراقية، ماعدا بعض النماذج المأخوذة من الآبار الضحلة والعميقة والتي اخترقت التكوينات الحاوية على صخور المتبخرات والتي تقع جنوب منطقة الدراسة فانها لايمكن استخدامها لأغراض معينة.

لأول مرة على مستوى كردستان والعراق، تم عمل خريطة للمياه الجوفية تبين الأماكن الأقل والأكثر عرضة للتلوث مستخدما طريقة ال DRASTIC ومستعينا بنظام المعلومات الجغرافية GIS. تم تصنيف الخريطة المتشكلة على اربعة اصناف رئيسة. أظهرت النتائج بان معظم مناطق الدراسة قليلة العرضة للتلوث (low vulnerable) ماعدا بعض الجيوب لأماكن صغيرة والواقعة في مناطق جبلية وتحديدا شرق جبلي أولوبلاغ و كويك مع بعض الأنطقة الصغيرة الأخرى والواقعة في جناحي الشمال و الجنوب الغربي لمنطقة الحوض والتي تمتاز بقلة النشاط البشري فإن تعرضها للتلوث عالية نسبيا (high vulnerable).

پوختە

ئاوزێڵی باسەڕە کە شێوەیەکی لاکێشەیی هەیە و ڕووبەرێکی 573 کم^2 دا پۆشیوە، دەکەوێتە باکوری ڕۆژهەڵاتی عێراق بە نزیکەی 25 کم لە ڕۆژئاوای شاری سلێمانی لەنێوان هەردوو هێڵی درێژیی (496652 و 537752) بەئاڕاستەی ڕۆژهەڵات وە هەردوو هێڵی پانی (3911038 و 3951906) بەئاڕاستەی باکوور.

لەڕووی تەکتۆنی یەوە، ئەم ئاوزێڵە کەوتۆتە ناوچەیەکی ئاڵۆزی ناجێگیری سەر بە سەکۆی عەرەبی کەناسراوە بە پشتێنەی لێکترازاوی پاڵنراوی زاگرۆس (ZFTB)، بەدرێژایی سنوری باشوری ڕۆژئاوای نوشتاوە باڵاکان (High folded zone) کەهاوسنوورە لەگەڵ ناوچە پاگردەکان (Foothill zone). پرۆسەی نوشتانەوەو لێکترازان لەکاتی دروستبوونی شاخەکان لەسەردەمی ئەلبایندا، کاریگەری تەواوی لەسەر ئەم ناوچانە جێهێشتووە. زۆربەی ئاوەڕۆی ئاوی سەرزەوی و ئاوی ژێرزەوی ئەم ئاوزێڵە بە ئاڕاستەی دەربەندی باسەڕە گوزەر دەکات، ئەویش لەڕێگای سێ چەمی سەرەکی و چەند چەمێکی تری لاوەکی.

بەمەبەستی دۆزینەوەی بڕی هەڵمینی ئاو بەبەکارهێنانی هاوکێشەی (FAO – Penman Monteith)، بارانی کاریگەر وە بڕی ئاوی پێویست بۆ مەبەستی ئاودێری کردنی چەند جۆرێکی دیاریکراو لە ڕووەکی چێندراو لە ناوچەکەدا، ڕێگای هاوسەنگیی ئاوی بەروبومی کشتوکاڵ (Crop Water Balance) بە بەکارهێنانی بەرنامەی کۆمپیوتەری تایبەت بەم بیردۆزەیە (CROPWAT 8.0) بەکارهێنرا، ئەویش بە پشتن بەستن بەئاماری کەشناسی مانگانە بۆ ساڵەکانی (1980-2009).

دەرئە نجامەکانی هەردوو بیردۆزەی هاوسەنگیی ئاوی بۆ خاک (soil water balance) وە (SCS) دەریا نخست کەوا بڕی چاوەڕووان کراوی ئاوی سەرڕێژ لە تێکڕای ئەو بڕە بارانەی کەساڵانە بەسەر ناوچەکەدا دەبارێت دەگاتە 149 ملم کەئەمیش دەکاتە ڕێژەی سەدی 21.5٪، وە ئەو ڕێژە ئاوەی کە دزە دەکاتە ناو زەوی و دەگاتە ئاوی ژێرزەوی ئەوا بە بڕی 168 ملم یان 24٪ لە تێکڕای بارانی ساڵانە ئەژمارکراوە.

تێکڕای چینە بەردینەکانی ئەم ناوچەیە چینە بەردینی نیشتوون کە مێژووەکەیان دەگەڕێتەوە بۆ چاخی ژیانی نوێ (Cenozoic) بەشێوازێك پێکهاتووی کۆلۆش کۆنترینیانە وە نیشتووە ڕووبارییەکان تازەترینیانە.

دەرئە نجامەکانی جیۆلۆجیای ئاوی ئەم توێژینەوەیە دەریا نخست کەوا سێ جۆر ئاوە کۆگای ژێر زەوی (Aquifer) لەناوچەکەدا بوونیان هەیە. جۆری یەکەمیان ناونرا بە ئاوەکۆگای کارستی درزی ئیۆسینی (EKFA)، جۆری دووەمیان کە نیشتووە ڕووبارییەکان و نیشتووە پلایۆسینیەکان دەگرێتەوە ناونرا بە ئاوە کۆگای دەنکۆڵەی نێوانی (Intergranular aquifer)، لە کاتێکدا جۆری سێهەم کە کەمترینیانە ناونرا بە ئاوە کۆگای ئاڵۆزی مایۆسینی (MCA).

بەمەبەستی هەڵسەنگاندن و زانینی سیفاتە هایدرۆلیکیەکانی هەر سێ ئاوەکۆگا سەرەکیەکانی ناوچەکە، تاقی کردنەوەی ترومپای ئاوی بە پشت بەستن بە هەڵکەندنی دوو بیری پیزۆمیتری کە هەردوو چینە

بەردینی سنجار وە پیلاسپی تێپەڕاندبوو، وە هەروەها بە بەکارهێنانی بیرێکی هەڵکەندراوی پێشوو کە چینە بەردینەکانی ئاوە کۆگای دەنکۆڵەی نێوانی بڕیوە ئەنجام درا.

تێکڕای قەبارەی ئەو ئاوەی کەلە بارانەوە دزە دەکات و دەگاتە ئاوی ژێرزەوی بە 96 ملیۆن م^3 خەملێنرا، لەم بڕە نزیکەی 10 ملیۆن م^3 بۆ مەبەستی بەکارهێنانی ناوماڵ و کشتوکاڵ و پیشەسازی بەکاردەبرێت. ڕێژەی چاوەڕوان کراوی نێوان بەرهەمی ساڵانە بەبەراورد لەگەڵ بوژانەوەی ساڵانە بۆ هەر سێ ئاوزێڵی "بازیان، هەنجیرە و تلێ" دەگاتە نزیکەی 71.5٪، 68٪ وە 16٪ بۆ هەر یەکێکیان بەجیا.

بە پشت بەستن بە پێوەرەکانی ڕێکخراوی تەندروستی جیهانی و عێراقی، وە پاش ئەنجام دانی شیکاری کیمیاوی بۆ 65 نمونەی ئاوی کانی و بیری دەستی و بیری قوڵ، دەرکەوت کەوا جۆری ئەو ئاوەی کەلەناوچەکەدا بڵاوە بریتی یە لە ئاوی کلسی بیکاربۆنی ($CaHCO_3$) کەئەمەش بە یەکێك لە جۆرە باشەکان دادەنرێت، بێجگە لە چەند نمونەیەك کەوەرگیراوە لەو بیرانەی کەچینەکانی نیشتوی هەڵمینی بڕیوە (evaporate) وەکەوتۆتە باشوری ئەم ئاوزێڵەوە ئەوا جۆری ئاوەکەی باش نییەو بە کەڵکی چەند مەبەستێکی دیاری کراو نایەت.

بۆیەکەم جار لەسەرئاستی کوردستان و عێراق، وە بە پشت بەستن بەرنامەی GIS نەخشەیەك بۆ ئاوی ژێرزەوی دروستکرا بۆ نیشاندانی ئەو ناوچانەی کەزۆرترین وە کەمترین مەترسییان لەسەر پیسبوونی ئاوی ژێرزەوی هەیە. لەم نەخشەیەدا ناوچەکە دابەشکرا بەسەر چوار پۆلی سەرەکی لەڕوویی مەترسی پیسبونەوە. خۆشبەختانە دەرئەنجامەکانی ئەم نەخشەیە دەریانخست کەوا زۆربەی ناوچەکە لەڕوویی مەترسی پیسبونەوە پۆلێن کراوە بە سەر ناوچەی کەم مەترسی (low vulnerable)، بێجگە لەچەند ناوچەیەکی شاخاوی کەکەوتۆتە ڕۆژهەڵاتی شاخەکانی ئۆڵوبلاغ و کۆیك وە چەند جێگایەکی تر کەکەوتۆتە باکوور و باشووری خۆرئاوای ناوچەکە، ئەوا مەترسی پیسبونیان لەسەرە (high vulnerable).

هەڵسەنگاندنی هایدرۆجیۆلۆجی و نەخشەی هەستیاری ئاوی ژێرزەوی لە ئاوزێڵی باسەڕە، پارێزگای سلێمانی، هەرێمی کوردستانی عێراق

نامەیەکە

پێشکەش کراوە بە ئەنجومەنی کۆلیجی زانست لە زانکۆی سلێمانی وەك بەشێکی تەواوکەر بۆ بەدەست هێنانی دکتۆرای فەلسەفە لە زانستی جیۆلۆجی دا

لەلایەن

دارا فائق حمەمین

ماستەر لە زانستی هایدرۆجیۆلۆجی – ٢٠٠4

بەسەرپەرشتی

پ. ی. د. صلاح الدين سعيد علی

جۆزەردان-٢7١١ کوردی   مایس- ٢٠١١ زایینی